

Case study

Carbon emissions assessment of concrete and quantitative calculation of CO₂ reduction benefits of SCMs: A case study of C30-C80 ready-mixed concrete in China

Zuojiang Lin ^a, Guangyao Lyu ^b, Kuizhen Fang ^{b,*}^a China Construction First Group Construction & Development Co., LTD., Beijing 100102, China^b Department of Civil Engineering, Tsinghua University, Beijing 100084, China

ARTICLE INFO

Keywords:

Carbon emissions
Ready-mixed concrete
Supplementary cementitious materials
Manufactured sand
Transport distance

ABSTRACT

This study elucidates the changes in carbon footprint variations in concrete production processes and component contributions due to the use of supplementary cementitious materials (SCMs) and changes in raw material transport distances through the establishment of a large-scale concrete mix proportion database and life-cycle assessment (LCA). The average carbon emissions for C30-C80 concrete were calculated to range from 262.21 to 401.78 kgCO₂e/m³, with data showing significant dispersion due to uncertainties in raw materials and experimental conditions. The incorporation of SCMs leads to substantial and unstable changes in cement content, but still generally reduces carbon emissions of concrete by 5 %-30 % at the same strength level, and increased transport distances have little effect on this reduction rate, which diminishes to zero only when distance exceeds 4166 km. In contrast, transporting aggregates over long distances (from 100 km to 500 km) increases carbon emissions by more than 10 % due to huge mass. Manufactured sand (MS) reduces transport emissions when replacing 50 % and 100 % of natural fine aggregates (NFA) but is scarcely beneficial to total CO₂e emission due to its higher production energy consumption and negative impact on concrete strength. This study highlights the low-carbon potential of SCMs and underscores that reducing production energy consumption and enhancing material performance are crucial for maximizing the comprehensive low-carbon benefits of MS.

1. Introduction

As an energy and material intensive industry, construction accounts for approximately 36 % of global carbon emissions [1], with the production phase of building materials alone generating around 64.5 % of the total emissions over a building's life cycle [2]. In response, China launched the Building Materials Carbon Label Project in 2024, aiming to establish a grading system based on material carbon emissions. This initiative is expected to drive low-carbon transformation in the construction sector [3]. At present, ready-mixed concrete remains the most widely used construction material in China, and it has a large carbon emission factor due to the decomposition of calcium carbonate during the cement production process. Song et al. [4] undertook a life-cycle assessment (LCA) of a typical Chinese cement production line, reporting total carbon emissions of 678 kgCO₂e/t, with 88.3 % attributed to the calcination process.

* Corresponding author.

E-mail address: fangkuizhen@163.com (K. Fang).

Turner et al. [5] made a comparison between Grade 40 concrete mixtures with geopolymer and OPC binders and the estimated carbon emission were calculated as 354 kgCO_{2e}/m³ and 320 kgCO_{2e}/m³, respectively. Thorne et al. [6] found that C45 pure cement concrete (PC) emitted 496.5 kgCO_{2e}/m³ based on a life-cycle inventory flow chart. Additionally, Cong et al. [7] analyzed C30, C40, and C50 PC, observing carbon emissions growth of 19.6 kgCO_{2e}/m³ and 16.7 kgCO_{2e}/m³ as strength levels increased. However, many of these studies only used limited mix proportions, and the results varied widely due to differing carbon emission factors. To address this, it is essential to leverage ready-mixed concrete mix proportions on a national scale, enabling large-scale calculations under unified emission factors to establish reliable grading standards for carbon emissions from ready-mixed concrete in China.

One effective approach to producing low-carbon concrete is to substitute supplementary cementitious materials (SCMs) for ordinary Portland cement (OPC), a strategy that is both well-studied and increasingly adopted. A literature review of the pathways towards low-carbon concrete was conducted by Busch et al. [8] and SCMs was listed as one of the consensus on the primary technical measures to decarbonize. Celik et al. [9] found that replacing 30 % of OPC with fly ash (FA) reduced concrete's carbon emissions by 160 kgCO_{2e}/m³ with only a slight drop in compressive strength (2.9 MPa at 28 days). Wang et al. [10] reported continued strength improvement in C60 recycled aggregate concrete when granulated blast furnace slag powder (GGBS) comprised 0–30 wt%. In another study, Wang et al. [11] assessed optimal replacement levels of red mud (10 %) and GGBS (15 %) based on strength, durability, and environmental impact. Jiang et al. [12] evaluated the influence of silica fume (SF) on mechanical properties and carbon emission of reactive powder concrete and found that 15 % substitution rate of SF achieved the lowest carbon emissions efficiency. Hossain et al. [13] compared the environment impacts of natural volcanic ash (VA) and typical SCMs in concrete, and the results showed that over 10 % carbon emission was reduced by incorporating 20 %-30 % VA instead of GGBS and FA when strength was considered comprehensively. Sinkhonde et al. [14] used waste brick powder (WBP) and waste tire rubber (WTR) to produce C20-C30 concrete and find the combination of 5 % WBP and 5 % WTR in concrete mixes kept a reasonable compressive strength and successfully reduced the carbon dioxide emissions. These studies confirm that SCMs can effectively lower concrete's carbon footprint. However, most research examines SCMs substitution under constant binder mass, which does not reflect real conditions, as SCMs may weaken concrete's mechanical properties. Consequently, SCM-blended concrete (SCMC) may require more cementitious material to match the strength of PC at similar levels. Thus, defining a standardized CO₂ reduction rate for SCMs that maintains equivalent strength levels is urgently needed.

At the same time, conventional high-quality SCMs, like FA and GGBS, face issues of uneven regional distribution and declining production in China, leading to potentially increased transport distances. Additionally, newer SCMs such as lithium and magnesium slag powders require further study for engineering applications. The impact of SCM transport distance on carbon reduction benefits must therefore be considered. Marian et al. [15] observed 3.9 %-11 % higher concrete emissions over FA transport distances of 15.1–504 km compared to non-transported FA. DeRousseau et al. [16] used LCA data to estimate FA's breakeven transport distances as 2655 km and 15110 km for truck and ship transport, respectively. However, these studies did not fully illustrate the complete reduction trend of CO₂ benefits as transport distances increase. Similarly, natural aggregates, particularly high-quality natural fine aggregates (NFA) like river sand, face restrictions due to environmental concerns [17]. Manufactured sand (MS) is an acceptable alternative but demands more energy for extraction and processing [18]. When long-distance transport is needed for NFA, a more flexible production location for MS may reduce transport emissions. Zhu et al. [19] established a compressive strength and carbon emission prediction model for MS concrete and found that combining 24.5 % FA and 8.33 % limestone powder (LP) can reduce carbon emissions by more than 23 %. However, Guan et al. [20] pointed out that the use of MS could lead to 5 %-40 % loss in compressive strength of concrete, which may result in an increase in cement mass, offsetting MS's low-carbon effect. Thus, the specific low-carbon potential of MS should be evaluated more comprehensively.

To address the limitations in the aforementioned research, this paper aims to establish a reliable concrete mix proportion dataset with sufficient scale for accurate carbon emission accounting. Breaking the traditional assumption of variable control in research, this study realistically considers the impact details of the introduction of SCMs and MS on various life stages (raw material production, transportation, etc.) and the usage of other components, clarifying the carbon emission allocation and synergistic mechanisms of different components and production processes. Thus, the low-carbon potential and limitations of SCMs and MS are proposed at the market average scale.

In this study, the calculating method on ready-mixed concrete carbon emissions was determined under the guidance of IPCC [21] and ISO 14040 [22]. A dataset for C30-C80 ready-mixed concrete mix proportions was developed using literature and data from mixing plants across China. Carbon emissions for C30-C80 concrete were then calculated, and growth trends were analyzed based on variations in key design parameters as strength levels increased. To assess SCMs' CO₂ reduction benefits, the carbon reduction index (CR^l) was defined and evaluated across different strength levels, with relationships between CR^l and SCMs substitution rates analyzed. Finally, to avoid unnecessary long-distance transport, a CR^l -transport distance variation curve was plotted, along with a scenario comparison to weigh MS's high energy consumption against its potentially lower carbon impact due to shorter transport distances. This research supports the establishment of carbon labeling for ready-mixed concrete and encourages the effective, low-carbon use of SCMs and MS.

2. Methodology

2.1. System boundary

The life cycle and system boundary for ready-mixed concrete are presented in Fig. 1. The "cradle to gate" system boundary was

widely adopted by researchers [9,15]. In addition to that, the system boundary in this study also includes the transportation of concrete from the mixing plant to the construction site to account for responsibility allocation. However, the construction, maintenance, disposal and recycle of concrete are excluded from the system boundary as the primary focus is on the material production and selection in this study.

2.2. Calculation method

The functional unit in this study is 1 m³ ready-mixed concrete, the total carbon emission of which should be calculated under the guidance of IPCC [21] based on the system boundary as Eq. (1) shows. To be noted, the carbon emission has taken other greenhouse gases (e.g., methane (CH₄), nitrous oxide (N₂O)) into consideration, their impact on global warming has been factored into the calculation of carbon emission factors and expressed in terms of carbon dioxide equivalents (CO₂e) in order to have a single unit of measure of emission.

$$E = E_{\text{material}} + E_{\text{tran1}} + E_{\text{manu}} + E_{\text{tran2}} \# \quad (1)$$

where E_{material} represents the embodied carbon emissions from raw material production; E_{tran1} is the transport emissions for raw materials; E_{manu} is the emissions from the manufacturing of ready-mixed concrete; and E_{tran2} is the emissions from transporting the ready-mixed concrete. These 4 types of emissions are calculated by Eq. (2)-(5) respectively:

$$E_{\text{material}} = \sum_i M_i \times EF_i \# \quad (2)$$

$$E_{\text{tran1}} = \sum_i M_i \times D_i \times EF_{\text{tran1},i} \# \quad (3)$$

$$E_{\text{manu}} = AD_{\text{fuel}} \times EF_{\text{fuel}} + AD_{\text{ele}} \times EF_{\text{ele}} \# \quad (4)$$

$$E_{\text{tran2}} = \rho \times D \times EF_{\text{tran2}} \# \quad (5)$$

where M_i is the mass of each raw material (kg/m³); EF_i is the carbon emission factor of each raw material (kgCO₂e/kg); D_i is the transport distance of each raw material (km); $EF_{\text{tran1},i}$ is the carbon emission factor for the transport equipment (kgCO₂e/(kg·km)); AD_{fuel} represents fuel consumption during concrete manufacturing (t/m³); EF_{fuel} is the carbon emission factor for fuel (kgCO₂e/t); AD_{ele} is the power consumption during concrete manufacturing (kWh/m³); EF_{ele} is the carbon emission factor for power (kgCO₂e/kWh); ρ is the bulk density of concrete (kg/m³); D is the transport distance for the ready-mixed concrete; EF_{tran2} is the carbon emission factor for concrete transport equipment (kgCO₂e/(kg·km)).

2.3. Carbon emission factors

The carbon emission factors of raw materials and their respective references are presented in Table 1.

The emission factor for transport equipment is based on values in the appendix of GB/T 51366–2019 (Standard for Building Carbon Emission Calculation) [23]. It is assumed that all raw materials are transported by heavy-duty diesel trucks with an 18-ton load capacity, yielding a carbon emission factor of $EF_{\text{tran1},i} = 0.000129$ kgCO₂e/(kg·km).

Diesel is the primary fuel consumed in the production and transportation of ready-mixed concrete. According to fuel parameters in the appendix of GB/T 32151.8–2023 (Requirements of the carbon emissions accounting and reporting-Part8: Cement enterprise) [30], the carbon emission factor of diesel is calculated as $EF_{\text{fuel}} = 3096$ kgCO₂e/t. And the carbon emission factor of power is taken as the latest national average value released by the Ministry of Ecology and Environment, set at $EF_{\text{ele}} = 0.5568$ kgCO₂e/kWh.

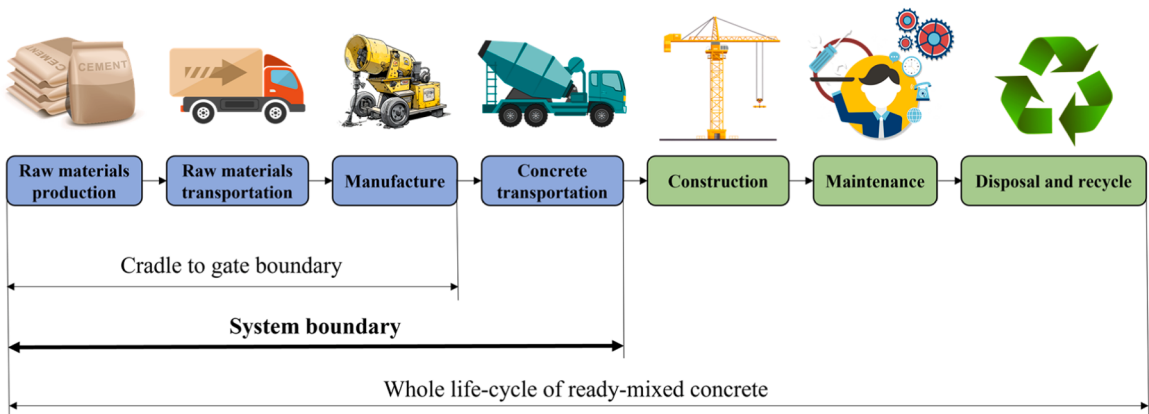


Fig. 1. Whole life cycle and system boundary of ready-mixed concrete.

Table 1
Carbon emission factors of raw materials (kgCO₂e/kg).

Raw material	EF_i	Ref
42.5 Cement	0.735	GB/T 51366–2019 [23]
52.5 Cement	0.889	DB3502/Z 5053–2019 [24]
NCA	0.00218	GB/T 51366–2019 [23]
NFA	0.00251	GB/T 51366–2019 [23]
MS	0.03485	Pan et al., 2024 [25]
FA	0.010	Matthew et al., [26]
GGBS	0.083	Matthew et al., [26]
SS	0.0442	DB 64/T 1954–2023 [27]
LP	0.017	Matthew et al., [26]
SF	0.00841	Zhong et al., [28]
SP	1.11	Kong et al., [29]

Note: 42.5 Cement and 52.5 Cement includes the cement type of P.O, P.I and P.II; NCA: natural coarse aggregate; SS: steel slag powder; LP: limestone powder; SF: silica fume; SP: superplasticizer; The carbon emission factor of SF additionally considers the transportation of undisturbed SF.

2.4. Activity data

2.4.1. Mix proportions of concrete

440 pieces of C30-C80 ready-mixed concrete (excluding fibers) mix proportions from 141 data sources in 29 provinces are collected in [Table S1](#), with 40 pieces for each strength level. The strength level was determined by the test values of 28d compressive strength of each sample, and the detailed rules were based on Chinese standard JGJ 55–2011 (Specification for mix proportion design of ordinary concrete) [31]. And the raw material types are limited in [Table 1](#). As [Fig. 2](#) shows, the dataset includes actual production data nationwide except for some remote regions.

2.4.2. Transport distance of raw materials

The transport distance of raw materials should prioritize the actual values in production, but due to the limited accessibility, hypothetical values from a baseline scenario are used instead, and the influence of increased transport distance of SCMs is discussed in [Section 3.6](#).

Under the baseline scenario, raw materials of C30-C80 ready mixed concrete have transport distances as shown in Table 2. The transport distance settings are based on the data provided by numerous Chinese ready-mixed concrete production enterprises, with consideration of the shortage of sources for obtaining natural aggregates and SCMs [32,33].

2.4.3. Fuel and power consumption

The fuel and power consumption during the manufacture stage are based on the limit values of DB 64/T 1954–2023 (Calculation method and evaluation standard of carbon emission from concrete) [27] and GB 36888–2018 (The norm of energy consumption per unit product of ready-mixed concrete) [34], which reflect the average energy consumption of concrete production in China. In order to verify the representativeness of the data provided by these two standards, this study additionally considered the data in two latest studies. Wu et al. [35] and Pan et al. [36] provided primary data on actual energy consumption monitoring form ready-mixed concrete production sites, and the calculation results are highly consistent with the standard as shown in Section 3.3, which demonstrates the rationality of the data selection in this study.



Fig. 2. The data sample sizes of different regions in China.

Table 2
Transport distances of raw materials under the baseline scenario (km).

Raw material	D_i
Cement	50
SCMs	200
NCA	100
NFA	100
MS	50
SP	50

2.4.4. Transportation of concrete

The transportation of ready-mixed concrete is carried out by concrete mixer trucks, typically with a transport volume from 2 to 18 m³. Assuming an average volume of 10 m³ and a concrete density of 2400 kg/m³, the corresponding carbon emission factor for a heavy-duty diesel truck with a load capacity of 30 tons is 0.078 kgCO_{2e}/t-km). The transport distance of concrete is assumed to be 40 km according to the average value in the carbon footprint reports provided by Chinese enterprises.

2.5. Normalization of carbon emission

A common practice for evaluating both mechanical properties and environmental impact is to compare the comprehensive benefits of ready-mixed concrete at different strength levels using $E_{normalized}$:

$$E_{normalized} = \frac{E}{l} \# \quad (6)$$

where l represents the strength level of the ready-mixed concrete.

2.6. CO₂ reduction rate of SCMs

Aiming at quantify the CO₂ reduction benefits of SCMs, the carbon reduction rate CR^l is defined according to Eq. (7):

$$CR^l = \frac{E_{pure}^l - E_{scm}^l}{E_{pure}^l} \times 100\% \# \quad (7)$$

where E_{pure}^l represents the total carbon emissions of PC at a given strength level; E_{scm}^l represents the total carbon emissions of SCMC at the same strength level.

2.7. Scenario settings to compare NFA and MS

To compare the carbon emission benefits of NFA and MS, four scenarios are considered as shown in Table 3.

In Scenario 1, the transport distance of NFA remains 100 km, and the MS ratio is 0, which means the fine aggregates in Scenario 1 are totally composed of NFA. In Scenario 2, the transport distance of NFA increases to 500 km to simulate the future shortage of NFA, but the MS ratio remains 0. In Scenario 3 and 4, the transport distance of NFA is still 500 km, and the MS ratio increases to 50 % and 100 % respectively to simulate the strategy of using MS with shorter transport distance instead of NFA. Meanwhile, in order to consider the different performances of MS in low-strength and high-strength concrete, C30 and C60 concrete is compared. It should be noted that the mix proportion used here was still derived from our large-scale dataset and the particle size range of MS was controlled. We extracted samples with MS ratios of 0, 0.5, and 1 from the C30 and C60 groups for analysis in 4 Scenarios. The emissions discussed in Section 3.6 are the average values of the corresponding samples.

Table 3
Parameter settings in different scenarios.

Scenario	1	2	3	4
D_i of NFA	100 km	500 km	500 km	500 km
D_i of MS	50 km	0	50 %	100 %
MS ratio	0	0	50 %	100 %

3. Results and discussion

3.1. Embodied carbon emission of raw materials

The embodied carbon emissions of raw materials were obtained by multiplying the mass of each component in the dataset and its corresponding carbon emission factor. In order to explore the influence of strength levels, the mean embodied carbon emission of each raw material under different strength levels is added up to obtain Fig. 3a, and the proportion of embodied carbon of each component is quantified as Fig. 4b. As shown in Fig. 3a, the average embodied carbon emissions from raw materials for C30-C80 ready-mixed concrete gradually increase from 226.9 kgCO_{2e}/m³ to 374.7 kgCO_{2e}/m³. The error bar demonstrates large standard deviation of each strength level group, which indicates high uncertainty of concrete mix proportions, mainly due to the fluctuations in raw material quality, diverse curing environments nationwide, as well as the acceptable ranges for test strength values. Fig. 3b further illustrates the emission ratio of different components, the ratio of cement gradually increases from 89 % to 93 %. Considering the continuous increase in the total amount of embodied carbon emission, 4 % increase in ratio actually reflects a huge change in the embodied carbon emission of cement, which is about 135 kgCO_{2e}/kg. And overall, cement accounts for about 90 % of the total embodied emission from raw materials, the ratio is even higher at high strength levels. Table 4 also indicates that the huge standard deviation is mainly caused by cements. Thus, the SCMs substitution rate will have significant impact on the total emission by reducing cement usage, leading to greater data variability.

However, Fig. 4a shows that the growth rate of $E_{material}$ with increasing strength levels is non-uniform, with rapid growth observed in the C30-C50 range, a slowdown at C50, and a return to moderate growth at C70. As the primary source of CO₂ emissions, the changes in $E_{material}$ of cement exhibit similar growth patterns. The $E_{material}$ of aggregates, however, shows a fluctuating downward trend, which aligns closely with the MS ratio curve, and this can be neatly explained as MS has a carbon emission factor nearly 14 times higher than NFA due to the high energy consumption in the MS production stage. The $E_{material}$ values for SCMs and SP both increase with strength level, but the magnitude of these changes does not exceed 10 kgCO_{2e}/m³ and thus has limited impact.

In order to further investigate the causes of uneven growth in total $E_{material}$, Fig. 5 shows the trends in some key design parameters for ready-mixed concrete. It can be observed that the total binder mass did not show a three-stage growth pattern like $E_{material}$, and keeps a relatively steady growth rate instead, implying the increasing usage of SCMs and 52.5 cement. Fig. 5b illustrates the three-growth mechanism of the strength and $E_{material}$. Between C30 and C50, strength gains primarily result from a rapid decrease in the water-to-binder (W/B) ratio and a sharp increase in cement mass, driving rapid growth in $E_{material}$. However, from C50 to C70, the cement mass growth rate slows, primarily due to shifts in application scenarios. Concrete above C50 strength is often used in mass concrete structures, where thermal crack control is a concern [33,36]. But the binder mass maintains the original growth rate for the request of strength, accompanied by the introduction of 52.5 cement into the system. However, as $E_{material}$ is dominated by cement mass, and the 52.5 cement mass remains relatively stable, the growth rate in stage 2 turns quite low. Between C70 and C80, the mass of 52.5 cement rises rapidly to satisfy strength requirements, along with a slight recovery of total cement mass, resulting in a moderate growth rate for $E_{material}$.

3.2. Transport emission of raw materials

E_{tran1} calculated from the mix proportion dataset and Table 2 is shown in Fig. 6. Unlike $E_{material}$, the variation of E_{tran1} is minimal and

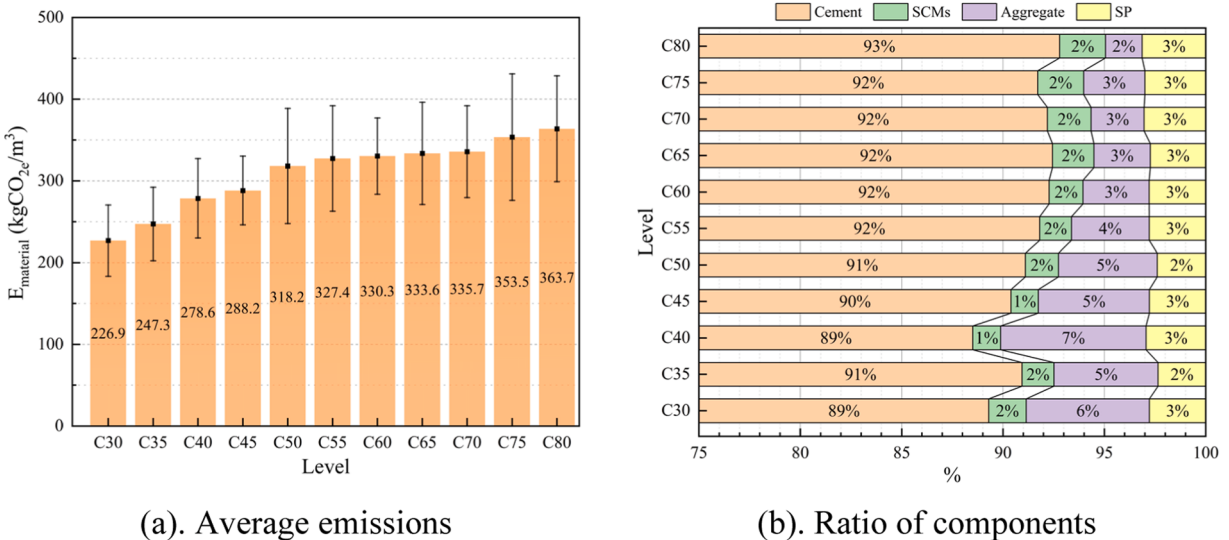


Fig. 3. Embodied carbon emission from raw materials of C30-C80 ready-mixed concrete.

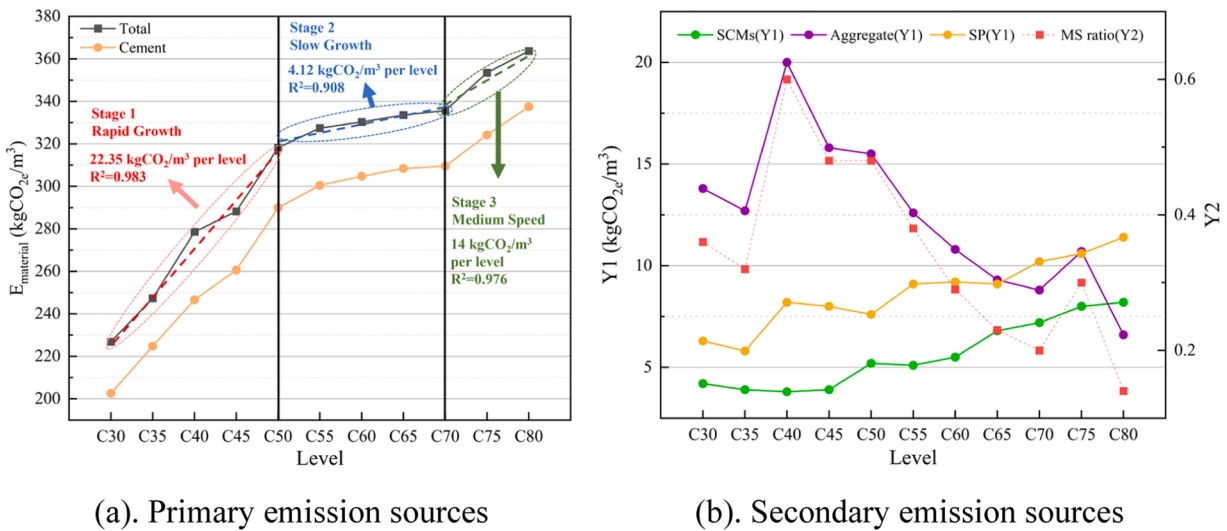


Fig. 4. Trends of embodied carbon emissions changes of each raw material.

Table 4
Standard deviation of $E_{\text{materials}}$ for 4 main components.

Component	Cement	SCMs	Aggregate	SP
Std	55.72	3.59	10.83	4.27

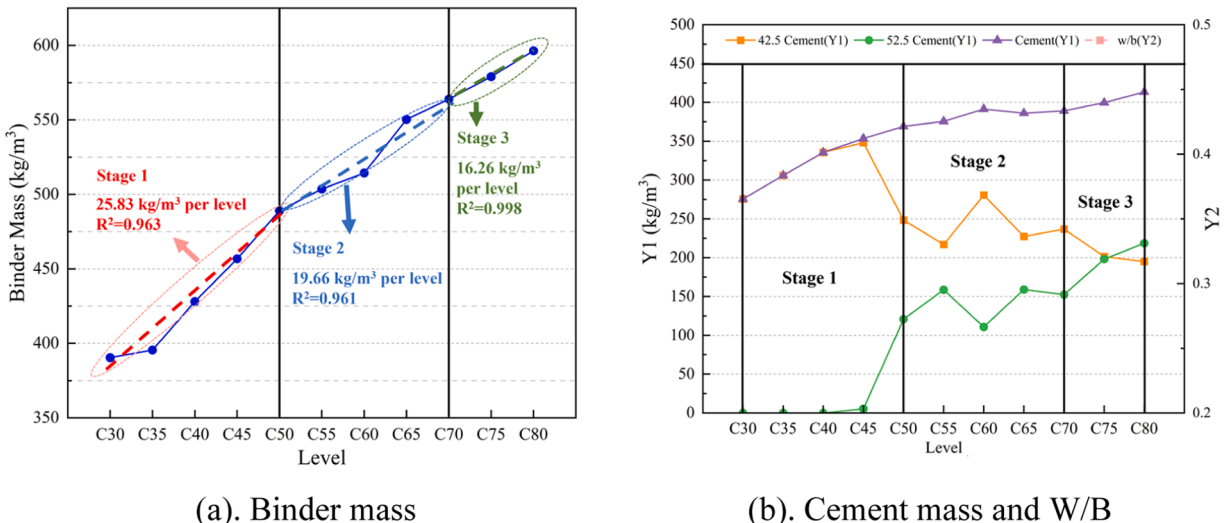


Fig. 5. Trends in design parameters changes for C30-C80 ready-mixed concrete.

is primarily generated from aggregates due to their large mass. The huge ratio of both NCA and NFA in transport emission indicates that when the transport distance of natural aggregates increases several times compared to the baseline situation, which is actually happening in Chinese market [10,11,15], the total carbon emission of concrete may be significantly affected. However, the change between adjacent strength levels is still mainly caused by binders, as E_{tran1} of aggregates remains steady with their mostly constant mass as strength rises. And despite a significant increase in the dosage of SP, the corresponding E_{tran1} of it is almost negligible due to its low total mass.

3.3. Manufacture and transport emission of concrete

Given the minimal changes in fuel and power consumption during the manufacture and transportation of ready-mixed concrete

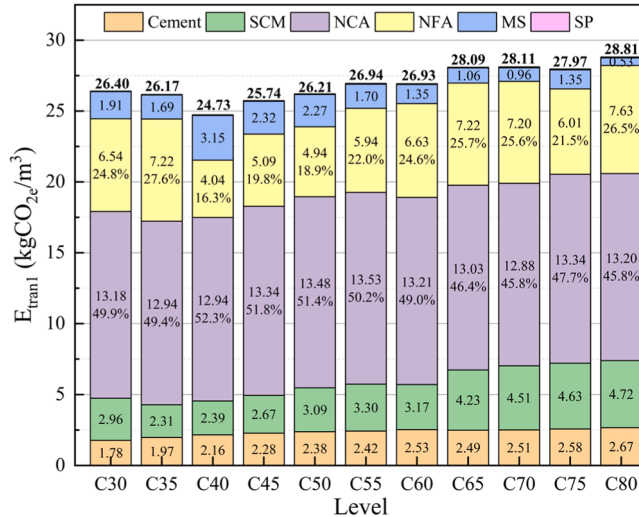


Fig. 6. Transport carbon emissions from raw materials of C30-C80 ready-mixed concrete.

across different strength levels, a unified calculation for E_{manu} and E_{tran2} is applied to all strength levels. Details of the E_{manu} calculation are provided in Table 5, where standard coal consumption has been converted to diesel consumption based on equivalent calorific values [37].

Carbon emissions caused by the transportation of concrete is calculated with the data in Section 2.4.4 as follows:

$$E_{tran2} = 2.4 \times 40 \times 0.078 \text{ kgCO}_2\text{e}/\text{m}^3 = 7.49 \text{ kgCO}_2\text{e}/\text{m}^3 \# \quad (8)$$

3.4. Total carbon emission

Fig. 7a shows the total carbon emissions and their composition for ready-mixed concrete across 4 life cycle stages, from raw material production to transportation. The average carbon emissions for C30-C80 ready-mixed concrete range from 262.61 kgCO_{2e}/m³ to 401.78 kgCO_{2e}/m³, with the majority of the emissions stemming from $E_{material}$, which accounts for 86.4–90.5 % of the total. Consequently, the growth pattern of total carbon emissions mirrors that of $E_{material}$. E_{tran1} is the second largest contributor, as its values have not changed significantly, the corresponding proportion has decreased from 10.1 % to 7.2 %. Together, $E_{material}$ and E_{tran1} contribute about 96 %-98 % of the total carbon emissions.

Fig. 7b compares the results of this study with those from other researchers and reference values reported in standard documents [23,24,26,27,38–43]. Overall, the carbon emission factors in this study are relatively low, likely due to the significant emphasis on SCM-blended concrete. The choice of cement carbon emission factor also plays a key role—for example, the EF_i values for cement used by Matthew et al. [26] and Li et al. [39] exceeded 900 kgCO_{2e}/m³ and they both reported extremely higher values as a result. However, the results presented in this study remain within a reasonable range and may be more forward-looking, as the use of low-carbon cement and SCMs is pivotal for the development of low-carbon concrete in the future.

Fig. 8 presents the results of $E_{normalized}$ calculated by Eq. (6), which steadily decreases from 8.75 to 5.02 kgCO_{2e}/(m³·MPa) as the strength level increases. The range is similar to the findings summarized in the review of Olsson et al. [44]. However, it is important to note that the use of high-strength concrete in structures does not necessarily lead to lower total carbon emissions. This assertion requires a comprehensive consideration of the balance between concrete usage and emission factors.

Table 5
Calculation of E_{manu} .

Energy consumption	E_{manu} (kgCO _{2e} /m ³)	Ref
0.214 kg/m ³ (diesel)	2.04	DB 64/T 1954–2023
2.47 kWh (power)		
0.7 kg/m ³ (standard coal)	1.49	GB 36888–2018
3.6 kWh (power)	2.00	Wu et al., 2024 [35]
0.214 kg/m ³ (diesel)	1.64	Pan et al., 2024 [32]
2.47 kWh (power)		

Average E_{manu} : 1.79 kgCO_{2e}/m³

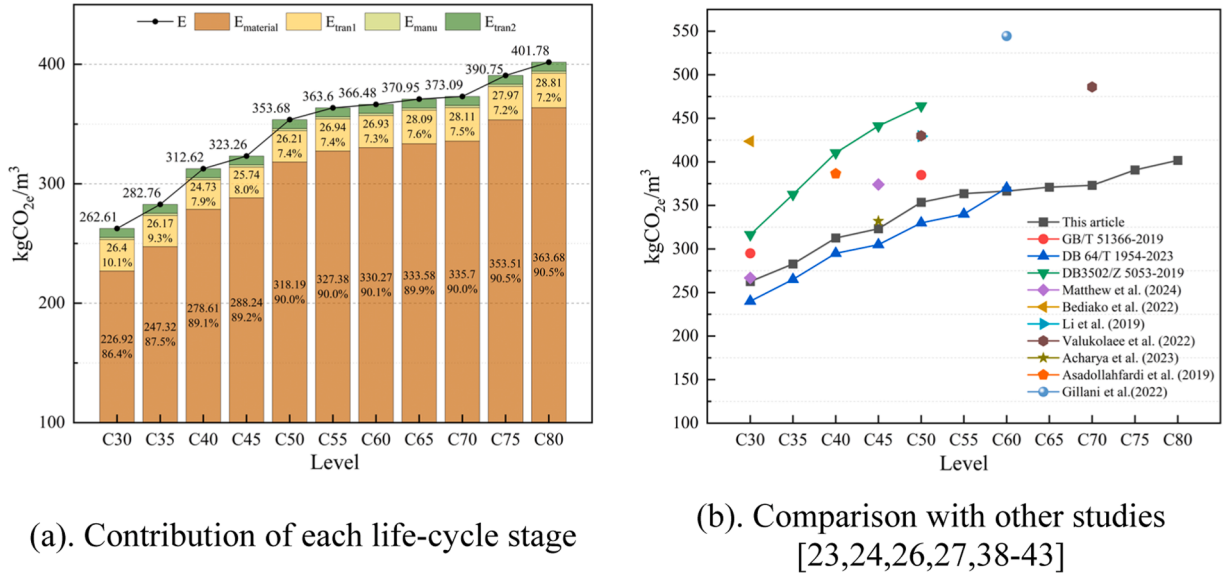


Fig. 7. Total carbon emissions of C30-C80 ready-mixed concrete.

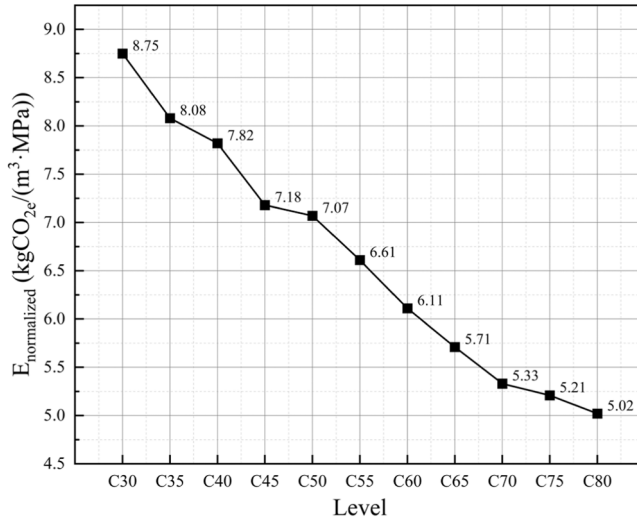


Fig. 8. Carbon emission factors normalized by strength levels.

3.5. CO_2 reduction benefits of SCMs

As noted earlier, the total carbon emission of ready-mixed concrete primarily stem from the embodied carbon emissions of cement, so substituting cement with SCMs offers significant low-carbon benefits. However, improper use of SCMs may lead to deterioration of the mechanical properties of concrete, which has been proved in many studies before [6,9,10], thus requiring the use of more cementitious materials to achieve the same strength level. Thus, a comparison between the total binder mass of PC and SCMC at the same strength level was conducted and the results were shown in Fig. 9. It can be noticed that the total binder mass used in SCMC is more than that in PC at most strength levels except for the outlier at C50. Therefore, it is not reasonable to directly derive a formula for calculating CR^l under the assumption of constant binder mass, as is common in many studies. This requires extensive data collection and calculation across various mix proportions to accurately reflect real-world scenarios.

Average CR^l values, ranging from 5 % to 30 %, are observed at different strength levels, as shown in Fig. 10a. 11 % of all samples even exhibit negative CR^l values, likely due to raw material variability and amplified test errors at low substitution rates, indicating that the improper use of SCMs may not reach the low-carbon object due to the uncertainty of raw materials. Nevertheless, SCMs generally demonstrate a strong low-carbon effect. To examine the relationship between SCM substitution rate and CR^l , a linear fit was performed, as shown in Fig. 10b. Despite a strong positive Pearson correlation coefficient, the large fluctuation range of CR^l values at

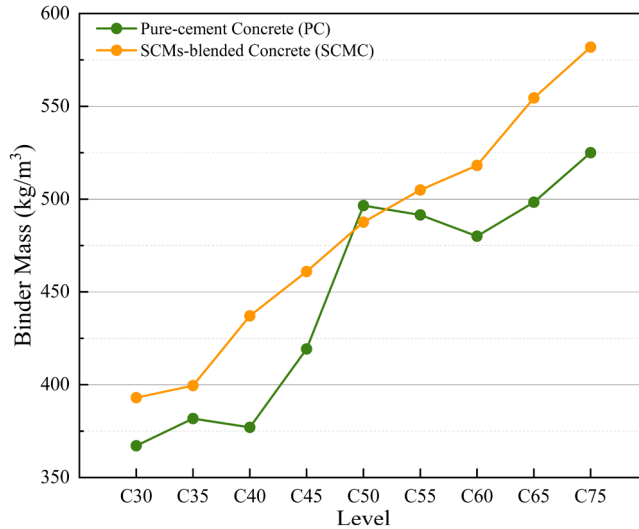


Fig. 9. Comparison of total binder mass in PC and SCMC.

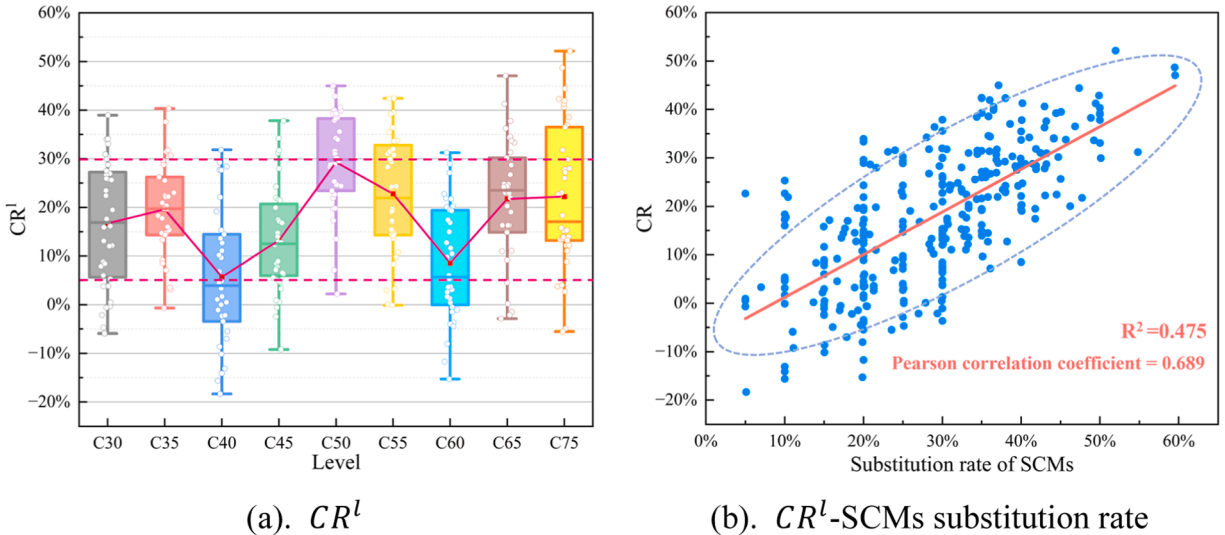


Fig. 10. CR^l at different strength levels and its correlation with SCMs substitution rate.

the same SCM substitution rate results in a low R^2 , indicating the difficulty of accurately predicting CR^l based solely on the SCM substitution rate.

3.6. Influence of transport distance

In the baseline scenario, the transport distance of SCMs is assumed to be 200 km, with an average CR^l (CR) of 17.78 % across all samples. However, due to the growing scarcity of SCMs, cross-provincial transportation of SCMs is becoming more common in China, potentially offsetting the low-carbon benefits. Therefore, there is a must to change the baseline transport distance of SCMs in Table 2 and recalculate the CR of SCMs to discuss the impact extent. Fig. 11 illustrates the variation in CR as SCMs transport distances increase under three different transportation modes. CR decreases linearly with transport distance, but the rate of decrease is minimal. For truck transportation, every 100 km increase in distance results in a reduction of approximately 0.45 % in CR, which indicates that the carbon emissions reduction achieved by using SCMs to lower cement consumption far outweighs the relatively small increase in emissions caused by the extended transport distance of SCMs. At a transport distance of 4166 km, the carbon reduction benefits of SCMs are entirely negated, and it becomes clear that transportation costs become prohibitive much earlier. Therefore, when considering only the total carbon emissions, the increase in emissions due to SCMs transport distance does not fully eliminate the low-carbon benefits of replacing cement with SCMs. Moreover, if alternative transportation methods, such as rail or shipping, are used over long distances,

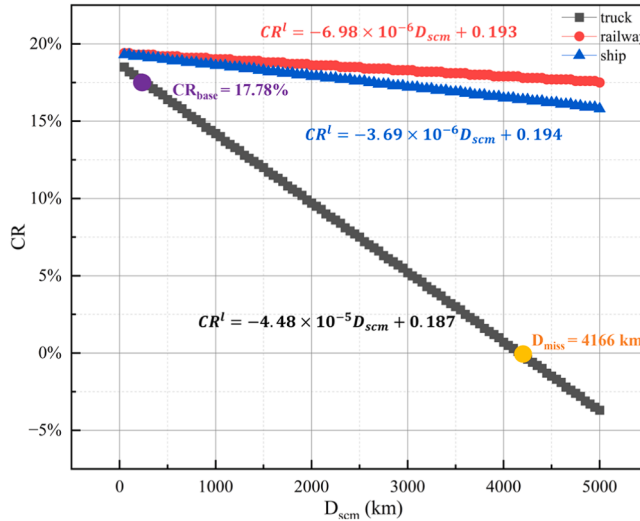


Fig. 11. Influence of SCMs transport distance on CR.

the carbon reduction rate can remain above 15 %.

Fig. 12 presents the carbon emissions under the four scenarios set as Table 3 shows. When the transport distance of NFA increases from 100 km to 500 km, E_{tran1} of NFA and the total emissions increase by $41.02 \text{ kgCO}_{2e}/\text{m}^3$ and $37.54 \text{ kgCO}_{2e}/\text{m}^3$ in C30 and C60 concrete. As the MS ratio rises from Scenario 2 to Scenario 4, the combined emissions from MS and FA decrease, demonstrating that the advantage of shorter transport distances for MS outweighs its higher production energy consumption. However, due to the reduction in concrete compressive strength caused by the use of MS, other components, particularly cement, are used in larger quantities in Scenarios 3 and 4, finally leading to similar total carbon emissions in Scenario 2–4. Similar patterns are observed in both C30 and C60 concrete. In fact, weak interfacial transition zones (ITZ) and compressive strength of MS tends to confer a reduction in concrete's mechanical properties [45]. As a result, using a high MS ratio does not currently offer obvious low-carbon benefits, but this conclusion could change in the future as energy consumption decreases and the performance of MS is optimized.

4. Conclusion

This study provides a detailed calculation of carbon emissions associated with C30-C80 ready-mixed concrete in China, using a large-scale dataset of mix proportions. The carbon emissions and their distribution across four life cycle stages were analyzed, and the carbon reduction benefits of SCMs were quantitatively assessed through the definition of CR^l . Additionally, the impact of transport distance was examined. The main conclusions are as follows:

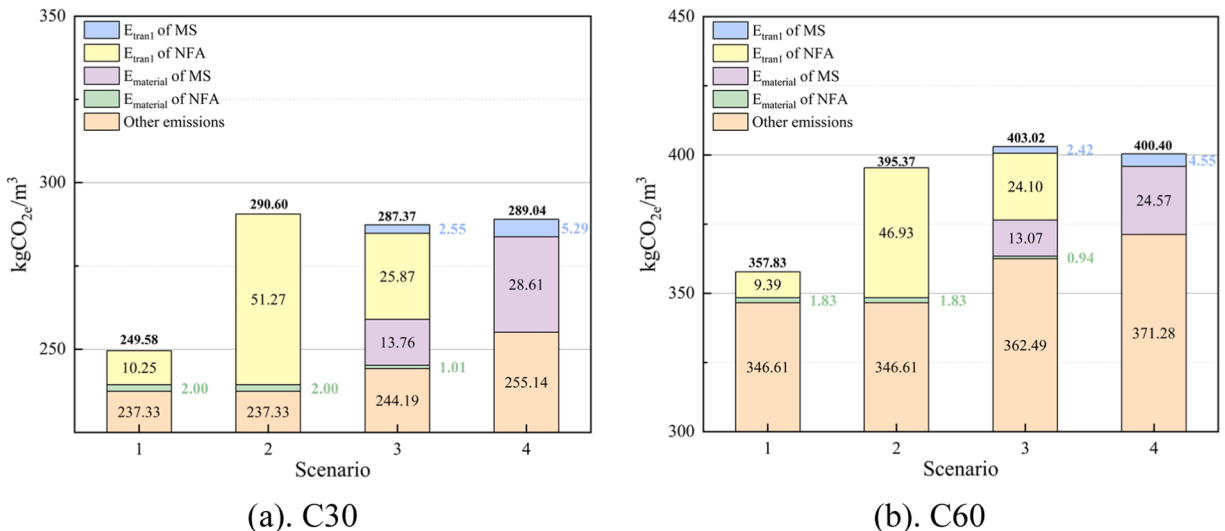


Fig. 12. Carbon emissions of ready-mixed concrete under 4 scenarios.

1. The carbon emissions of C30-C80 ready-mixed concrete ranged from 262.61 kgCO_{2e}/m³ to 401.78 kgCO_{2e}/m³. Embodied carbon from raw materials accounted for 86.4–90.5 % of the total emissions, with 89–93 % of this coming from the cement production process. Therefore, variations in cement dosage due to the incorporation of SCMs are the primary cause of the large standard deviation in carbon emissions at each strength level. The synergistic mechanism of SCMs and cement, as well as the changes in the use scenarios of ready-mixed concrete, explains the uneven growth of carbon emissions.
2. The CR^l values for SCMs in C30-C80 ready-mixed concrete range from 5 % to 30 %. While there is a positive correlation between the SCM substitution rate and CR^l, the degree of linear fit is very low. This indicates that CR^l cannot be directly calculated from the substitution rate alone, highlighting the importance of raw material quality and the rational use of SCMs.
3. The CR^l of SCMs is relatively insensitive to changes in transport distance. For truck transportation of SCMs, the CR only reaches zero when the transport distance exceeds 4166 km. Furthermore, if railway or shipping transport is used for distances up to 5000 km, the CR will not fall below 15 %.
4. When the transport distance for NFA increases from 100 km to 500 km, the carbon emissions of C30 and C60 ready-mixed concrete increase by approximately 16 % and 10 %. If the MS ratio is increased from 0 % to 50 % and 100 %, the advantage of shorter transport distances for MS can offset its higher production energy consumption, but total emissions remain almost unchanged, due to MS's deterioration of compressive strength.
5. There are still limitations to this study. Due to the high uncertainty of the performance of various raw materials in concrete, although some important indicators (e.g., the type of SCMs and the particle size range of MS) have been controlled, the differences in other raw materials between different mix proportions (e.g., the activity index of SCMs and the gradation of MS) are unavoidable. This study only discusses and summarizes the macroscopic laws from the perspective of market averages.

CRediT authorship contribution statement

Lyu Guangyao: Writing – review & editing, Validation, Supervision, Conceptualization. **Lin Zuojiang:** Methodology, Formal analysis. **Fang Kuizhen:** Writing – review & editing.

Declaration of Competing Interest

The authors declare that they have no known competing financial interests or personal relationships that could have appeared to influence the work reported in this paper.

Acknowledgements

Authors would like to acknowledge The National Key Research and Development Program of China (2023YFC3807200).

Appendix A. Supporting information

Supplementary data associated with this article can be found in the online version at [doi:10.1016/j.cscm.2025.e04287](https://doi.org/10.1016/j.cscm.2025.e04287).

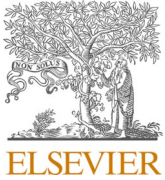
Data availability

The authors do not have permission to share data.

References

- [1] X.M. Ma, Y. Cai, *China's Low-Carbon Finance Development Report*, Peking University Press, 2014.
- [2] Yu Zhao, Tingwei Wang, Wen Yi, Energy-accounting-based comparison of carbon emissions of solid waste recycled concrete, *Constr. Build. Mater.* 387 (2023) 131674, <https://doi.org/10.1016/j.conbuildmat.2023.131674>.
- [3] The building materials carbon label and environmental label (EPD) project officially launches, *China Build. Mater.* 04 (2024) 35–36, <https://doi.org/10.16291/j.cnki.zgjc.2024.04.020>.
- [4] Dan Song, Jin Yang, Bin Chen, Tasawar Hayat, Ahmed Alsaedi, Life-cycle environmental impact analysis of a typical cement production chain, *Appl. Energy* 164 (2016) 916–923, <https://doi.org/10.1016/j.apenergy.2015.09.003>.
- [5] Louise K. Turner, Frank G. Collins, Carbon dioxide equivalent (CO₂-e) emissions: a comparison between geopolymers and OPC cement concrete, *Constr. Build. Mater.* 43 (2013) 125–130, <https://doi.org/10.1016/j.conbuildmat.2013.01.023>.
- [6] J. Thorne, D.V. Bompa, M.F. Funari, N. Garcia-Troncoso, Environmental impact evaluation of low-carbon concrete incorporating fly ash and limestone, *Clean. Mater.* 12 (2024) 100242, <https://doi.org/10.1016/j.clema.2024.100242>.
- [7] Peiliang Cong, Ruyan Du, Huanlin Gao, Zhihui Chen, Comparison and assessment of carbon dioxide emissions between alkali-activated materials and OPC cement concrete, *J. Traffic Transp. Eng. (Engl. Ed.)* 11 (2024) 918–938, <https://doi.org/10.1016/j.jtte.2023.07.011>.
- [8] Pablo Busch, Alissa Kendall, Colin W. Murphy, Sabbie A. Miller, Literature review on policies to mitigate GHG emissions for cement and concrete, *Resour., Conserv. Recycl.* 182 (2022) 106278, <https://doi.org/10.1016/j.resconrec.2022.106278>.
- [9] Kemal Celik, Cagla Meral, A. Petek Gursel, P.Kumar Mehta, Arpad Horvath, Paulo J.M. Monteiro, Mechanical properties, durability, and life-cycle assessment of self-consolidating concrete mixtures made with blended portland cements containing fly ash and limestone powder, *Cem. Concr. Compos.* 56 (2015) 59–72, <https://doi.org/10.1016/j.cemconcomp.2014.11.003>.

- [10] Jiabin Wang, Zhihao Che, Kaifeng Zhang, Yijie Fan, Ditao Niu, Xiao Guan, Performance of recycled aggregate concrete with supplementary cementitious materials (fly ash, GBFS, silica fume, and metakaolin): mechanical properties, pore structure, and water absorption, *Constr. Build. Mater.* 368 (2023) 130455, <https://doi.org/10.1016/j.conbuildmat.2023.130455>.
- [11] Yuanzhan Wang, Jing Liao, Zhen Liu, Service life prediction and environmental impact evaluation of recycled aggregate concrete with supplementary cementitious materials, *Constr. Build. Mater.* 395 (2023) 132270, <https://doi.org/10.1016/j.conbuildmat.2023.132270>.
- [12] Chengzhi Jiang, Wei Zhao, Laibo Li, Youmin Qin, Lingchao Lu, Influence of silica fume on pore structure, mechanical properties and carbon emission of reactive powder concrete prepared by ice crystal homogenization technology, *Case Stud. Constr. Mater.* 21 (2024) e03972, <https://doi.org/10.1016/j.cscm.2024.e03972>.
- [13] Md. Uzzal Hossain, Rongjin Cai, S.Thomas Ng, Dongxing Xuan, Hailong Ye, Sustainable natural pozzolana concrete – a comparative study on its environmental performance against concretes with other industrial by-products, *Constr. Build. Mater.* 270 (2021) 121429, <https://doi.org/10.1016/j.conbuildmat.2020.121429>.
- [14] David Sinkhonde, Tajebe Bezabih, On the computational evaluation of carbon dioxide emissions of concrete mixes incorporating waste materials: a strength-based approach, *Clean. Waste Syst.* 8 (2024) 100149, <https://doi.org/10.1016/j.clwas.2024.100149>.
- [15] Marian Sabau, Dan V. Bompă, Luis F.O. Silva, Comparative carbon emission assessments of recycled and natural aggregate concrete: environmental influence of cement content, *Geosci. Front.* 12 (2021) 101235, <https://doi.org/10.1016/j.gsf.2021.101235>.
- [16] M.A. DeRousseau, J.H. Arehart, J.R. Kasprzyk, W.V. Srubar, Statistical variation in the embodied carbon of concrete mixtures, *J. Clean. Prod.* 275 (2020) 123088, <https://doi.org/10.1016/j.jclepro.2020.123088>.
- [17] Y. Yu, F. Pacheco-Torgal, X.Y. Zhao, Wang, Cleaner production of the precast concrete industry: comparative life cycle analysis of concrete using recycled aggregates from crushed precast rejects, *Eur. J. Environ. Civ. Eng.* 28 (5) (2023) 1014–1038, <https://doi.org/10.1080/19648189.2023.2240828>.
- [18] Yong Yu, Guo-Hua Fang, Rawaz Kurda, Ashikur Rahman Sabuj, Xin-Yu Zhao, An agile, intelligent and scalable framework for mix design optimization of green concrete incorporating recycled aggregates from precast rejects, *Case Stud. Constr. Mater.* 20 (2024) e03156, <https://doi.org/10.1016/j.cscm.2024.e03156>.
- [19] Xiangchen Zhu, Yunsheng Zhang, Zhiyong Liu, Hongxia Qiao, Fukai Ye, Zhang Lei, Research on carbon emission reduction of manufactured sand concrete based on compressive strength, *Constr. Build. Mater.* 403 (2023) 133101, <https://doi.org/10.1016/j.conbuildmat.2023.133101>.
- [20] Minsheng Guan, Ruolin Yao, Junhua Wang, Xin Wang, Yong Li, Compressive behavior of manufactured sand recycled coarse aggregate concrete-filled steel tubular short columns, *Constr. Build. Mater.* 451 (2024) 138907, <https://doi.org/10.1016/j.conbuildmat.2024.138907>.
- [21] IPCC, *IPCC Guidelines for National Greenhouse Gas Inventories Prepared by the National Greenhouse Gas Inventories Program*, 2006, IGES, Tokyo, 2006.
- [22] Technical Committee ISO/TC 207. ISO 14040. Environmental management, Life cycle assessment. Principles and framework, International Organization for Standardization, Geneva, 2006.
- [23] Standardization Administration of the People's Republic of China, GB/T 51366-2019, Standard for Building Carbon Emission Calculation, 2019.
- [24] Xiamen Construction Bureau, DB3502/Z 5053-2019, Standard for Building Carbon Emission Accounting, 2019.
- [25] Dawei Pan, Wenduo Xue, Le Niú, Carbon emission reduction accounting of sand and gravel aggregate production from mining waste rock, *Ind. Miner. Process.* (2024) 1–11, <http://kns.cnki.net/kcms/detail/32.1492.TQ.20240627.1248.002.html>.
- [26] Matthew A. Jungclaus, Sarah L. Williams, Jay H. Arehart, Wil V. Srubar, Whole-life carbon emissions of concrete mixtures considering maximum CO₂ sequestration via carbonation, *Resour., Conserv. Recycl.* 206 (2024) 107605, <https://doi.org/10.1016/j.resconrec.2024.107605>.
- [27] Market Supervision and Administration Department of Ningxia Hui Autonomous Region, DB 64/T 1954-2023, Calculation method and evaluation standard of carbon emission from concrete, 2023.
- [28] Rui Zhong, Kay Wille, Roberto Viegas, Material efficiency in the design of UHPC paste from a life cycle point of view, *Constr. Build. Mater.* 160 (2018) 505–513, <https://doi.org/10.1016/j.conbuildmat.2017.11.049>.
- [29] Y.K. Kong, K. Kurumisawa, S.H. Chu, Infilled cementitious composites (ICC) – a comparative life cycle assessment with UHPC, *J. Clean. Prod.* 377 (2022) 134051, <https://doi.org/10.1016/j.jclepro.2022.134051>.
- [30] Standardization Administration of the People's Republic of China, GB/T 32151.8-2023, Requirements of the carbon emissions accounting and reporting-Part8: Cement enterprises, 2023.
- [31] Ministry of Housing and Urban-Rural Development of the People's Republic of China, JGJ 55-2011, Specification for mix proportion design of ordinary concrete, 2011.
- [32] Yuanshan Pan, Jian Gong, Kun Zhang, Calculation and analysis of carbon footprint of ready-mixed concrete based on LCA and research on carbon emission reduction technology, *N. Build. Mater.* 51 (2024) 145–149.
- [33] Tzu-Han Wen, Terry Y.P. Yuen, Victor K.S. Li, Albert T. Yeung, A case study on early-age cracking of high-strength concrete construction by coupled thermal-mechanical analysis and field monitoring, *Case Stud. Constr. Mater.* 21 (2024) e03436, <https://doi.org/10.1016/j.cscm.2024.e03436>.
- [34] Standardization Administration of the People's Republic of China, GB 36888-2018, The norm of energy consumption per unit product of ready-mixed concrete, 2018.
- [35] Bing Wu, Chao Ma, Meijin Gao, Carbon emission and economic evaluation of CO₂ mineralization ready-mixed concrete, *Clean. Coal Technol.* (2023) 1–9, <http://kns.cnki.net/kcms/detail/11.3676.TD.20230615.1409.002.html>.
- [36] Sufen Dong, Xinyue Wang, Huining Xu, Jialiang Wang, Baoguo Han, Incorporating super-fine stainless wires to control thermal cracking of concrete structures caused by heat of hydration, *Constr. Build. Mater.* 271 (2021) 121896, <https://doi.org/10.1016/j.conbuildmat.2020.121896>.
- [37] Fan Meng, Guoqiang Rong, Ruiji Zhao, Bo Chen, Xiaoyun Xu, Hao Qiu, Xinde Cao, Ling Zhao, Incorporating biochar into fuels system of iron and steel industry: carbon emission reduction potential and economic analysis, *Appl. Energy* 356 (2024) 122377, <https://doi.org/10.1016/j.apenergy.2023.122377>.
- [38] Mark Bediako, Luca Valentini, Strength performance and life cycle assessment of high-volume low-grade kaolin clay pozzolan concrete: a Ghanaian scenario, *Case Stud. Constr. Mater.* 17 (2022) e01679, <https://doi.org/10.1016/j.cscm.2022.e01679>.
- [39] Jiaqi Li, Wenxin Zhang, Chen Li, Paulo J.M. Monteiro, Green concrete containing diatomaceous earth and limestone: workability, mechanical properties, and life-cycle assessment, *J. Clean. Prod.* 223 (2019) 662–679, <https://doi.org/10.1016/j.jclepro.2019.03.077>.
- [40] Saber Fallah-Valukolaei, Reza Mousavi, Arash Arjomandi, Mahdi Nematzadeh, Mostafa Kazemi, A comparative study of mechanical properties and life cycle assessment of high-strength concrete containing silica fume and nanosilica as a partial cement replacement, *Structures* 46 (2022) 838–851, <https://doi.org/10.1016/j.istruc.2022.10.024>.
- [41] Prasanna Kumar Acharya, Sanjaya Kumar Patro, Evaluation of environmental disturbance indicator using functional performance and life cycle assessment of ferrochrome waste concrete, *J. Build. Eng.* 65 (2023) 105788, <https://doi.org/10.1016/j.jobe.2022.105788>.
- [42] G. Asadollahfardi, A. Katabi, P. Taherian, Panahandeh, Environmental life cycle assessment of concrete with different mixed designs, *Int. J. Constr. Manag.* 21 (2019) 665–676, <https://doi.org/10.1080/15623599.2019.1579015>.
- [43] S.T.A. Gillani, K. Hu, B. Ali, et al., Life cycle impact of concrete incorporating nylon waste and demolition waste, *Environ. Sci. Pollut. Res.* 30 (2023) 50269–50279, <https://doi.org/10.1007/s11356-023-25905-w>.
- [44] Josefina A. Olsson, Sabbie A. Miller, Joshua D. Kneifel, A review of current practice for life cycle assessment of cement and concrete, *Resour., Conserv. Recycl.* 26 (2024) 107619, <https://doi.org/10.1016/j.resconrec.2024.107619>.
- [45] Yong Yu, Yu Zheng, Xin-Yu Zhao, Mesoscale modeling of recycled aggregate concrete under uniaxial compression and tension using discrete element method, *Constr. Build. Mater.* 268 (2021) 121116, <https://doi.org/10.1016/j.conbuildmat.2020.121116>.



A comprehensive analysis of process-related CO₂ emissions from Iran's cement industry



Bahman Massoumi Nejad ^{a,*} , Sara Enferadi ^a, Robbie Andrew ^b

^a Asia West Cement (AWCC), Torbat-e-Jam, Razavi Khorasan, Iran

^b CICERO Center for International Climate Research, Oslo, 0349, Norway

ARTICLE INFO

Keywords:

Process-related CO₂ emissions
Iran's cement industry
Clinker-to-cement ratio
Supplementary cementitious materials (SCMs)
Climate change mitigation

ABSTRACT

Direct emissions from the cement industry account for 7%–8% of global anthropogenic CO₂ emissions, primarily from thermal decomposition of carbonates (i.e., calcination) during clinker production. Iran ranks among the world's top ten cement producers and is the seventh-largest CO₂ emitter globally. Despite its significant contribution to global emissions, Iran's process-related CO₂ emissions (i.e., chemically derived CO₂ from calcination) remain underreported in international datasets. This study addresses this gap by analyzing CO₂ emissions from carbonate decomposition in 77 Iranian cement plants from 2013 to 2023, highlighting regional and plant-specific emission factors. Utilizing plant-specific clinker data, the study applied methodologies aligned with the 2006 IPCC Guidelines and the WRI/WBCSD Greenhouse Gas Protocol to calculate emission factors and CO₂ emissions. The findings show notable geographical variations and a substantial national trend, with emissions rising from 28.75 million tonnes (Mt) in 2016 to 39.33 Mt in 2023. A primary contributor is Iran's high clinker-to-cement ratio, averaging 94.1% in 2023, underscoring the urgent need for sustainable production practices, particularly through the adoption of supplementary cementitious materials (SCMs) like pozzolans and industrial by-products. To address this, the study recommends a two-pronged policy approach: reducing clinker content in cement by promoting blended alternatives, such as Portland Composite Cement (PCC) and Portland Pozzolana Cement (PPC), through regulatory controls and economic incentives. These results emphasize the importance of targeted, data-driven policies for sustainable cement production, offering critical insights for stakeholders and policymakers aiming to align Iran's cement sector with global emissions reduction goals.

1. Introduction

Climate change, driven by rising CO₂ emissions, significantly threatens our planet. Mitigating climate change is crucial for humanity's future, involving both reducing CO₂ emissions and adapting to inevitable changes. While fossil fuels and land-use changes are well-known drivers of anthropogenic CO₂ emissions, the cement industry deserves particular attention as a significant contributor to releasing CO₂ from decomposing carbonates (Redlin et al., 2021). Globally, the cement industry contributes approximately 7–8% of total anthropogenic CO₂ emissions (Agency, 2018; Monteiro et al., 2017). These emissions vary significantly by region, driven by local production practices and raw material use.

The annual Global Carbon Budget (GCB) report (Budget, 2023), published by the Global Carbon Project, an international science team established to monitor progress towards international climate goals,

identifies Iran as a top-ten CO₂ emitter globally in 2022. While Iran trails major emitters like China and the United States, it has high emissions, ranking 7th globally, and contributing 1.86% of total emissions, with a per capita emission of 8.5 tonnes and annual emissions of 690.64 million tonnes (Mt) of CO₂ (Friedlingstein et al., 2023). This data highlights the urgent need for Iran to implement effective CO₂ reduction measures to tackle climate change and ensure a sustainable future.

Manufacturing one tonne of cement releases between 0.8 and 0.95 tonnes of CO₂ (Ali et al., 2019; Scrivener et al., 2018; Gartner et al., 2011). This variation depends on the clinker-to-cement ratio, fuel efficiency, fuel mix, electricity mix, and other factors (Gursel et al., 2014). Cement production results in CO₂ emissions from two aspects: direct and indirect sources. Directly, CO₂ is released from the chemical process of calcining CaCO₃ and MgCO₃, the combustion of fossil fuels for kiln heat generation, on-site power generation, and even wastewater treatment due to the carbon content. Indirect emissions come from the electricity

* Corresponding author.

E-mail address: Bahman.Massoumi@gmail.com (B. Massoumi Nejad).

consumed during external production, purchased clinker production and processing, as well as the production and transport of fuels and materials by third parties ((CSI) and W.C.S.I., 2011). Approximately 60% of CO₂ emissions in cement production, termed process-related CO₂ emissions, is attributed to the thermal decomposition of calcium carbonate in the calcination process (Cement, 2021), where limestone (primarily composed of CaCO₃) decomposes at high temperatures during pyroprocessing. This process contributes approximately 520 kg of CO₂ per tonne of clinker, which is the main constituent of cement. (CARB) and C.A.R.B., 2018).

In addition to calcination emissions, the remaining 40% of CO₂ emissions, termed energy-related CO₂ emissions, come from burning fuel for high temperatures and electricity use (100–120 kWh/tonne cement), both of which contribute significantly to overall CO₂ emissions (Cement, 2021). Electricity's share varies (1–10%) based on energy source and grid efficiency. Additionally, raw material extraction and transportation add about 5% to the industry's CO₂ footprint (Ali et al., 2019).

In global emissions inventories, these process-related and energy-related emissions are most often reported separately (Le Quéré, 2018; Eggleston et al., 2006). Our study focuses exclusively on CO₂ emissions from calcination, referred to as process-related CO₂ emissions, as fossil fuel and electricity emissions consumed during cement production are usually attributed to the energy sector in CO₂ inventories.

Studies by Andrew (2018a) indicate that process emissions from global cement production peaked in 2014 at around 1.5 GtCO₂, with a slight decline to 1.46 GtCO₂ by 2016. These emissions currently contribute roughly 4% to global CO₂ emissions from fossil sources. Cumulative emissions from 1928 to 2016 are estimated at 37.8 GtCO₂, with a significant increase (66%) occurring since 1990. Estimates for the years 2020, 2021, and 2022 show process emissions of 1.63 GtCO₂, 1.69 GtCO₂, and 1.61 GtCO₂ respectively (Friedlingstein et al., 2023).

Despite ranking sixth globally in cement production, Iran lacks comprehensive data on industry-specific CO₂ emissions. Some studies estimate these emissions using national cement-production data (e.g., GCB), but this method does not accurately reflect the nuances of Iran's

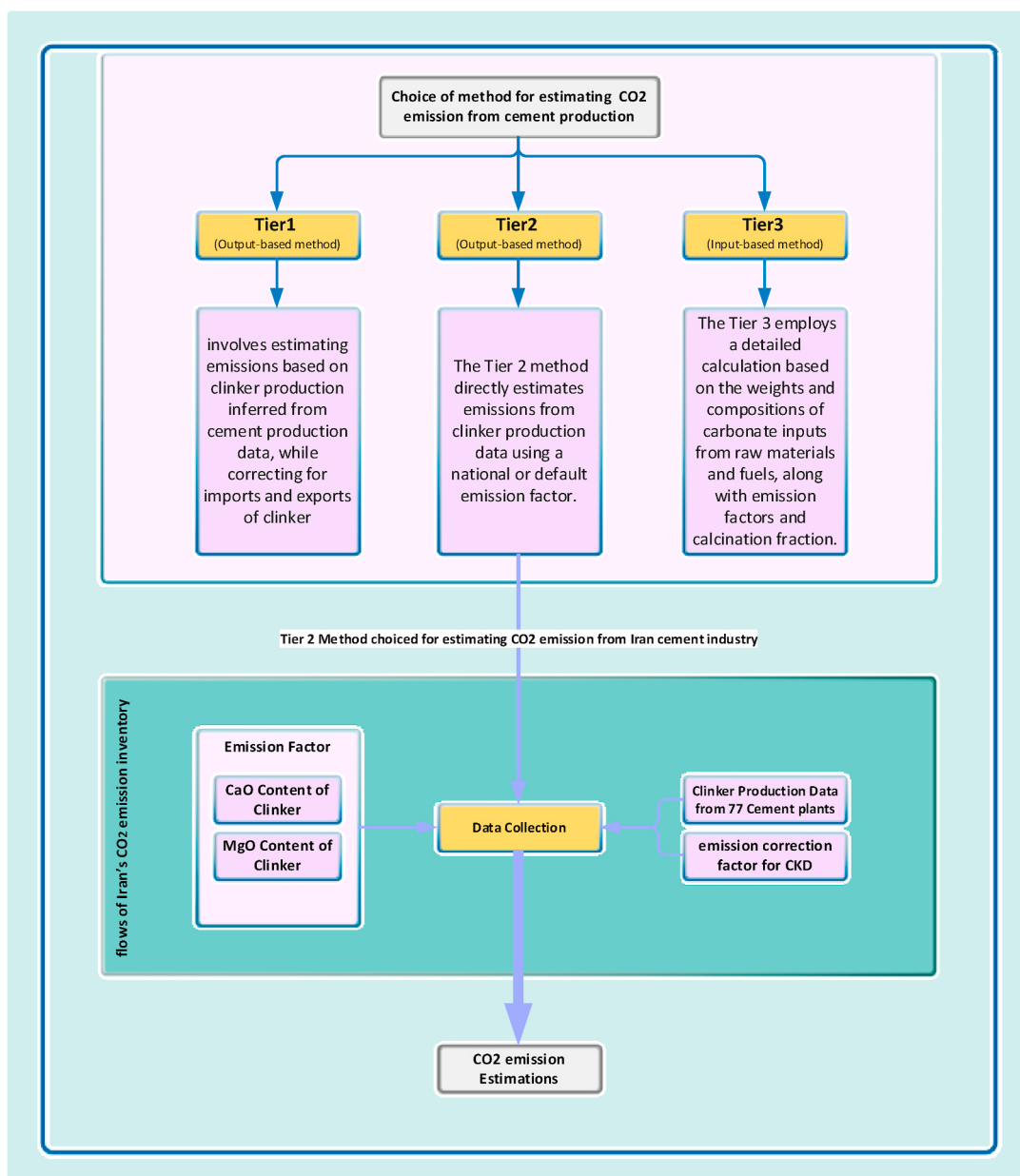


Fig. 1. Overview of the IPCC guideline method and choice of method for estimating CO₂ emission from cement production.

specific industry, partly due to international sanctions imposed that limit its representation in global datasets. These estimates often rely on regional averages and default clinker-to-cement ratios, which do not account for significant variations in production practices and raw material use across different plants in Iran. As a result, national emissions estimates based on these averages underestimate Iran's true CO₂ emissions.

Iran, one of the world's largest cement producers, has ranked among the top 10 countries in cement production in recent years ([Survey and U.S.G., 2023; Iran 8th Biggest Cement Producer, 2023](#)). In 2023, Iran produced 65 Mt of cement, making it the world's sixth-largest producer, according to a United States Geological Survey report ([Survey and U.S.G., 2024](#)). Global production decreased from 4.4 billion tonnes in 2021 to 4.1 billion in 2023.

The Iranian cement industry began in 1933 with a 100 t/day plant near Tehran by Danish company FLSmidth. Capacity grew to 9000 t/yr in 1937 and expanded further in the 1950s and 1960s. By the late 1970s, capacity reached 8 Mt/yr ([Written by Peter Edwards, 2017](#)). Post-revolution (1979), Iran's cement industry witnessed significant growth driven by population increase, post-war reconstruction, infrastructure needs, and low prices. Abundant resources like limestone, clay, silica, iron ore, and natural gas and fossil fuel, aided this expansion, production capacity surging 207% from 32 Mt in 2004 to 66.5 Mt in 2014. ([Fig. 1s in the SM](#)). Despite this impressive growth, a shortage of cement supply persisted until 2007. Since 2006, Domestic cement consumption in Iran has been consistently lower than production capacity. This overcapacity has been exacerbated by the stagnation in housing and construction projects, coupled with limited government planning. As a result, despite domestic consumption reaching 69.82 Mt in 2023, production capacity currently stands at a surplus of 89 Mt.

Iran is home to 77 cement plants ([Fig. 2s in the SM](#)) with a total production capacity of 89 Mt for cement and 86.5 Mt for clinker, crucial for domestic needs and export markets. However, this capacity lacks strategic distribution across the nation. The Iranian standard INSO 389 ([Organization and I.N.S., 2020](#)) categorizes OPC into five types: Type I, II, III, IV, and V. Additionally, INSO 17518-1 ([Organization and I.N.S., 2014](#)) defines 27 distinct types of common cements, including all blended cements such as Portland Pozzolana Cement (PPC) and Portland Composite Cement (PCC). Both align with international ASTM C150/C150M and EN 197-1:2011.

No studies have been reported on CO₂ emissions from cement

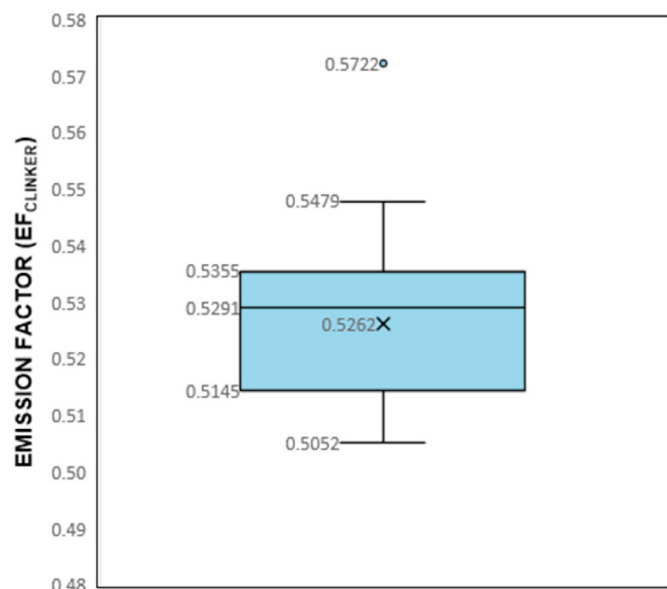


Fig. 2. Variation in emission factor (EF_{clinker}) of Clinker (T CO₂/T clinker) across Iranian cement plants (2023).

production in Iran. This study addresses this critical gap by quantifying process-related CO₂ emissions using actual clinker production data collected. This unique dataset provides a more accurate assessment and a scientific basis for analyzing Iran's emissions and developing effective CO₂ control measures. The primary objective is to quantify CO₂ emissions from the calcination process across 77 cement plants in Iran, utilizing clinker production data from 2013 to 2023.

The approach for this study involves calculating the Emission Factor (EF_{clinker}) using specific CaO and MgO data from individual cement plants. While several organizations provide default emission factors, these generic values do not accurately represent Iranian cement plants. The IPCC Tier 2 method suggests default emission factors to be used when country-specific clinker data is unavailable, with 65% CaO, assuming it's entirely from calcium carbonate, adjusted by a 2% correction factor for CKD. This results in a clinker emission factor of 0.52 tonnes CO₂ per tonne clinker ([Prepared by the National Greenhouse Gas Inventories Programme et al., 2006](#)). In contrast, China's emission factors, provided by the cement-based method by Emissions Database for Global Atmospheric Research (EDGAR), The Carbon Dioxide Information Analysis Center (CDIAC), and Carbon Emission Accounts and Datasets (CEADs) also vary considerably, ranging from 0.2906 to 0.499 tonnes CO₂ per tonne of cement ([Shen et al., 2014](#)), highlighting the variability and limitations of these generalized factors.

For Iran, relying solely on IPCC's default assumptions does not capture the unique production characteristics of Iranian cement plants. This study, therefore, emphasizes the importance of collecting CaO and MgO data at each facility to calculate emission factors independently, providing a more accurate basis for quantifying CO₂ emissions. This approach aligns with the principles of the Cement Sustainability Initiative (CSI) ([CSI and W.C.S.I., 2011](#)) and is critical for developing effective, localized emissions mitigation strategies.

Iran's cement industry is facing high CO₂ emissions, requiring sustainable mitigation strategies. Accelerated CO₂ emissions reduction strategies, supportive policies, public-private collaboration, and financing mechanisms are needed. This article focuses on Iran's opportunities for reducing emissions in cement production. Identifying the most effective strategy is crucial, as no study has yet highlighted the optimal approach. In the following sections, we aim to discuss Iran's potential pathways for emissions reduction in cement production.

2. Methods

2.1. Process-related CO₂ Emission calculation method

This study aims to quantify process-related CO₂ emissions from Iran's cement industry, focusing on plant-specific emission factors derived from clinker production data collected from 77 plants across 31 provinces. The scope of the study is limited to process-related emissions, excluding energy-related and indirect emissions. We employed methodologies aligned with the 2006 IPCC Guidelines ([Prepared by the National Greenhouse Gas Inventories Programme et al., 2006](#)), along with the WRI/WBCSD Greenhouse Gas Protocol ([CSI and W.C.S.I., 2011](#)). Furthermore, we utilized the Guidelines for Monitoring and Reporting of Greenhouse Gas Emissions (MRG) within the European Emission Trading System (EU ETS). These frameworks provide a comprehensive approach for accurately calculating process-related CO₂ emissions from cement production, particularly at the plant level.

Based on these procedures, there are two basic techniques used for estimating CO₂ emission at the plant level: the **input method**, which uses the quantity of CaCO₃ and MgCO₃ in the raw meal, and the **output method**, which relies on the quantity and composition of clinker produced, as well as any dust exiting the pyroprocessing system. Both methods are theoretically equivalent and are included in the 2006 IPCC Guidelines (Output Tier 1 and 2, Input Tier 3), WRI/WBCSD Greenhouse Gas Protocol (Input Methods (A1) and (A2), Output Methods (B1) and (B2)) and the MRG in the European Emission Trading System (EU ETS,

Input Method A, Output Method B). For this study, we predominantly employed the output method based on plant-specific clinker production data, due to its practicality and accuracy within the Iranian context.

The IPCC framework defines three tiers for estimating CO₂ emissions from cement production (Fig. 1). The Tier 1 method involves estimating emissions based on clinker production inferred from cement production data while correcting for imports and exports of clinker. The Tier 2 method directly estimates emissions from clinker production data using a national or default emission factor. Tier 3 employs a detailed calculation based on the weights and compositions of carbonate inputs from raw materials and fuels, along with emission factors and calcination fraction.

It is not suitable with good practice to calculate CO₂ emissions directly from cement production (i.e., using a fixed cement-based emission factor) by Tier 3 method. Alternatively, if national clinker production data and carbonate input data are unavailable, cement production data can be used to estimate clinker production by accounting for the types and quantities of cement produced, their clinker contents, and a correction for imports and exports of clinker. When estimating emissions from this source, it's crucial to take clinker imports and exports into consideration.

The Tier 3 method for reporting CO₂ emissions based on raw material inputs faces challenges in many cement plants due to the extensive inputs and continuous monitoring required for their chemical composition. The Cement Sustainability Initiative's (CSI) Task Force suggested alternative methods for input-based reporting, based on determining raw meal consumption in the kiln system, proving more practical than Tier 3 of the 2006 IPCC. However, obtaining precise raw meal data from all cement factories in Iran over the past decade was unfeasible, hindering the application of methods relying on measuring raw materials for calculating CO₂ emissions.

2.2. Data collection

Clinker production data and CaO and MgO content were collected from 77 cement plants across 31 provinces in Iran. These data were obtained from plant-specific reports and verified through laboratory analysis in collaboration with the Iran Cement Association. A key limitation of this methodology is the reliance on plant-reported data, which may vary in accuracy.

2.3. Emission factor calculation

Emission factors were calculated using Equation (1).

$$\text{CO}_2 \text{ Emissions} = M_{\text{clinker}} \times EF_{\text{clinker}} \times CF_{\text{ckd}} \quad (1)$$

CO₂ Emissions = emissions of CO₂ from cement production process, tonnes. M_{clinker} = weight of clinker produced, tonnes. EF_{clinker} = plant-specific emission factor of clinker (t CO₂/t clinker). CF_{ckd} = emissions factor for partially calcined cement kiln dust (CKD) leaving the kiln system, (t CO₂/t CKD) dimensionless.

According to the calcination reaction formula, the emission factor for clinker is determined by Eq. (2):

$$EF_{\text{clinker}} = \left(\text{CaO}_{\text{Clinker}} \times \frac{44}{54} \times R_{\text{CaCO}_3} \right) + \left(\text{MgO}_{\text{Clinker}} \times \frac{44}{40} \times R_{\text{MgCO}_3} \right) \quad (2)$$

where CaO_{Clinker} and MgO_{Clinker} represent the CaO and MgO content in the clinker, while R_{CaCO₃} and R_{MgCO₃} denote the CaO and MgO derived from calcium and magnesium carbonate. The typical CaO_{Clinker} and MgO_{Clinker} in Portland cement clinker are 65% and 1.8%, respectively (Shah et al., 2022). In countries like China, the R_{CaCO₃} is set at 95% due to the use of solid wastes such as carbide mud, fly ash, and steel slag as calcium sources (Shen et al., 2015). In contrast, in Iran, R_{CaCO₃} is considered 100% CaCO₃-derived, as solid wastes are not used as calcium sources in raw materials for clinker production during pyroprocessing,

resulting in no CO₂ emissions from these materials. While the circular economy approach, which involves using waste materials as resources, can offer significant benefits such as reduced emissions, waste management, and cost savings, it has not yet been implemented in Iran's cement industry. R_{MgCO₃} varies from 0 to 100% in each plant based on the magnesium mineralogy specific to that plant. Because MgO may also come from a non-carbonate source and is deliberately kept low in Portland cement, the true MgO from carbonate is likely to be very small. Using this equation, we estimate the emission factor of each cement plant separately.

CF_{ckd} (Cement Kiln Dust Correction Factor) is used in CO₂ emission calculations to consider emissions from cement kiln dust (CKD) not recycled back into the kiln system. In the Iranian cement sector, almost all CKD is recycled, leading to minimal CKD emissions. Hence, the CF_{ckd} value for Iran is usually set to one in Eq. (1) and It is assumed that 100 percent of the CKD is first captured.

This calculation follows the principle followed in the 'calcb2' of the Cement Sustainability Initiative (CSI) approach ((CSI) and C.S.I., 2013), stressing the need for plant-specific data to calculate emission factors accurately.

3. Results

3.1. Emission factor

This study analyzes emission factors for clinker production across all cement plants in 2023. Fig. 2 presents a box-and-whisker plot illustrating the distribution of emission factors, ranging from 0.5052 to 0.5722 t CO₂/t clinker, with an average of 0.5262 t CO₂/t clinker. The narrow interquartile range and low standard deviation (0.0126) indicate a high degree of consistency across the sector. However, variations exist, and our analysis reveals a correlation between emission factors and clinker MgO content. Plants with emission factors above the average, represented by the upper quartile, predominantly have higher MgO content, such as Shargh White Cement (0.5722 t CO₂/t clinker), Isfahan White (0.5479 t CO₂/t clinker), and Grey Shargh (0.5445 t CO₂/t clinker). While most plants exhibit emission factors close to the average, the 0.5722 t CO₂/t clinker data point associated with Shargh White Cement stands out as an outlier, notably higher than the rest of the data set. This higher emission factor attributed to specific characteristics of the raw materials used at this plant, particularly the high MgO content in the clinker. The presence of elevated MgO levels leading to an increase in CO₂ emissions. The average emission factor across the sector is 0.5262 t CO₂/t clinker, while the median is slightly higher at 0.5291 t CO₂/t clinker. This small difference between the average and the median suggests a relatively symmetric distribution of emission factors, with a slight tendency toward higher values in the dataset. However, the outlier at 0.5722 t CO₂/t clinker pulls the average slightly lower than the median, indicating that while most plants are near the central tendency, a few plants, such as Shargh White Cement, significantly deviate from this trend. In contrast, plants in the lower quartile, including Khash (0.5052 t CO₂/t clinker), Azar Abadgan Khoi (0.5078 t CO₂/t clinker), and Kavir Kashan (0.5085 t CO₂/t clinker), generally exhibit lower MgO and CaO contents, resulting in reduced emissions.

Fig. 3 presents the distribution of clinker emission factors across the Iranian cement plants studied. The histogram reveals a concentration of facilities (61 enterprises, representing 70.22%) with emission factors clustered within a narrow band of 0.51–0.54 t CO₂/t clinker. This observation suggests that alternative raw materials were not widely utilized in the Iranian cement industry during the study period. Iranian cement plants employ a limited set of raw materials (limestone, alluvium, marl, and iron ore) for clinker production. This homogeneity in raw materials likely contributes to the observed uniformity in emission factors.

From 2013 to 2023, we considered the emission factor content of each cement plant within each province and calculated the provincial

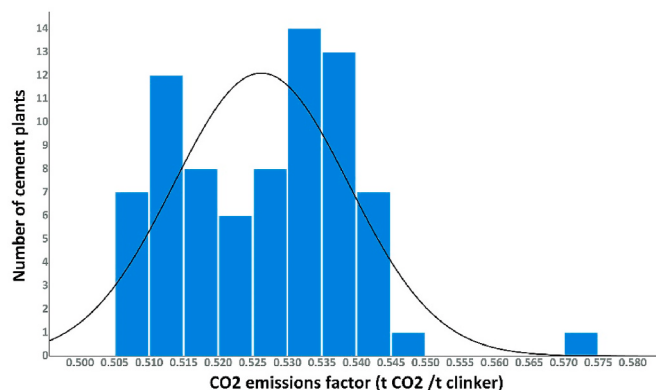


Fig. 3. Histogram of emission factor of all cement plants.

emission factor based on clinker production. The analysis revealed clinker emission factors ranging from 0.50962 to 0.53756 tonnes of CO₂ per tonne of clinker. In 2023, our study identified notable variations in emission factors among provinces. Razavi Khorasan (0.5376), Kohgiluyeh and Boyer-Ahmad (0.5372), and Bushehr (0.5359) exhibited the highest emission factors, while Qazvin (0.5096), West Azerbaijan (0.5103), and Yazd (0.5123) had the lowest figures. These results emphasize the importance of considering both plant-specific and provincial variations for accurate emissions assessment in the cement industry. The final provincial clinker emission factors are detailed in Table 1.

3.2. Process-related CO₂ emissions in Iran's cement industry

Fig. 4 illustrates the fluctuation in clinker production over the past

Table 1

Clinker emission factors of 31 provinces of Iran from 2013 to 2023 (tonne CO₂ per tonne clinker).

Province	2013	2015	2017	2019	2021	2023
Isfahan	0.5216	0.5219	0.5224	0.5228	0.5231	0.5257
West Azerbaijan	0.5093	0.5105	0.5096	0.5099	0.5107	0.5103
South Khorasan	0.5046	0.5060	0.5094	0.5112	0.5162	0.5174
Razavi Khorasan	0.5246	0.5239	0.5256	0.5285	0.5281	0.5376
North Khorasan	0.5343	0.5399	0.5378	0.5375	0.5306	0.5302
Khuzestan	0.5210	0.5213	0.5221	0.5212	0.5238	0.5251
Zanjan	0.5131	0.5300	0.5271	0.5228	0.5216	0.5213
Sistan and Baluchestan	0.5200	0.5130	0.5130	0.5132	0.5149	0.5180
Fars	0.5209	0.5222	0.5232	0.5216	0.5238	0.5239
Kerman	0.5111	0.5116	0.5135	0.0000	0.5133	0.5162
Kermanshah	0.5312	0.5325	0.5323	0.5335	0.5343	0.5313
Kohgiluyeh and Boyer-Ahmad	0.5393	0.5355	0.5392	0.5287	0.5371	0.5372
Markazi	0.5225	0.5218	0.5198	0.5230	0.5247	0.5267
Hormozgan	0.5128	0.5139	0.5160	0.5134	0.5141	0.5192
Hamedan	0.5248	0.5244	0.5292	0.5312	0.5292	0.5322
Yazd	0.5107	0.5123	0.5116	0.5123	0.5108	0.5123
Gilan	0.5349	0.5327	0.5331	0.5319	0.5311	0.5342
Lorestan	0.5228	0.5228	0.5230	0.5243	0.5244	0.5250
Tehran	0.5211	0.5231	0.5242	0.5256	0.5344	0.5301
East Azerbaijan	0.5325	0.5354	0.5404	0.5367	0.5385	0.5342
Semnan	0.5217	0.5225	0.5244	0.5260	0.5286	0.5313
Bushehr	0.5331	0.5323	0.5320	0.5332	0.5336	0.5359
Kurdistan	0.5146	0.5173	0.5165	0.5182	0.5208	0.5136
Ardabil	0.5322	0.5306	0.5305	0.5326	0.5308	0.5328
Qom	0.5153	0.5166	0.5153	0.5183	0.5186	0.5237
Ilam	0.5074	0.5088	0.5113	0.5108	0.5106	0.5127
Golestan	0.5200	0.5147	0.5087	0.5131	0.5143	0.5127
Chaharmahal and Bakhtiari	0.5364	0.5373	0.5361	0.5379	0.5356	0.5356
Mazandaran	0.5221	0.5245	0.5272	0.5270	0.5259	0.5277
Qazvin	0.5072	0.5072	0.5064	0.5087	0.5063	0.5096

decade, ranging from a low of 55.79 Mt in 2016 to a peak of 74.82 Mt in 2023. Correspondingly, Process-related CO₂ emissions rose from 28.75 Mt to 39.33 Mt during the same period. These results underscore the escalating environmental footprint of Iran's cement industry.

4. Discussion

4.1. Discrepancies between study findings and Global Carbon Budget (GCB) estimates

Our estimates for Iran's process-related CO₂ emissions differ significantly from those reported thus far by the Global Carbon Budget (GCB). The GCB, a key initiative of the Global Carbon Project (GCP), tracks global emissions and plays a vital role in monitoring progress towards the Paris Agreement's climate goals. This discrepancy arises from the limited availability of high-quality, granular data for Iran's cement industry. Due to international sanctions and the subsequent lack of collaboration with global institutions, Iran's cement production data is often underrepresented in international databases, such as the GCB. Consequently, the GCB relies on regional averages and default clinker-to-cement ratios for its CO₂ emissions estimates for Iran. These regional estimates may not accurately reflect Iran's specific production practices, raw material compositions, or technological differences. Our investigation reveals a substantial difference in estimated Process-related CO₂ emissions compared to the GCB data, indicating that the regional clinker ratio used by the GCB was too low for Iran's industry. This highlights the importance of incorporating industry-specific data for accurate CO₂ emission assessments and making such data more widely available. Fig. 5 compares our findings on process-related CO₂ emissions with estimates from the 2023 edition of the GCB (Andrew et al., 2023).

4.2. Cement plant analysis for process-related CO₂ emission and spatial distribution

Iran's cement industry demonstrates significant production capacity. In 2023, the top 4 largest cement production enterprises collectively produced 14.3 Mt of cement, representing 16.6% of the total national production. These top four producers were Abyek Cement (4.50 Mt), Tehran Cement (4.21 Mt), Sepahan Cement (3.08 Mt), and Khuzestan Cement (2.49 Mt).

Fig. 6 presents the cumulative emissions curve for the cement enterprises in our study. The enterprises were first ranked by their CO₂ emissions in descending order before calculating the cumulative percentage. The top 7 emitters contributed a significant share (22.8%) of the total emissions. This concentration is further emphasized by the finding that the top 34 emitters were responsible for a substantial 67.7% of the total Process-related CO₂ emissions.

Breaking down the distribution by emission magnitude, we observed a single enterprise (Tehran cement) emitting over 1.5 Mt of CO₂/yr, accounting for 4.2% of the total. Additionally, 6 enterprises emitted between 1.0 and 1.5 Mt, contributing 18.6% of the total emissions. Notably, 27 enterprises emitted between 0.5 Mt and 1.0 Mt, representing a moderate share (44.8%) of the total.

The data also reveals a significant presence of smaller facilities. We found 27 enterprises emitting between 0.2 Mt and 0.5 Mt, contributing 27.9% of the total emissions. Finally, 16 enterprises emitted less than 0.2 Mt, collectively responsible for only 4.4% of the total CO₂ emissions. Combining these observations (43 enterprises emitting less than 0.5 Mt, representing 32.3% of the total), on the data, it is clear that there are numerous small cement facilities still operational. A key point to consider is that these smaller facilities may lack advanced technology and resources to invest in modern solutions. With fewer facilities, transitioning to cleaner production methods and implementing modern technology for CO₂ reduction becomes more feasible.

Fig. 3s in the SM illustrates the spatial distribution of Iranian cement

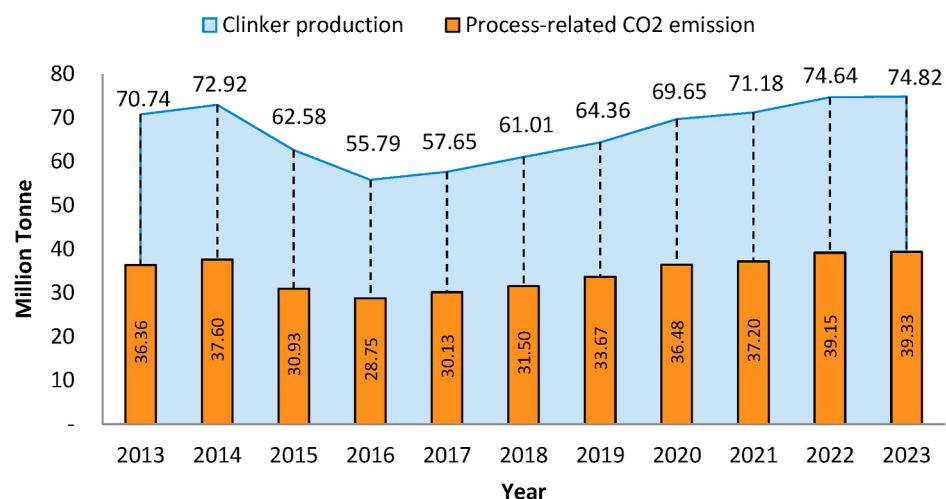


Fig. 4. Clinker production and process-related CO₂ emissions in the Iranian cement industry (2013–2023).

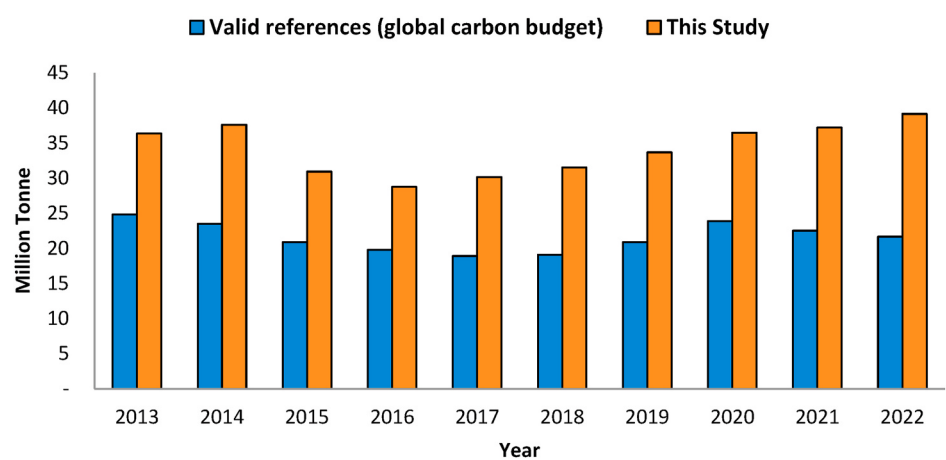


Fig. 5. Comparison of Process-Related CO₂ Emissions Estimates for Iran: Our Study vs. Global Carbon Budget (GCB).

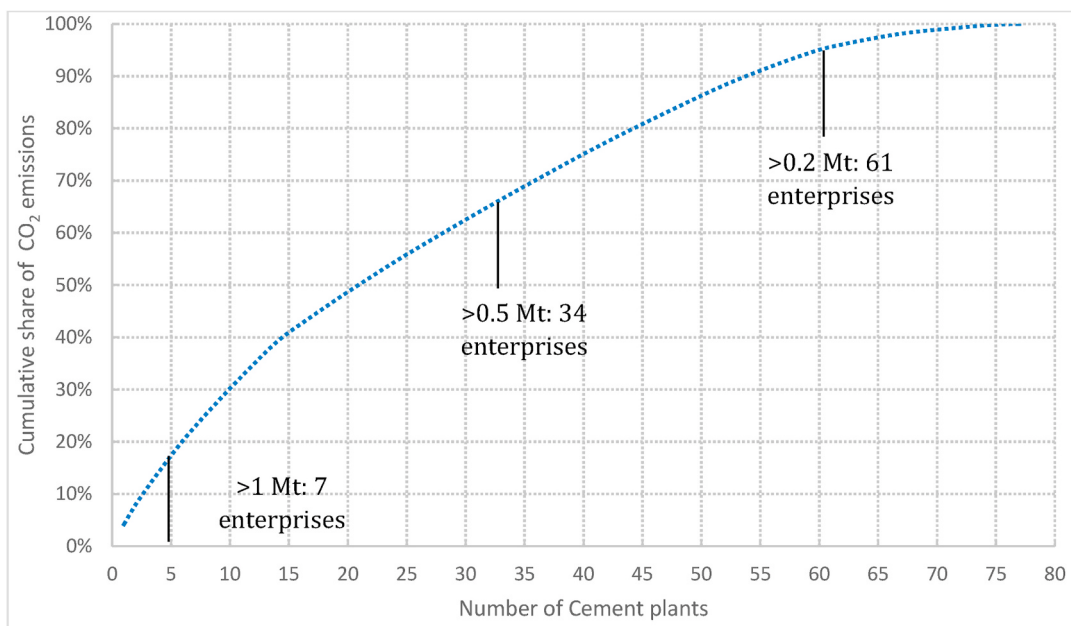


Fig. 6. the cumulative Process-related CO₂ emissions of Iranian cement factories, ranked from highest to lowest emitter (%).

facilities across the country, except the Dasht-e Lut desert, a sparsely populated region in the provinces of Kerman and Sistan-Baluchestan. Notably, major urban centers appear to influence facility size. Tehran, Qazvin, and Isfahan, all prominent Iranian cities, host larger production facilities, such as Tehran Cement (1.64 Mt CO₂ emissions, 4.2% of Iran's total CO₂ emissions in 2023) and Abyek Cement (3.8% of Iran's total CO₂ emissions in 2023). Sepahan Cement (3.2% of Iran's total CO₂ emissions in 2023) in Isfahan and Khuzestan Cement (3.1% of Iran's total CO₂ emissions in 2023) in Khuzestan province further exemplify this trend. Saveh Cement (3.0% of Iran's total CO₂ emissions in 2023) is another significant contributor. Collectively, these top facilities account for approximately 8% of Iran's total clinker production and a substantial share of the nation's CO₂ emissions in 2023.

We employed kernel density estimation to delve deeper into understanding the spatial distribution of Process-related CO₂ emissions from Iranian cement facilities (Fig. 7). This nonparametric method allows us to estimate the probability density function of CO₂ emissions across the country. By applying kernel density analysis to the CO₂ emissions data of each facility, we were able to calculate the magnitude of emissions per unit area. This analysis helped us identify hotspots – areas with particularly high concentrations of CO₂ emissions – and visualize the overall gradient, or gradual change, in emission levels across Iran's cement industry.

Fig. 7 reveals Tehran and Qazvin as the major hotspots of cement CO₂ emissions in Iran. These neighboring metropolises, with Tehran (239.4 t CO₂/km²) being the hottest, reflect the market radius of the cement industry. Their dominance stems from a combination of factors: economic development, population density, and proximity to consumers. Other notable hotspots include Bushehr (southwest) and Hamedan (west), with 88.5 and 76.9 t CO₂/km² emissions, respectively. Conversely, provinces with vast areas, like Kerman (southeast) and Sistan and Baluchestan (southwest), exhibit lower emissions per square kilometer (ranging from 5.7 to 7.7 t CO₂/km²).

4.3. A provincial look at process-related CO₂ emissions in Iran's cement industry and spatial distribution

Utilizing data on process-related CO₂ emissions from cement plants and their provincial locations, this study estimates provincial emissions from the Iranian cement industry. Fig. 8 visually depicts the distribution of emissions (in Mt) across different provinces over the past decade. Notably, the data shows significant variation in process carbon emissions in Mt between provinces.

Fig. 9 illustrates the current status of Process-related CO₂ emissions

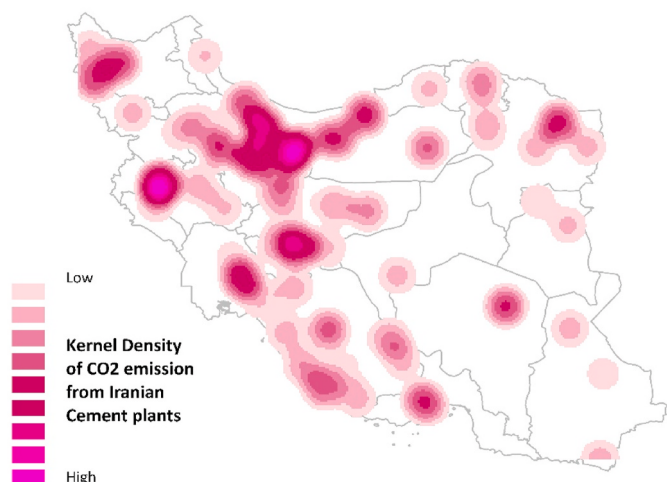


Fig. 7. Kernel density estimation of process-related CO₂ emissions from Iranian cement plants.

from the cement production process across various Iranian provinces in 2023. The data reveals that Isfahan, Tehran, Fars, and Khorasan Razavi provinces hold the highest levels of process-related CO₂ emissions, contributing 3.41 Mt CO₂, 3.11 Mt CO₂, 3.10 Mt CO₂, and 2.84 Mt CO₂, respectively. In contrast, Ardabil, Kurdistan, Lorestan, Golestan, and Qom provinces exhibit the lowest emission levels, all falling below 0.5 Mt CO₂. Specifically, these provinces contribute 0.41 Mt CO₂, 0.43 Mt CO₂, 0.44 Mt CO₂, 0.45 Mt CO₂, and 0.48 Mt CO₂, respectively. One province – Alborz – lacks cement plants and therefore has zero CO₂ emissions associated with cement production.

As illustrated in Fig. 10, a significant variation exists in the ratio of process CO₂ emissions to cement production across Iranian provinces over a decade. This ratio, also known as CO₂ emission intensity, highlights the amount of CO₂ emitted per unit of cement produced. The figure reveals substantial discrepancies between provinces.

Bushehr province stands out with the highest emission intensity throughout the decade. This can be attributed to several factors. Firstly, cement plants in Bushehr, like Dashtestan, Monde Dashti, and Saroog Bushehr, are major clinker exporters. Clinker requires less processing than cement and has a lower associated CO₂ emission per unit weight. Secondly, the domestic consumption of cement in Bushehr is lower than its clinker production capacity. This suggests that a significant portion of the produced clinker is exported without being converted into cement, potentially leading to a higher CO₂ emission intensity for the province's overall cement production.

While Bushehr held the top position for most of the decade, Lorestan province surpassed it in 2023 with the highest emission intensity (1.15 kg CO₂ per ton cement). In contrast, Khuzestan province consistently exhibits the lowest emission intensity throughout the period. This is likely because Khuzestan houses three major cement facilities (Karoon, Behbahan, and Khuzestan) that focus primarily on cement production for export. Since their clinker is entirely converted into cement for export, their CO₂ emissions are likely associated with the complete production cycle, resulting in a lower emission intensity per unit of cement produced.

4.4. Potential of lowering CO₂ emissions in the iranian cement sector

This section explores key pathways for CO₂ mitigation within Iran's cement industry, focusing on strategies with significant potential impact. These key strategic measures include Improving energy efficiency, switching to alternative fuels (less carbon-intensive fuels), reducing the clinker-to-cement ratio, and integrating carbon capture. Carbon capture and reducing clinker content hold the most potential for cutting CO₂ emissions in the cement industry by 2050, contributing 48% and 37% of the required reductions for a 2 °C warming scenario. The rest of the emissions cuts are switching to lower-carbon fuels and being more energy efficient (Agency, 2018).

One of the best ways to lower CO₂ emissions is to reduce clinker content by using material-based approaches such as SCMs. These materials may include natural pozzolan (e.g., volcanic fly ashes), artificial pozzolan (e.g., silica fume, low-calcium fly ash, metakaolin), and hydraulic materials (e.g., Ground Granulated Blast Furnace Slag (GGBFS), high-calcium fly ash) that can partially replace clinker in cement production (Pacewska et al., 2020). Utilizing SCMs alongside clinker reduction offers several advantages: lower CO₂ footprint due to reduced clinker content, enhanced performance with improved concrete strength, durability, and resistance to environmental factors, and improved workability of fresh concrete.

Research by Shah et al. (2022) report that using SCMs can significantly reduce greenhouse gas (GHG) emissions in cement production, with potential global reductions of up to 44% through maximized SCMs utilization. Blended cements like PPC and PCC, which incorporate SCMs and have lower clinker-to-cement ratios, offer a pathway for significantly reducing CO₂ emissions (Prakasan et al., 2020). Although several countries have already implemented SCMs and lower clinker ratios, Iran

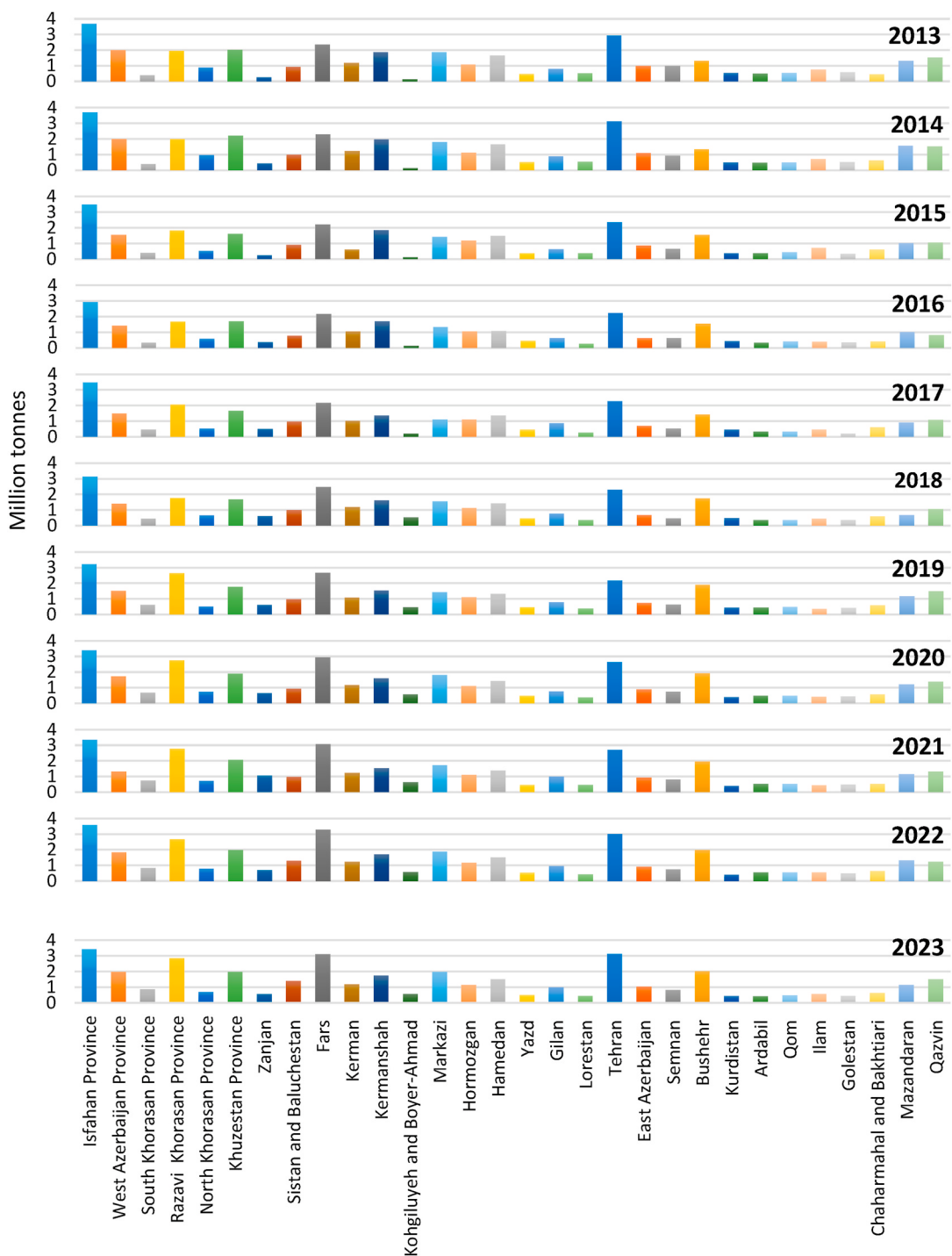


Fig. 8. Process-related CO₂ emissions distribution (Mt) across Iranian provinces (2013–2023).

has substantial potential to increase its use of these strategies.

Iran is situated in a region with diverse geology and rich in inorganic material. The area is abundant in volcanic rocks naturally possessing pozzolan properties (Sobhani et al., 2020; AR, 2007; Stöcklin, 1974) and also rich in pure limestone and blast furnace slag from iron production (particularly in Isfahan, Shiraz, Kerman and Zanjan), which can be used to produce PPC and PCC. Ramezanianpour et al. (Ramezanianpour, 2014) studied the use of SCMs and blended cement in concrete worldwide, especially in Iran. Using these alternative cement types presents a promising approach to mitigating carbon emissions by reducing the clinker content of Cement. By focusing on domestic resources of SCMs in Iran like high quality pozzolan and GGBFS and lime stone for PPC and

PCC production, Iran can significantly reduce its CO₂ footprint and reduce energy consumption and costs from the cement sector.

Reducing the clinker-to-cement ratio is a crucial strategy for lowering the CO₂ footprint in cement production, particularly relevant to Iran's reliance on clinker-heavy Ordinary Portland Cement (OPC).

Building on research by Andrew (2018b), who estimated the global clinker-to-cement ratio using emissions and cement production data, this study reveals a decline in the average ratio from 0.83 in 1990 to 0.66 in 2016. This decline aligns with the International Energy Agency's estimate of 0.65 for 2014. However, recent data suggests the ratio might be rising again (over 0.7) due to policy changes in some countries, like China phasing out lower-quality cements.

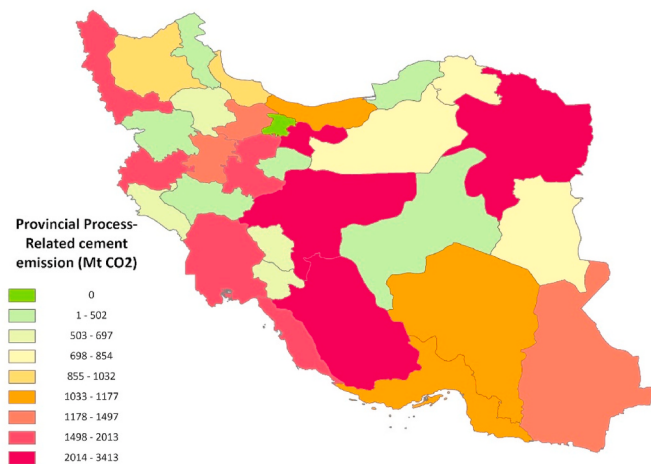


Fig. 9. Provincial process emissions of process-related CO₂ from Iranian cement production (Mt, 2023).

According to the International Energy Agency (IEA) (IEA et al., 2023), global cement production's clinker-to-cement ratio varied roughly between 0.7 and 0.71 from 2018 to 2022. This shift is projected to achieve a global clinker-to-cement ratio of 0.68 by 2050 and 0.61 in 2070, leading to a 35% emissions reduction related to material efficiency and 14% total emissions reductions in the cement industry due to lowering the clinker-to-cement ratio (IEA, 2020). However, the availability of these materials declines in the Sustainable Development Scenario, leading to a greater reliance on alternatives like limestone and calcined clay.

While Iran lacks comprehensive data on its clinker-to-cement ratio, estimates for 2023 place it at a high 94.1%, based on clinker production, exports, and cement production data. This contrasts with the Middle Eastern average of 81% reported by the World Business Council for Sustainable Development's Getting the Numbers Right (GNR) initiative (Development and W.B.C.f.S., 2016). However, this figure may be skewed due to its reliance on survey responses (covering only 15% of regional production) and potential bias from responding countries.

OPC, heavily reliant on clinker (typically exceeding 90%), dominated the Iranian cement market in 2023, accounting for approximately 95.5% of the total production and sales data collected from the Iranian Cement Association (ICA), The Ministry of Industry, Mine and Trade (MIMT), and the Iran Mercantile Exchange (IME). This dominance suggests a high clinker content in Iranian cement production. Production of PPC and PCC followed, representing 2.75% and 1.96% of the market share, respectively. Fig. 4s in the SM provides a detailed breakdown of these figures. High OPC production in Iran suggests a likely high clinker factor in the cement industry.

Blended cements like PPC and PCC, which incorporate SCMs and rely on lower clinker content, offer substantial environmental benefits over OPC, given the minimal or even negligible carbon footprint of some substitutes. By increasing the production and use of PPC and PCC, the Iranian cement industry can significantly reduce its CO₂ emissions.

4.5. Limitations of the current study and prospects for future investigations

While this study provides a comprehensive analysis of process-related CO₂ emissions in Iran's cement industry, it is important to recognize some of its limitations. The focus is exclusively on emissions from clinker production, without considering energy-related or indirect emissions, which significantly contribute to the overall environmental impact of the industry. Incorporating these additional factors could offer a more complete understanding of the sector's CO₂ emissions profile.

Over 70% of Iran's energy portfolio is dependent on gas, from

households to industries and power plants. The cement industry primarily depends on natural gas as its main energy source due to its relative abundance. However, during winter, increased domestic demand for gas leads to shortages, forcing cement plants to switch to substitute fuels such as fuel oil. This shift not only raises pollution emissions but also presents logistical and regulatory challenges, particularly due to restrictions imposed by the Ministry of Oil.

Future research should aim to assess energy-related emissions comprehensively, exploring the effects of fuel switching, improving energy efficiency, and integrating renewable energy sources. Such an approach would provide a more holistic view of the industry's carbon footprint and identify viable strategies for reducing energy-related emissions.

A key avenue for further investigation is conducting a Life Cycle Assessment (LCA) of cement production in Iran. Expanding the analysis to encompass energy-related emissions, transportation, raw material extraction, and end-of-life disposal would yield a more thorough evaluation of the industry's environmental impact. Preliminary LCAs on select Iranian cement plants suggest that blended cements such as Portland Pozzolana Cement (PPC) and Portland Composite Cement (PCC) offer significant CO₂ reductions compared to Ordinary Portland Cement (OPC). Future research should include a comparative LCA of OPC, PPC, and PCC to quantify potential CO₂ savings, accounting for both process and energy-related emissions. This comprehensive approach would generate more accurate data, facilitating the development of effective low-carbon cement strategies.

5. Conclusion

This study has offered a thorough analysis of process-related CO₂ emissions within Iran's cement sector, highlighting critical geographical and plant-specific variations. The findings underscore that the industry's high clinker-to-cement ratio, averaging 94.1% in 2023, is a significant contributor to these emissions. This highlights an urgent need for reform in cement production practices, with a particular focus on reducing the clinker content and promoting the use of SCMs such as pozzolans and industrial by-products. These SCMs provide a promising pathway not only for reducing CO₂ emissions but also for enhancing the durability and performance of cement products.

The localized approach of this study has proven effective, offering more accurate and actionable insights compared to broader national estimates. This localized data can serve as a crucial foundation for implementing targeted CO₂ reduction strategies, tailored to the unique conditions of each region and plant in Iran. The study also emphasizes the importance of data-driven decision-making in addressing climate change challenges, advocating for more granular data collection to improve the precision of emissions assessments.

To achieve meaningful reductions in CO₂ emissions, both policymakers and industry stakeholders need to collaborate on strategies that promote lower-emission alternatives, such as blended cements like PPC and PCC. A two-pronged policy approach is recommended to address this environmental challenge.

Firstly, it is crucial to encourage the production and use of alternative cements with lower clinker content, such as PPC and PCC. Implementing stricter emission regulations or limitations on OPC production quotas could drive this shift. Additionally, offering tax breaks or subsidies for PPC and PCC production would enhance their economic competitiveness compared to OPC.

Secondly, leveraging the current government-controlled pricing system presents an opportunity to incentivize consumer adoption of lower-emission alternatives. Setting lower prices for blended cements like PPC and PCC compared to OPC would directly influence consumer choices and promote the use of more sustainable options.

By implementing these combined policy measures, Iran's cement industry can significantly reduce its CO₂ emissions and contribute to global efforts in combating climate change. This transition towards

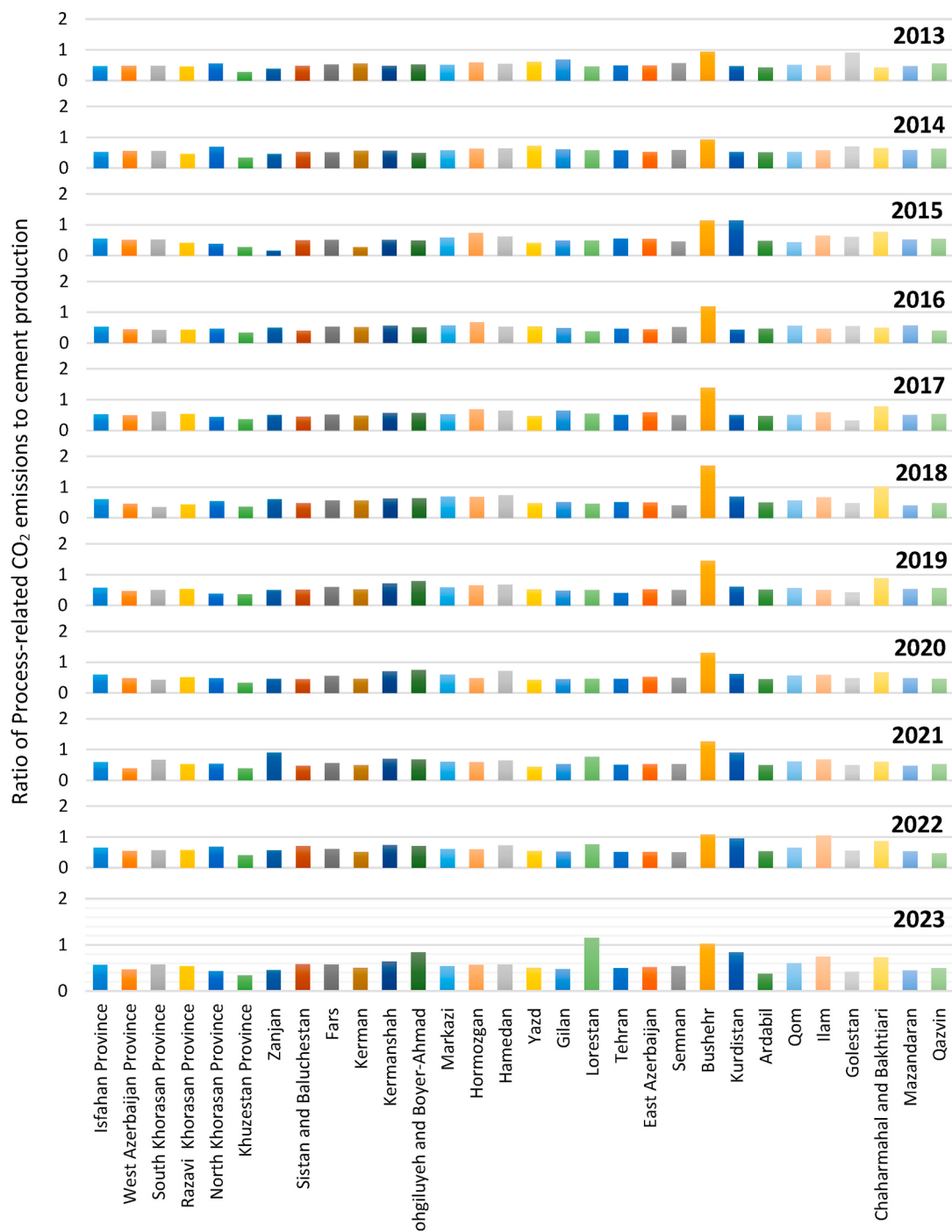


Fig. 10. Process-related CO₂ emissions per ton of cement produced in Iranian provinces (2013–2023).

lower-emission cement not only benefits the environment but also promotes long-term sustainability for Iran's construction sector.

CRediT authorship contribution statement

Bahman Massoumi Nejad: Writing – original draft, Software, Resources, Project administration, Methodology, Investigation, Funding acquisition, Formal analysis, Data curation, Conceptualization. **Sara Enferadi:** Writing – review & editing, Writing – original draft. **Robbie Andrew:** Supervision.

Declaration of generative AI and AI-assisted technologies in the writing process

While preparing this work the author(s) used **Gemini** and also **ChatGPT** to improve language and readability. After using this tool/service, the author(s) reviewed and edited the content as needed and take(s) full responsibility for the publication's content.

Declaration of competing interest

The authors declare that they have no known competing financial interests or personal relationships that could have appeared to influence

the work reported in this paper.

Appendix A. Supplementary data

Supplementary data to this article can be found online at <https://doi.org/10.1016/j.cesys.2024.100251>.

Data availability

Data will be made available on request.

References

- Agency, I.E., 2018. Technology Roadmap - Low-Carbon Transition in the Cement Industry. International Energy Agency, Paris.
- Ali, Hasanbeigi, Cecilia Springer, G.E.C.I., 2019. CALIFORNIA'S CEMENT INDUSTRY, FAILING THE CLIMATE CHALLENGE. Global Eciency Intelligence, San Francisco, CA.
- Andrew, R.M., 2018a. Global CO₂ emissions from cement production. *Earth Syst. Sci. Data* 10 (1), 195–217.
- Andrew, R.M., 2018b. Global CO₂ emissions from cement production. *Earth Syst. Sci. Data* 10 (1), 195–217.
- Andrew, R.M., Peters, G.P., 2023. The Global Carbon Project's Fossil CO₂ Emissions Dataset, 2023v36. Zenodo.
- Ar, B., 2007. Pozzolan: application in cement industry and distribution in Iran. *Journal of Mining Engineering Society of Iran* (In Persian).
- Budget, G.C., available at: : <https://globalcarbonbudgetdata.org/>. 2023, (Global Carbon Budget).
- (CARB), C.A.R.B., 2018. Staff Report - Initial Statement of Reasons for Rulemaking - Portland Cement Manufacturing.
- Cement, G., 2021. Concrete Future: the GCCA 2050 Cement and Concrete Industry Roadmap for Net Zero Concrete. GCCA, London, UK.
- (CSI), C.S.I., 2013. Cement Sustainability Initiative (CSI). "CSI_ProtocolV3.1 _09December2013." Cement sustainability Initiative. URL: http://www.cement-co-2-protocol.org/en/Content/Resources/Downloads/CSI_ProtocolV3_1_09December2013.xls.
- (CSI), W.C.S.I., 2011. CO₂ and Energy Accounting and Reporting Standard for the Cement Industry. World Business Council for Sustainable Development.
- Development, W.B.C.F.S., 2016. Cement Industry Energy and CO₂ Performance: Getting the Numbers Right (GNR). W.B.C.F.S. Development. URL: <https://docs.wbcsd.org/2016/12/GNR.pdf>.
- Eggleslon, H., et al., 2006. 2006 IPCC Guidelines for National Greenhouse Gas Inventories.
- Friedlingstein, P., et al., 2023. Global carbon budget 2023. *Earth Syst. Sci. Data* 15 (12), 5301–5369.
- Gartner, E.M., Macphee, D.E., 2011. A physico-chemical basis for novel cementitious binders. *Cement Concr. Res.* 41 (7), 736–749.
- Gursel, A.P., et al., 2014. Life-cycle inventory analysis of concrete production: a critical review. *Cement Concr. Compos.* 51, 38–48.
- IEA, 2020. Energy Technology Perspectives 2020. IEA, Paris. <https://www.iea.org/reports/energy-technology-perspectives-2020>. Licence: CC BY 4.0. IEA (2020); Paris.
- (IEA), T.I.E.A., IEA, 2023. CO₂ emitted and captured in the cement sector and clinker-to-cement ratio in the Net Zero Scenario, 2015–2030, available at : [https://www.iea.org/data-and-statistics/charts/co2-emitted-and-captured-in-the-cement-sector-and-clinker-to-cement-ratio-in-the-netzero-scenario-2015-2030_2023](https://www.iea.org/data-and-statistics/charts/co2-emitted-and-captured-in-the-cement-sector-and-clinker-to-cement-ratio-in-the-net-zero-scenario-2015-2030_2023).
- Iran 8th Biggest Cement Producer in 2022, 2023. USGS. Available from: <https://financialtribune.com/node/117585>
- Le Quéré, C., et al., 2018. Global carbon budget 2018. *Earth Syst. Sci. Data* 10 (4), 2141–2194.
- Monteiro, P.J., Miller, S.A., Horvath, A., 2017. Towards sustainable concrete. *Nat. Mater.* 16 (7), 698–699.
- Organization, I.N.S., 2014. INSO 17518-1 — cement - Part 1: specifications. In: Iranian National Standardization Organization: Islamic Republic of Iran, 1st.Edition, p. 35.
- Organization, I.N.S., 2020. INSO 389 Portland cement — specifications. Iranian National Standardization Organization: Islamic Republic of Iran.
- Pacewska, B., Wilińska, I., 2020. Usage of supplementary cementitious materials: advantages and limitations: Part I. C-S-H, C-A-S-H and other products formed in different binding mixtures. *Journal of Thermal Analysis and Calorimetry* 142 (1), 371–393.
- Prakasan, S., Palaniappan, S., Gettu, R., 2020. Study of energy use and CO₂ emissions in the manufacturing of clinker and cement. *J. Inst. Eng.: Series A* 101, 221–232.
- Prepared by the National Greenhouse Gas Inventories Programme, E.H.S., 2006. Chapter 2: mineral industry emissions. In: Buendia, L., Miwa, K., Ngara, T., Tanabe, K. (Eds.), Industrial Processes and Product Use, vol. 3. Published by the Institute for Global Environmental Strategies (IGES), Hayama, Japan on behalf of the IPCC Japan.
- Ramezaniapour, A.A., 2014. Cement Replacement Materials, vol. 10. Springer geochemistry/mineralogy, p. 978, 3.
- Redlin, M., Gries, T., 2021. Anthropogenic climate change: the impact of the global carbon budget. *Theor. Appl. Climatol.* 146 (1), 713–721.
- Scrimmer, K.L., John, V.M., Gartner, E.M., 2018. Eco-efficient cements: potential economically viable solutions for a low-CO₂ cement-based materials industry. *Cement Concr. Res.* 114, 2–26.
- Shah, I.H., et al., 2022. Cement substitution with secondary materials can reduce annual global CO₂ emissions by up to 1.3 gigatons. *Nat. Commun.* 13 (1), 5758.
- Shen, L., et al., 2014. Factory-level measurements on CO₂ emission factors of cement production in China. *Renew. Sustain. Energy Rev.* 34, 337–349.
- Shen, W., et al., 2015. Quantifying CO₂ emissions from China's cement industry. *Renew. Sustain. Energy Rev.* 50, 1004–1012.
- Sobhani, J., Pourkhorshidi, A.R., Masoudi, F., 2020. Iranian eocene green tuffs as natural pozzolan for use in cement industries. *Journal of Civil Engineering and Materials Application* 4 (3), 133–140.
- Stöcklin, J., 1974. Northern Iran: Alborz mountains. Geological Society, London, Special Publications 4 (1), 213–234.
- Survey, U.S.G., 2023. Cement. In: Mineral Commodity Summaries. U.S. Geological Survey, U.S.A.
- Survey, U.S.G., 2024. Cement. In: Mineral Commodity Summaries. U.S. Geological Survey.
- Written by Peter Edwards, G.C.M., 2017. The Cement Sector of Iran. *Global Cement Magazine*.

Article

The Environmental Profile of Clinker, Cement, and Concrete: A Life Cycle Perspective Study Based on Ecuadorian Data

Daniel M. Petroche  and Angel D. Ramirez  *

Facultad de Ingeniería en Mecánica y Ciencias de la Producción, Escuela Superior Politécnica del Litoral, ESPOL, Campus Gustavo Galindo, Km. 30.5 Vía Perimetral, Guayaquil P.O. Box 09-01-5863, Ecuador; dpetroch@espol.edu.ec

* Correspondence: aramire@espol.edu.ec; Tel.: +593-042-269-351; Fax: +593-042-852-804

Abstract: Concrete is the most-used material in the construction industry, and the second most-used after water. Cement is the main component of concrete. A total of 8% of global CO₂ emissions correspond to the cement industry; CO₂ is the main greenhouse gas contributing to global warming. To mitigate climate change, it is necessary to design buildings with a lower environmental impact, and therefore, it is crucial to assess the environmental profile of the local production of construction materials. This study uses the life cycle assessment methodological framework to evaluate the environmental sustainability of the cement and concrete industry in Ecuador. The inventory accounts for 62.8% of national cement production, with data corresponding to 2019. The OpenLCA software was used to perform the life cycle inventory and impact assessment calculations. Eight impact categories were assessed, including Global Warming Potential (GWP). Clinker has a GWP result of 897.04 kg CO₂-Eq/ton. Hydraulic cement types MH, GU, and HE have GWPs ranging from 465.89 to 696.81 kg CO₂-Eq/ton. Results of ready-mixed concrete range from 126.02 to 442.14 kg CO₂-Eq/m³. Reducing the content of clinker in cement and concrete should be the aim so as to improve their environmental profiles. This study contributes to the development of regional life cycle inventory data for Latin America. This research is the first to be developed regarding construction materials in Ecuador and contributes to the sustainable design of structures with pozzolan-lime cement and concrete.

Keywords: LCA; carbon footprint; cement; concrete; clinker



Citation: Petroche, D.M.; Ramirez, A.D. The Environmental Profile of Clinker, Cement, and Concrete: A Life Cycle Perspective Study Based on Ecuadorian Data. *Buildings* **2022**, *12*, 311. <https://doi.org/10.3390/buildings12030311>

Academic Editors: João Gomes Ferreira and Ana Isabel Marques

Received: 28 January 2022

Accepted: 2 March 2022

Published: 6 March 2022

Publisher's Note: MDPI stays neutral with regard to jurisdictional claims in published maps and institutional affiliations.



Copyright: © 2022 by the authors. Licensee MDPI, Basel, Switzerland. This article is an open access article distributed under the terms and conditions of the Creative Commons Attribution (CC BY) license (<https://creativecommons.org/licenses/by/4.0/>).

1. Introduction

World population growth is expected to increase by 22% by 2050, from 7.6 to 9.7 billion people [1], leading to migration, urbanization, and the construction of cities [2]. As a result, the consumption of raw materials and greenhouse gas (GHG) emissions will increase. In 2015, the United Nations Member States approved 17 Sustainable Development Goals (SDGs) as part of the 2030 Agenda [3]. The understanding of the key trends in urbanization likely to unfold over the coming years is critical for the SDGs' implementation, with a particular focus on SDG 9: build resilient infrastructure, promote inclusive and sustainable industrialization, and foster innovation; SDG 11: make cities and human settlements inclusive, safe, resilient, and sustainable; and SDG 13: take urgent action to combat climate change and its impacts [4].

Climate change has been a constant topic of debate, which is why the environmental impacts of industries are more perceived, and it has led to the introduction of legislation and incentives to regulate and reduce GHG emissions [5,6]. Reducing the emission of GHG from the construction sector is of the utmost importance. Thus, it is necessary to quantify GHG emission throughout its value chain [5].

Construction is one of the main economic sectors, contributing significantly to the increase of the gross domestic product of different countries [7]. The construction industry

is a dynamic sector in economic growth due to increased investments in infrastructure, construction, energy, and transport. It is one of the most important sectors in Latin America, mainly due to its ability to generate jobs. In Ecuador, it represents 7.5% of the total suitable jobs for 2019 [8]. This activity is transversal to other strategic sectors, such as agriculture, industry, commerce, and services since they require buildings to develop their activities.

Cement is one of the most commercialized materials worldwide [9]. It is estimated that global cement consumption was 4.08 billion tons in 2019 [10]. Its use is essential in the manufacture of concrete, the construction phase, and the maintenance of buildings [5,11]. From 5 to 8% of global CO₂ emissions correspond to the cement industry [12–14] due to the calcination of limestone and the combustion of fossil fuels. Additionally, a large electricity supply is required for the limestone-, clinker-, and cement-crushing processes. Cement production consumes 7% of the global industrial energy [15]. Cement production also causes other environmental impacts in addition to GHG emissions [16]; for example, nitrogen oxides (NO_x) and volatile organic compounds (VOC) are generated that can produce photochemical ozone formation in the air. This, in contact with people, causes health problems [17] and affects ecosystems [18]. Nitrogen oxides (NO_x), ammonia (NH₃), and sulfur dioxide (SO₂) exposed in high concentrations to the soil cause acidification, which would cause problems in the growth and development of vegetation [19,20].

According to FICEM (2020), cement production in Ecuador for the year 2019 was 6030 thousand metric tons [21]. Cement production in the coastal zone of Ecuador has a production capacity of 5.4 million metric tons. The coastal zone, the north, and the center-south contribute 62.8%, 18.6%, and 18.6% of the volume of Ecuadorian cement, respectively [22]. Ecuador is the country in Latin America with the highest consumption per capita with 355 kg cement per capita, followed by Mexico and Peru with 343 and 333 kg cement per capita, respectively (adapted from FICEM, 2020). Orienting the construction industry in Ecuador towards sustainability is a significant challenge to include in national agendas, and determining the environmental performance of the raw material of this sector is the first step.

Concrete is a widely used material in construction, and it is composed mainly of cement, crushed stone, sand, and water. The combination, proportion, number of components, and additions of these raw materials will result in the final properties of the concrete [23,24]. The versatility in its manufacture, that can be on-site or ready-mixed, the ease of being molded into different shapes and sizes, combined with its mechanical properties, durability, chemical inertness, thermal energy storage, and cost make it an essential material in the construction sector [25–27]. It is the most-consumed material after water [28]; 30 billion tons of concrete are used every year, 3 times more than 40 years ago on a per capita basis [29]. This extensive use makes evaluating and analyzing its environmental impacts essential, considering concrete production and its impact on climate change [30]. In Ecuador, 86% of the structures built in 2019 were made of reinforced concrete, with a lesser proportion of metallic structures at 11%, and wood and others occupying 3% [31]. In recent infrastructure projects built in Ecuador, 29% of the total cost corresponds to concrete structures [32].

Life cycle assessment (LCA) is a tool that allows obtaining quantitative results when evaluating the environmental performance of a service or product in each of the stages of its life cycle [33]. Given the growing interest of government groups in the environmental impacts of the industry [34], LCA has been widely used for the generation of environmental product declarations (EPDs), particularly in the manufacture of materials [35]. In the last decade, the analysis of the environmental impacts of the cement industry has increased [16]. In Europe, LCAs for clinker production have been developed [36–38]; these results serve as input for the preparation of Portland cement (PC) or added cement. Some studies analyze ordinary Portland cement (OPC) as the main product, as well as the process and composition alternatives [36,38–41]. In Asia, OPC and proposals for environmental improvement measures are analyzed; others compare the environmental performance between cements [9,42–44]. In Latin America, there are fewer studies on the environmental

performance of cement using LCA. In Peru, the GWP of the cement industry and the partial replacement of clinker with other additions, such as pozzolan, slag, and calcareous filler, has been studied using LCA methodology in bags of cement (42.5 kg) from 3 different plants, having results between 24–32 kg CO₂-Eq/cement bag (42.5 kg); adapting this result to tons, it is 564–752 kg CO₂-Eq/ton of cement [45]. Regarding ready-mixed concrete (RMX), studies from Europe and Asia have analyzed conventional concrete and concrete environmental improvements by adding waste, recycled components, using fly ash, slag, or combining these options [46–49], resulting in GWP reductions between 1 and 23% in similar, characteristic, compressive strength. For North America, South America, and South Africa, life cycle inventories [50–52] and LCA [53,54] for conventional concrete with characteristic compressive strengths produced results between 20 and 50 MPa.

Constructing structures for the development of human activities is a need; making it sustainable is a challenge for different stakeholders, such as the public and private sectors and academia. It is necessary to measure the environmental impact in the construction sector with tools such as LCA. There is no quantitative environmental performance information regarding the main construction material used in Ecuador. Therefore, it is essential to develop life cycle inventories of the main raw materials, those being clinker, cement, and ready-mixed concrete. This information will allow the calculation of the environmental performance of buildings and construction projects that will serve as a baseline for optimizing and reducing the environmental impact of construction. This study aims to quantify the environmental performance of clinker, cement, and ready-mixed concrete using the LCA methodological framework to identify hotspots in the studied systems.

2. Materials and Methods

2.1. Life Cycle Assessment

Life cycle assessment (LCA) is based on the guidelines of ISO 14040–14044, which describes four steps for its development: Goal and scope definition, Inventory analysis, Impact assessment, and Interpretation [55]. A life cycle includes stages such as the extraction of raw materials, production, product components and the product itself, use, and recycling or final disposal. It is important to note that it is not necessary to prepare an LCA with all the stages of the life cycle; it can be adjusted to the needs of the project. The life cycle inventory analysis is a compilation of all the environmentally relevant input and output of the system, which are obtained or adapted from primary and secondary data. All the input and output is quantified according to the functional unit. The impact assessment phase includes the use of characterization models, which include emissions and resource use factors that are used to transform the environmentally relevant input and output into the life cycle environmental impact indicator results. The use of LCA has been very useful in evaluating the performance of materials and energy in a system, the variations of the levels of environmental efficiency between processes, and generating baselines for future eco-efficient improvements [56].

Although LCA is the main tool to evaluate the environmental profile of product and services, including GHG emissions and carbon footprint, some authors have used some approaches that are not explicitly labeled as life cycle tools. Similarly, these tools quantify the GHG emissions with a focus on the product or service. Park et al. [57], in their study of metakaolin composite concrete, use emission factors adapted from Long et al. [58] for the calculation of CO₂ emissions, energy, and resource consumption [57,58]. Similarly, authors such as Ghalehnovi et al. [59] and Shamsabadi et al. [60] use a global warming index derived from Lippiatt [61], based on the GWP of each material and its weight.

Other authors have used an index, the Building Material Sustainability Potential (BMSP), which relates the structural performance, service life, and the environmental impact to describe the sustainability of a building material [62–64]. It should be noted that the GWP have been used as the descriptor of environmental performance, and that in LCA, the performance and service life of a building material should be expressed in the functional unit.

2.2. Scope

The study includes the extraction and processing of virgin raw materials; the processing of raw materials; the transportation of raw materials to the manufacturer; and the manufacturing of clinker, cement, and ready-mixed concrete. Three systems are studied: clinker, cement, and concrete (Figure 1). Primary data for all the systems is for the year 2019. The functional units are 1 ton of clinker, 1 ton of type GU (general use) cement, 1 ton of type HE (high early strength) cement, 1 ton of type MH (moderate heat of hydration) cement, under ASTM C1157 [65], and 1 m³ of ready-mixed concrete (RMX) with characteristic compressive strengths between 2.5 and 80 MPa.

The systems studied for clinker and cement accounted for 62.8% of the cement used in Ecuador in 2019. The clinker, cement, and concrete systems have cradle-to-gate approaches. Technical system boundaries for clinker include extraction and transport of raw materials, fuels, rotary kiln, and cooling. Technical system boundaries for cement include the clinker system, additional raw materials, and cement manufacturing. The technical system boundaries for concrete include the cement system, aggregate production, transport to the concrete plant, concrete production, and recycling.

2.3. Life Cycle Inventory Analysis

2.3.1. Primary Data Collection

Material and energy inputs to produce clinker, cement, and concrete were obtained from plants' sustainability reports. Access was provided to the data of the registering system of raw materials consumption, fuels, and electricity use in each phase of the three systems. Monthly emission data for CO₂, NO_x, SO₂, PM, and VOCs was obtained from the continuous emission-monitoring system of each clinker kiln. Pollutant emissions such as ammonia, antimony, arsenic, benzene, cadmium, hydrogen chloride, cobalt, copper, chromium, dioxins, mercury, carbon monoxide, nickel, lead, thallium, and vanadium were obtained from the biannual measurement reports of each clinker kiln. Reports on the consumption of oils, heavy machinery, and maintenance equipment were obtained from logistics records. The average production of the last five years was used, and a life span of 50 years was used to include the construction of the production plants.

2.3.2. Secondary Data

The main components of the clinker production process are limestone, clay, and other mineral correctors. Life cycle inventory datasets for those were taken from ecoinvent 3.7.1 [66], considering the transport from each factory (see Table S1 in Supplementary Materials). In the cement production process, the raw materials, such as limestone and gypsum, were taken from ecoinvent 3.7.1 (see Table S2 in Supplementary Materials).

In the concrete manufacturing process, production of the tap water available for Peru (PE) and diesel for Colombia (CO) are used due to their geographical proximity, crushed stone, sand, and admixtures were used from global processes (see Table S3 in Supplementary Materials) available in ecoinvent 3.7.1 [66].

The electricity process was created by Ramirez et al. [67,68], who carry out a life cycle assessment covering all types of power plants available in the country, taking the national energy balance of 2018. Regarding diesel from Ecuador, the physical properties used for the calculation: density of 850 kg/m³ and a heat capacity of 40.8 MJ/kg, available in reports from the Ministry of Energy and Non-Renewable Natural Resources [69].

2.4. Life Cycle Impact Assessment

The impact analysis method used is ReCiPe Midpoint (H) V1.13 [70]. The following impact categories are considered: global warming potential (GWP100), terrestrial acidification potential (TAP100), freshwater eutrophication potential (FEP), marine eutrophication potential (MEP), ozone depletion potential (ODPinf), photochemical oxidant formation potential (POFP), particulate matter formation potential (PMFP), and fossil depletion potential (FDP). It should be noted that the GWP category indicator results are often called "carbon footprint."

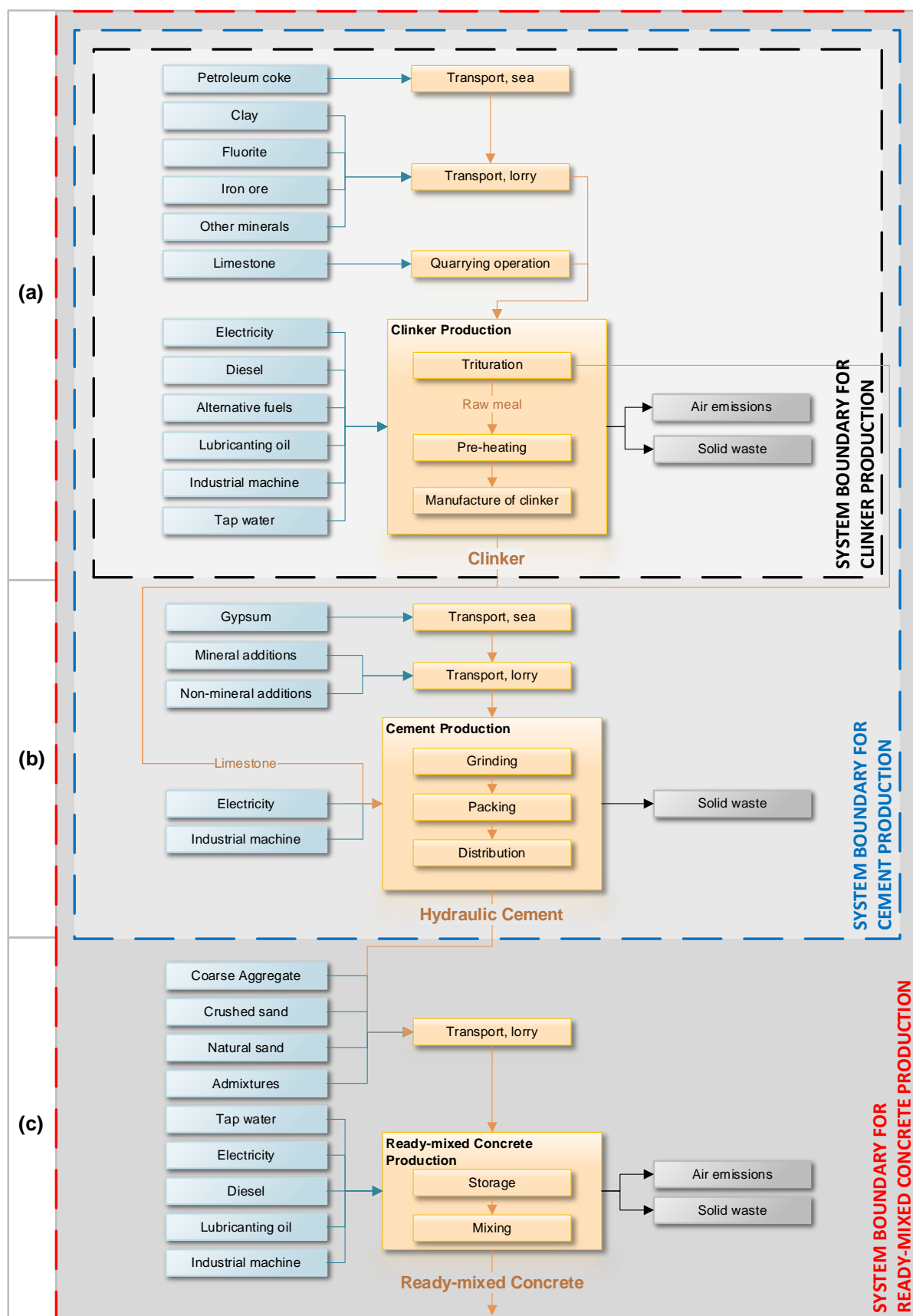


Figure 1. Cradle-to-gate system boundaries for the production of clinker, cement, and concrete in Ecuador: (a) clinker production, (b) cement production, and (c) ready-mixed concrete production.

Calculation

The software used for the life cycle inventory and impact assessment calculations is OpenLCA 1.10.3, GreenDelta, Berlin, Germany [71].

3. Results and Discussion

3.1. Life Cycle Inventory

In the production of clinker, 86% of the total raw materials are composed of limestone (the most used material). Four types of clays are used, which come from different parts of Ecuador; these clays represent 11% by mass, and other raw materials of mineral correction represent 3% (see Table S4 in Supplementary Materials).

The process that consumes the greatest amount of electricity is the manufacture of clinker, followed by the crude material mills. Using the heat capacity of fuels, petroleum coke and diesel represent 91.1% of thermal energy and 8.9% of alternative fuels. The clinker and cement manufacturing processes do not consume water as a raw material. The life cycle inventory for compound hydraulic cements from Ecuador is not presented because of a confidentiality agreement with the companies analyzed in this study.

In regard to ready-mix concrete, the city with the highest consumption is Guayaquil, with 38.1%, followed by Quito with 30.8%; other cities, such as Cuenca, Machala, Ambato, and Manta, represent 10.2%, 8.4%, 6.5%, and 6%, respectively. Conventional concretes (18–40 MPa) are the most-used in the construction industry in Ecuador, with 88% of the total studied, while high compressive strength concretes (≥ 40 MPa), 6.5%, and low compressive strength concretes (≤ 18 MPa), 5.5%. (Life cycle inventory is presented in Table S5 in Supplementary Materials).

The most-used concrete has a compressive strength of 28 MPa, representing 22.5% of national production. This concrete is typical in the construction of elements such as columns, beams, and building foundations. The second most-used concrete has a compressive strength of 21 MPa, with 20.1%, and is commonly used in slabs.

3.2. Life Cycle Impact Assessment

3.2.1. Clinker

The different stages of clinker production are classified and compared. Figure 2 shows the contribution result in the selected impact categories. Table 1 shows the environmental impact category indicator results for clinker.

Table 1. Result of life cycle assessment impact categories for 1 ton of clinker.

Impact Categories	Unit	This Study	Literature Reviewed
Global Warming Potential—GWP100	kg CO ₂ -Eq	897.04	850–929 ¹
Terrestrial Acidification Potential—TAP100	kg SO ₂ -Eq	1.52	8.41 ²
Freshwater Eutrophication Potential—FEP	kg P-Eq	0.42×10^{-2}	1.21×10^{-2} ³
Marine Eutrophication Potential—MEP	kg N-Eq	0.08	—
Ozone Depletion Potential—ODPinf	kg CFC ⁻¹¹ -Eq	4.51×10^{-5}	—
Photochemical Oxidant Formation Potential—POFP	kg NMVOC-Eq	2.08	1.24 ³
Particulate Matter Formation Potential—PMFP	kg PM10-Eq	0.65	—
Fossil Depletion Potential—FDP	kg oil-Eq	86.48	—

¹ [36,37,40]; ² [40]; ³ [41].

Regarding GWP100, the manufacture of clinker is the process with the highest contribution of GWP, with 842.69 kg CO₂-Eq/ton of clinker; this represents 93.9% of this indicator. This is due to the CO₂ generated in the clinker kiln by the combustion of petroleum coke and the release of CO₂ in the chemical process of the change of calcium carbonate (CaCO₃)

into calcium oxide (CaO) [72]. The production of petroleum coke is the second process with the highest contribution to GWP, resulting in 30.21 kg CO₂/ton of clinker and a share of 3.37%. Electricity supply contributes 1.19% to the GWP because 82% of the electricity mix in Ecuador in 2018 was hydropower [67]. In the literature, GWP results range between 850 and 929 kg CO₂-Eq/ton of clinker [36,37,40]; this study has a GWP result of 897.04 kg CO₂-Eq/ton of clinker, which is within the range found in the literature.

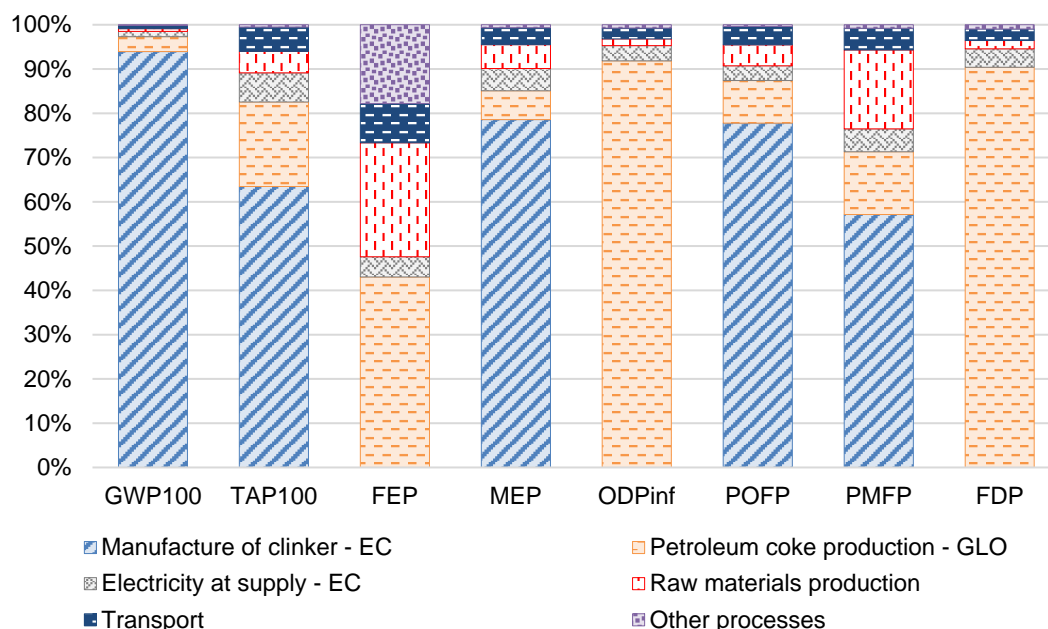


Figure 2. Contribution analysis for each environmental impact category for processes per ton of clinker (functional unit). GWP100: global warming potential; TAP100: terrestrial acidification potential; FEP: freshwater eutrophication potential; MEP: marine eutrophication potential; ODPinf: ozone depletion potential; POFP: photochemical oxidant formation potential; PMFP: particulate matter formation potential; FDP: fossil depletion potential; EC: Ecuador; and GLO: global.

Nitrogen oxides (NO_x), sulfur dioxide (SO₂), and ammonia (NH₃) are the main emissions contributing to TAP100, which are present in the flue gases from clinker kilns. This process contributes 0.964 kg SO₂-Eq/ton of clinker, corresponding to 63.5% of the indicator. The production of petroleum coke contributes 0.29 kg SO₂-Eq/ton of clinker, representing 19.25% of this category; the result is 1.52 kg SO₂-Eq/ton of clinker. Çankaya & Pekey [40] obtained results of terrestrial acid/nutri in 8.41 SO₂-Eq/ton of clinker for a traditional scenario, and 6.75 SO₂-Eq/ton of clinker for an alternative scenario, clinkering contributes 75%, raw materials, 13%; and electricity, 6.5%. Most of the difference between Çankaya & Pekey [40] and this study is due to the composition of fossil fuels (such as petroleum coke, lignite, fuel oil, and natural gas) and the use of alternative fuels.

The results of FEP for this study are lower than García-Gusano et al. [41], with 0.42×10^{-2} kg and 1.21×10^{-2} P-Eq/ton of clinker, respectively. Figure 2 shows that the process with the greatest contribution is the manufacture of petroleum coke, with 43.04%, and electricity, 4.55% of the total FEP. García-Gusano et al. [41] found that the fossil fuel combustion and electricity consumed entail 40% and 37%, respectively. These differences are mostly due to the electricity mix and the efficiency of electrical consumption; this study has 71.24 kWh/t of clinker, and the Spanish industry has 92 kWh/t of clinker in 2010. Regarding MEP, the result obtained for Ecuador is 0.08 kg N-Eq/ton of clinker. The clinker production process contributes 78.6% to the MEP results due to the NO_x emitted during clinkering.

The result for ODPinf is 4.51×10^{-5} kg CFC-11-Eq/ton of clinker, and for FDP, it is 86.48 kg oil-Eq/ton of clinker. The dominant process in ODPinf is producing petroleum

coke, and it is also dominant for the impact category FDP. Regarding POFP, the most contributing process is clinkering, with 77.8%, due to the VOC in the gases emitted from the clinker kiln. García-Gusano et al. (2015a) obtained as a result 1.24 kg NMVOC-Eq/ton of clinker [41], a value close to the result of this study: 2.08 kg NMVOC-Eq/ton of clinker. The result for PMFP, 0.65 kg PM10-Eq/ton of clinker, is due to primary aerosols, such as PM, and secondary aerosols, such as SO_2 , NH_3 , and NO_x , present in the flue gases from clinkering.

3.2.2. Cement

This study presents the environmental performance of the three most-sold types of cement in Ecuador. Type GU cement is the one with the highest consumption. The carbon footprint of cement in Ecuador ranges from 465.89 to 696.81 kg CO₂-Eq/ton (Table 2). The results for type GU were 545.78 kg CO₂-Eq/ton of cement. The GWP range for ordinary Portland cement ranges from 632 to 950 kg CO₂-Eq/ton of cement, according to the literature [36–40,45,73,74], while the GWP of cement with additions, such as pozzolan, slag, limestone, and fly ash, vary from 452 to 850 kg CO₂-Eq/ton of cement [36,40,45,53].

Table 2. Result of life cycle evaluation impact categories for 1 ton of composite hydraulic cement.

Impact Categories	Unit	GU ¹	This Study HE ²	MH ³	Literature Reviewed
Global Warming Potential—GWP100	kg CO ₂ -Eq	545.78	696.81	465.89	632–950 ⁴ 452–850 ⁵
Terrestrial Acidification Potential—TAP100	kg SO ₂ -Eq	1.03	1.27	0.88	1.467–4.1 ⁶ 0.87–1.16 ⁷
Freshwater Eutrophication Potential—FEP	kg P-Eq	3.59×10^{-3}	4.23×10^{-3}	3.22×10^{-3}	1.23×10^{-2} ⁸
Marine Eutrophication Potential—MEP	kg N-Eq	0.054	0.067	0.047	—
Ozone Depletion Potential—ODP	kg CFC ⁻¹¹ -Eq	2.83×10^{-5}	3.59×10^{-5}	2.43×10^{-5}	9.60×10^{-9} 4.20×10^{-5} ⁹
Photochemical Oxidant Formation Potential—POFP	kg NMVOC-Eq	1.34	1.68	1.16	1.09 ⁸
Particulate Matter Formation Potential—PMFP	kg PM10-Eq	0.48	0.56	0.42	—
Fossil Depletion Potential—FDP	kg oil-Eq	54.85	69.30	47.14	—

¹ GU: General use cement; ² HE: High early strength cement; ³ MH: Moderate heat of hydration cement; ⁴ Ordinary Portland cement, GWP results [36–40,45,73,74]; ⁵ Cement with additions, GWP results [36,40,45,53]; ⁶ [37,38,43,46,53,74]; ⁷ Cement with additions, TAP100 result [40]; ⁸ [41]; ⁹ [9,40,41,53,73].

The results of this study rank in the lower limits due to the levels of additions in the cement and because of the efficiency of the plant of 3.01 GJ/ton of cement in thermal energy consumption compared to that in the literature, that being from 2.81 to 5.4 GJ/ton of cement [43,74,75]. The clinkering production process contributes 98% of the total GWP of the composite hydraulic cement in Ecuador (Figure 3) due to the GHG emitted in the clinkering process, followed by the electricity generation process, with a range between 0.9 and 1.4%.

Regarding TAP100, the cement from Ecuador ranges between 0.88 to 1.27 kg SO₂-Eq/ton of cement. These values are close to those found in the literature, which are between 1.467 and 4.1 kg SO₂-Eq/ton of cement [37,38,43,46,53,74]. Çankaya & Pekey [40] report values between 0.87 to 1.16 kg SO₂-Eq/ton for pozzolanic cements with similar additions and compositions to the ones in Ecuador. NO_x is the largest contributor to this category, followed by SO₂, both produced by the clinkering process.

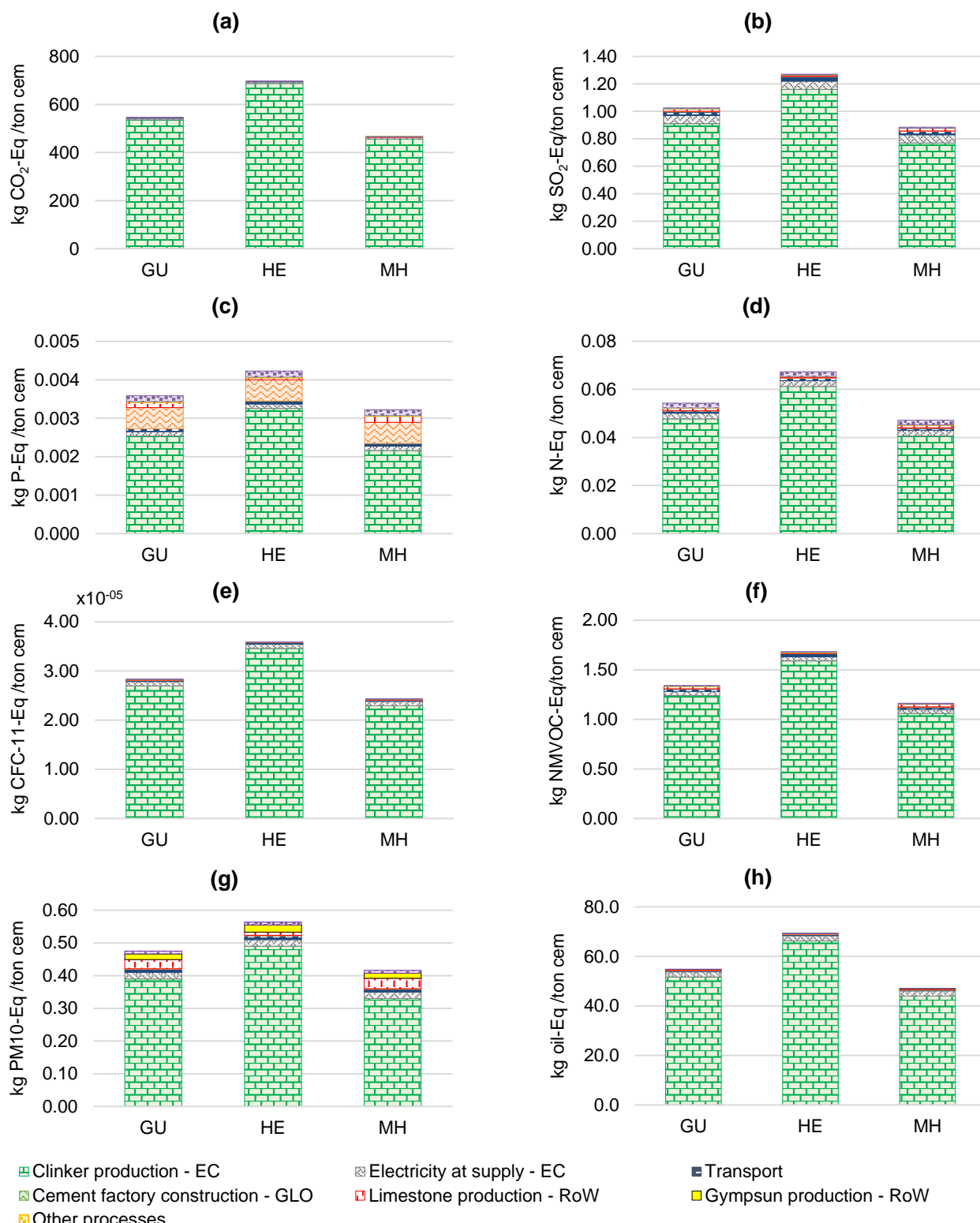


Figure 3. Characterization results for impact categories. The graphs show the impact results per ton cement (functional unit) by type: GU: General use, HE: High early strength, and MH: Moderate Heat of Hydration, and a contribution analysis for processes. (a) Global warming potential—GWP100; (b) Terrestrial acidification potential—TAP100; (c) Freshwater eutrophication potential—FEP; (d) Marine eutrophication potential—MEP; (e) Ozone depletion potential—ODPinf; (f) Photochemical oxidant formation potential—POFP; (g) Particulate matter formation potential—PMFP; (h) Fossil depletion potential—FDP; EC—Ecuador; GLO—global; and RoW—Rest of world.

For the Spanish cement industry, García-Gusano et al. [41] calculated for freshwater eutrophication (FEP) a value of 1.23×10^{-2} kg P-Eq/ton of cement. This study determines values between 3.22×10^{-3} to 4.23×10^{-3} kg P-Eq/ton of cement. The process with the greatest contribution is the manufacture of clinker. Comparing both studies, the results are in similar ranges. In marine eutrophication (MEP), the results obtained are 0.047 to 0.067 kg N-Eq/ton of cement.

Results of ODPinf in Ecuadorian cements are between 2.43×10^{-5} and 3.59×10^{-5} kg CFC⁻¹¹-Eq/ton of cement. Literature results vary between 9.60×10^{-9} and 4.20×10^{-5} kg CFC⁻¹¹-Eq/ton of cement [9,40,41,53,73]. The process with the greatest contribution is clinker production. The same situation also occurs for FDP, as this category represents the depletion of fossil resources.

The results for POFP in this study ranged from 1.16 to 1.68 kg NMVOC-Eq/ton of cement due to the emissions of VOC, NO_x, and SO₂ from the manufacture of clinker. The result of POFP is similar to that obtained by García-Gusano et al. [41] of 1.09 kg NMVOC-Eq/ton of cement. Results of PMFP for cements in Ecuador are in the range of 0.42 to 0.56 kg PM10-Eq/ton of cement, with NO_x being the highest contributor to the flow followed by PM.

The critical input in the manufacture of cement in Ecuador is the clinker. Clinker has the greatest share in the impact categories analyzed, as shown in Figure 3.

3.2.3. Concrete

The impact category indicator results for 1 m³ of ready-mixed concrete with characteristic compressive strengths between 2.5–80 MPa for Ecuadorian production are presented in Table 3. These results represent the average production of ready-mixed concrete in Ecuador, based on the distribution percentage of the concrete output per plant.

Table 3. Result of life cycle evaluation impact categories for 1 m³ of ready-mixed concrete with different compressive strengths in Ecuador.

Compressive Strength	GWP100 kg CO ₂ -Eq	TAP100 kg SO ₂ -Eq	FEP kg P-Eq	MEP kg N-Eq	ODPinf kg CFC ⁻¹¹ -Eq	POFP kg NMVOC-Eq	PMFP kg PM10-Eq	FDP kg Oil-Eq
2.5 MPa	126.02	0.35	5.79×10^{-3}	0.019	0.93×10^{-5}	0.50	0.17	22.55
15 MPa	206.80	0.49	8.04×10^{-3}	0.027	1.35×10^{-5}	0.67	0.23	30.17
18 MPa	225.84	0.54	9.40×10^{-3}	0.029	1.45×10^{-5}	0.72	0.25	33.43
21 MPa	237.22	0.55	9.73×10^{-3}	0.030	1.50×10^{-5}	0.75	0.26	34.85
24 MPa	256.08	0.60	10.2×10^{-3}	0.033	1.63×10^{-5}	0.81	0.28	37.89
28 MPa	267.54	0.62	10.3×10^{-3}	0.034	1.66×10^{-5}	0.83	0.29	38.91
30 MPa	290.85	0.67	11.4×10^{-3}	0.036	1.85×10^{-5}	0.90	0.32	43.17
35 MPa	310.31	0.69	11.2×10^{-3}	0.038	1.88×10^{-5}	0.93	0.32	44.87
40 MPa	355.38	0.77	11.8×10^{-3}	0.041	2.07×10^{-5}	1.02	0.35	50.86
45 MPa	379.38	0.83	11.2×10^{-3}	0.045	2.29×10^{-5}	1.12	0.39	52.25
50 MPa	382.03	0.82	12.0×10^{-3}	0.044	2.23×10^{-5}	1.10	0.38	53.37
60 MPa	419.55	0.89	13.3×10^{-3}	0.048	2.40×10^{-5}	1.17	0.41	59.18
80 MPa	442.14	0.91	12.3×10^{-3}	0.048	2.46×10^{-5}	1.19	0.41	60.25

GWP100: global warming potential; TAP100: terrestrial acidification potential; FEP: freshwater eutrophication potential; MEP: marine eutrophication potential; ODPinf: ozone depletion potential; POFP: photochemical oxidant formation potential; PMFP: particulate matter formation potential; FDP: fossil depletion potential.

The results of GWP100 show that low compressive strength concrete (18 MPa) has approximately 29% of the GWP of the high compressive strength concrete (>40 MPa); this is due to different cement contents (Figure 4). It can be seen that cement production is the critical process within this impact category, with an influence between 84 and 88% in conventional concrete (18 at 40 MPa). For low compressive strength concrete, cement production contribution is approximately 76% because there is greater use of fine aggregate instead of cement. For high compressive strength concrete, the consumption of cement increases; this causes that cement production to contribute 89–92%. Transport is the second process with the highest contribution in this category, with values between 1.13 and 8.30%. For high compressive strength concrete (>40 MPa), transport shows low contribution values (1.13–2.83%).

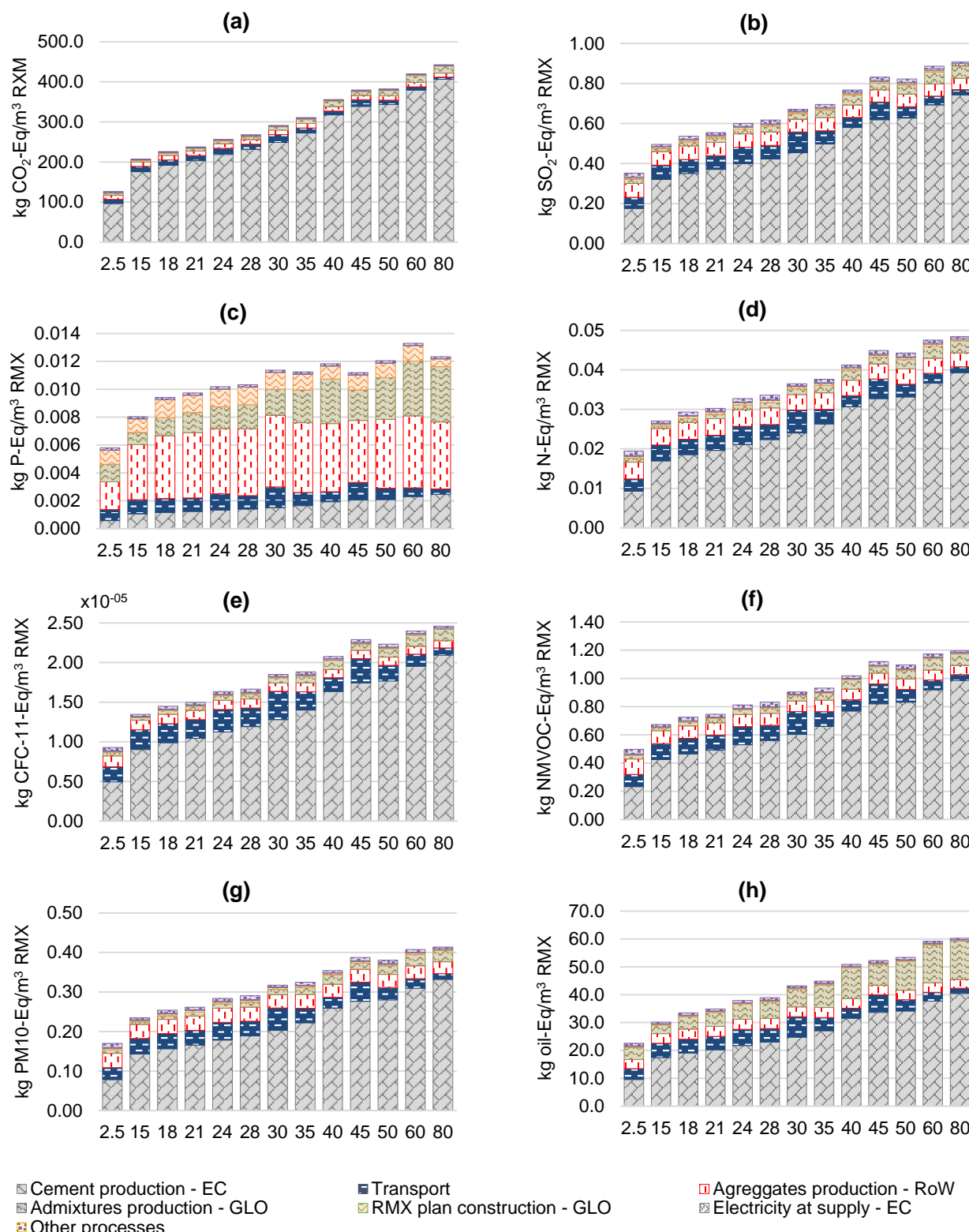


Figure 4. Characterization of results for impact categories. The graphs show the impact results per m^3 of ready-mixed concrete (functional unit) with compressive strength between 2.5 and 80 MPa and a contribution analysis for processes. (a) Global warming potential—GWP100; (b) Terrestrial acidification potential—TAP100; (c) Freshwater eutrophication potential—FEP; (d) Marine eutrophication potential—MEP; (e) Ozone depletion potential—ODPinf; (f) Photochemical oxidant formation potential—POFP; (g) Particulate matter formation potential—PMFP; (h) Fossil depletion potential—FDP; RMX: ready-mixed concrete; EC: Ecuador; GLO: global; and RoW: Rest of world.

The following two processes with significant contributions are aggregate production and admixture production. Within aggregate production, there is a consumption between 67 and 84% per m^3 of the concrete's total mass; also, there is a low amount of CO_2 emission per kg of aggregate. Admixture consumption is between 0.01 and 0.02% per m^3 , with a high content of CO_2 emission per kg of admixture. Other processes, such as electricity, fuel, and water consumption represent between 0.5 and 2% of the GWP.

The results of terrestrial acidification—TAP100—vary between 0.35 and 0.91 $\text{kg SO}_2\text{-Eq}/\text{m}^3$ of ready-mixed concrete. Cement production is the critical process, with a contribution between 49.79 and 81.83%. The content (and contribution) is higher when higher characteristic compressive strength is required. TAP100 for transport increases for concrete plants where a greater distance from the cement factory is observed. The values of this study for characteristic compressive strengths between 21 and 50 MPa are 0.55–0.83 $\text{kg SO}_2\text{-Eq}/\text{m}^3$ of ready-mixed concrete, lower than studies from Colombia, Peru, South Africa, Brazil, and Canada for the same compressive strengths. The value of TAP100 varies from 0.622 at 1.73 $\text{kg SO}_2\text{-Eq}/\text{m}^3$ of ready-mixed concrete [50–52,54], due to low levels of SO_2 in flue gas from the production of clinker, due to the composition of fossil fuels and use of alternative fuels in kilns. This is reflected in the value chain of cementitious materials, such as concrete production, having lower TAP100 values than the literature reviewed.

For the freshwater eutrophication—FEP impact category, the values reported within this research range from 55.79×10^{-3} to 13.3×10^{-3} $\text{kg P-Eq}/\text{m}^3$ of ready-mixed concrete. The process with the highest contribution is aggregate production, with values between 34 and 49%. The production of crushed aggregate has a greater contribution than the production of natural sand. The second process with the highest contribution is admixture production, ranging between 10.96 and 32.10%. Results of marine eutrophication—MEP range from 0.019 to 0.048 $\text{kg N-Eq}/\text{m}^3$ of ready-mixed concrete. The critical process is the production of cement due to the NO_x emissions in the production of clinker. The value of other processes is relatively constant, with values between 0.009 and 0.011 $\text{kg N-Eq}/\text{m}^3$ of ready-mixed concrete. Gursel & Ostertag [76] in their study of ready-mixed concrete with OPC report values between 0.18 and 0.395 $\text{kg N-Eq}/\text{m}^3$ of ready-mixed concrete; the results in their research are high due to the marine transport of aggregates to Singapore from other countries. Adapting that research to this study, where no transport of aggregates is considered, results in values between 0.1 and 0.19 $\text{kg N-Eq}/\text{m}^3$ of ready-mixed concrete, which is lower than the results for this study.

Regarding ozone depletion—ODPinf, the results of this study are between 0.93×10^{-5} and 2.46×10^{-5} $\text{kg CFC}^{-11}\text{-Eq}/\text{m}^3$ of ready-mixed concrete. Cement production is the process with the highest contribution, with 53.18 to 85.10%. The second process is transport, contributing between 3.72 and 20%; this result varies depending on the distance between the concrete plant and the cement factory. According to previous literature, characteristic compressive strengths between 21 to 50 MPa are 6.93×10^{-6} to 9.2×10^{-5} $\text{kg CFC}^{-11}\text{-Eq}/\text{m}^3$ of concrete ready-mixed [50–52,54]; in this research, those values are similar for characteristic compressive strengths between 21 and 50 MPa, which is 1.50×10^{-5} to 2.23×10^{-5} $\text{kg CFC}^{-11}\text{-Eq}/\text{m}^3$ of ready-mixed concrete.

NO_x and VOC are the main substances that contribute to the photochemical oxidant formation—POFP impact category. These are mainly emitted during clinker production; hence, cement production is the critical process in this category, contributing from 46.73 to 82.43%. The POFP values for this study are between 0.50 and 1.19 $\text{kg NMVOC-Eq}/\text{m}^3$ of ready-mixed concrete; the result of all processes except for cement production remains between 0.20 and 0.30 $\text{kg NMVOC-Eq}/\text{m}^3$ of ready-mixed concrete. Adapting the study by Gursel & Ostertag [76], the result without aggregates' marine transport is 2.8 to 4 $\text{kg NMVOC-Eq}/\text{m}^3$ of ready-mixed concrete with OPC cement, a higher range than the ones calculated in this study.

Figure 4 shows the result of Particulate matter formation—PMFP, with values between 0.17 and 0.41 $\text{kg PM10-Eq}/\text{m}^3$ of ready-mixed concrete; the study by Gursel & Ostertag [76] has been adapted by removing the aggregate transport process, obtaining values between

1.70 and 2.25 kg PM10-Eq/m³ of ready-mixed concrete; this is related to the low levels of PM in this study, focused on the production of Ecuadorian cement, the use of control equipment for the reduction and reuse of PM in the process, causing the PMFP to be lower than in the studies reviewed. The critical process of the impact category described is cement production, with contributions between 46.10 to 80.23%. As with most impact categories, the contribution increases as the cement content increases to improve the compressive strength of the concrete.

Fossil depletion—FDP was analyzed; the results obtained ranged from 22.55 to 60.25 kg oil-Eq/m³ of ready-mixed concrete. The cement production process and admixture production are critical processes due to the consumption of thermal energy used in clinker production and organic chemicals. The contribution of cement and admixture production are between 42.28 and 67.09% and 10.17 and 23.02%, respectively. Both contributions increase due to the progressive consumption of these materials to improve concrete characteristic compressive strength.

Figure 5 shows a comparison of Global warming potential—GWP100 results between this research and previous results in the literature with compressive strengths of 20 to 70 MPa [49–52,54]. The study by Hossain et al. [48] of concrete in China analyzes compressive strengths between 59 and 70 MPa.

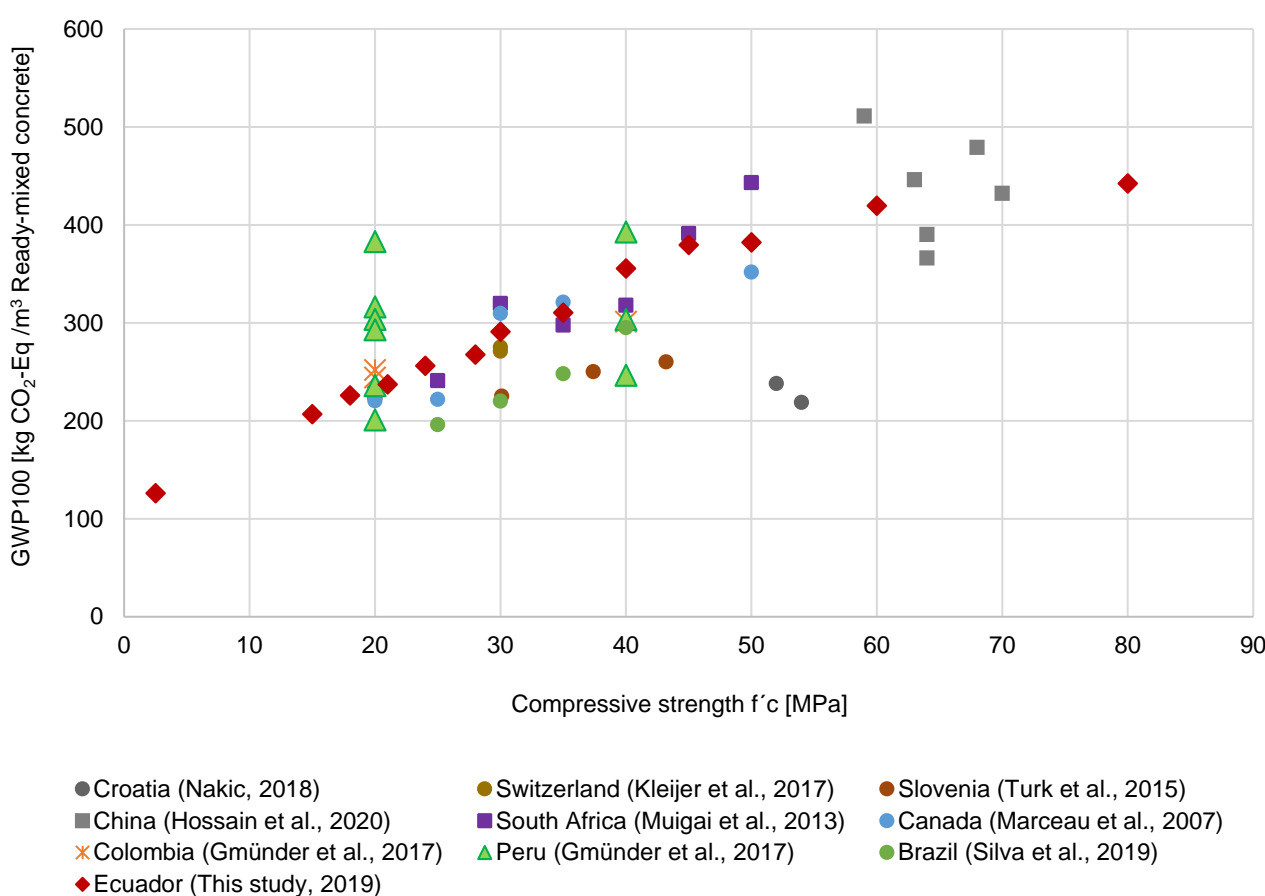


Figure 5. Global warming potential results of ready-mixed concrete in literature reviewed and this study.

The result of this study for Ecuadorian 21 MPa is 237.22 kg CO₂-Eq/m³ of ready-mixed concrete. Studies with similar characteristic compressive strength (20 MPa) are from Peru, Colombia, Canada, and South Africa. The most similar values are those of Peru and Colombia, where pozzolanic cement concrete is used, with a differential between 0.60 to 6.19%. Concrete with limestone from Peru uses raw materials similar to those of Ecuador,

with results between 55.68 and 66.20 kg CO₂-Eq/m³ of ready-mixed concrete. OPC concrete shows a difference between 79.01 and 145.60 kg CO₂-Eq/m³ of ready-mixed concrete due to the high clinker content of OPC.

The result for this study for 24 MPa is 256.08 kg CO₂-Eq/m³ of ready-mixed concrete. Results in the literature for 25 MPa range from 221.85 to 240 kg CO₂-Eq/m³ of ready-mixed concrete [49,51,52]. This study reports a higher value. The same authors report results between 246.5 and 392.74 kg CO₂-Eq/m³ for 40 MPa ready-mixed concrete; this study result is 355.37 kg CO₂-Eq/m³ of ready-mixed concrete, which is within the aforementioned results, the main differences between the studies are due to the components of the concrete, such as recycled material, fly ash, and slag.

For the compressive strength of 30 MPa, this study reports a value of 290.85 kg CO₂-Eq/m³ of ready-mixed concrete. The results of Canada and South Africa are 6.44 and 9.91% higher, respectively. This study has a result of 310.30 kg CO₂-Eq/m³ for 35 MPa ready-mixed concrete. This result is within the range of 297.56 to 320.97 kg CO₂-Eq/m³ of ready-mixed concrete for Canada and South Africa [51,52]. The study for Slovenia presents values below the average of the rest of the countries due to the use of steel slags and foundry sands [49], in particular, 22.64 and 19.43% lower compared to the results for 30 and 35 MPa concretes of this study. The results for South Africa 45 MPa concrete are similar to this study's result with a difference of +11.71 kg CO₂-Eq/m³ of ready-mixed concrete. For 50 MPa, studies from South Africa and Canada show results between 443.05 and 351.65 kg CO₂-Eq/m³ of ready-mixed concrete; this study reports a higher value of 382.03 kg CO₂-Eq/m³ of ready-mixed concrete.

Hossain et al. [48] analyzed the production of high compressive strength concrete in China with compressive strengths between 59 and 70 MPa. Concrete with characteristic compressive strengths between 59 and 64 MPa, with values of 390 at 511 kg CO₂-Eq/m³ of ready-mixed concrete, is comparable to the 60 MPa concrete of this study with a result of 419.54 kg CO₂-Eq/m³ of ready-mixed concrete, which is similar to 63 MPa results with +26.45 kg CO₂-Eq/m³ of ready mixed concrete. The results of 68 and 70 MPa from the same study are close to the result for 80 MPa of this study, with +36.86 and -10.13 kg CO₂-Eq/m³ of ready-mixed concrete, respectively. The influence of the use of materials, such as pozzolan and slag in the composition of Ecuadorian cement, was a determining factor in the reduction of GWP in concrete with high compressive strength compared to the literature reviewed.

4. Conclusions

The environmental performance of the production of clinker, cement, and concrete in Ecuador has been quantified using the life cycle assessment methodological framework. Input and output inventories of matter and energy have been generated for 62.8% of the cement industry and 55% of the concrete industry in Ecuador.

Environmental impacts of clinker production are mainly caused by gases generated in the combustion in clinker kilns, which is necessary to transform calcium carbonate into calcium oxide. This process becomes critical throughout the value chain of cement and concrete products in most of the established impact categories. The result for the environmental performance result of clinker of this study is similar to those found in the literature review in terms of GWP; other indicators such as TAP100 and FEP are reduced due to emissions control equipment, energy efficiency, and the Ecuadorian electricity mix. The environmental performance of clinker is necessary throughout the value chain of construction materials based on cement since this presents a baseline for the evaluation of environmental improvements at the cement production level. Improvement strategies that can be assessed include replacing clinker with alternative materials, such as pozzolan, slag, and fly ash, and the use of alternative fuels.

The environmental impact of the Ecuadorian cement industry has been determined using inventory data of cement types: GU, HE, and MH, used in conventional construction and the ready-mixed concrete industry. The results of impact assessment of cement based

in Ecuador are at the lower range than those found in the literature due to the levels of additions in Ecuadorian cement and cement plant efficiency.

A range of compressive strengths has been covered in the quantification of the environmental performance of ready-mixed concrete from 2.5 MPa to 80 MPa; each conventional concrete used by the construction industry has been included in detail (18, 21, 24, 28, 30, 35, and 40 MPa).

Main strategies for improving the environmental profile of clinker, cement, and concrete should be focused on decreasing the environmental impact of the clinkering process. For the clinker production system, this can be done by increasing the thermal efficiency and using fuels with lower environmental impacts. For the cement and the concrete systems, measures should be focused on reducing the content of clinker.

Cement and concrete environmental profiles obtained in this study are used to calculate the environmental performance of structural elements (columns, beams, foundations, etc.) and also structures, such as housing, buildings, and mega-infrastructure projects that use cement and concrete. The results of this study, based on local inventories, can be used in research on sustainable construction in Ecuador and countries with similar conditions for the production of materials and construction systems, such as the Latin American region. Using its GWP, it will be possible to determine reductions in CO₂ by materials. This makes it possible to quantify the current status and the improvements in compliance with SDG 13: Climate Action and seek solutions to make cities and human settlements inclusive, safe, resilient, and sustainable, according to SDG 11: Sustainable Cities and Communities.

Supplementary Materials: The following supporting information can be downloaded at: <https://www.mdpi.com/article/10.3390/buildings12030311/s1>: Table S1: Summary of processes taken from ecoinvent database for LCIA Clinker in Ecuador; Table S2: Summary of processes taken from ecoinvent database for LCIA Cement in Ecuador; Table S3: Summary of processes taken from ecoinvent database for LCIA Concrete in Ecuador; Table S4: Life cycle inventories of clinker production in Ecuador (per ton of clinker); and Table S5: Life cycle inventories of concrete production in Ecuador (per m³ of ready-mixed concrete).

Author Contributions: Conceptualization, D.M.P. and A.D.R.; methodology, D.M.P. and A.D.R.; investigation, D.M.P.; writing—original draft, D.M.P.; writing—review & editing, A.D.R.; visualization, D.M.P.; supervision, A.D.R.; project administration, A.D.R. All authors have read and agreed to the published version of the manuscript.

Funding: The study was funded by the Escuela Superior Politecnica del Litoral, ESPOL, Ecuador.

Data Availability Statement: All data generated or analyzed during this study are presented or can be reproduced using the life cycle inventories that are presented and references indicated.

Acknowledgments: The authors wish to thank Escuela Superior Politecnica del Litoral, ESPOL for funding. The APC is covered by Escuela Superior Politecnica del Litoral, ESPOL.

Conflicts of Interest: D.M.P works for a company that provided data for this study. A.D.R declares no conflicts of interest.

References

- United Nations; Department of Economic and Social Affairs; Population Division. *World Urbanization Prospects*; The 2018 Revision; United Nations: New York, NY, USA, 2019; pp. 9–10.
- United Nations. *World Cities Report 2020: The Value of Sustainable Urbanization*; UN-Habitat: Nairobi, Kenya, 2020; Volume 1, pp. 18–20.
- United Nations. Transforming Our World: The 2030 Agenda for Sustainable Development. United Nations Sustainable Knowledge Platform. Sustainable Development Goals. 2015; pp. 1–35. Available online: <https://sustainabledevelopment.un.org/content/documents/21252030%20Agenda%20for%20Sustainable%20Development%20web.pdf> (accessed on 1 February 2022).
- United Nations. *The World's Cities in 2018*; United Nations: New York, NY, USA, 2018.
- Sagastume Gutiérrez, A.; Cabello Eras, J.J.; Gaviria, C.A.; Van Caneghem, J.; Vandecasteele, C. Improved selection of the functional unit in environmental impact assessment of cement. *J. Clean. Prod.* **2017**, *168*, 463–473. [CrossRef]
- Imbabi, M.S.; Carrigan, C.; McKenna, S. Trends and developments in green cement and concrete technology. *Int. J. Sustain. Built Environ.* **2012**, *1*, 194–216. [CrossRef]

7. Tatari, O.; Kucukvar, M. Sustainability Assessment of U.S. Construction Sectors: Ecosystems Perspective. *J. Constr. Eng. Manag.* **2012**, *138*, 918–922. [[CrossRef](#)]
8. Banco Central del Ecuador. *Reporte Trimestral del Mercado Laboral (Diciembre 2019)*; Banco Central del Ecuador: Quito, Ecuador, 2019.
9. Chen, W.; Hong, J.; Xu, C. Pollutants generated by cement production in China, their impacts, and the potential for environmental improvement. *J. Clean. Prod.* **2015**, *103*, 61–69. [[CrossRef](#)]
10. International Cement Review. *The Global Cement ReportTM*, 13th ed.; International Cement Review: Dorking, UK, 2019.
11. Rodrigues, F.A.; Joekes, I. Cement industry: Sustainability, challenges and perspectives. *Environ. Chem. Lett.* **2011**, *9*, 151–166. [[CrossRef](#)]
12. Supino, S.; Malandrino, O.; Testa, M.; Sica, D. Sustainability in the EU cement industry: The Italian and German experiences. *J. Clean. Prod.* **2016**, *112*, 430–442. [[CrossRef](#)]
13. Humphreys, K.; Mahasenan, M. *Towards a Sustainable Cement Industry. Substudy 8: Climate Change*; World Business Council for Sustainable Development: Geneva, The Switzerland, 2002.
14. Ellis, L.; Badel, A.; Chiang, M.; Park, R.; Chiang, Y. Toward electrochemical synthesis of cement—An electrolyzer-based process for decarbonating CaCO₃ while producing useful gas streams. *Proc. Natl. Acad. Sci. USA* **2020**, *117*, 12584–12591. [[CrossRef](#)]
15. International Energy Agency. *Technology Roadmap—Low-Carbon Transition in the Cement Industry*; International Energy Agency: Paris, France, 2018.
16. Salas, D.A.; Ramirez, A.D.; Rodríguez, C.R.; Petroche, D.M.; Boero, A.J.; Duque-Rivera, J. Environmental impacts, life cycle assessment and potential improvement measures for cement production: A literature review. *J. Clean. Prod.* **2016**, *113*, 114–122. [[CrossRef](#)]
17. World Health Organization. *Health Risks of Air Pollution in Europe—HRAPIE Project, Recommendations for Concentration–Response Functions for Cost–Benefit Analysis of Particulate Matter, Ozone and Nitrogen Dioxide*; World Health Organization: Copenhagen, Denmark, 2013.
18. Van Goethem, T.M.W.J.; Azevedo, L.B.; Van Zelm, R.; Hayes, F.; Ashmore, M.R.; Huijbregts, M.A.J. Plant Species Sensitivity Distributions for ozone exposure. *Environ. Pollut.* **2013**, *178*, 1–6. [[CrossRef](#)] [[PubMed](#)]
19. Zvereva, E.L.; Toivonen, E.; Kozlov, M.V. Changes in species richness of vascular plants under the impact of air pollution: A global perspective. *Glob. Ecol. Biogeogr.* **2008**, *17*, 305–319. [[CrossRef](#)]
20. Roem, W.J.; Berendse, F. Soil acidity and nutrient supply ratio as possible factors determining changes in plant species diversity in grassland and heathland communities. *Biol. Conserv.* **2000**, *92*, 151–161. [[CrossRef](#)]
21. FICEM. *Cemento & Concreto de Iberoamérica y el Caribe*; FICEM: Bogota, Colombia, 2020.
22. Acebo, M.; Vera, J.; Rodríguez, J.; Zambrano, J. *Estudios Industriales, Orientación Estratégica Para la Toma de Decisiones: Industria de la Construcción*; ESPAE-ESPOL: Guayaquil, Ecuador, 2016.
23. Anderson, R.; Dewar, J.D.; McKee, H.; Treasaden, I. *Manual of Ready-Mixed Concrete*; CRC Press: London, UK, 1992.
24. Neville, A. *Properties of Concrete*, 4th ed.; Longman Group: Harlow, UK, 1995; ISBN 0-582-23070-5.
25. Mehta, P.K.; Monteiro, P. *Concrete. Structure, Properties and Materials*, 2nd ed.; Prentice-Hall, Inc.: Hoboken, NJ, USA, 1993; ISBN 0131756214.
26. Das, S.K.; Mishra, J.; Mustakim, S.M. Rice Husk Ash as a Potential Source Material for Geopolymer Concrete: A Review. *Int. J. Appl. Eng. Res.* **2018**, *13*, 81–84.
27. Egüez Álava, H.; Tsangouri, E.; De Belie, N.; De Schutter, G. Chloride interaction with concretes subjected to a permanent splitting tensile stress level of 65%. *Constr. Build. Mater.* **2016**, *127*, 527–538. [[CrossRef](#)]
28. Gagg, C.R. Cement and concrete as an engineering material: An historic appraisal and case study analysis. *Eng. Fail. Anal.* **2014**, *40*, 114–140. [[CrossRef](#)]
29. Monteiro, P.J.M.; Miller, S.A.; Horvath, A. Towards sustainable concrete. *Nat. Mater.* **2017**, *16*, 698–699. [[CrossRef](#)]
30. Van Den Heede, P.; De Belie, N. Environmental impact and life cycle assessment (LCA) of traditional and “green” concretes: Literature review and theoretical calculations. *Cem. Concr. Compos.* **2012**, *34*, 431–442. [[CrossRef](#)]
31. INEC. *Encuesta Nacional de Edificaciones (ENED)*, 2019; INEC: Quito, Ecuador, 2020.
32. McDermot, E.; Agdas, D.; Rodríguez Díaz, C.R.; Rose, T.; Forcael, E. Improving performance of infrastructure projects in developing countries: An Ecuadorian case study. *Int. J. Constr. Manag.* **2020**. [[CrossRef](#)]
33. ISO. ISO-14040 Environmental Management—Life Cycle Assessment—Principles and Framework: International Organization for Standardization. 2006. Available online: <https://www.iso.org/obp/ui#iso:std:iso:14040:ed-2:v1:en> (accessed on 1 February 2022).
34. Concrete needs to lose its colossal carbon footprint. *Nature* **2021**, *597*, 593–594. [[CrossRef](#)]
35. Sartori, T.; Drogemuller, R.; Omrani, S.; Lamari, F. A schematic framework for Life Cycle Assessment (LCA) and Green Building Rating System (GBRS). *J. Build. Eng.* **2021**, *38*, 102180. [[CrossRef](#)]
36. Feiz, R.; Ammenberg, J.; Baas, L.; Eklund, M.; Helgstrand, A.; Marshall, R. Improving the CO₂ performance of cement, part I: Utilizing life-cycle assessment and key performance indicators to assess development within the cement industry. *J. Clean. Prod.* **2015**, *98*, 272–281. [[CrossRef](#)]
37. García-Gusano, D.; Garraín, D.; Herrera, I.; Cabal, H.; Lechón, Y. Life cycle assessment of the Spanish cement industry: Implementation of environmental-friendly solutions. *Clean Technol. Environ. Policy* **2015**, *17*, 59–73. [[CrossRef](#)]
38. Stafford, F.N.; Dias, A.C.; Arroja, L.; Labrincha, J.A.; Hotza, D. Life cycle assessment of the production of Portland cement: A Southern Europe case study. *J. Clean. Prod.* **2016**, *126*, 159–165. [[CrossRef](#)]

39. Valderrama, C.; Granados, R.; Cortina, J.L.; Gasol, C.M.; Guillem, M.; Josa, A. Implementation of best available techniques in cement manufacturing: A life-cycle assessment study. *J. Clean. Prod.* **2012**, *25*, 60–67. [CrossRef]
40. Çankaya, S.; Pekey, B. A comparative life cycle assessment for sustainable cement production in Turkey. *J. Environ. Manag.* **2019**, *249*, 109362. [CrossRef] [PubMed]
41. García-Gusano, D.; Garraín, D.; Herrera, I.; Cabal, H.; Lechón, Y. Life Cycle Assessment of applying CO₂ post-combustion capture to the Spanish cement production. *J. Clean. Prod.* **2015**, *104*, 328–338. [CrossRef]
42. Li, C.; Nie, Z.; Cui, S.; Gong, X.; Wang, Z.; Meng, X. The life cycle inventory study of cement manufacture in China. *J. Clean. Prod.* **2014**, *72*, 204–211. [CrossRef]
43. Tun, T.Z.; Bonnet, S.; Gheewala, S.H. Life cycle assessment of Portland cement production in Myanmar. *Int. J. Life Cycle Assess.* **2020**, *25*, 2106–2121. [CrossRef]
44. Yang, D.; Fan, L.; Shi, F.; Liu, Q.; Wang, Y. Comparative study of cement manufacturing with different strength grades using the coupled LCA and partial LCC methods—A case study in China. *Resour. Conserv. Recycl.* **2017**, *119*, 60–68. [CrossRef]
45. Vázquez-Rowe, I.; Ziegler-Rodriguez, K.; Laso, J.; Quispe, I.; Aldaco, R.; Kahhat, R. Production of cement in Peru: Understanding carbon-related environmental impacts and their policy implications. *Resour. Conserv. Recycl.* **2019**, *142*, 283–292. [CrossRef]
46. Nakic, D. Environmental evaluation of concrete with sewage sludge ash based on LCA. *Sustain. Prod. Consum.* **2018**, *16*, 193–201. [CrossRef]
47. Kleijer, A.L.; Lasvaux, S.; Citherlet, S.; Viviani, M. Product-specific Life Cycle Assessment of ready mix concrete: Comparison between a recycled and an ordinary concrete. *Resour. Conserv. Recycl.* **2017**, *122*, 210–218. [CrossRef]
48. Hossain, M.U.; Cai, R.; Ng, S.T.; Xuan, D.; Ye, H. Sustainable natural pozzolana concrete—A comparative study on its environmental performance against concretes with other industrial by-products. *Constr. Build. Mater.* **2020**, *270*, 121429. [CrossRef]
49. Turk, J.; Cotič, Z.; Mladenovič, A.; Šajna, A. Environmental evaluation of green concretes versus conventional concrete by means of LCA. *Waste Manag.* **2015**, *45*, 194–205. [CrossRef] [PubMed]
50. Gmünder, S.; Myers, N.; Laffley, J.; Rubio, L.; Belizario Silva, F. *Life Cycle Inventories of Cement, Concrete and Related Industries—Colombia and Peru for the SRI Project*; Ecoinvent Association: Zürich, Switzerland, 2017.
51. Muigai, R. *Life Cycle Inventories of Cement, Concrete and Related Industries—South Africa*; Ecoinvent Association: Zürich, Switzerland, 2017.
52. Marceau, M.L.; Nisbet, M.A.; VanGeem, M.G. Life Cycle Inventory of Portland Cement Concrete. SN3011 Portl. Cem. Assoc. Skokie Ill. PCA; 2007. Available online: <https://www.osti.gov/servlets/purl/1223003> (accessed on 1 February 2022).
53. Bushi, L.; Meil, J. *An Environmental Life Cycle Assessment of Portland-Limestone and Ordinary Portland Cements in Concrete*; Cement Association of Canada: Ottawa, Canada, 2014.
54. Silva, F.B.; Oliveira, L.A.; Yoshida, O.S.; John, V.M. Variability of environmental impact of ready-mix concrete: A case study for Brazil. *IOP Conf. Ser. Earth Environ. Sci.* **2019**, *323*, 012132. [CrossRef]
55. ISO. ISO 14044:2006. Environmental Management—Life Cycle Assessment—Requirements And Guidelines ISO 14044. *Int. Organ. Stand.* **2006**, *2006*. Available online: <https://www.iso.org/obp/ui/es/#iso:std:iso:14044:ed-1:v1:en> (accessed on 1 February 2022).
56. Ross, S.; Evans, D.; Webber, M. How LCA studies deal with uncertainty. *Int. J. Life Cycle Assess.* **2002**, *7*, 47–52. [CrossRef]
57. Park, K.B.; Lin, R.S.; Han, Y.; Wang, X.Y. Model-Based Methods to Produce Greener Metakaolin Composite Concrete. *Appl. Sci.* **2021**, *11*, 10704. [CrossRef]
58. Long, G.; Gao, Y.; Xie, Y. Designing more sustainable and greener self-compacting concrete. *Constr. Build. Mater.* **2015**, *84*, 301–306. [CrossRef]
59. Ghalehnovi, M.; Roshan, N.; Taghizadeh, A.; Shamsabadi, E.A.; Hadigheh, S.A.; de Brito, J. Production of Environmentally Friendly Concrete Incorporating Bauxite Residue and Silica Fume. *J. Mater. Civ. Eng.* **2021**, *34*, 04021423. [CrossRef]
60. Shamsabadi, E.A.; Ghalehnovi, M.; de Brito, J.; Khodabakhshian, A. Performance of Concrete with Waste Granite Powder: The Effect of Superplasticizers. *Appl. Sci.* **2018**, *8*, 1808. [CrossRef]
61. Lippiatt, B.C. BEES 4.0: Building for Environmental and Economic Sustainability. Technical Manual and User Guide | NIST. *Natl. Inst. Stand. Technol. Gaithersbg.* **2000**. Available online: <https://nvlpubs.nist.gov/nistpubs/TechnicalNotes/NIST.TN.2032.pdf> (accessed on 1 February 2022).
62. Konečný, P.; Ghosh, P.; Hrabová, K.; Lehner, P.; Teplý, B. Effective methodology of sustainability assessment of concrete mixtures. *Mater. Struct.* **2020**, *53*, 1–15. [CrossRef]
63. Müller, H.S. Sustainable structural concrete—From today's approach to future challenge. *Struct. Concr.* **2013**, *14*, 299–300. [CrossRef]
64. Mueller, H.S.; Haist, M.; Moffatt, J.S.; Vogel, M. Design, Material Properties and Structural Performance of Sustainable Concrete. *Procedia Eng.* **2017**, *171*, 22–32. [CrossRef]
65. ASTM International. ASTM International. ASTM C1157/C1157M—20a, standard performance specification for hydraulic cement. In *Annual Book of ASTM Standards*; ASTM International: West Conshohocken, PA, USA, 2020; Volume 04.01, ISBN 978-1-6822-1426.
66. Wernet, G.; Bauer, C.; Steubing, B.; Reinhard, J.; Moreno-Ruiz, E.; Weidema, B. The ecoinvent database version 3 (part I): Overview and methodology. *Int. J. Life Cycle Assess.* **2016**, *21*, 1218–1230. [CrossRef]
67. Ramirez, A.D.; Boero, A.; Rivela, B.; Melendres, A.M.; Espinoza, S.; Salas, D.A. Life cycle methods to analyze the environmental sustainability of electricity generation in Ecuador: Is decarbonization the right path? *Renew. Sustain. Energy Rev.* **2020**, *134*, 110373. [CrossRef]

68. Ramirez, A.D.; Rivela, B.; Boero, A.; Melendres, A.M. Lights and shadows of the environmental impacts of fossil-based electricity generation technologies: A contribution based on the Ecuadorian experience. *Energy Policy* **2019**, *125*, 467–477. [CrossRef]
69. MERNNR; Ministerio de Ambiente y Agua MAAE; Agencia de Regulación y Control de Energía y Recursos Naturales No; Renovables ARCERNR; Operador Nacional de Electricidad CENACE. *Factor de Emisión de CO₂ del Sistema Nacional Interconectado de Ecuador 2019*; MERNNR: Quito, Ecuador, 2020. Available online: https://www.ambiente.gob.ec/wp-content/uploads/downloads/2020/11/factor_de_emision_de_co2_del_sistema_nacional_interconectado_de_ecuador_-_informe_2019.pdf (accessed on 1 February 2022).
70. Goedkoop, M.; Heijungs, R.; De Schryver, A.; Struijs, J.; Van Zelm, R. ReCiPe 2008 A Life Cycle Impact Assessment Method Which Comprises Harmonised Category Indicators at the Midpoint and the Endpoint Level First Edition (Version 1.08) Report I: Characterisation Mark Huijbregts 3. 2013. Available online: https://www.rivm.nl/sites/default/files/2018-11/ReCiPe%202008_A%20lcia%20method%20which%20comprises%20harmonised%20category%20indicators%20at%20the%20midpoint%20and%20the%20endpoint%20level_First%20edition%20Characterisation.pdf (accessed on 1 February 2022).
71. GreenDelta openLCA.org | openLCA Is a Free, Professional Life Cycle Assessment (LCA) and Footprint Software with a Broad Range of Features and Many Available Databases, Created by GreenDelta since 2006. Available online: <https://www.openlca.org/> (accessed on 5 February 2021).
72. Fennell, P.S.; Davis, S.J.; Mohammed, A. Decarbonizing cement production. *Joule* **2021**, *5*, 1305–1311. [CrossRef]
73. Chen, C.; Habert, G.; Bouzidi, Y.; Jullien, A. Environmental impact of cement production: Detail of the different processes and cement plant variability evaluation. *J. Clean. Prod.* **2010**, *18*, 478–485. [CrossRef]
74. Li, C.; Cui, S.; Nie, Z.; Gong, X.; Wang, Z.; Itsubo, N. The LCA of portland cement production in China. *Int. J. Life Cycle Assess.* **2015**, *20*, 117–127. [CrossRef]
75. Josa, A.; Aguado, A.; Cardim, A.; Byars, E. Comparative analysis of the life cycle impact assessment of available cement inventories in the EU. *Cem. Concr. Res.* **2007**, *37*, 781–788. [CrossRef]
76. Gursel, A.P.; Ostertag, C. Comparative life-cycle impact assessment of concrete manufacturing in Singapore. *Int. J. Life Cycle Assess.* **2017**, *22*, 237–255. [CrossRef]

Carbon Footprint Analysis of Cement Production in India

Sunita Kumari¹, Saurabh Jaglan¹, Arti Chouksey¹, Rinku Walia², Aman Ahlawat¹, Atul Garg¹, Manvendra Verma³

¹DCRUST, Civil Engineering Department, Murtthal, Sonipat, Haryana, India

²IKGPTU, Civil Engineering Department, Kapurthala, Jalandhar, Punjab, India

³GLA, Civil Engineering Department, Mathura, Uttar Pradesh, India

*Author to whom correspondence should be addressed:

E-mail: sunitakumari.civil@dcrustm.org

(Received May 23, 2024; Revised September 2, 2024; Accepted October 4, 2024).

Abstract: As the global imperative to mitigate climate change grows, the cement industry becomes a focal point due to its significant carbon dioxide (CO₂) emissions. This study seeks to evaluate the carbon emission factors associated with direct manufacturing, manufacturing processes, neat emissions, and the entire life cycle of cement production, with a special focus on raw material extraction and cement manufacturing within cement plants. This study uses a variety of units, including raw material extraction rates, fuel consumption metrics, electricity usage data, transportation distances, and concrete life cycle assessments, to provide a comprehensive understanding of the carbon footprint inherent in each stage of cement production. It is concluded that the carbon dioxide emission factor with clinker is 0.3838t/ton of limestone and 0.4373t/ton of cement based on manufacturing neat emission and the life cycle of cement in the cement industries. By taking a comprehensive approach that considers both direct and indirect emissions, stakeholders can make decisions incorporating advanced technology, process modification, and sustainable materials and practices to reduce the carbon intensity of cement manufacturing while advancing sustainability goals.

Keywords: Carbon dioxide emission; Cement; Manufacturing Process; Limestone; Clinker

1. Introduction

Cement, a fundamental construction component, has played a pivotal role in shaping the modern built environment. As societies evolve and urbanize, the demand for robust and sustainable infrastructure has intensified, making cement a crucial material for meeting these challenges. According to the Statista Research Department 2023 report, the volume of cement production has increased by 206 million metric tons to 381 million metric tons in the last two decades¹⁾. At Present, India is having 333 cement manufacturing units out of which 150 are large integrated cement plants, 116 are griding, 62 mini cement plant and 5 clinkering plants. Where, Madhya Pradesh, Chhattisgarh, Andhra Pradesh, Rajasthan, and Gujarat, are the highest cement manufacturer states in India. This versatile binding agent is utilized in many construction applications, ranging from towering and expansive bridges to residential homes and essential public amenities. The per capita demand for 200-250 kg cement is intricately tied to global population growth and urbanization²⁾. As more people migrate to cities, the need for housing, transportation networks, and commercial spaces has

surged³⁾. This has led to consistent and escalating demand for cement as a primary construction material.

Additionally, emerging economies and developing nations are investing heavily in infrastructure projects, that further contributing to the global demand for cement^{4,5)}. Per capita consumption in India is 200- 250 kg/yr. as compared to Global per capita consumption of 500-550kg⁶⁾. it is expected to grow by 8 to 15 percent over the next few years, driven by rural housing demand and the government's strong focus on infrastructure development and a multimodal transportation network. The increased demand for cement directly boosts carbon dioxide emissions.

Cement production requires high-temperature processes, particularly the calcination of limestone (calcium carbonate), which produces clinker, the primary ingredient in cement. This calcination process produces CO₂ as a byproduct of the chemical reaction in which limestone decomposes into lime (calcium oxide) and CO₂. Furthermore, the grinding of raw materials, the production of clinker in kilns, and the grinding of cement all require significant energy inputs, primarily from fossil fuels like coal and natural gas—the combustion of these fuels releases CO₂ directly into the atmosphere. Limestone,

95% of the raw material used, plays an indispensable role in clinker production, contributing to the strength, durability, and overall quality of Portland cement. Its calcination process and fluxing properties ensure the formation of essential clinker compounds. Figure 1 shows the production of limestone and Cement Production of limestone & Cement in India. In 2021, Global cement production was 4.37 billion tons, while in India it was 349.12 metric ton which is the world's second-largest cement manufacturing country⁷⁾. State wise CO₂ emission from cement plant is not available. Production of cement is 10 to 15% less than the limestone used. In the upcoming decade, the Indian cement industry is poised for remarkable growth, with anticipated demand set to soar to 2.5 to 2.7 times its current volumes, reaching an estimated 550 to 600 million metric tons per annum (MTPA) by 2025⁸⁾. Meanwhile, China maintains its dominance, consuming a staggering 2119 million tons in 2022, representing 52% of global demand. The second-largest consumer, with 387.335 million tons in 2022, experienced an 8.1% expansion in 2023. This growth is attributed to persistent urbanization and industrialization trends, supporting both consumption and a rapid pace of capacity expansion for the foreseeable future.

On the other hand, demand in the US, the world's third-largest consumer, faced a slight setback, with an estimated 2.7% decline in 2023, reaching 108 million tons. This dip is attributed to challenges posed by interest rates, impacting homebuilders and homebuyers. Despite this setback, the global cement landscape showcases dynamic trends, with each region navigating its unique set of factors influencing demand and consumption⁹⁾.

Cement production also requires transporting raw materials, fuels, and finished products over long distances, contributing to additional CO₂ emissions. Because cement markets are global, raw materials can be sourced in one region, transported to manufacturing facilities in another, and distributed to construction sites in various locations, resulting in significant transportation emissions.

Concrete is made by mixing cement with aggregates (such as sand and gravel) and water, and the chemical reaction between cement and water emits additional CO₂. Furthermore, the carbonation of concrete over time results in the absorption of atmospheric CO₂, but this process is relatively slow, with 100 years of concreting considered. Assessment of CO₂ includes the emission during the life cycle of cement (Cradle to Grave), from the quarry of raw material to the demolition of concrete¹¹⁾. The direct emissions of CO₂ from clinker, OPC, PPC, PSC, and composite cement are 779kgCO₂/t clinker, 740 kgCO₂/t, 507kgCO₂/t, 312kgCO₂/t and 315kgCO₂/t of cement respectively. While for the manufacturing process, these are 850kgCO₂/t clinker, 84kgCO₂/t, 582kgCO₂/t, 318kgCO₂/t, and 418kgCO₂/t of cement respectively¹⁰⁾. In China, manufacture direct emission, manufacture direct process manufacture neat emission of CO₂ for clinker are 0.7628t/t, 0.8143t/t, and 0.4878t/t of clinker respectively.

Similarly, for OPC these values are 0.7265t/t, 0.8077t/t, and 0.4646t/t of cement respectively. The CO₂ emission of the Cement life cycle is 0.5884t/t of cement as calculated by W. Shen¹³⁾.

The objective of this study is to comprehensively quantify the carbon emissions associated with various stages of cement production, focusing on direct manufacturing, manufacturing processes, and the entire life cycle. This study is based on a detailed understanding of the carbon footprint, particularly in raw material extraction and cement manufacturing within cement plants. By utilizing a variety of metrics, including raw material extraction rates, fuel consumption, electricity usage, transportation distances, and life cycle assessments. The final output is to determine the carbon dioxide emission factors with clinker and, subsequently, propose recommendations for stakeholders to reduce the carbon intensity of cement manufacturing by incorporating advanced technology, process modification, and adopting sustainable materials.

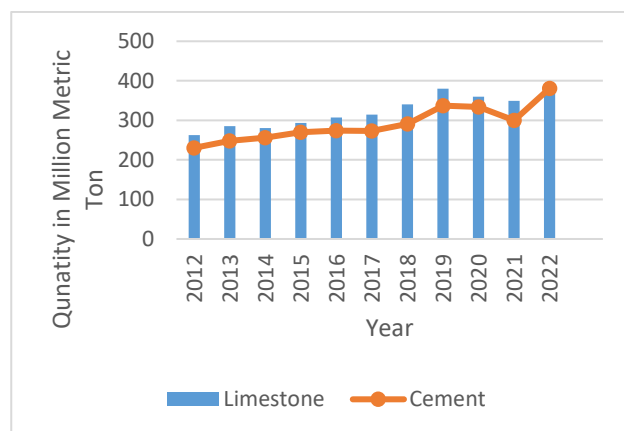


Fig. 1: Limestone and Cement consumption by the Indian cement industry

2. Manufacturing of cement

Raw materials for cement production are typically obtained from quarries or mines near the cement plant. The primary ingredient, limestone, is extracted from open-pit mines via drilling, blasting, and hauling techniques. Limestone deposits are commonly found in sedimentary rock formations and are high in calcium carbonate, making them ideal for cement production. Once extracted, limestone is crushed and screened to reduce size and remove impurities. This crushed limestone and other raw materials like clay and iron ore are then delivered to the cement plant for further processing.

Clinker, the most important component of cement, is made from a mixture of raw materials such as limestone, sand, and clay. Sand and clay provide the remaining silica, alumina, and iron requirements that are not met by limestone. The powdered raw material is thoroughly mixed and preheated to 900°C to burn impurities in the kiln. The materials are then heated to 1450°C for de-carbonation in a cement kiln, where CO₂ is liberated from

the burning of limestone, and a slurry of the materials is formed. Material heating converts slurry into small balls known as clinker. Clinkers are ground into fine powder in

a ball mill after cooling. Gypsum is also added in small amounts during the grinding process to control cement

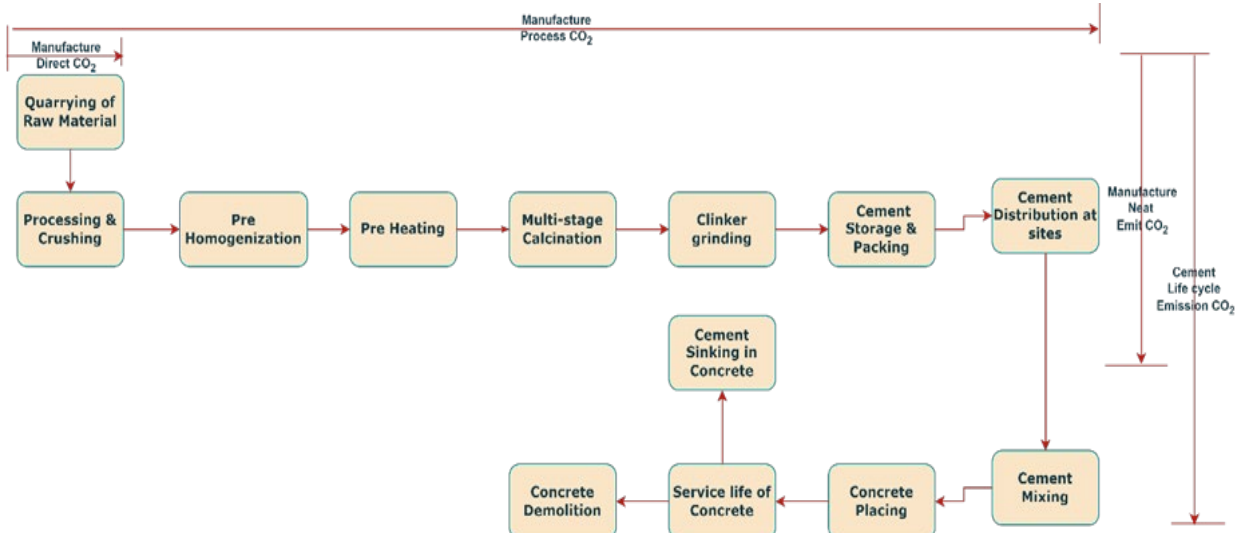


Fig.2: Manufacturing Process of Cement

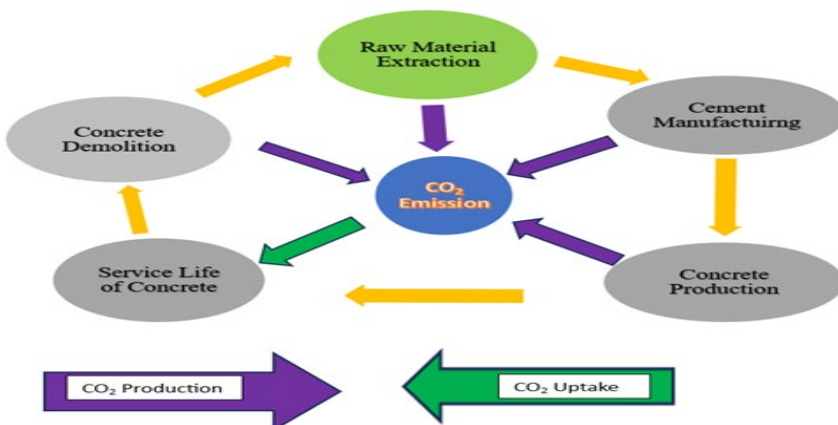


Fig. 3: Carbon Footprint during Life Cycle of Cement

setting. The manufactured cement is transported directly to silos and packaged in 50 kg bags^{10,12)}. After that, cement is transported to the distributor to sell for construction purposes. At the construction site, concrete mix is prepared using all ingredients like Cement, fine & Coarse aggregates, SCM, and water. The placement of concrete is done as per the infrastructure design /element. Concrete serves till any damage or renovation takes place in the structure. Carbonation sinks carbon dioxide during the concrete service life or in landfilling after demolition¹³⁾. Further, the boundary system of Direct manufacture, Direct manufacture process, manufacture neat emission, and cement life cycle of CO₂ emission¹³⁾ is also shown in Fig. 2.

Extraction of raw material, manufacturing of cement, Concrete Production, and demolition emit CO₂ into the atmosphere while concrete during its service life uptake the CO₂ from the atmosphere which is also called the

sinking of carbon dioxide¹³⁾ as shown in Fig. 3.

According to (the World Business Council for Sustainable Development¹⁴⁾, the direct manufacturing process emissions source of CO₂ includes raw material - calcination, direct stationary combustion in furnaces, fossil fuels, and mobile emissions from the company-vehicle used in the cement manufacturing process. At the same time, the indirect emission is the electricity purchased for a cement manufacturing plant.

3. CO₂ emission from various units in the Indian Cement industry

(a) CO₂ emission from raw materials Carbon emission from raw materials is the summarization of CaO and MgO available in the raw materials, which can be calculated by eq. (i)

$$RM\text{-CO}_2 = M_{CaO} \times (44/56) \times R_{CaCO_3} + M_{MgO} \times (44/40) \times R_{MgCO_3} \quad (1)$$

Where Cao and MgO are 65% and 2% respectively, the average percentage in the clinker. R_{CaCO_3} and R_{MgCO_3} are 95% and 75% respectively. The percentage of CaO and MgO of OPC - 43 are obtained from chemical analysis of material shown in Table 1. The high percentage of CaO (57.21%) suggests that this cement is rich in calcium, a key component for strength development during the hydration process.

The SiO_2 content (20.58%) indicates a significant presence of silica, contributing to the cement's overall structure. Al_2O_3 and Fe_2O_3 together make up about 8.9%, influencing the cement's color and stability. The presence of Na_2O and K_2O indicates potential susceptibility to alkali-silica reactions, which may need attention during concrete mix design.

From above eq.1, RM-CO₂ emission obtained is 0.501t CO₂/t clinker and 0.4762 t/t of cement, which is slightly less than the worldwide and Indian emission of CO₂ from one ton of clinker is 0.507t /ton of clinker and 0.528t/t clinker respectively^{15,16}). According to the IPCC method, the emission factor is 0.510t/t clinker without MgO¹⁷). With the CSI clinker-based method the emission is 0.525t/t clinker with MgO.

Table 1. Chemical composition of OPC 43

Parameter	OPC 43
SiO ₂	20.58
Al ₂ O ₃	4.98
Fe ₂ O ₃	3.89
CaO	57.21
Na ₂ O	0.15
SO ₂	2.54
K ₂ O	0.57
MgO	1.27
LOI	4.0

Use of Calcium sulphaaluminate contains a high amount of limestone and unused overburden bauxite from mining can be used as raw material to reduce two- third of the CO₂ emission¹⁸). The use of Geopolymer concrete instead of OPC concrete can reduce CO₂, it has good mechanical strength and durability properties^{19,20,21,22}.

(b) CO₂ emission from fuel used

It is the emission from the fuel used in the calcination of clinker and the machine used in the plant, except the vehicle to transport the raw materials.

$$Fuel\text{-CO}_2 = P/29.307x EF_{coal} + V_{diesel} \times EF_{diesel}/1000 \quad (2)$$

Where P is Thermal energy consumption by the clinker system, e.g., Five stage cyclone pre-heater plus pre-calciner with energy efficient cooler, is 3.026GJ/t clinker and 3.4GJ/t cement (Including clinker) in India^{23,24}. V is

the total amount of diesel used in machines during cement manufacturing 1.72Lt/t clinker and 4.83 Lt/ton cement (including clinker)^{25,26}. During the heating and burning process of raw materials in the kiln, decomposition reactions, transformation, and new phases occur. The cement manufacturing plant consumes approximately 70-80 percent of total energy in the form of thermal energy and the remaining energy (20-30%) is electrical energy^{27,28}. Coal and Diesel emission factors are 2.4567tCO₂/t of coal and 2.764 kgCO₂/Lt of diesel^{29,30}. Fuel – CO₂ emission for clinker is 0.2584t/t of clinker and 0.2455t/t of cement. The emission of CO₂ is 0.2953t/t of clinker based on fuel; the value may vary as per production technology adopted in China¹⁷.

Using biomass, solid-derived fuel (SDF), and Refuse-derived fuel (RDF) instead of coal can reduce CO₂ emissions, Waste lubricant oils, Plastics, Used tires, Sewage sludge, Timber waste, etc. Although all fuels emit CO₂, certain alternative fuels are considered CO₂-neutral. Growing organic materials capture CO₂, which is then released when burned, resulting in zero CO₂ emissions. Using alternative materials, such as used tires, can also be considered an environmentally responsible alternative to dumping them in landfills^{31,32}.

(c) CO₂ emission from electricity consumption

Electric energy is required in cement plants to extract and prepare raw materials, clinker production, fuel grinding, cement grinding, and cement packaging and loading.

$$ED\text{-CO}_2 = \sum M \times EI \times EF_{electricity} \quad (3)$$

M= Mass of material used to manufacture one ton of cement is 1.55-ton clinker²⁵). EI is the electricity used in the crusher, raw mill, Kiln & cooler, and Coal mill is 40.37kWh/t, and in the Cement mill and packaging plant is 30.74kWh/t evaluated by Shakti Sustainability Energy Foundation³³). EF electricity emission factor in India is 1.19kgCO₂/kWh as per the Electricity GHG Inventory Report³⁴. Electricity consumed in the Indian cement industry is purchased from the regional grid and, therefore, is not included in the calculation. Electricity CO₂ emission is found to be 0.0749 t/t of clinker and 0.0846t/t of cement, which is generated from waste heat recovery technology. It is 0.02633t CO₂/t clinker in China because electricity consumption in the kiln is less (23.14Kwh/t clinker) than in India¹⁷.

Developing and implementing low-carbon cement grinding technology and equipment can help reduce power consumption and up to 10% CO₂ emission while improving clinker quality³⁵). Application of 10%Zelolite, 15%kaoline, or 25% combination of both can reduce CO₂ emission to a large extent due to the similar properties of cement³⁶.

(d) CO₂ emission from vehicles used for transportation

It summarizes CO₂ emitted while transporting raw material, gypsum SCM to the cement plant, placing fresh concrete, and disposal of C&D concrete waste.

$$TD\text{-CO}_2 = \sum M \times D \times FC \times EF_{diesel} \quad (4)$$

Where M is the mass of material transported, D is the distance covered by the vehicle. FC is the fuel consumption during transportation.

EF diesel vehicles are 0.1023 CO₂/t-km for LDV and have a loading capacity of more than 3.5T, as per India's GHG program 2015³⁷⁾. The average distance traveled for raw material is 10km, where Gypsum and coal are 300km, admixture traveled 10km, and fresh and demolished concrete and vehicles covered 20km and 50 km, respectively. The quantity of material for manufacturing cement is considered as Raw material – 1.5t/one ton of cement, Gypsum – 0.050t/one ton of cement²³⁾, Coal-0.215t/one ton of clinker³²⁾. TD – CO₂ emission of Clinker, Cement, and Concrete are shown in Table 2–

Table 2: CO₂ emission from the transportation of materials.

Table 2: CO ₂ emission from the transportation of materials.					
Product	Material	Mass (t)	D (km)	EF (kgCO ₂ /t-km)	CO ₂ (t)
Clinker	Raw Material	1.50	10	0.1023	0.00153
	Coal	0.215	300	0.1023	0.00660
Cement	Raw Material	1.50	10	0.1023	0.00153
	Coal	0.215	300	0.1023	0.00660
	Gypsum	0.05	300	0.1023	0.00153
Concrete	Cement	1.00	100	0.1023	0.01023
	Fresh concrete	1.43	20	0.1023	0.00293
	Waste concrete	1.43	50	0.1023	0.00731

Transportation accounted for up to 20% of total emissions^{33).}

(e) LC-CO₂ emission at the life cycle of concrete

Water is responsible for cement hydration, workability, and strength development in concrete. Therefore, the CO₂ emission from water with the cement is included during the life cycle of concrete. The total quantity of material flow in the concrete life cycle is equivalent to the mass of cement paste. The life cycle of concrete involves activities like mixing, placing, and demolition of concrete, and CO₂ emissions are 0.0004kgCO₂, 0.0025kgCO₂, and 0.000538 kgCO₂ per kg of concrete^{29,30}. This paper uses 406.604kg cement, Fine & Coarse (FA & CA) aggregates with 0.43 water–cement ratio to prepare 1 m³ M35 grade concrete. The total quantity of material flow is 1.43, excluding the FA & CA.LC-CO₂ = 0.00492t/t cement used in concrete

(f) CO₂ sinking during carbonation (S-CO₂)

Concrete will absorb atmospheric CO₂ over time if exposed to air. This is known as carbonation, an inherent property of Portland cement-based concrete. Carbonation will occur both during and after the service life of a concrete structure. The carbonation rate may be affected if the concrete contains supplementary cementitious

materials, either as part of the cement or added directly at the concrete batch plant. Limestone increases the carbonation rate by lowering the clinker content per unit volume of concrete. The paste's buffering capacity decreases because less hydration product or CaO per unit volume can be carbonated.

$$\text{CO}_2 \text{ absorbed by concrete (kg/m}^3 \text{ concrete)} = 0.75 \times C \\ = 0.383x C, \text{ where } C \text{ is the amount of cement in } 1m^3 \text{ concrete} \quad (5)$$

For these calculations, a lifetime of 100 years was used, with the service life of the concrete estimated to be 70 years. Carbonation of demolished concrete was calculated for 30 years⁴⁰). CO₂ sinking is 0.365t/t of cement.

CO₂ emission at various phases of cement production in the cement industry based on the values shown in Table 3^{40,41)}:

Manufacture Direct CO₂ = RM-CO₂ + FD-CO₂.... (6)

Manufacture Process CO₂ = RM-CO₂ + FD-CO₂ + ED- CO₂ + TD-CO₂ (Cement produce) (7)

Manufacture Neat Emit = RM-CO₂ + FD-CO₂ + TD-CO₂ (Cement produce) + S-CO₂.....(8)

Cement Life Cycle Emission CO₂ = RM-CO₂ + FD-CO₂ + ED-CO₂ + TD-CO₂ (Cement produce) + S-CO₂ + LC-CO₂ + TD-CO₂ (Concrete life Cycle) (9)

Table 3: Emission of CO₂ at various phases of cement manufacturing

Phases	Clinker	OPC Cement
RM - CO₂	0.5012	0.4371
FD - CO₂	0.2584	0.2455
ED - CO₂	0.0749	0.0846
TD - CO₂	0.0081	0.0097
LC -CO₂	---	0.0049
TD -CO₂(Con)	---	0.0205
S - CO₂ (-ve)	0.3840	0.3650

Table 4: The CO₂ emission factor of cement production

CO₂ emission from	Clinker	OPC Cement
Manufacture Direct	0.7597	0.6826
Manufacture Process	0.8427	0.7769
Manufacture Neat Emit	0.3838	0.3273
Cement Life Cycle	----	0.4373

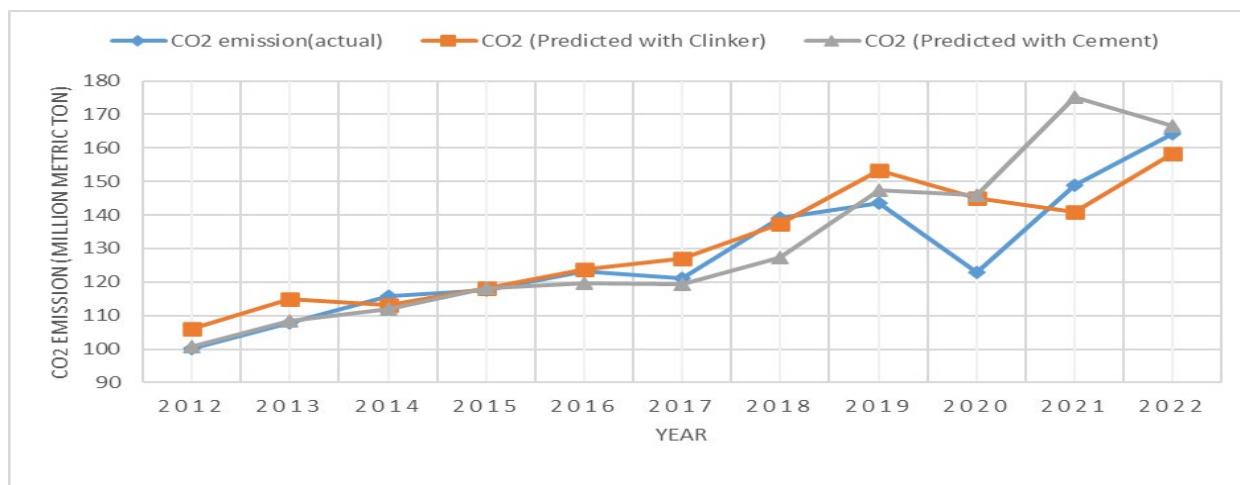


Fig. 4: CO₂ emitted from Indian Cement Industry.

Table 4 shows that CO₂ emission factors are calculated at different phases based on the inventory for cement production. The Manufacture direct CO₂ emissions factors for Clinker and cement are 0.7597t/t & 0.6826t /t respectively. It is the sum of CO₂ emissions from raw material and fuel used during calcination in machines.

The direct manufacture CO₂ emission factor is 0.0771 more for Clinker, as the quantity of raw material and material to be calcined in the kiln is 1.5 times the cement produced. The range in developing countries is 0.825t – 0.890t CO₂/t of clinker, while worldwide, it is 0.840t/t of clinker³⁰.

The total CO₂ emission factors during the manufacturing process of clinker and Ordinary Portland Cement are 0.842t/t clinker & 0.819t /t respectively, similar to the estimated values by researchers Parth & Shrivastava^{16,42,43}. In Spain it is found to be 0.9245t/t clinker²⁴. It is obtained by adding CO₂ emission from consumption of fuel and energy, during transportation of material and calcination. The manufacturing process CO₂ emission factor of clinker is 0.0658 more than the cement because it depends upon the clinker factor (the mass ratio of clinker to cement) and production technologies⁴⁴.

The Neat CO₂ emission factor of clinker includes the CO₂ emitted from raw material, fuel consumed, and transportation, except electricity used in grinding because the industry purchases it. For clinker and cement it is equivalent to 0.3838t/ton of clinker and 0.3273t/ton of cement respectively. The Neat CO₂ emission value in Spain is 0.3471t/ton of clinker³⁰.

The cement life Cycle Emission is the sum of CO₂ from Neat emission from cement produced and the lifecycle emission of concrete. Therefore, clinker has zero values while cement used in manufacturing concrete is 0.4373t/ton of cement.

Total CO₂ emission during cement manufacturing from the cement industry calculated by –

$$\text{Total CO}_2 \text{ emission (Yearly)} = 0.3838 \times \text{limestone consumption in cement industries yearly....} \quad (5)$$

$$\text{Total CO}_2 \text{ emission (Yearly)} = 0.4373 \times \text{Cement produced in that year} \quad (6)$$

3.2 Assessment of Carbon emission from the Indian cement Industry

CO₂ emission from the cement industries (2011 – 2022) is assessed by equations 5 &6 based on the quantity of limestone extracted and cement produced in the respective years as shown in Fig.4. All the values of CO₂ emissions except in the years 2020 & 2021 due to COVID-19, with limestone and cement are approximately the same Limestone is 95% of the raw material; therefore, it is used to evaluate CO₂ emissions as clinker. The overall CO₂ emissions varied, with notable peaks in 2019, 2021, and 2022. CO₂ emission shows a 64 % increase in the year 2022 as compared to 2012.

CO₂ emissions per unit of clinker produced ("CO₂ (Clinker)") showed variability, reaching a peak in 2019. It offers a 49% increase in 2022 as compared to 2012.

In FY 2023 – 2024 the production of limestone is 450MMT⁴⁵) and it is predicted that CO₂ emission from the cement industry will be 172.71MMT.

4. Application of CO₂ emission factors –

Assessing carbon emission factors from cement plants is critical for understanding and mitigating the environmental impact of cement production, which is well known for its significant contribution to global carbon dioxide (CO₂) emissions. By quantifying the amount of CO₂ emitted per tonne of cement produced, stakeholders can better understand the true scope of emissions associated with cement manufacturing, providing valuable insights into its impact on climate change.

Furthermore, evaluating carbon emission factors makes comparing cement production facilities to industry standards and peers easier. This comparative analysis identifies areas for improvement and establishes targets for lowering carbon emissions, fostering a culture of continuous improvement in the industry⁴⁶.

Identifying key stages in the manufacturing process that contribute the most to CO₂ emissions, such as clinker production and energy consumption, is critical for cement plants looking to reduce their environmental impact. Adopting cleaner production technologies, such as alternative fuels, energy-efficient kilns, and carbon capture and storage systems, provides tangible pathways to emission reduction and sustainability⁸⁾.

Furthermore, accurate carbon emission factors are critical inputs for performing life cycle assessments (LCA) on cement products. LCA assesses the

environmental impacts of products from raw material extraction to end-of-life disposal, allowing for informed decisions about sustainable procurement. This comprehensive approach ensures a thorough understanding of the environmental performance of cement products⁴⁷⁾.

Determining carbon emission factors is even more critical in areas with carbon pricing mechanisms or participation in carbon markets. This data is required for calculating carbon liabilities and credits associated with cement production, allowing involvement in carbon trading schemes and incentivizing cost-effective emission reduction measures^{48,49,50)}.

5. Conclusion

In conclusion, this study has successfully quantified the carbon emissions at various critical stages of cement production, providing a comprehensive overview of the industry's environmental impact. The identified carbon dioxide emission factors, particularly with clinker, offer precise metrics crucial for understanding and addressing the challenges associated with carbon intensity in cement manufacturing.

The findings reveal a carbon dioxide emission factor of 0.3838t/ton of limestone and 0.4373t/ton of cement based on manufacturing neat emissions and the entire life cycle of OPC cement.

The assessment is based on dry cement manufacturing process in India. It may vary with the Chemical composition of Cao and Mgo in raw material and distance from the mining & cement industry which is 10km and 300km considered in the present study.

By partially or fully replacement of cement, use of biomass as fuel, type of vehicle and decreasing travelling distance, CO₂ emission can be reduced up to large extent.

The uniform emission factor underscores the need for targeted efforts to optimize transportation and explore sustainable sourcing and energy alternatives to mitigate environmental impact. Addressing these key factors across the entire production chain is imperative for the cement and concrete industry to contribute meaningfully to carbon reduction goals.

Overall, evaluating carbon emission factors from cement plants is critical for improving the sustainability of cement production. It forms the foundation of a more environmentally responsible cement industry by

informing decision-making, driving innovation, and facilitating efforts to mitigate climate change.

References

- 1) T. Ian, "CO₂ emissions from cement manufacturing in India 1960-2022. Delhi: Energy & Environment" (2023). <https://www.statista.com/statistics/1198693/carbon-dioxide-emissions-cement-manufacturing-china/>. (accessed on March 2024).
- 2) V. Malik, M. Sharma, and S. Bandyopadhyay, "Cement Industry: Trends and Prospects", Industry Outlook, Published by Infomerics Valuation and Rating Pvt. Ltd, pp. 1-7. (2022). https://www.infomerics.com/admin/uploads/Indian_Cement_Industry_Nov_19_2020.pdf. (accessed on November 23, 2023).
- 3) S. Irudaya, Rajan, and R.B. Bhagat, "Internal Migration in India: Integrating Migration with Development and Urbanization Policies," *KNOMAD, Policy Brief*, 12, pp. 1-5. (2021).
- 4) E. Subiyanto, "The relationship of Cement Consumption and Economic Growth: An Updated Approach," *European Research Studies Journal*, 23(3), 280-295 (2020). <http://dx.doi.org/10.35808/ersj/1638>.
- 5) H.U. Sverdrup, and A.H Olafsdottir, "Dynamical Modelling of the Global Cement Production and Supply System, Assessing Climate Impacts of Different Future Scenarios," *Water Air Soil Pollution*, 234(191) 1-19 (2023). doi.org/10.1007/s11270-023-06183-1.
- 6) Systematix, "Indian Cement Industry. Delhi," published by Systematix Shares and Stocks (India) Limited," (2021). <https://intra.systematixgroup.in/Institutional/IPOMail/Indian%20Cement%20Industry%20-%20IC%20-%2001-09-2021%20-%20Systematix.pdf>. (accessed on October 20, 2023).
- 7) Jaganmohan, and Madhumitha, "Limestone production volume in India FY 2012-2023. USA: statista," (2023). <https://www.statista.com/statistics/1198693/carbon-dioxide-emissions-cement-manufacturing-china/> (accessed March 14, 2024).
- 8) Construction. com., "Green Building Practices with Prefabrication. Manchester: Utilities One," (2023).
- 9) Cement.Com. 2024. "Cement industry looks forward to sustainable progress in 2024.", Jakarta, Indonesia: Cement News, 1. Accessed February 26, 2024. <https://www.cemnet.com/Conference/Item/193101/cemtech-asia-2024.html>.
- 10) Global Cement and Concrete Association, "Blended Cement - Green, Durable & Sustainable - 2022," published in April 2022, gccassociation.org (Accessed on 15August 2024)
- 11) Olagunju, D. Busola, and O. A. Olanrewaju, "Life

- Cycle Assessment of Ordinary Portland Cement (OPC) Using both Problem Oriented (Midpoint) Approach and Damage Oriented Approach (Endpoint)", Edited by Antonella Petrillo and Fabio De Felice. (2021). doi: 10.5772/intechopen.98398.
- 12) Y. K. Verma, D. Ghime, B. Mazumdar, and P. Ghosh, "Emission reduction through process integration and exploration." *International Journal of Environmental Science and Technology*, (2023). pp.13329 - 13346.
- 13) W. Shen, L. Cao, Q. Li, W. Zhang, G. Wang and C. Li, "Qunatifying CO₂ emission from China's cement industry," *Renewable and Sustainable Energy Review*, 50 1004 - 1012. (2015). <https://doi.org/10.1016/j.rser.2015.05.031>
- 14) World Business Council for Sustainable Development (WBCSD, 2005). "Cement Tool Guidance Document: India Version 1.0. Delhi: TERI." (2005). https://ghgprotocol.org/sites/default/files/2023-03/India_Cement_tool_guidance.pdf. (accessed January 15, 2024).
- 15) M.J Gibbs, P. Soyka, D. Conneely, and M Kruger, "CO₂ Emissions from Cement Production. Good Practice Guidance and Uncertainty Management in National Greenhouse Gas Inventories," *Industrial Processes*, pp.175-182. USA. (2000). https://www.ipcc-nnigip.iges.or.jp/public/gp/bgp/3_1_Cement_Product ion.pdf.
- 16) Shrivastava, K. Amit, A. Vashishth, and B. Jayant, "Deterministic approach for calculation of Carbon Footprint for Cement plants in India," *Research Square*, pp. 1-20. (2020). doi.org/10.21203/rs.3.rs-285464/v1.
- 17) T. Gao, M. Shen, L. Shen, F. Chen, L. Liu, and L. Gao, "Analysis on differences of carbon dioxide emission from cement production and their major determinants," *Journal of Cleaner Production*, (103)160 - 170 (2015). <http://dx.doi.org/10.1016/j.jclepro.2014.11.026>.
- 18) Negrão, L. B. Ayres, H. Pöllmann, and M. L. da Costa, "Production of low-CO₂ cements using abundant bauxite overburden," *Sustainable Materials. and Technique*, 29. pp. 1-11 (2021) doi:10.1016/j.susmat.2021.e00299.
- 19) M. Verma, and M. Nigam, "Effect of FRP on the strength of geopolymers concrete," AIP Conf. Proceeding, FSAET - 2021, 2721 020030 (2023). doi.org/10.1063/5.0154114
- 20) M. Nigam and M. Verma, "Effect of nan-silica on the fresh and mechanical properties of conventional concrete," *Force in Mechanics*, (10) 1-7. (2023). doi.org/10.1016/j.finmec.2022.100165.
- 21) R. Kumar, M. Verma, and N. Dev, "Investigation on the effect of seawater condition, sulphate attack, acid attack, freeze - thaw condition, and wetting - drying on the geopolymers concrete," *Iranian Journal of Science and Technology, Transactions of Civil Engineering*, (46) 2823 - 2852. (2022). doi.org/10.1007/s40996-021-00767-9.
- 22) U. Sharma, N. Gupta, and M. Verma, "Prediction of compressive strength of GGBFS and flyash - based geopolymer composite by linear regression, lasso regression, and ridge regression," *Asian Journal of Civil Engineering*, 24 (8) 3399 - 3411. (2023). doi.org/10.1007/s42107-023-00721-2.
- 23) Technical EIA Guidance Manual for Cement Industry. Delhi: IL&FS Ecosmart Limited, pp.1-185, https://dste.py.gov.in/SEIAA/pdf/Sector/Isolated_Sto rages.pdf. (accessed on 12 December 2023).
- 24) A. Mokhtar, and M. Nasooti, "A decision support tool for cement industry to select energy efficiency measures," *Energy Strategy Reviews*, 28, pp.1-14 (2020). <https://doi.org/10.1016/j.esr.2020.100458>.
- 25) Ei. Thwe, D. Khatiwada, and A. Gasparatos, "Life cycle assessment of a cement plant in Naypyitaw, Myanmar," *Cleaner Environment System*, 2, 1 - 9. (2021). doi.org/10.1016/j.cesys.2020.100007.
- 26) A. Setiawan, Md. Y. J. Purwanto, and K. Siregar, "The Life Cycle Assessment of Cement Product with Alternative Fuels Usage in Indonesia," *Journal of Natural Resources & Environment Management*, 11 (3) 474-489. (2021). doi.org/10.29244/jpsl.11.3.474-489.
- 27) Y. K. Verma, B. Mazumdar, and P. Ghosh, "Thermal energy consumption and its conservation for a cement production unit," *Environment Engineering Research*, 26 (3) 1 - 17 (2021). <https://doi.org/10.4491/eer.2020.111>.
- 28) S. Kumari and R. Walia, "A comparative study of life cycle assessment of sustainable concrete mixes," *Journal of Materials and Engineering Structures*, 9. 187 - 196 (2022).
- 29) A. Loijos, "Life cycle assessment of concrete pavements: impacts and opportunities," Massachusetts Institute of Technology. (2011).
- 30) M.A. Sanjuán, M. Ángel, C. Andrade, P. Mora, and A. Zaragoza, "Carbon Dioxide Uptake by Cement-Based Materials: A Spanish Case study," *Applied Science*, 10 (339) 1-16 (2020). <https://doi.org/10.3390/app10010339>.
- 31) E. Beguedou, S. Narra, E. A. Armoo, K. Agboka, and M. K. Damgou, "Alternative Fuels Substitution in Cement Industries for Improved Energy Efficiency and Sustainability," *Energies*, 16(8) 3533 (2023). <https://doi.org/10.3390/en16083533>.
- 32) GCP Applied Technologies, "Using alternatives fuels in cement production," published September 15(2020). <https://gcpat.com/en/about/news/blog/using-alternative-fuels-cement-production>. (accessed on 21 December 2023).
- 33) SSEF (2012), "A study of Energy Efficiency in the Indian Cement Industry. Bangalore: Centre for Study

- of Science, Technology and Policy,” 1-184. <https://shaktifoundation.in/wp-content/uploads/2017/06/A-study-of-EE-in-the-cement-industry.pdf>. (accessed on November 12, 2023).
- 34) V. Gilani, “GHG Inventory report for Electricity generation and consumption in India,” cBalance Blog. (2014). <https://cbalance.in/2014/05/ghg-inventory-report-for-electricity-generation-and-consumption-in-india/>. (accessed on 28 October 2023).
- 35) Zerbe, Rüdiger. 2024. Grinding for green goals. China: ICR Research.
- 36) S. A. A. Wahab, E. M. Hassan, K. S. Al-Jabri, and K. Yetilmezsoy, “Application of zeolite/kaolin combination for replacement of partial cement clinker to manufacture environmentally sustainable cement in Oman,” *Environmental Engineering Research*, 24 (2) 246-253 (2019). <https://doi.org/10.4491/eer.2018.047>.
- 37) GHG, India. 2015. India- Specific -Road-Transport-Emission- Factor. Delhi: WRI-2015.
- 38) J. D. Bapat, “Quality of coal for Indian cement industry,” *Indian Cement Review*, 28 (8): 41- 42 (2014).
- 39) A. A. L. Pachecoa, L. S. Oliveira, V. M. John, and S. C. Anguloa, “Transportation impact on CO₂ emissions of concrete: a case study in Rio Branco/Brazil,” *IBRACON Structures and Material Journal*, 15 (6) 1-13. (2022). <https://doi.org/10.1590/S1983-41952022000600009>.
- 40) P. Claus, and M. Guimaraes, “The CO₂ uptake of concrete in a 100 year perspective,” *Cement and Concrete Research*, 37 (9) 1348-1356 (2007). <https://doi.org/10.1016/j.cemconres.2007.06.009>.
- 41) W. Shen, L. Cao, Q. Li, W. Zhang, G. Wang, and C. Li, “Quantifying CO₂ emissions from China’s cement industry,” *Renewable and Sustainable Energy Reviews*, 50 (1) 1004 - 1012 (2015). <http://dx.doi.org/10.1016/j.rser.2015.05.031>.
- 42) Kumar, Parth. 2023. *Cementing possibilities*. Down to Earth, New Delhi, Published on September 27, 2023. <https://www.downtoearth.org.in/news/environment/cementing-possibilities-91980>. (accessed on November 15, 2023).
- 43) M. Antunes, R. L. Santos, J. Pereira, P. Rocha, R. B. Horta, and R. Colaço, “Alternative Clinker Technologies for Reducing Carbon Emissions in Cement Industry: A Critical Review,” *Materials*, 15 (1) 1-19 (2022). <http://dx.doi.org/10.3390/ma15010209>.
- 44) K. W. Rychter, and A. Smoliński, “Multi-Case Study on Environmental and Economic Benefits through Co-Burning Refuse-Derived Fuels and Sewage Sludge in Cement Industry,” *Materials*, 15(12)1-18. (2022). <https://doi.org/10.3390/ma15124176>.
- 45) Energyworld.com, “India's key mineral production sees robust growth in Q1 FY 2024 - 25”, published in August 2024,. <https://energy.economictimes.indiatimes.com/news/copal/indias-key-mineral-production-sees-robust-growth-in-q1-fy-2024-25/112190534> (Accessed August 15, 2024).
- 46) S. Prakasan, S. Palaniappan, and R. Gettu, “Study of Energy Use and CO₂ Emissions in the Manufacturing of Clinker and Cement,” *Journal Institute of Engineers Series A*, 1-12 (2019). doi: 10.1007/s40030-019-00409-4.
- 47) A. Kumar, “Present Scenario of Green Buildings in India,” *International Journal of Trend in Scientific Research and Development*, 6 (5) 538 – 543 (2022). https://issuu.com/ijtsrd.com/docs/67_present_scenario_of_green_buildings_in_india.
- 48) C. Chea, P. Ket, L. Taing, S. Kong, D. Um, C. Taing, C. Or, S. Aun, and L. Hang, “Life-Cycle Impact Assessment of Air Emissions from a Cement Production Plant in Cambodia,” *Open Journal of Air Pollution*, 11 (4) 1-19 (2022). <https://doi.org/10.4236/ojap.2022.114007>. (Accessed March 03, 2024).
- 49) S. Nie, J. Zhou, F. Yang, M. Lan, J. Li, Z. Zhang, Z. Chen, M. Xu, Hui Li, and J. G. Sanjayan, “Analysis of theoretical carbon dioxide emissions from cement production: Methodology and application”. *Journal of Cleaner Production*, 334, pp.1-18 (2022). <https://doi.org/10.1016/j.jclepro.2021.130270>.
- 50) B. Bakhtyar, T. Kacemi, and Md. A. Nawaz, “A Review on Carbon Emissions in Malaysian Cement Industry,” *International Journal of Energy Economics and Policy*, 7 (3) 282-286 (2017).

scientific data



OPEN

DATA DESCRIPTOR

Global CO₂ uptake by cement materials accounts 1930–2023

Songbin Wu^{1,2,10}, Zi Shao^{3,4,10}, Robbie M. Andrew⁵, Longfei Bing^{1,6,7}, Jiaoyue Wang^{1,6,7}, Le Niu^{1,2}, Zhu Liu⁶✉ & Fengming Xi^{1,6,7,9}

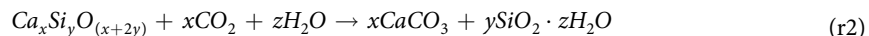
The majority of the carbon footprint of the cement industry originates from the decomposition of alkaline carbonates during clinker production. Recent studies have demonstrated that calcium oxides and other alkaline oxides in cement materials can sequester CO₂ through the carbonation process and partially offset the carbon emissions generated during cement production. This study employs a comprehensive analytical model to estimate the CO₂ uptake via hydrated cement carbonation, including concrete, mortar, construction waste, and cement kiln dust (CKD), covering major cement production and consumption regions worldwide from 1930 to 2023. In 2023, the global annual cement CO₂ uptake reached 0.93 Gt/yr (95% CI: 0.80–1.13 Gt/yr). From 1930 to 2023, the global cumulative cement CO₂ absorption reached 23.89 Gt (95% CI: 20.47–28.74 Gt), equivalent to 52.32% of the CO₂ process emissions from cement production during the same period. Our system for estimating cement emissions and uptake is updated annually, providing consistent and accurate data for the cement industry and carbon cycle studies. This data supports improved adaptation to future challenges.

Background & Summary

Over the past two decades, global cement consumption has significantly increased, mainly due to rapid urbanization and the demand for large-scale infrastructure construction, which have greatly driven up cement demand¹. It is projected that global cement annual production will increase by 50% by 2050². Additionally, sustained economic growth and increased housing demand have further accelerated the rapid expansion of cement consumption³. Cement production generates large amounts of carbon dioxide, including that directly released from the calcination of limestone, the burning of fossil fuels during high-temperature calcination, electricity consumption, and emissions from the transportation and processing of raw materials⁴. The global carbon emissions reached 36.8 billion tones in 2023, with cement production accounting for about 7–8% of this total⁵. Currently, the Global Carbon Project releases annual estimates of global cement industry emissions, including emissions caused by the decomposition of carbonates (mainly CaCO₃) during the cement production process, namely cement production process-related emissions, and emissions from fossil fuel combustion. Such estimates serve to formulate a global carbon budget⁶. Andrew^{7,8} publishes regularly updated estimates of annual global cement production process-related emissions from 1880, a dataset that is incorporated into several global emissions datasets⁹.

However, when examining the carbon emission issue associated with cement production from a life cycle standpoint, it is imperative to consider the inherent carbon absorption capacity of cement materials. Specifically, alkaline components such as calcium hydroxides and silicate components within these materials interact with atmospheric CO₂ to form stable compounds like calcium carbonate in humid conditions^{10–12}. This process of CO₂ absorption occurs naturally in cement materials, as illustrated by the following equations:

¹Institute of Applied Ecology, Chinese Academy of Sciences, Shenyang, 110016, China. ²University of Chinese Academy of Sciences, Beijing, 100049, China. ³Department of Geography, The University of Hong Kong, Pok Fu Lam, Hong Kong SAR, China. ⁴Institute for Climate and Carbon Neutrality, University of Hong Kong, Pok Fu Lam, Hong Kong SAR, China. ⁵CICERO Center for International Climate Research, Oslo, 0349, Norway. ⁶Key Laboratory of Pollution Ecology and Environmental Engineering, Chinese Academy of Sciences, Shenyang, 110016, China. ⁷Key Laboratory of Terrestrial Ecosystem Carbon Neutrality, Liaoning Province, Shenyang, 110016, China. ⁸Department of Earth System Science, Tsinghua University, Beijing, 100084, China. ⁹University of Science and Technology Beijing, Beijing, 100049, China. ¹⁰These authors contributed equally: Songbin Wu, Zi Shao. ✉e-mail: zhliu@tsinghua.edu.cn; xifengming@ustb.edu.cn



The process of carbonation in cement materials, which reabsorbs atmospheric CO_2 , is a gradual one that accumulates over time and persists throughout the entire lifecycle of cement products. Xi *et al.*¹³ indicated that the cumulative CO_2 sequestered by this carbonation process over recent decades constituted 43% of the process emissions from cement production during the same timeframe (excluding fuel emissions). Guo *et al.*¹⁴ and Huang *et al.*¹⁵ proceeded to construct a comprehensive analysis model based on Xi's study, which showed that annual cement CO_2 uptake reached up to 0.89 Gt in 2019 and 0.96 Gt in 2021. This uptake is equivalent to mitigating approximately 52%–55% of the process emissions during the same period^{14,15}. This analysis model considers historical data changes and combines clinker factors and production data from different countries and regions, providing a more comprehensive assessment of emission reductions.

However, that analysis model used the 75%–97% clinker factor range based on IPCC guidelines^{16,17} to calculate global cement clinker production before 1990. After 1990, except for China and India for which specific clinker factor parameters were adopted, the analysis still used this ratio for Europe, the United States, and other regions, which is biased because different cement production conditions and development paths among countries and regions lead to significant differences in clinker factors and trends. In addition, the ratio of cement production to cement consumption shown in statistical data (about $\pm 30\%$)^{14,15} within a specific year range had been used to estimate the cement consumption for years without consumption records, which introduced considerable calculation uncertainty for cement CO_2 uptake.

On the other hand, the usage of cement materials exhibits regional variations globally. In the United States, Japan, and most European nations, more than 70% of cement is used in concrete production¹⁸, but in Russia and Turkey, the proportion of cement used for concrete and mortar is almost equal¹⁸. This difference is further exacerbated by architectural styles: concrete building service lives in Europe are generally longer than those in Latin America, East Asia, and Southeast Asia^{19,20}. Such longevity implies a long material turnover cycle, limiting the carbon absorption capacity of concrete structures¹¹. Finally, the utilization and distribution of concrete strength in buildings across various regions exhibit significant variations. These differences are ultimately reflected in the range of carbonation rate coefficient (k) values and directly influences the carbon absorption rate of both concrete structures and fragments^{21,22}. However, when considering regional differences for cement usage parameters as mentioned above, previous studies were limited to China, Europe, the United States, India, and all other regions combined^{14,15}. This coarse division inevitably affects the accuracy of global and regional carbon absorption estimates for cement materials when using the bottom-up method.

In this study, we refer to more comprehensive cement clinker production and ratio recorded in national reports and statistical lists^{7,23–26}, while using detailed clinker trade data (imports and exports)²⁷ to replace the rough estimates of cement clinker production and consumption in previous studies. At the same time, we divide the world into 7 regions (China, North America, Latin America, Europe & Central Eurasia, Africa, mainland Asia (excluding China and former Soviet Union countries), and Southeast Asia & Oceania), and distinguish the cement use in different regions by using various cement usage ratios (separately for concrete and mortar), concrete building service lives and concrete strength class distribution, so as to facilitate the comparison of carbon sequestration capabilities by cement materials across diverse global regions and improve the accuracy of our bottom-up calculation model of global cement carbon uptake. This model includes the total carbon absorption of four types of cement production and consumption products (including concrete, mortar, construction waste and cement kiln dust) in three life stages (including service, demolition and second use). The updated cement CO_2 uptake inventory from this ongoing work can also provide data support for global and targeted regions and countries in formulating cement carbon reduction policies. The cement industry can further reduce its net carbon emissions and achieve near-zero emissions through enhancing carbon capture technology, using waste concrete as a carbon storage material, employing low-carbon alternative materials, and optimizing production processes.

Methods

Accounting scope. In this study, a comprehensive analytical model for cement CO_2 uptake accounting is created based on the Life Cycle Assessment (LCA) and Greenhouse Gas (GHG) analysis method, through which the CO_2 absorption of cement materials throughout their life cycle and the process-related CO_2 emissions during the cement production was calculated. The uncertainty of the calculation results was also evaluated using the Monte Carlo simulation method recommended by the Intergovernmental Panel on Climate Change (IPCC). The process of constructing an inventory of CO_2 absorption in cement materials and process-related CO_2 emissions of cement production is shown in Fig. 1.

Calculation of cement production process-related CO_2 emission. The calcination reaction inherent in the cement clinker production process triggers the endothermal decomposition of carbonates present in cement, such as limestone and $CaCO_3$, yielding corresponding oxides and CO_2 . Consequently, when assessing emissions from a specific region's cement manufacturing process, the CO_2 emission is typically calculated by multiplying the regional cement clinker yield with the process emission coefficient.

$$E_{cement} = W_{cement} \times f_{cement}^{clinker} \times EF_{CO_2} \quad (1)$$

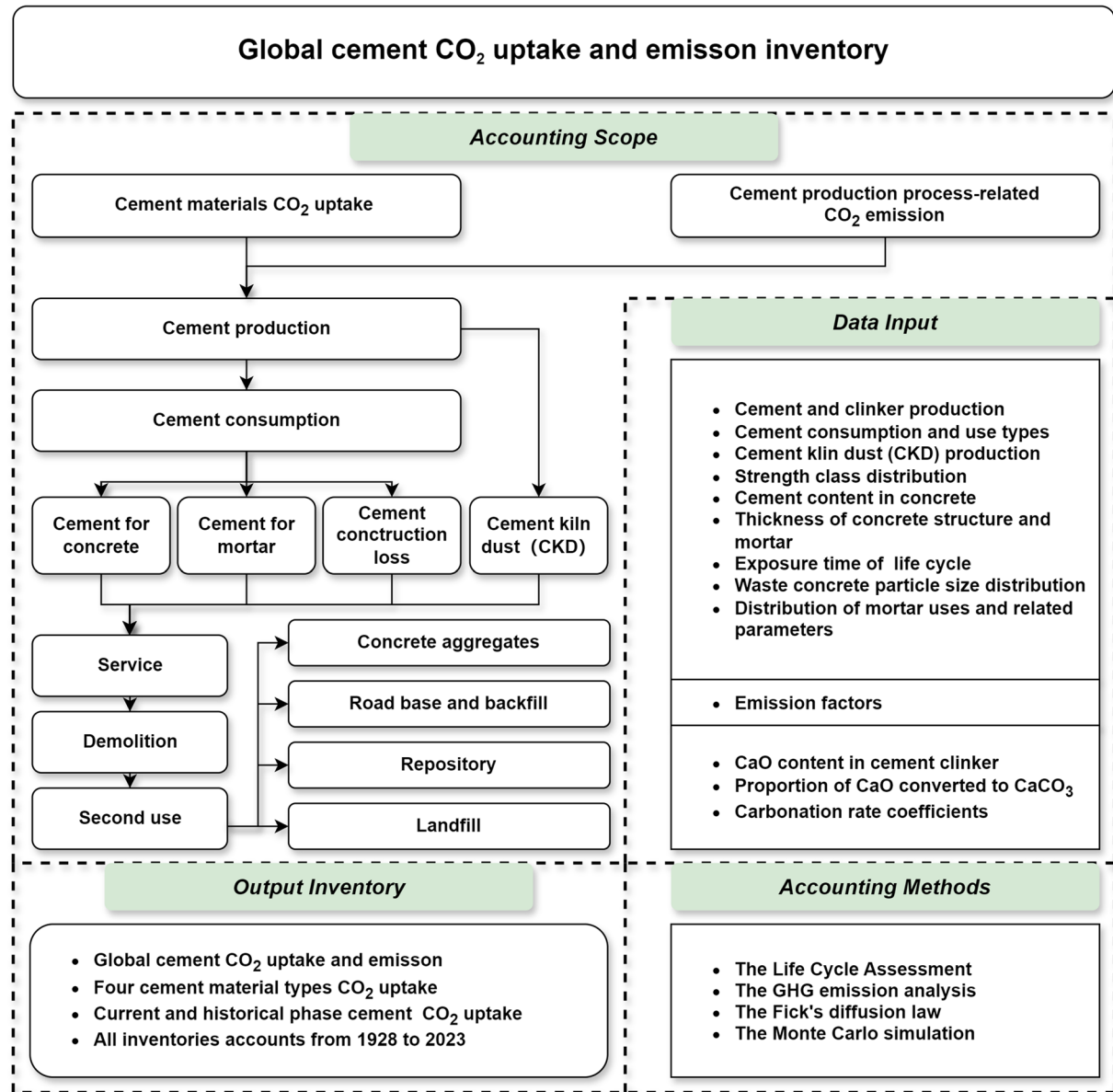


Fig. 1 Diagram of global cement CO₂ uptake and emission inventory construction.

Where E_{cement} is the cement process emissions of each region, W_{cement} is the cement production, $f_{cement}^{clinker}$ and EF_{CO_2} are the clinker factor and cement production process-related CO₂ emission factor, respectively.

Estimation of cement materials CO₂ uptake. The comprehensive life cycle analysis method was employed to compute the cement carbon absorption. The life cycle of the cement was segmented into three distinct phases: the service period, the demolition period, and the secondary utilization stage. This segmentation allowed for a detailed accounting of four types of absorption: concrete, mortar, construction waste, and CKD. The entire calculation process can be articulated as follows:

$$U_{cement} = U_{concrete} + U_{mortar} + U_{loss} + U_{CKD} \quad (2)$$

$$U_{concrete} = U_{cs} + U_{cd} + U_{cu} \quad (3)$$

$$U_{mortar} = U_{mr} + U_{mm} + U_{mmr} \quad (4)$$

$$U_{loss} = U_{lc} + U_{lm} \quad (5)$$

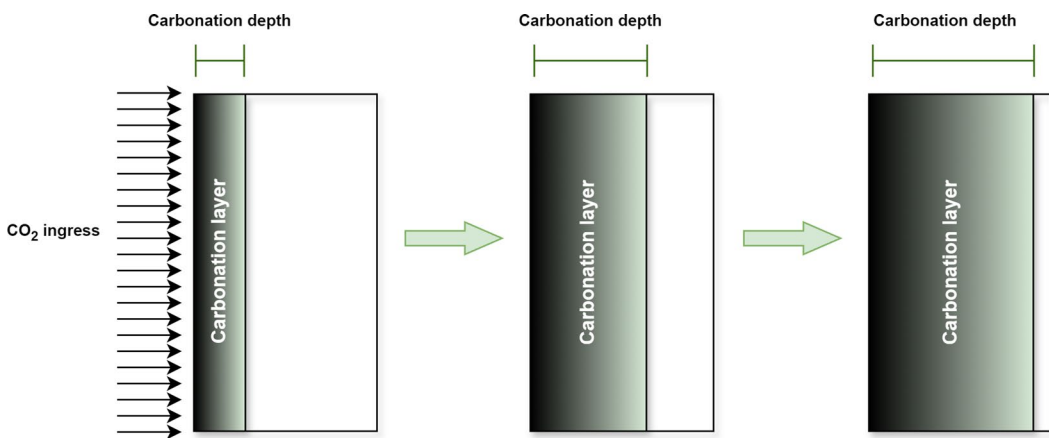


Fig. 2 Schematic diagram of the concrete and mortar carbonation model.

Where U_{cement} is the cumulative carbon absorption from cementitious materials. Additionally, $U_{concrete}$, U_{mortar} , U_{loss} , and U_{CKD} are the respective carbon absorption from concrete, mortar, construction waste, and cement kiln dust. Furthermore, U_{cs} , U_{cd} , and U_{cu} are respectively the CO₂ absorption associated with concrete during its service stage, demolition stage, and second use stage. U_{mr} , U_{mm} , and U_{mmr} are the CO₂ uptake of mortar for (1) rendering and plastering, (2) masonry, (3) maintenance and repairing. Lastly, U_{lc} is the CO₂ absorption of concrete waste, U_{lm} is the CO₂ absorption of mortar waste.

Based on the principle of hydrated cement carbonation, the annual cement CO₂ uptake (U) can be calculated as follows:

$$U = W_{cement} \times f_{cement}^{clinker} \times f_{clinker}^{CaO} \times \frac{M_{CO_2}}{M_{CaO}} \times \gamma \times F \quad (6)$$

Where $f_{clinker}^{CaO}$ is the proportion of CaO in cement clinker (including both the original CaO and the CaO converted from MgO, where the conversion factor is taken as 1.4 according to molecular weight comparison), γ is the proportion of CaO that can be converted to CaCO₃, M_{CO_2} , M_{CaO} are respectively the relative molecular mass of CO₂ and CaO, which are taken as 44 and 56. Lastly, F is the annual carbonation ratio and is associated with the kinetic process of carbon absorption by cementitious materials, which is established through Fick's diffusion law that there exists a direct correlation between the carbonation depth d and the diffusion time \sqrt{t} of these materials:

$$d = k\sqrt{t} \quad (7)$$

Where k is the diffusion coefficient of the cement material.

Moreover, the diffusion plate model is employed to delineate the carbonation process of cement materials¹⁴ (Fig. 2). The following assumptions are made: firstly, it is postulated that the diffusion front aligns with the carbonation front, implying that the area beyond the diffusion front undergoes complete carbonization; secondly, within the plate model, the extent of carbonation is quantified as a function of the concrete's exposed surface area, carbonation depth, and cementitious content. Specifically, concrete from various global regions is categorized based on compressive strength to elucidate the impact of exposure conditions and material characteristics on the carbonation process of concrete. The detailed calculation procedure is provided below.

CO₂ uptake by concrete. When describing the carbonation process of concrete during its service life, the compressive strength of the concrete material itself and the influence of environmental conditions on the rate of carbonation should be considered^{10,28,29}. Thus, the carbonation rate during service period ($k_{ci,s}$) is calculated as follows:

$$k_{ci,s} = \beta_{env} \times \beta_{add} \times \beta_{CO_2} \times \beta_{CC} \quad (8)$$

Where β_{env} , β_{add} , β_{CO_2} and β_{CC} are the carbonation coefficients of concrete in various environments, cement admixtures, CO₂ concentration, and coatings and covers, respectively.

In accordance with Fick's diffusion law, the depth of concrete carbonation ($d_{ci,s}$) is defined as follows:

$$d_{ci,s} = k_{ci,s} \sqrt{t_{ci,s}} \quad (9)$$

$$W_{ci,s} = C_{ci,s} \times d_{ci,s} / T_{ci,s} \quad (10)$$

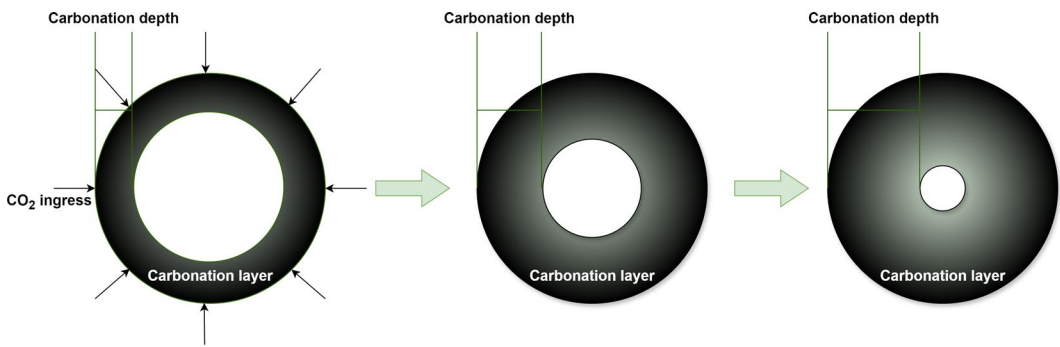


Fig. 3 Schematic diagram of the concrete carbonation model during demolition.

$$U_{ci,s} = W_{ci,s} \times f_{cement}^{clinker} \times f_{clinker}^{CaO} \times \gamma_c \times \frac{M_{CO_2}}{M_{CaO}} \quad (11)$$

Where $W_{ci,s}$ is the mass of carbonized cement in different kinds of concrete during service period, $C_{ci,s}$ is the cement content in different kinds of concrete, $T_{ci,s}$ is the average thickness of structure in different kinds of concrete, $U_{ci,s}$ is the amount of carbon uptake of different kinds of concrete during service period. γ_c is the proportion of CaO that can be converted to $CaCO_3$ in concrete.

The concrete structure will be demolished after the service period, and it is broken into numerous fragments and particles during the demolition period. A simplified spherical diffusion model is introduced to describe the carbonation process of concrete during the demolition period (Fig. 3), and it is assumed that carbonation starts from the outer surface and diffuses inward along the diameter direction. Based on the maximum carbonation depths (D_{0i}) of concrete with different compressive strengths and its particle size distribution [a, b] (a and b are the lower and upper limits of particle size respectively), three different numerical relationships are defined to calculate the carbonation fraction (F_{di}):

$$F_{di} = \begin{cases} 1 - \int_a^b \frac{\pi}{6} (D - D_{0i})^3 / \int_a^b \frac{\pi}{6} D^3 & (a > D_{0i}) \\ 1 - \int_{D_{0i}}^b \frac{\pi}{6} (D - D_{0i})^3 / \int_a^b \frac{\pi}{6} D^3 & (a \leq D_{0i} < b) \\ 1 & (b \leq D_{0i}) \end{cases} \quad (12)$$

$$D_{0i} = 2d_{ci,d} = 2k_{ci,d} \sqrt{t_{ci,d}} \quad (13)$$

Where $k_{ci,d}$ is the diffusion coefficient of different types of concrete at the demolition period, and $t_{ci,d}$ is the demolition time.

The cement absorption amount $U_{ci,d}$ during the demolition period is calculated as:

$$U_{ci,d} = (W_{ci} - W_{ci,s}) \times F_{di} \times f_{cement}^{clinker} \times f_{clinker}^{CaO} \times \gamma_c \times \frac{M_{CO_2}}{M_{CaO}} \quad (14)$$

Where W_{ci} is the amount of cement used for different kinds of concrete.

A part of the concrete after the demolition period will be reused. The reused concrete will have a decrease in its overall carbonation rate due to the existed carbonation layer on its surface, and thus when considering the depth of carbonation ($d_{ci,u}$) of the concrete during the second use period, a correction term is added:

$$d_{ci,u} = \sqrt{k_{ci,d} \times \sqrt{t_{ci,d}} \times k_{ci,u} \times \sqrt{t_{ci,u}}} \quad (15)$$

Where $k_{ci,u}$ is the diffusion coefficient of concrete in the secondary utilization period, and $t_{ci,u}$ is the secondary utilization time.

Similar to the demolition period, the carbonized fraction F_{ui} is calculated as follows:

$$F_{ui} = \begin{cases} 1 - \int_a^b \frac{\pi}{6} (D - D_{ti})^3 / \int_a^b \frac{\pi}{6} D^3 - F_{di} & (a > D_{0i}) \\ 1 - \int_{D_{0i}}^b \frac{\pi}{6} (D - D_{ti})^3 / \int_a^b \frac{\pi}{6} D^3 - F_{di} & (a \leq D_{0i} < b) \\ 1 & (b \leq D_{0i}) \end{cases} \quad (16)$$

The carbon absorption of cement material during secondary use period $U_{ci,u}$ is calculated as follows:

$$U_{ci,u} = (W_{ci} - W_{ci,s} - W_{ci,d}) \times F_{ui} \times f_{cement}^{clinker} \times f_{clinker}^{CaO} \times \gamma_c \times \frac{M_{CO_2}}{M_{CaO}} \quad (17)$$

CO₂ uptake by mortar. The rendering and plastering mortar draw on the diffusion plate model of concrete, then the carbonation depth (d_{mr}) is calculated as:

$$d_{mr} = k_m \sqrt{t_{mr}} \quad (18)$$

$$f_{mr,t} = (d_{mr,t} - d_{mr,t-1})/T_{mr} \quad (19)$$

Where k_m is the diffusion coefficient of cement mortar, T_{mr} is the exposure time of rendering mortar, $f_{mr,t}$ is the annual carbonation rate of rendering mortar at year t, $d_{mr,t}$ and $d_{mr,t-1}$ are the carbonation depth of rendering mortar at year t and (t-1), respectively, T_{mr} is the utilization thickness of rendering and plastering mortar.

Then the rendering mortar CO₂ absorption amount ($U_{mr,t}$) is calculated as:

$$U_{mr,t} = W_m \times \xi_{mr} \times f_{mr,t} \times f_{cement}^{clinker} \times f_{clinker}^{CaO} \times \gamma_m \times \frac{M_{CO_2}}{M_{CaO}} \quad (20)$$

Where W_m is the total amount of mortar cement, ξ_{mr} is the proportion of rendering mortar cement in the total mortar cement, and γ_m is the ratio of CaO carbonized into CaCO₃ in the mortar.

The carbon uptake of the maintenance and repairing mortar is calculated similarly to that of the rendering and plastering mortar. For masonry mortar, the calculation scenarios are divided into three categories according to the type of masonry wall: double-sided rendered wall, one-sided rendered wall, and no rendered wall. The carbon absorption of masonry mortar can then be calculated as follows:

$$U_{mm} = U_{mmd} + U_{mmo} + U_{mmn} \quad (21)$$

The CO₂ absorption of masonry mortar in double-sided rendered wall is calculated as:

$$d_{mmd} = \begin{cases} 0 & (t_{mm} \leq t_r) \\ 2(k_m \sqrt{t_{mm}} - T_{mr}) & (t_{mm} > t_r) \end{cases} \quad (22)$$

$$f_{mmd,t} = \begin{cases} 0 & (t_{mm} \leq t_r) \\ d_{mmd,t} - d_{mmd,t-1}/T_w & (t_r \leq t_{mm} < T) \\ 1 - (d_{mmd,T}/T_w) & (t_{mm} = T + 1) \end{cases} \quad (23)$$

$$U_{mmd,t} = W_m \times \xi_{mm} \times \xi_{mmd} \times f_{mmd,t} \times f_{cement}^{clinker} \times f_{clinker}^{CaO} \times \gamma_m \times \frac{M_{CO_2}}{M_{CaO}} \quad (24)$$

Where d_{mmd} is the carbonation depth of masonry mortar in double-sided rendered wall, t_{mm} is the exposure time of masonry mortar, t_r is the time for rendering mortar to be completely carbonated, T_{mr} is the thickness of rendered mortar on masonry wall, $f_{mmd,t}$ is the annual carbonation rate of masonry mortar in double-sided rendered wall in year t, $d_{mmd,T}$ and $d_{mmd,t-1}$ are the carbonation depth of masonry mortar in double-sided rendered wall in year t and (t-1), respectively, T_w is the thickness of masonry wall, T is the service life of building, $d_{mmd,T}$ is the total carbonation depth of masonry mortar in double-sided rendered wall during life, $U_{mmd,t}$ is the annual carbon absorption amount of masonry mortar in double-sided rendered wall in year t, ξ_{mm} is the proportion of masonry mortar in cement mortar, and ξ_{mmd} is the proportion of masonry mortar for double-sided rendered wall.

The CO₂ absorption of masonry mortar in one-sided rendered wall is calculated as:

$$d_{mmo} = \begin{cases} k_m \times \sqrt{t_{mm}} & (t_{mm} \leq t_r) \\ k_m \times \sqrt{t_{mm}} + (K_m \times \sqrt{t_{mm}} - T_{mr}) & (t_{mm} > t_r) \end{cases} \quad (25)$$

$$f_{mmo,t} = \begin{cases} (d_{mmo,t} - d_{mmo,t-1})/T_w & (t_r < t_{mm} \leq T) \\ 1 - (2d_{mmo,T} - T_{mr})/T_w & (t_{mm} = T + 1) \end{cases} \quad (26)$$

$$U_{mmo,t} = W_m \times \xi_{mm} \times \xi_{mmo} \times f_{mmo,t} \times f_{cement}^{clinker} \times f_{clinker}^{CaO} \times \gamma_m \times \frac{M_{CO_2}}{M_{CaO}} \quad (27)$$

Where d_{mmo} is the carbonation depth of masonry mortar in one-sided rendered wall, $f_{mmo,t}$ is the annual carbonation rate of masonry mortar in one-sided rendered wall in year t, $d_{mmo,t}$ and $d_{mmo,t-1}$ are the carbonation depth of masonry mortar in one-sided rendered wall in year t and (t-1), $U_{mmo,t}$ is the annual carbon absorption amount of masonry mortar in one-sided rendered wall in year t, ξ_{mmo} is the proportion of masonry mortar for one-sided rendered wall.

The CO₂ absorption of masonry mortar in no rendered wall is calculated as:

$$d_{mmn} = 2k_m \times \sqrt{t_{mm}} \quad (28)$$

$$f_{mmn,t} = \begin{cases} 2(d_{mmn,t} - d_{mmn,t-1})/T_w & (t_{mm} \leq T) \\ 1 - 2d_{mmn,T}/T_w & (t_{mm} = T + 1) \end{cases} \quad (29)$$

$$U_{mmn,t} = W_m \times \xi_{mm} \times \xi_{mmn} \times f_{mmn,t} \times f_{cement}^{clinker} \times f_{clinker}^{CaO} \times \gamma_m \times \frac{M_{CO_2}}{M_{CaO}} \quad (30)$$

Where d_{mmn} is the carbonation depth of masonry mortar in no rendered wall, $f_{mmn,t}$ is the annual carbonation rate of masonry mortar in no rendered wall in year t, $d_{mmn,t}$ and $d_{mmn,t-1}$ are the carbonation depth of masonry mortar in no rendered wall in year t and (t-1), $U_{mmn,t}$ is the annual carbon absorption amount of masonry mortar in no rendered wall in year t, ξ_{mmn} is the proportion of masonry mortar for no rendered wall.

CO₂ uptake by construction waste. The CO₂ uptake formula for cement construction wastes are as follows:

$$U_{lc} = (\sum_1^n W_{ci} \times l_{con} \times f_{con}) \times f_{cement}^{clinker} \times f_{clinker}^{CaO} \times \gamma_c \times \frac{M_{CO_2}}{M_{CaO}} \quad (31)$$

$$U_{lm} = (\sum_1^n W_{mi} \times l_{mor} \times f_{mor}) \times f_{cement}^{clinker} \times f_{clinker}^{CaO} \times \gamma_m \times \frac{M_{CO_2}}{M_{CaO}} \quad (32)$$

Where W_{ci} is the total quantity of cement utilized for different types of concrete, l_{con} is the loss rate of concrete during the construction phase, f_{con} is the annual carbonation ratio of concrete waste. For mortar, W_{mi} is the total amount of cement used for different types of mortar, l_{mor} is the loss rate of mortar at the construction stage, and f_{mor} is the annual carbonation ratio of mortar waste.

CO₂ uptake by cement kiln dust (CKD). With is very high surface-to-volume ratio, CKD has a high rapid carbonation rate, and it is often assumed to be fully carbonized within a year when discussing its carbonation status, with calculations limited to a single year. The CO₂ absorption formula for CKD is as follows:

$$U_{CKD} = W_{cement} \times \xi_{CKD} \times \xi_{landfill} \times f_{cement}^{clinker} \times f_{CKD}^{CaO} \times \gamma_{CKD} \times \frac{M_{CO_2}}{M_{CaO}} \quad (33)$$

Where W_{cement} is the total quantity of cement utilized for different types of concrete, ξ_{CKD} is the CKD yield at the point of cement clinker production, $\xi_{landfill}$ is the ratio of CKD to landfills, which is between 0.52 and 0.9¹³, f_{CKD}^{CaO} is the proportion of CaO present in CKD, and γ_{CKD} is the conversion rate of CaO in CKD to CaCO₃.

Data Records

The dataset “Global cement CO₂ uptake and emission accounts 1930–2023” (Version v4) consists of five core tables, each uploaded in Excel file format and openly shared. The total dataset includes 30684 data records. All the data described in this study are accessible at <https://doi.org/10.5281/zenodo.1394147>³⁰.

- 3948 of these records present cement production and consumption in 7 regions worldwide, including “Cement production, Clinker production and consumption, Construction waste and CKD production”. There are a total of 5 tables of long time-series data, for the period 1930–2023. [File ‘Input data 1. Global cement clinker production and consumption’]
- 1180 are the cement materials usage in 7 regions worldwide, as well as CO₂ emission and uptake factors, including “Cement usage ratio (for concrete or for mortar), Distribution of concrete by strength class and cement content, Concrete carbonation rate coefficients (k), Exposure times of cement materials in life cycle, Waste concrete treatment and particle size distribution, Distribution of mortar uses and related parameters, Thickness of concrete construction and mortar, Chinese survey statistics for walls with various extents of

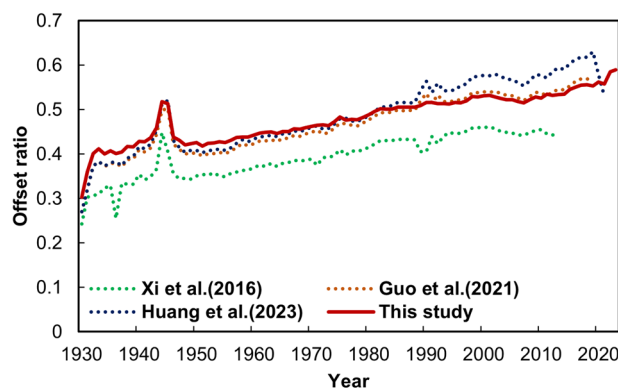


Fig. 4 Global cement production process-related CO₂ emission offset by cement carbonation since 1930 (comparing with previous study).

mortar rendering, mortar carbonation rate coefficients and CaO converted to CaCO₃ in China, cement production process-related CO₂ emission factors". There are total of 12 tables. [File 'Input data 2. Global cement usage parameters and CO₂ uptake factors']

- 71 are 24 sources of uncertainty in the global cement production process-related CO₂ emissions and uptake accounting, as well as their distribution patterns, parameter descriptions, and value ranges. These are used for our Monte Carlo analysis. [File 'Input data 3. Variables considered in the cement CO₂ uptake uncertainty analysis using Monte Carlo method']
- 22383 are the accounting results of global cement production process-related CO₂ emissions and uptake across 7 regions, including "Annual carbon uptake by cement materials and regions, Global carbon uptake by cement materials, Annual global carbon uptake by cement material and relevant lag time, Process CO₂ emissions from cement production by regions, Global process CO₂ emissions from cement production and carbon uptake by cement materials carbonation", There are total of 5 tables of long-term sequence data, accounts 1930–2023. [File 'Output data 1. Global cement CO₂ emission and uptake results']
- 3102 are the uncertainty results of global cement materials CO₂ uptake across 7 regions, accounts 1930–2023. [File 'Output data 2. Uncertainty of global cement CO₂ uptake']

Technical Validation

Comparison with existing estimates. The proportion of global cement production-related CO₂ emissions offset by the carbon absorption effect of cement materials in this study (52.32%) falls within the range of previous studies (43.16%–55.07%) (Fig. 4), which is attributed to: (1) we used regional scale clinker factor and trade data, making our input cement consumption slightly larger than previous studies, which feeds back positively to the increase in CO₂ absorption of cement materials; (2) We accounted for different cement usage parameters (cement usage ratios, concrete building service lives and concrete strength class distribution) for various accounting regions, thereby balancing the increase in CO₂ absorption accounting, due to previous studies treated China-India-USA-Europe & Central Eurasia separately and used a single set of parameters for the rest of the world, resulting in overly high theoretical values and an overestimation of global CO₂ uptake by cement materials. Specifically:

- For cement clinker production and consumption, we directly collated and utilized the national carbon emission reports regularly submitted by the 43 UNFCCC signatories²⁶, which cover the cement clinker production of each country since 1990. For non-signatory countries that did not provide consecutive annual clinker production data, we calculated their annual cement clinker production based on cement production data and the collated clinker factor. This study continued to adopt USGS cement production data as the primary input source, as USGS provides continuous time series cement production data for 164 countries and regions worldwide, covering the period from 1930 to 2022²³. Additionally, USGS offers rough cement production estimates for 13 major cement producing countries in 2023³¹. Furthermore, we obtained the 2023 production data for some countries from the ccf2up database²⁴ as a supplement and correction. For other countries that did not provide the latest cement production data, we referenced their 2022 production data. Regarding clinker factor parameters, the data sources for China are consistent with previous studies^{23,32–35}, while the clinker factor parameters for other countries and regions are based on data from WBCSD's Getting the Numbers Right initiative²⁵ and Andrew's compilation and assumptions⁷. Finally, we utilized cement clinker trade data (import and export data) provided by the UN COMTRADE dataset²⁷, combined with our collated clinker production data, to estimate cement consumption data for each country. For countries and years where trade data were not available, we used clinker production data as an approximate substitute, which greatly reduced the uncertainty in our estimates of national cement clinker consumption compared to our previous work.
- For cement usage parameters, we conducted an exhaustive survey of regional cement market consumption^{36–39} and construction type⁴⁰, detailing the distribution of cement usage in concrete products and mortar

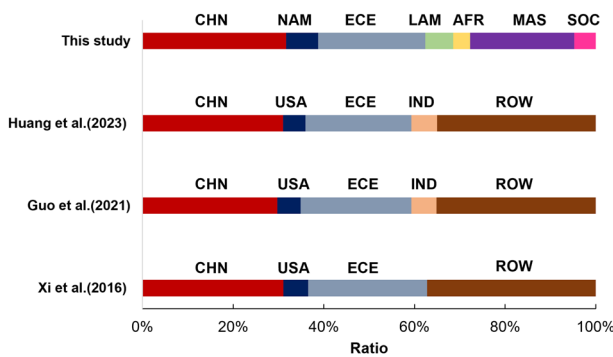


Fig. 5 Allocation of cumulative cement materials CO₂ uptake by regions from 1930 to 2023 (comparing with previous study). (CHN: China; NAM: North America, includes the United States and Canada; LAM: Latin America, includes all Latin American countries included in the “USGS 2022 Cement Production Dataset”; ECE: Europe & Central Eurasia, includes all European countries and the former Soviet republics in Central Asia included in the “USGS 2022 Cement Production Dataset”; AFR: Africa, includes all African countries included in the “USGS 2022 Cement Production Dataset”; MAS: Mainland of Asia, includes all Asian countries included in the “USGS 2022 Cement Production Dataset” except China, the former Soviet republics in Central Asia, and Southeast Asia; SOC: Southeast Asia & Oceania, includes all Southeast Asian and Oceania countries included in the “USGS 2022 Cement Production Dataset”).

manufacturing and presenting the regional scale distribution of concrete building service life and concrete strength class, so as to estimate the global CO₂ uptake of cement materials based on bottom-up approach.

In contrast to prior research, this methodology for subdividing accounting regions enables a more granular comparison of CO₂ uptake in cement materials across broader regional scales (Fig. 5). When comparing across datasets for regions that datasets have in common, it is observed that China’s cement cumulative CO₂ uptake proportion is higher in our analysis (from 29.55% to 31.67%), whereas the ECE’s proportion is lower (from 26.25% to 23.63%). This trend aligns with the recent growth trajectory of cement production and consumption in China and ECE^{23,30}, thereby cross-validating the findings of this study.

Limitations and future work. There are still some limitations in our current dataset:

- Currently, our collection does not cover all countries involved in cement production globally in terms of clinker output and clinker factor parameters. Notably, prior to 1990, for countries where data on clinker production or clinker factors are not available, the clinker factor parameters were derived using Andrew’s assumption⁷: Most countries in the world only produced ordinary Portland cement (clinker factor of 0.95) at the beginning of the development of their cement industry, and gradually expanded the production of other cements with lower clinker factors over time. We set the clinker factor of 1970 and earlier years for these countries at 0.95, and then used linear interpolation to the earliest year for each country to obtain the clinker factor parameters and obtained the clinker factor parameters of the intermediate years. This approach represents an attempt to implement Occam’s Razor, avoiding unwarranted assumptions, but overlooks potential regional variations and compromises the accuracy of our global cement clinker output estimates. However, obtaining data on early clinker factors for these countries may be challenging.
- Despite the extensive collection of regional data on cement usage (cement usage ratio, concrete building service lives concrete strength class distribution), providing a preliminary understanding of specific parameter characteristics, a significant data deficit remains at the national level. Further detailed information at both regional and national-scales are required, which is crucial for constructing smaller-scale national cement materials CO₂ uptake inventories in the future.
- The carbonation rate coefficient (*k*) is closely associated with concrete strength class distribution, cement clinker content, concrete cement content, and the regional geographical location^{21,22}. Our current input database predominantly derives from surveys and literature data from China, the United States, and Europe. To accurately calculate the carbon sequestration capacity of cement across various regions and countries, it is imperative to collect and organize additional regional *k* values, especially based on climatic conditions and exposure environments.

Code availability

The programs used in the data generation is based on MATLAB or Python. The associated codes are available at <https://doi.org/10.5281/zenodo.13941475>³⁰.

Received: 2 September 2024; Accepted: 4 December 2024;

Published online: 19 December 2024

References

- Amran, M. *et al.* Global carbon recoverability experiences from the cement industry. *Case Stud. Constr. Mater.* **17**, e01439, <https://doi.org/10.1016/j.cscm.2022.e01439> (2022).
- Monteiro, P. J. M. *et al.* Towards sustainable concrete. *Nat. Mater.* **16**, 698–699, <https://doi.org/10.1038/nmat4930> (2017).
- Sing, J. & Singh, J. Sustainable use of industrial waste in cement industry. *Int. J. Environ. Ecol. Fam. Urban Stud.* **6**, 2250–0065 (2016).
- Hasanbeigi, A. *et al.* Carbon emissions mitigation methods for cement industry. *J. Clean. Prod.* **18**, 1509–1518, <https://doi.org/10.1016/j.jclepro.2009.12.014> (2010).
- International Energy Agency (IEA). Cement Technology Roadmap: Carbon Emissions Reductions up to 2050. International Energy Agency, Paris (2018).
- Friedlingstein, P. *et al.* Global Carbon Budget 2023. *Earth Syst. Sci. Data* **15**, 5301–5369, <https://doi.org/10.5194/essd-15-5301-2023> (2023).
- Andrew, R. M. Global CO₂ emissions from cement production, 1928–2018,. *Earth Syst. Sci. Data* **11**, 1675–1710, <https://doi.org/10.5194/essd-11-1675-2019> (2019).
- Andrew, R. M. Global CO₂ emissions from cement production (version: 240517) [Data set]. Zenodo. <https://doi.org/10.5281/zenodo.11207133> (2024).
- Gütschow, J. *et al.* The PRIMAP-hist national historical emissions time series (1750–2022) v2.5.1. Zenodo. <https://doi.org/10.5281/zenodo.10705513> (2024).
- Pade, C. & Guimaraes, M. The CO₂ uptake of concrete in a 100 year perspective. *Cement. Concr. Res.* **37**, 1348–1356, <https://doi.org/10.1016/j.cemconres.2007.06.009> (2007).
- Huntzinger, D. N. *et al.* Carbon dioxide sequestration in cement kiln dust through mineral carbonation. *Environ. Sci. Technol. Lett.* **43**, 1986–1992, <https://doi.org/10.1021/es0000748> (2009).
- Renforth, P. *et al.* Silicate production and availability for mineral carbonation. *Environ. Sci. Technol. Lett.* **45**, 2035–2041, <https://doi.org/10.1021/es103078j> (2011).
- Xi, F. *et al.* Substantial global carbon uptake by cement carbonation. *Nat. Geosci.* **9**, 880–883, <https://doi.org/10.1038/ngeo2834> (2016).
- Guo, R. *et al.* Global CO₂ uptake by cement from 1930 to 2019. *Earth Syst. Sci. Data* **13**, 1791–1805, <https://doi.org/10.5194/essd-13-1791-2021> (2021).
- Huang, H. *et al.* Global carbon uptake of cement carbonation accounts 1930–2021. *Earth Syst. Sci. Data*. <https://doi.org/10.5194/essd-15-469-2023> (2023).
- IPCC. *Guidelines for National Greenhouse Gas Inventories*. (1997).
- IPCC. *Guidelines for National Greenhouse Gas Inventories*. (2006).
- ERMCO. *European Ready-Mixed Concrete Industry Statistics 2003–2019*. <https://ermco.eu/statistics-previous-years> (2024).
- Pommer, K. & Pade, C. Guidelines: Uptake of Carbon Dioxide in the Life Cycle Inventory of Concrete. Nordic Innovation Centre (2006).
- da Silva, M. R. *et al.* Influence of concrete cover in the service life of a newly built reinforced concrete structure: a case study. *J. Build. Rehabil.* **5**, 9, <https://doi.org/10.1007/s40940-019-00048-6> (2020).
- Chen, Y. *et al.* Effects of Environmental Factors on Concrete Carbonation Depth and Compressive Strength. *Materials* **11**, 2167, <https://doi.org/10.3390/ma11112167> (2018).
- Hills, T. P. *et al.* Statistical analysis of the carbonation rate of concrete. *Cement Concr. Res.* **72**, 98–107, <https://doi.org/10.1016/j.cemconres.2015.03.006> (2015).
- USGS. *Cement statistics and information*. <https://www.usgs.gov/centers/national-minerals-information-center/cement-statistics-and-information> (2024).
- OneStone Consulting. Cement Market Report for 130 countries, 2 Updates per year. <https://ccf2up.com> (2024).
- WBCSD. *Getting the Numbers Right project: Reporting CO₂*. World Business Council for Sustainable Development. <http://www.wbcsdcement.org/GNR-2014/index.html> (2014).
- UNFCCC. National Inventory Submission 2023. <https://unfccc.int/ghg-inventories-annex-i-parties/2023> (2024).
- UN Comtrade. <https://comtrade.un.org/> (2024).
- Lagerblad, B. Carbon dioxide uptake during concrete life cycle - State of the art. Swedish Cement and Concrete Research Institute (2005).
- Andersson, R. *et al.* Calculating CO₂ uptake for existing concrete structures during and after service life. *Environ. Sci. Technol. Lett.* **47**, 11625–11633, <https://doi.org/10.1021/es401775w> (2013).
- Wu, S. *et al.* Global CO₂ uptake by cement materials accounts 1930–2023 [Data set]. Zenodo. <https://doi.org/10.5281/zenodo.13941475> (2024).
- USGS. *Mineral Commodity Summaries* (2024).
- China Cement Association (CCA). China Cement Almanac, China Building Industry Press, Beijing, China (2001–2015).
- Xu, J. H. *et al.* Energy consumption and CO₂ emissions in China's cement industry: A perspective from LMDI decomposition analysis. *Energ. Policy* **50**, 821–832, <https://doi.org/10.1016/j.enpol.2012.08.059> (2012).
- Cao, Z. *et al.* Elaborating the history of our cementing societies: An in-use stock perspective. *Environ. Sci. Technol.* **51**, 11468–11475, <https://doi.org/10.1021/acs.est.7b02048> (2017).
- MIIT. *Building materials*. <http://www.miit.gov.cn/n1146312/n1146904/n1648356/n1648361/index.html> (2020).
- Villagrán-Zaccardi, Y. *et al.* Overview of cement and concrete production in Latin America and the Caribbean with a focus on the goals of reaching carbon neutrality. *RILEM Tech. Lett.* **7**, 30–46, <https://doi.org/10.21809/rilemtechlett.2022.155> (2022).
- Muigai, R. *et al.* Cradle-to-gate environmental impacts of the concrete industry in South Africa. *J. South Afr. Inst. Civil Eng.* **55**, 02–07 (2013).
- Kumar, P. & Kaushik, S. Some trends in the use of concrete: Indian scenario. *Indian Concr J.* **77**, 1503–1508 (2003).
- Limsuwan, E. Thailand – Concrete Construction Industry – Cement Based Material and Civil Infrastructure (CBM-CI). Proc. CBM-CI International Workshop, Karachi, Pakistan (2007).
- CEIC Data. <https://www.ceicdata.com.cn/> (2024).

Acknowledgements

This work was supported by National Key R&D Program of China (Grant No. 2023YFE0113000); National Natural Science Foundation of China (41977290); the Youth Innovation Promotion Association, Chinese Academy of Sciences (2020201, Y202050); the Liaoning Xingliao Talents Project (XLYC1907148); the Natural Science Foundation of Liaoning Province (2022-MS-031); the Norwegian Environment Agency (24010001); and the Major Program of Institute for Applied Ecology, Chinese Academy of Sciences (IAEMP202201).

Author contributions

S.W. design the study, collected and assembled the data, conducted modelling, constructed the database, and prepared the manuscript. Z.S. collected and assembled the data, constructed the database, and revised the manuscript. R.A. design the study, collected and assembled the data, and revised the manuscript. L.B. conducted modelling. J.W. revised the manuscript. L.N. collected and assembled the data. Z.L. led the project. F.X. led the project, design the study.

Competing interests

The authors declare no competing interests.

Additional information

Correspondence and requests for materials should be addressed to Z.L. or F.X.

Reprints and permissions information is available at www.nature.com/reprints.

Publisher's note Springer Nature remains neutral with regard to jurisdictional claims in published maps and institutional affiliations.



Open Access This article is licensed under a Creative Commons Attribution-NonCommercial-NoDerivatives 4.0 International License, which permits any non-commercial use, sharing, distribution and reproduction in any medium or format, as long as you give appropriate credit to the original author(s) and the source, provide a link to the Creative Commons licence, and indicate if you modified the licensed material. You do not have permission under this licence to share adapted material derived from this article or parts of it. The images or other third party material in this article are included in the article's Creative Commons licence, unless indicated otherwise in a credit line to the material. If material is not included in the article's Creative Commons licence and your intended use is not permitted by statutory regulation or exceeds the permitted use, you will need to obtain permission directly from the copyright holder. To view a copy of this licence, visit <http://creativecommons.org/licenses/by-nc-nd/4.0/>.

© The Author(s) 2024

Potential of Reducing CO₂ Emissions in Cement Production through Altering Clinker Compositions

Franco Williams* and Aidong Yang



Cite This: *Ind. Eng. Chem. Res.* 2024, 63, 17158–17167



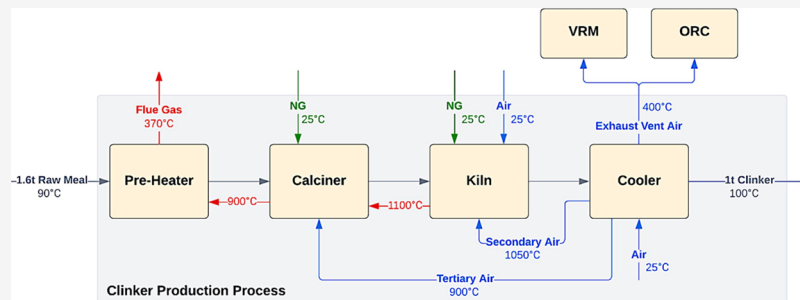
Read Online

ACCESS |

Metrics & More

Article Recommendations

Supporting Information



ABSTRACT: This study assessed seven cases of distinct raw material compositions with the aid of process simulation using Aspen Plus V12.1, focusing on reducing carbon dioxide (CO₂) emissions and energy demands from clinker production. Material and energy flows for the raw meal mixes were simulated in a natural gas-fueled plant. The results indicated up to 45.5% energy and 35.1% CO₂ reduction using alternative clinkers compared to ordinary Portland cement (OPC) clinker. Calcium silicate cement (CSC) clinker had the lowest energy consumption and CO₂ emissions, resulting from raw meal limestone reduction and a lower sintering temperature. Partially replacing OPC clinker with a supplementary cementitious material (SCM) from CO₂ mineralization reduced CO₂ emissions by ~45% compared to OPC. Location-dependent CO₂ emission analysis revealed that Brazil yielded the least emissions compared to the United States and China. These findings underscore the imperative for cement industries to adopt alternative clinkers, coupled with SCMs, as decarbonization measures.

INTRODUCTION

The global production of cement, the most used material in the world after water,¹ reached 4.4 billion tonnes in 2021 and reduced slightly to 4.1 billion tonnes in 2023.² Cement production was responsible for 2.9 billion tonnes of CO₂ emissions in 2021³ or about 8% of global anthropogenic carbon dioxide (CO₂) emissions.⁴ Toward the Net Zero targets by 2050 and aligning with the objectives established in the Paris Agreement, the World Business Council for Sustainable Development has urged the cement industry to achieve 20–25% CO₂ emission reductions by 2030.¹ These significant abatements are also widely expected by governmental bodies, financiers, and end users.⁵

Most of the CO₂ emissions of cement production arise from the process of producing clinker, the main component of ordinary Portland cement (OPC), which accounts for 95% of cement.⁶ Clinker production involves calcination, where limestone is decomposed into calcium oxide and CO₂,⁷ and the subsequent operation of the kiln, where clinker is formed.⁸ Both the calciner and the kiln require heating, which represents the main energy consumption in clinker production,⁹ along with electricity for grinding raw materials (known as raw meal),¹⁰ driving gas flows in the production process and other auxiliary uses.¹¹ In addition to the above-mentioned CO₂ production

from calcination, which accounts for ~60% of total emissions,¹² the combustion of fuels (predominantly coal or natural gas) in the calciner and kiln leads to about 28–35% CO₂ emissions from clinker production.^{9,13,14}

To tackle CO₂ emissions produced from cement production, carbon capture, utilization, and storage (CCUS) has been typically considered as a strategy to be applied to the flue gas of clinker production, which typically contains about 20% CO₂.¹⁵ CCUS has previously been reported to offer carbon capture efficiencies of 90%,¹⁶ 94%,¹⁷ and 99.7%¹⁸ through the use of MEA-based absorption, calcium looping, and advanced amine-based CO₂ capture, respectively. To aid CCUS, oxygen combustion (hereafter, oxy-combustion) offers more concentrated CO₂ to be produced from cement flue gases,⁷ leading to higher capture efficiencies up to 100%,¹⁷ and yields high-purity CO₂ streams, hence easing carbon capture.¹⁹ Although

Received: May 17, 2024

Revised: September 13, 2024

Accepted: September 13, 2024

Published: September 25, 2024



Table 1. Chemical Compositions of Raw Materials (wt %) in Six Different Simulated Clinker Cases^{a,b}

case ID	chemical composition of raw materials (wt %)					sintering temperature (°C)	compressive strength (MPa)	references
	CaCO ₃	SiO ₂	Al ₂ O ₃	Fe ₂ O ₃	CaSO ₄			
1. OPC	79.47	14.34	3.49	2.70	0.00	1500	32.5–55	37,38
2. HFC-a (4.34)	77.08	14.81	3.77	4.34	0.00	1375	73	31
3. HFC-b (3.72)	77.33	15.80	3.14	3.72	0.00	1350	60	32
4. HFC-c (3.93)	78.46	12.85	4.73	3.93	0.00	1350	45	30
5. BYFC	64.20	12.50	13.80	4.70	4.81	1350	45.9	28
6. CSC	61.86	35.61	1.93	0.59	0.00	1250	63	33
7. SCM + OPC	75% OPC + 25% SCM					Not specified; properties considered comparable with OPC		35

^aChemical compositions of raw materials, including CaCO₃, SiO₂, Al₂O₃, Fe₂O₃, and CaSO₄; with the addition of a case, where clinker is mixed with SCM; and including the combustion temperature of seven simulated cases (°C), ranging from 1250 to 1500 °C, with their respective mechanical strengths, where the strength of clinkers in case 7 was not identified as it was integrated with CO₂ mineralization but is assumed to be adequate as it shares similar raw material compositions as that of case 1, respectively. ^bIt is worth noting that the lower water-to-cement (w/c) ratio of CSC increases the compressive strength as less water relative to the amount of clinker is present.³⁶

substantial CO₂ emissions can be removed from the cement production process, the implementation of CCUS demands higher energy.¹⁸ Furthermore, while CCUS offers removal of CO₂ emissions from the cement production process, it does not prevent the generation of CO₂ but mitigates its release into the atmosphere.

Deep decarbonization in the cement sector necessitates the transition to cleaner production by reducing both the dependency on fossil fuels²⁰ and calcination-induced emissions.¹² Alternative fuels that have been considered for clinker production include hydrogen (H₂)^{9,21,22} and biomass.²³ Notably, a prior modeling study by Williams et al.⁹ achieved CO₂ reductions of ~28% in contrast with the conventional fossil fuel (natural gas based) process from the combustion with H₂ fuel. In industry, a report by Hanson Cement²⁴ successfully demonstrated the replacement of fossil fuels with a combination of H₂, biomass, and plasma-based energy supply at Hanson's Ribblesdale plant in the United Kingdom (UK), where it saved about 180,000 tonnes of CO₂ annually. Among alternative fuels, biomass demonstrated climate change mitigation of up to 31% in contrast with fossil fuels.¹² Modeling work by Association M. P. Ltd²⁵ demonstrated that alternative fuel replacement with 50% hydrogen and 50% biomass in the kiln and 83.3% biomass and 16.7% plasma in the calciner was used, leading to the removal of fuel-related CO₂ emissions. Despite these results, fuel-oriented measures alone can only achieve a limited extent of carbon abatement since they do not address emissions from calcination.⁹

The raw meal of Portland clinker consists of calcium carbonate (in the form of limestone, the main source of CO₂), argillaceous clays (silicon), aluminum, and iron, where the chemical compositions are CaCO₃, SiO₂, Al₂O₃, and Fe₂O₃.²⁶ The clinker product compositions include C₃S (alite), C₂S (belite), C₃A (calcium aluminate), and C₄AF (ferrite),⁷ in which C₃S (alite) is the most carbon-intensive component.¹ Targeting CO₂ reductions in calcination involves the use of different clinker types deviating from the conventional OPC clinker as follows:

1. Belite-ye'elinite ferrite (BYF) clinker, produced from a raw meal with a reduction in limestone²⁷ and an increase in aluminate, leads to a product containing ye'elinite (C₄A₃S) and elevated belite and ferrite in the absence of alite.²⁸ BYF also offers a reduction in the sintering temperature from the typical 1500 °C in the kiln for

producing OPC clinkers to the range of 1300–1350 °C.²⁹ BYF clinker displayed energy and CO₂ savings of 20% and 20–40% compared to the OPC clinker, respectively.²⁹

2. High-ferrite clinker (HFC), produced from a raw meal with increased Fe₂O₃ content, leads to a product containing increased ferrite (C₄AF) content. HFC decreases the combined proportion of C₂S and C₃S, offering a reduced sintering temperature by approximately 100 °C compared to traditional OPC.^{30,31} HFC demonstrated up to 20% energy and 18% CO₂ savings to be achieved relative to OPC.^{30–32}
3. Calcium silicate cement (CSC) clinker, which adopts a raw meal with increased silica to displace limestone, leads to a product containing low-lime calcium silicate phases and a significantly reduced sintering temperature at 1200°.³³ CO₂ and energy savings of 30% can be realized relative to OPC.³³

Along with holding potential for energy and CO₂ savings compared to OPC, these BYF, HFC, and CSC clinkers have been reported to offer sufficient mechanical properties needed for replacing OPC, as shown in refs 28, 30–32, and 33, respectively.

While the above-mentioned alternative clinkers are promising for the reduction of the inherent CO₂ emissions from calcination, to our knowledge, their production processes are yet to be systematically assessed and compared to quantify their potential on a consistent basis. By modeling these processes in the Aspen Plus V12.1 process simulator, this study aims to fill the gap and provide a comparative evaluation of these options in terms of energy consumption and CO₂ emissions. Additionally, recognizing the emerging proposal of supplementary cementitious materials (SCMs) derived from CO₂ mineralization that absorbs CO₂ emissions from cement production,^{34,35} a further option incorporating partial replacement of clinkers with SCMs is also evaluated in parallel with the alternative clinkers for comparison. The results from the study are poised to bring new insights into the carbon abatement potential of interventions from a materials perspective, complementing energy-oriented studies of cement production to promote deep decarbonization of this sector.

METHODS

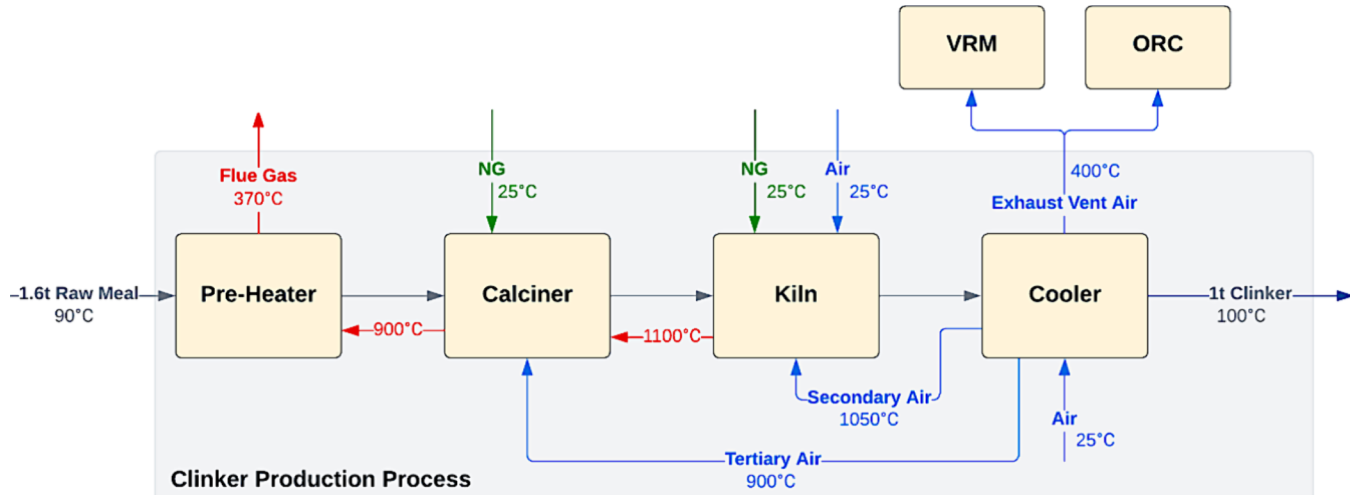
This study is centered on seven technical options for producing clinkers or equivalent products, which are introduced in the

Table 2. Chemical Reactions for the Formation of Clinker Components

cases	mineral component	chemical reaction
1–6	Belite	$2\text{CaO} + \text{SiO}_2 \rightarrow \text{C}_2\text{S}^{33}$
1–4	Alite	$\text{C}_2\text{S} + \text{CaO} \rightarrow \text{C}_3\text{S}^{33}$
1–4	Aluminate	$3\text{CaO} + \text{Al}_2\text{O}_3 \rightarrow \text{C}_3\text{A}^{33}$
1–5	Ferrite	$4\text{CaO} + \text{Al}_2\text{O}_3 + \text{Fe}_2\text{O}_3 \rightarrow \text{C}_4\text{AF}^{33}$
5	Calcium Sulfoaluminate	$3\text{Al}_2\text{O}_3 + 3\text{CaO} + \text{CaSO}_4 \rightarrow \text{Ca}_4\text{Al}_6\text{O}_{12}\text{SO}_4 (\text{C}_4\text{A}_3\text{S})^{39}$
6	Wollastonite	$\text{CaO} + \text{SiO}_2 \rightarrow \text{CaSiO}_3 (\text{CS})^{33}$
6	Rankinite	$3\text{CaO} + 2\text{SiO}_2 \rightarrow \text{Ca}_3\text{Si}_2\text{O}_7 (\text{C}_3\text{S}_2)^{33}$
6	Gehlenite/Melilite	$2\text{CaO} + \text{Al}_2\text{O}_3 + \text{SiO}_2 \rightarrow \text{Ca}_2\text{Al}_2\text{SiO}_7^{29}$

Table 3. Mineral Composition of Six Clinker Cases (wt %)^{29–33,37,38}

case ID	mineral composition of clinker cases (wt %)								
	C ₃ S	C ₂ S	C ₃ A	C ₄ AF	C ₄ A ₃ S	CS	C ₃ S ₂	melilite	amorphous
1. OPC	57.60	18.00	9.00	9.30	0	0	0	0	0
2. HFC-a (4.34)	42.10	28.40	2.80	18.10	0	0	0	0	0
3. HFC-b (3.72)	37.06	32.86	4.32	15.17	0	0	0	0	0
4. HFC-c (3.93)	59.10	8.60	8.50	17.20	0	0	0	0	0
5. BYFC	0	49.70	0	19.90	28.80	0	0	0	0
6. CSC	0	2.96	0	0	0	52.30	13.38	7.12	24.20

**Figure 1.** Schematic of the clinker production process. Air is represented in blue, natural gas in green, flue gas in red, and the material flows in gray. The raw meal mass flow rate and temperatures refer to the case of the OPC clinker production.

Cases for Evaluation section. The evaluation of these options is fundamentally based on the computer simulation of the clinker production processes, as presented in the **Process Simulation** section; the simulation results then provide the quantification of energy consumption and CO₂ emissions, following the approaches described in the **Quantification of Energy Demand and CO₂ Emissions of Clinker Production (Cases 1–6)** section and the **Quantification of Energy Demand and CO₂ Emissions for the Option Involving CO₂ Mineralization (Case 7)** section.

Cases for Evaluation. Seven cases were selected to scrutinize the effects of material composition on energy demand and CO₂ production, as shown in **Table 1**, where six cases contained distinct raw meal compositions for producing clinkers and one involved 25 wt % replacement of a clinker with an SCM produced through CO₂ mineralization. In all cases, natural gas was the assumed fuel for providing thermal energy.

For the reference case (case 1), the raw meal compositions were established following the parameters outlined in ref 11 to produce traditional OPC.

Cases two to four featured three variations of HFC based on the literature, with various Fe₂O₃ contents at 4.34 wt % (case 2),³¹ 3.72 wt % (case 3),³² and 3.93 wt % (case 4).³⁰ Also, according to these references, the sintering temperatures of these HFC cases are 100–150 °C lower than those of the OPC.

BYF clinker was adopted for case 5, with a lower lime (CaO) content and a greater alumina content in the raw meal. BYF required a lower sintering temperature similar to the HFC cases while containing a noticeably higher content of C₂S compared to the other clinkers.²⁹

Case 6 was introduced to represent the CSC clinker,³³ characterized by the lowest CaCO₃ content and the highest silica content in the raw meal among all clinker options. This was accompanied by the lowest sintering temperature of 1250 °C.

Case 7 integrated CO₂ mineralization (not explicitly modeled in this work) based on ref 35, with the utilization of CO₂ from cement flue gas to produce an SCM that contains 40% SiO₂, 50% MgCO₃, and 10% moisture, replacing 25% of OPC clinker.

In terms of the product properties, the literature-reported compressive strengths of the clinkers are listed in **Table 1**. There exist deviations between OPC and the alternative clinkers, although generally the latter have been considered being able to offer product properties comparable to OPC. The same comparability has been deemed valid for case 7,³⁵ although no specific measurements of mechanical strengths were reported.

The properties of each clinker are largely determined by its chemical composition.

Table 2 shows the chemical reactions leading to the key components of the clinkers. The composition of each clinker is shown in **Table 1**. Note that the composition of the raw meal for each of the cases (shown in **Table 1**) was determined according to its literature-reported clinker composition (shown in **Table 3**) by mass balance. Simulations in Aspen using these calculated raw meal inputs showed that the resultant clinker mineral compositions were consistent with the literature values.^{29–33}

Process Simulation. The mathematical modeling work of the clinker production process was based on adapting the Aspen Plus V12.1 simulation model established in an earlier study.⁹ The modeling itself was originally based on a plant producing 4200 tonnes of clinker daily in Alberta, Canada.¹¹ The process utilizes natural gas combustion in air, serving as a primary source of thermal energy, accompanied by electrical energy from the grid. A schematic representation of the production process is shown in **Figure 1**, with the Aspen Plus flowsheet provided in **Figure S1**. To produce OPC clinker, the process begins as the raw meal enters the preheater and is processed in the calciner, where limestone is decomposed at 900 °C to attain 95% calcination.⁴⁰ The calciner output then proceeds to the kiln, where decomposition, transition, and sintering reactions occur, with the sintering temperature reaching 1500 °C, before being cooled to 100 °C in the cooler and exiting the process. In the process, primary air and secondary air enter the kiln's combustor at 25 and 1050 °C, respectively, whereas tertiary air enters the calciner's combustor at 900 °C, following heat recovery.¹¹ The cooling vent air progresses through heat recovery phases, which supply a hot gas flow of 1762 kg/tonne clinker at 176.85 °C to satisfy the operation of a vertical roller mill.¹⁰ The remaining cooling exhaust coupled by the preheater exhaust then provides heat to operate the Organic Rankine Cycle (ORC) for further heat recovery.

The calciner and kiln combustors were modeled as stoichiometric reactors (RStoic), where a series of three RStoic reactors represented the three stages in the kiln. Heat losses were modeled for the combustors, including the calciner, kiln decomposition, kiln transition, and kiln sintering at 42.99 MJ/t clinker, 30.60 MJ/t clinker, 59.40 MJ/t clinker, and 90 MJ/t clinker, respectively.⁷

To simulate the production of an alternative clinker, the above Aspen Plus model was adapted by using a clinker-specific raw meal composition (**Table 1**), chemical reactions (**Table 2**), and their conversions as needed to attain the clinker composition (**Table 3**). Physical properties of new clinker components not present in the OPC clinker are summarized in **Table S1**. Clinker-specific sintering temperatures (**Table 1**) were also applied by adjusting the supply of natural gas and combustion air.

The physical property modeling of all the cases was also based on the previously established Aspen model for OPC clinker production.⁹ The information on new clinker components not available in the databases of Aspen is provided in **Table S1**.

Quantification of Energy Demand and CO₂ Emissions of Clinker Production (Cases 1–6).

Principal components responsible for the net energy consumption of the clinker production processes include the consumption of electrical (fans, raw meal preparation, and auxiliary) and thermal energy (natural gas), along with the recovery of thermal energy into electricity (ORC). The natural gas consumption values were extracted from Aspen simulations. The following assumptions were made in energetic analyses:

1. The scope of energy consumption modeling was set to “gate to gate”; processes that occur before or after the clinker production process were not included;
2. Natural gas was assumed to be 100% methane with a lower heating value of 50 MJ/kg;⁴¹
3. The auxiliary electricity consumption was assumed constant across all cases as 68 kWh/t clinker, according to ref 11;
4. Electricity required for raw meal preparation was presumed to be constant among the cases at 25.2 kWh/t clinker, as per ref 42.

The electrical energy demand for each fan (W_{fan}) was determined by scaling the reference fan power consumption, as per ref 11, where q_{ref} and W_{ref} are the volumetric gas flow and the power consumption of a reference fan, respectively, and q is the volumetric gas flow of the fan, as shown below:

$$W_{\text{fan}} = W_{\text{ref}} \times \left(\frac{q}{q_{\text{ref}}} \right)^3 \quad (1)$$

An ORC was incorporated into each clinker production process for waste heat recovery, which produces electricity to partially offset the process electricity demand. The ORC electricity output ($W_{\text{ORC}} = Q_{\text{in}} \times \eta_{\text{th}}$) was calculated using the recovered waste heat from the hot gas stream (Q_{in}), which was acquired from Aspen simulation results of each cooler. This represented the evaporator of the ORC, on the waste heat streams cooled to 130 °C, which was 20 °C higher (providing heat transfer driving force) compared to the working fluid of the ORC (at 110 °C), following the ORC design presented in ref 43. The ORC efficiency, η_{th} , was set to 0.225, according to the assumed organic working fluid.⁴⁴

On CO₂ emissions, both CO₂ directly emitted from the clinker production process, resulting from calcination and natural gas combustion (as quantified by Aspen simulations), and indirect emissions from the supply of grid electricity consumed in the clinker production process were considered. Other CO₂ emissions in the cement supply chain were not included. The carbon footprint of grid electricity is dependent on geographical locations. Three out of the top 10 cement producing countries with low, medium, and high carbon intensities (on a basis of kg of CO₂eq per MWh), namely, Brazil,⁴⁵ the United States,⁴⁵ and China,⁴⁶ were chosen to calculate location-sensitive emissions from electricity.

Quantification of Energy Demand and CO₂ Emissions for the Option Involving CO₂ Mineralization (Case 7). The CO₂ mineralization process was incorporated in case 7, involving the blending of 250 kg of SCM, derived from the mineralization of CO₂, with 750 kg of clinker, facilitating the production of 1 tonne of the final product, in accordance with ref 35. CO₂ was sourced by a monoethanolamide (MEA)-based process applied to the flue gas from clinker production with a capture efficiency of 90%.³⁵ The CO₂ mineralization process produced a stream of SCM consisting of 40% SiO₂, 50% MgCO₃, and 10% moisture (on a weight basis).³⁵

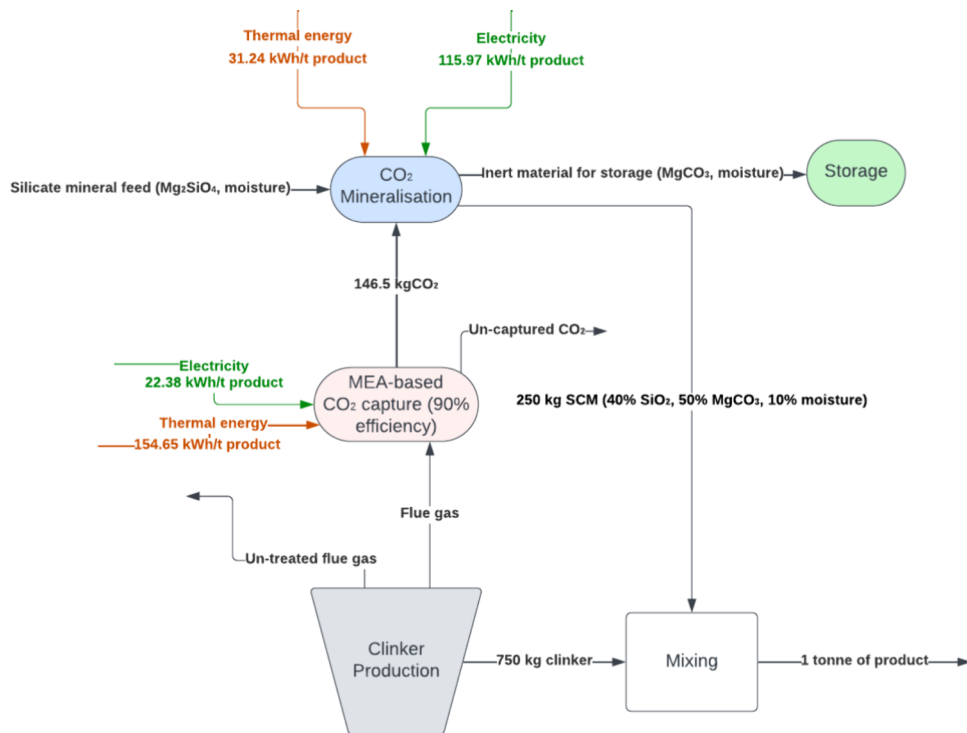


Figure 2. Process diagram for cases involving CO_2 mineralization. The electrical and thermal energy inputs were calculated from the paper;³⁰ the compositions of SCM were based on the literature.³⁵

Table 4. Key Players for the Electrical and Thermal Energy Demand of All Cases^a

	case 1 OPC	case 2 HFC-77.08	case 3 HFC-77.33	case 4 HFC-78.46	case 5 BYFC	case 6 CSC	case 7 SCM + OPC
Electrical Energy for clinker (kWh/t clinker)							
Fans (kWh/t)	165.66	86.65	77.76	91.63	62.28	37.20	124.25
Auxiliary (kWh/t)	68.00	68.00	68.00	68.00	68.00	68.00	51.00
ORC (kWh/t)	-73.79	-61.09	-59.33	-62.69	-48.15	-24.07	-55.34
Raw Meal Preparation (kWh/t)	25.20	25.20	25.20	25.20	25.20	25.20	18.90
MEA Capture (electrical)	N/A						22.38
Mineralization (electrical)							115.97
Total electrical energy (kWh/t clinker)	185.07	118.76	111.63	122.14	107.33	106.33	277.16
Thermal Energy for clinker (kWh/t clinker)							
Natural Gas (kWh/t)	1035.37	924.54	907.81	971.83	731.03	558.78	776.53
MEA Capture (thermal)	N/A						154.65
Mineralization (thermal)							31.24
Total thermal energy (kWh/t clinker)	1035.37	924.54	907.81	971.83	731.03	558.78	962.41
Net total energy (kWh/t clinker)	1220.44	1043.30	1019.45	1093.97	838.36	665.11	1239.57

^aAs CO_2 mineralization was only applicable to case 7, CO_2 mineralization energy (thermal and electrical) was not applicable to cases 1–6.

To determine the electrical and thermal energy requisites for the production of 750 kg of clinker, 75% of the corresponding values of the OPC (case 1) were taken, as illustrated in Figure 2.

For the production of 250 kg of SCM containing 40% or 100 kg of SiO_2 , the CO_2 demand was stoichiometrically determined to be 146.50 kg of CO_2 , according to the reaction equation of magnesium silicate carbonation (see eq 2). The thermal and electrical energy demands for MEA-based carbon capture were 3.8 MJ/kg CO_2 captured (thermal) and 0.55 MJ/kg CO_2 captured (electrical).⁴⁷ The electrical and thermal energy required for the CO_2 mineralization process leading to the production of 250 kg of SCM were 115.97 and 31.24 kWh, respectively.³⁵

The quantification of CO_2 emissions for case 7 included (see eq 1) (1) 75% CO_2 emissions from the production of 1 tonne of OPC clinker in case 1, as determined by the approach described in the Quantification of Energy Demand and CO_2 Emissions of Clinker Production (Cases 1–6) section; (2) deduction of 146.50 kg of CO_2 consumed by mineralization; (3) CO_2 emissions by the supply of thermal energy required for mineralization and MEA-based carbon capture at 241 kg CO_2/MWh ;³⁵ and (4) carbon footprint of the electricity consumed by mineralization and MEA-based carbon capture, based on the location-specific carbon intensities of grid electricity in the three chosen countries.

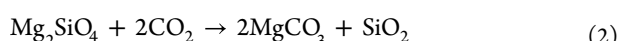


Table 5. CO₂ Emissions for Seven Simulated Cases in Three Different Geographical Locations of the United States (US), China, and Brazil

		OPC clinker production		SCM - MEA capture		SCM - CO ₂ mineralisation		net total CO ₂
		CO ₂ produced (kgCO ₂ /t clinker) - from Aspen	net electrical (kgCO ₂ /t clinker)	electrical (kgCO ₂ /t clinker)	thermal (kgCO ₂ /t clinker)	electrical (kgCO ₂ /t clinker)	thermal (kgCO ₂ /t clinker)	total (kgCO ₂ /t clinker)
Case 1 OPC	USA	741.50	67.92	N/A	N/A	N/A	N/A	809.42
	China	741.50	98.30	N/A	N/A	N/A	N/A	839.80
	Brazil	741.50	18.88	N/A	N/A	N/A	N/A	760.38
Case 2 HFC-a (4.34)	USA	695.80	43.58	N/A	N/A	N/A	N/A	739.38
	China	695.80	63.08	N/A	N/A	N/A	N/A	758.88
	Brazil	695.80	12.11	N/A	N/A	N/A	N/A	707.91
Case 3 HFC-b (3.72)	USA	694.43	40.97	N/A	N/A	N/A	N/A	735.40
	China	694.43	59.29	N/A	N/A	N/A	N/A	753.72
	Brazil	694.43	11.39	N/A	N/A	N/A	N/A	705.82
Case 4 HFC-c (3.93)	USA	718.62	44.83	N/A	N/A	N/A	N/A	763.45
	China	718.62	64.88	N/A	N/A	N/A	N/A	783.50
	Brazil	718.62	12.46	N/A	N/A	N/A	N/A	731.08
Case 5 BYF	USA	537.28	39.39	N/A	N/A	N/A	N/A	576.67
	China	537.28	57.01	N/A	N/A	N/A	N/A	594.29
	Brazil	537.28	10.95	N/A	N/A	N/A	N/A	548.23
Case 6 CSC	USA	481.34	39.02	N/A	N/A	N/A	N/A	520.36
	China	481.34	56.48	N/A	N/A	N/A	N/A	537.81
	Brazil	481.34	10.85	N/A	N/A	N/A	N/A	492.18
Case 7 SCM + OPC	USA	409.63	50.94	8.21	37.27	42.56	7.53	556.14
	China	409.63	73.73	11.89	37.27	61.60	7.53	601.63
	Brazil	409.63	14.16	2.28	37.27	11.83	7.53	482.69

RESULTS AND DISCUSSION

This section presents and discusses the results pertaining to energy consumption and carbon intensity, offering a comparative analysis of various cases. Specifically, we examine the thermal energy input from natural gas and the electrical energy requirement. The carbon intensity is assessed, determining the amount of CO₂ produced and the carbon footprint associated with electricity, which extends across three distinct locations, namely, the United States, China, and Brazil.

Energy Intensity. The energy consumption results are presented in Table 4. All alternative clinkers (cases 2–6) were predicted to gain energy savings compared to the OPC clinker (case 1), as projected in previous studies.^{29–33} In particular, case 6 (CSC clinker) is the most energy-efficient, with a total energy intensity of 665.1 kWh/tonne clinker, which represents a ~46% reduction in thermal and total energy, compared to case 1 (OPC). Its energy savings can be attributed to the significantly lower sintering temperature (1250 °C) and CaCO₃ input (989.7 kg/tonne clinker) corresponding to significantly lower contents of C₃S and C₂S. In comparison, case 1 (OPC) had a sintering temperature of 1500 °C and a CaCO₃ input of 1271.5 kg/tonne clinker, both demanding greater thermal energy input.

Case 5 (BYF) shared a similar CaCO₃ content with case 6 but with a higher sintering temperature (by 100 °C) and a substantial amount of C₂S in the clinker composition, making it the second most energy-efficient alternative clinker, saving thermal energy and total energy by 29.4 and 31.3%, respectively, compared to those of the case for the OPC.

Among the high-ferrite cases (cases 2–4), electricity and thermal energy consumption were comparable, with differences below 10%, resulting from minor variations in the raw meal and clinker compositions. Notably, among the high-ferrite options, case 3 (HFC-b), with the lowest alite content, exhibited the

lowest thermal and total energy consumption with 12.3 and 16.5% savings, respectively, compared to those of OPC.

The case involving SCM (case 7) was the most energy-intensive process, even more demanding than case 1, which supplied 75% of its product. This suggests that, on a basis of 1 kg of product (SCM or clinker), the energy required for mineralization and MEA-based carbon capture (1.30 kWh/kg SCM) was greater than that required for OPC clinker production (1.22 kWh/kg).

Finally, it is worth noting that thermal energy from natural gas emerged as the key contributor to the total energy demand, contributing 63–89% of the total energy demand across all the cases. Besides, it was observed that case 1 had the highest and case 6 had the lowest heat recovery value from ORC as the amount of recoverable waste heat was correlated with the natural gas input in the processes.

Carbon Intensity. As shown in Table 5, all non-OPC options (cases 2–7) were predicted to have a carbon intensity lower than that of the OPC clinker (case 1). Among the alternative clinkers (cases 2–6), the trend in carbon intensity agrees well with that in thermal energy consumption, where reduced natural gas consumption was coupled with a reduced CaCO₃ content in the raw meal, both contributing to the reduction of CO₂ emissions. Case 6 (CSC) was projected to achieve a 35.1% reduction in direct emissions (i.e., excluding carbon footprint of electricity) compared to case 1, followed by 27.5% and 3.1–6.4% reduction by case 5 (BYF) and cases 2–4 (HFC clinkers), respectively. These values of CO₂ savings were comparable to the literature, suggesting 30%, 20–40%, and up to 18% in contrast with OPC for CSC, BYF, and HFC clinkers, respectively^{29–33} (shown in Table 7). When the carbon footprint of electricity is included, the results differ between the three countries, although their difference was within 10% despite the significant gap in the carbon intensity of grid

electricity. This was a result of the relatively low share of electricity in total energy consumption. Comparing case 6 with case 1, the reductions of total carbon intensity for producing 1 tonne of clinker were 35.7, 36, and 35.3% for the US, China, and Brazil, respectively.

For the option involving CO₂ mineralization (case 7), the impact of replacing 250 kg of clinker with the SCM on total carbon intensity was dictated by the combined effect of three elements: (1) CO₂ removal through the mineralization process, (2) avoided CO₂ emissions from the replaced 250 kg of clinker, and (3) CO₂ emissions associated with the supply of electrical and thermal energy for CO₂ capture and mineralization. The second and third elements are differentially affected by the carbon intensity of the grid electricity in different locations. Compared to case 1 (OPC), case 7 clearly shows, for all three countries, that the benefit of CO₂ savings (elements 1 and 2) outweighs the CO₂ burden of additional energy consumption (element 3), leading to 31.3, 28.4, and 36.5% reduction in total carbon intensity for the US, China, and Brazil, respectively (shown in Table 5). These findings were comparable to the literature, where CO₂ savings of 33% were realized from the substitution of 25% SCM from CO₂ mineralization.³⁵ However, the comparison of case 7 with case 6 shows that while Brazil was predicted to (slightly) benefit from the SCM replacement from its rather “green” electricity grid, the higher energy consumption in the case involving the replacement resulted in a worse overall carbon intensity for the US and China compared to a low-carbon clinker (CSC).

Further Discussion. From the results presented above on alternative clinkers, lowering the sintering temperature and CaCO₃ content in the raw meal both played a role in reducing energy consumption and CO₂ emissions. A less understood aspect was the relative contributions of these two factors. To shed light on this, additional supporting simulation of OPC clinker production at 1400 °C (which is the lower end of the practical range⁴⁸) was conducted, as per Table 6. Furthermore,

Table 6. Reference of the OPC Case Compared to a Lower Sintering Temperature Scenario (1400 °C) and Hypothetical Additional Simulations with Changes to the Sintering Temperatures of 1350 °C (H1-OPC) and 1250 °C (H2-OPC)

reference OPC vs hypothetical supporting simulations	sintering temperature (°C)	energy consumption (kWh/t clinker)	CO ₂ produced (kgCO ₂ /t clinker)
OPC (reference)	1500	1220.4	741.5
OPC (low sintering T)	1400	1134.5	733.8
H1-OPC	1350	1063.8	730.1
H2-OPC	1250	1006.9	722.3

two hypothetical lower sintering temperatures for the OPC clinker, 1350 and 1250 °C, directly corresponding to those adopted for BYF and CSC clinkers, respectively, were simulated (see Tables 6, S2 and S3). These additional simulations showed reductions between 7.0 and 17.5% in total energy consumption and between 1.0 and 2.6% in average CO₂ emissions, all in contrast with case 1 (OPC). In comparison, and as shown earlier, the assessed alternative clinkers achieved up to 45.5% energy reductions and 35.1% CO₂ reductions. The contrast of these percentage savings suggests that adopting a low-limestone raw meal plays a more significant role in CO₂ and energy reductions in comparison to lowering the sintering temperature.

The alternative clinkers studied in this work have previously been considered to be able to achieve energy and CO₂ savings (shown in Table 7). Here, we can compare the previously stated

Table 7. Energy and CO₂ Savings from the Literature Compared to Traditional OPC Clinker, with Corresponding Literature References, and Energy and CO₂ Savings from the Results Compared to the Reference Case 1

alternative clinkers	energy savings (literature)	CO ₂ savings (literature)	energy savings (results)	CO ₂ savings (results)	literature references
HFC-a	17–20%	15–18%	14.5%	6.2%	31
HFC-b	N/A	N/A	16.5%	6.4%	32
HFC-c	5%	5%	10.4%	3.1%	30
BYF	20%	20–40%	31.3%	27.5%	29
CSC	30%	30%	45.5%	35.1%	33

CO₂ and energy performances with what was predicted in this study through consistent modeling. As shown in Table 7, both cases 5 (BYF) and 6 (CSC) demonstrate a notable agreement with the existing literature^{29,33} regarding CO₂ savings; however, the findings of this study indicate higher energy savings in comparison with the literature. This difference may be caused by the assessment’s consideration of various energy types and distinct comparison baselines. Whist existing studies provide a comparison with coal-combusted OPC,^{29–33} this study uses natural gas-combusted OPC as a benchmark. In contrast, the HFC cases in the results only exhibited modest CO₂ savings of up to 6.4% from the calcination process in contrast with the literature, which projected CO₂ savings of up to 18%³¹ (shown in Table 7). This was predominantly a result of the minor reductions in the CaCO₃ content in the raw meal.

Examining the underlying chemical and physical mechanisms, the decomposition of CaCO₃ to CaO involves the decomposition reaction, $\text{CaCO}_3 \rightarrow \text{CaO} + \text{CO}_2$, releasing 0.44 kg of CO₂ per tonne of CaCO₃ converted. Additionally, the reaction requires an input of 179.4 kJ/kmol of heat at 900 °C.⁷ This emphasizes that both CO₂ and energy savings can be realized from the reduction of the CaCO₃ content in the raw material composition, a key target that has been aimed at by all the alternative clinkers. In the kiln processes, silica (SiO₂) reacts with CaO to form alite (C₃S) and belite (C₂S), which are the primary components of clinker, requiring 12.0 kJ/kmol and releasing 135.0 kJ/kmol of heat, respectively.⁷ Furthermore, the clinker raw materials, iron oxide (Fe₂O₃) and aluminum oxide (Al₂O₃), demand conversion temperatures of up to 1280 °C, releasing heat of 41.3 kJ/kmol and requiring 19.7 kJ/kmol, respectively, for the formation of C₄AF and C₃A.⁷ Energetically, the above suggests that C₂S and C₄AF would be preferred over C₃S and C₃A, respectively, which has been broadly reflected in the contrast of compositions between the OPC clinker and the alternative clinkers studied in this work.

With the use of SCMs, the main study presented above assumed 25% of replacement, although a lower-level replacement may be favored due to concerns such as product workability.⁴⁹ If 20% of clinker were to be replaced with SCMs, an additional option suggested by Strunge et al.,³⁵ our additional assessment showed that CO₂ reductions in the results observed in case 7 compared with case 1 would be 25.1, 22.8, and 29.2% for the United States, China, and Brazil, respectively. These reductions represent 6.2, 5.6, and 7.3% decreases in CO₂ savings compared to the scenario with 25% SCM replacement in

these respective countries. Despite these decreases, the CO₂ savings potential of this technical option remains significant.

As a final comment, although the electricity consumption is relatively minor compared to the thermal energy demand in clinker production that is dominated by thermal processes (i.e., the operation of the calciner and the kiln), the introduction of an SCM could potentially alter the picture, depending on the production method of the SCM. In the example included in this study, 22.4% of the total energy consumption of the CO₂ mineralization processes is electricity, higher than that of OPC production. A higher share of electricity in total energy consumption, among other impacts, will lead to greater differentiation in the total carbon emissions between countries with diverse carbon intensities in their electricity supply, potentially making some options more suitable for certain countries than others.

CONCLUSIONS

With the aid of process simulation, this work quantified how CO₂ emissions and energy consumption of the cement production process can be reduced by altering the composition of the clinker. The energy demand and CO₂ production in 7 evaluated cases were found to vary according to four key factors: limestone content in the raw meal, alite (C₃S) content in the clinker, sintering temperature, and substituting conventional clinker with SCMs from CO₂ mineralization.

1. The limestone (CaCO₃) content in the raw meal plays a key role, as the chemical reaction of calcination is a significant source of both thermal energy demand and direct CO₂ emissions. All the cases alternative to OPC clinker featured reduction of the use of CaCO₃, albeit to different extents, leading to reduced fuel consumption for calcination and lower combined CO₂ emissions from fuel combustion and CaCO₃ decomposition in the calcination step.
2. Reduction of the alite content of the clinker is advantageous in achieving lower CO₂ output from the cement production process, as particularly demonstrated by cases 5 (BYC) and 6 (CSC). This is in line with the literature, which determined that alite was the most carbon-intensive clinker mineral when compared to the rest.
3. The alternative clinkers were accompanied by a lower sintering temperature compared to OPC, which was a contributing factor to the lower energy demand and CO₂ emissions, although more significant contributions were shown to stem from the alteration of the raw meal and hence the clinker compositions.
4. The use of an SCM derived through mineralizing part of the CO₂ emissions from conventional clinker production (OPC) to partially substitute OPC clinkers demonstrated a significant reduction of CO₂. However, it did not lead to the lowering of energy demand due to the high energy (thermal and electrical) requirement of CO₂ mineralization.

Overall, case 6 (CSC) emerges as the winner in energy efficiency (45.5% energy reduction compared to case 1, OPC), with the lowest CaCO₃ content in the raw meal, zero alite in the clinker, the lowest sintering temperature, and the absence of the energy demand associated with SCM. In terms of direct CO₂ emissions from the production process (i.e., excluding the carbon footprint of electricity), CSC clinker achieved a 35.1%

reduction from the OPC clinker, which is the second best, next to case 7 (SCM + OPC), which achieved a 44.8% reduction. However, when the carbon footprint of electricity is included in the total CO₂ emissions, the SCM+OPC case retains its superiority over the CSC case only in Brazil from its low-carbon grid but only in China and the United States. This indicates the importance of decarbonizing electricity generation, particularly in production options, where the electrical energy demand is significant.

The encouraging results of this modeling study on alternative clinkers warrant further experimental testing of these products, as well as their production processes, so that their potential in decarbonizing the cement industry can be firmly established. Additionally, future work can explore cements used in concretes with equivalent performance, allowing for more detailed and in-depth comparisons.

ASSOCIATED CONTENT

Data Availability Statement

All energy and flow data are referenced within the main text with simulation data obtained using Aspen Plus software.

Supporting Information

The Supporting Information is available free of charge at <https://pubs.acs.org/doi/10.1021/acs.iecr.4c01885>.

Data involving the physical properties of clinker minerals, energy and CO₂ performance of hypothetical cases, and process flow diagram for Aspen Plus V12.1 modeling for the cement production process ([PDF](#))

AUTHOR INFORMATION

Corresponding Author

Franco Williams – Department of Engineering Science, University of Oxford, Oxford OX1 3PJ, U.K.;  orcid.org/0000-0001-8192-312X; Email: franco.williams@eng.ox.ac.uk

Author

Aidong Yang – Department of Engineering Science, University of Oxford, Oxford OX1 3PJ, U.K.;  orcid.org/0000-0001-5974-247X

Complete contact information is available at: <https://pubs.acs.org/10.1021/acs.iecr.4c01885>

Author Contributions

F.W.: Conceptualization, methodology, investigation, software, analysis, writing—original draft. A.Y.: Conceptualization, supervision, validation, writing—review and editing.

Notes

The authors declare no competing financial interest.

ACKNOWLEDGMENTS

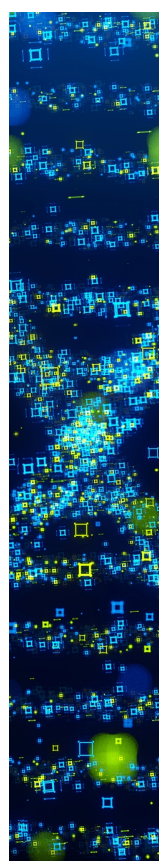
The authors are grateful to Till Strunge for providing supporting data on CO₂ mineralization for this paper.

REFERENCES

- (1) Scrivener, K. L.; John, V. M.; Gartner, E. M. Eco-Efficient Cements: Potential Economically Viable Solutions for a Low-CO₂ Cement-Based Materials Industry. *Cem. Concr. Res.* **2018**, *114*, 2–26.
- (2) Jaganmohan, M. Production volume of cement worldwide from 1995 to 2023; Statista. <https://www.statista.com/statistics/1087115/global-cement-production-volume/> (accessed 2024-07-01).

- (3) Supriya; Chaudhury, R.; Sharma, U.; Thapliyal, P. C.; Singh, L. P. Low-CO₂ Emission Strategies to Achieve Net Zero Target in Cement Sector. *J. Clean. Prod.* **2023**, *417*, No. 137466.
- (4) Cormos, C. C. Decarbonization Options for Cement Production Process: A Techno-Economic and Environmental Evaluation. *Fuel* **2022**, *320*, No. 123907.
- (5) Nie, S.; Zhou, J.; Yang, F.; Lan, M.; Li, J.; Zhang, Z.; Chen, Z.; Xu, M.; Li, H.; Sanjayan, J. G. Analysis of Theoretical Carbon Dioxide Emissions from Cement Production: Methodology and Application. *J. Clean. Prod.* **2022**, *334*, No. 130270.
- (6) British Geological Survey. *Cement Raw Materials British Geological Survey Mineral Profile*; United Kingdom, 2005.
- (7) Faria, D. G.; Carvalho, M. M. O.; Neto, M. R. V.; de Paula, E. C.; Cardoso, M.; Vakkilainen, E. K. Integrating Oxy-Fuel Combustion and Power-to-Gas in the Cement Industry: A Process Modeling and Simulation Study. *Int. J. Greenh. Gas Control* **2022**, *114*, No. 103602.
- (8) The European Cement Association *The Story of Cement Manufacture*; Cembureau. <https://cembureau.eu/media/wm0jmdw/cementmanufacturing.pdf> (accessed 2024-01-09).
- (9) Williams, F.; Yang, A.; Nhuchhen, D. R. Decarbonisation Pathways of the Cement Production Process via Hydrogen and Oxy-Combustion. *Energy Convers. Manag.* **2024**, *300*, No. 117931.
- (10) Ghalandari, V.; Esmaeilpour, M.; Payvar, N.; Toufiq Reza, M. A Case Study on Energy and Exergy Analyses for an Industrial-Scale Vertical Roller Mill Assisted Grinding in Cement Plant. *Adv. Powder Technol.* **2021**, *32* (2), 480–491.
- (11) Nhuchhen, D. R.; Sit, S. P.; Layzell, D. B. Decarbonization of Cement Production in a Hydrogen Economy. *Appl. Energy* **2022**, *317*, No. 119180.
- (12) Cavalett, O.; Watanabe, M. D. B.; Voldsgaard, M.; Roussanaly, S.; Cherubini, F. Paving the Way for Sustainable Decarbonization of the European Cement Industry. *Nat. Sustain.* **2024**, *7* (5), 568–580.
- (13) Antunes, M.; Santos, R. L.; Pereira, J.; Rocha, P.; Horta, R. B.; Colaço, R. Alternative Clinker Technologies for Reducing Carbon Emissions in Cement Industry: A Critical Review. *Materials (Basel)* **2022**, *15*, 209.
- (14) Klee, H. *The Cement Sustainability Initiative - Cement Industry Energy and CO₂ Performance*; 2009.
- (15) Baker, R. W.; Freeman, B.; Kniep, J.; Huang, Y. I.; Merkel, T. C. CO₂ Capture from Cement Plants and Steel Mills Using Membranes. *Ind. Eng. Chem. Res.* **2018**, *57* (47), 15963–15970.
- (16) Gardarsdóttir, S. O.; De Lena, E.; Romano, M.; Roussanaly, S.; Voldsgaard, M.; Pérez-Calvo, J. F.; Berstad, D.; Fu, C.; Anantharaman, R.; Sutter, D.; Gazzani, M.; Mazzotti, M.; Cinti, G. Comparison of Technologies for CO₂ Capture from Cement Production—Part 2: Cost Analysis. *Energies (Basel)* **2019**, *12* (3), 542.
- (17) Rolfe, A.; Huang, Y.; Haaf, M.; Pita, A.; Rezvani, S.; Dave, A.; Hewitt, N. J. Technical and Environmental Study of Calcium Carbonate Looping versus Oxy-Fuel Options for Low CO₂ Emission Cement Plants. *Int. J. Greenh. Gas Control* **2018**, *75*, 85–97.
- (18) Jiang, K.; Yu, H.; Sun, Z.; Lei, Z.; Li, K.; Wang, L. Zero-Emission Cement Plants with Advanced Amine-Based CO₂ Capture. *Environ. Sci. Technol.* **2024**, *58* (16), 6978–6987.
- (19) Guo, Y.; Luo, L.; Liu, T.; Hao, L.; Li, Y.; Liu, P.; Zhu, T. A Review of Low-Carbon Technologies and Projects for the Global Cement Industry. *J. Environ. Sci.* **2024**, *136*, 682–697.
- (20) Chatterjee, A.; Sui, T. Alternative Fuels—Effects on Clinker Process and Properties. *Cem. Concr. Res.* **2019**, *123*, No. 105777.
- (21) El-Emam, R. S.; Gabriel, K. S. Synergizing Hydrogen and Cement Industries for Canada's Climate Plan—Case Study. *Energy Sources A: Recovery Util. Environ. Eff.* **2021**, *43* (23), 3151–3165.
- (22) Juangsa, F. B.; Cezeliano, A. S.; Darmanto, P. S.; Aziz, M. Thermodynamic Analysis of Hydrogen Utilization as Alternative Fuel in Cement Production. *S. Afr. J. Chem. Eng.* **2022**, *42*, 23–31.
- (23) Kusuma, R. T.; Hiremath, R. B.; Rajesh, P.; Kumar, B.; Renukappa, S. Sustainable Transition towards Biomass-Based Cement Industry: A Review. *Renew. Sustain. Energy Rev.* **2022**, *163*, No. 112503.
- (24) Hanson. *Hydrogen trial | Hanson UK*. <https://www.hanson.co.uk/en/socialvalue/climate/hydrogen-trial> (accessed 2023-05-09).
- (25) Association, M. P.; Ltd, C. *Options for switching UK cement production sites to near zero CO₂ emission fuel: Technical and financial feasibility*. https://assets.publishing.service.gov.uk/government/uploads/system/uploads/attachment_data/file/866365/Phase_2_-_MPA_-_Cement_Production_Fuel_Switching.pdf (accessed 2023-07-11).
- (26) Mikulčić, H.; Klemes, J. J.; Vujanović, M.; Urbaniec, K.; Duić, N. Reducing Greenhouse Gases Emissions by Fostering the Deployment of Alternative Raw Materials and Energy Sources in the Cleaner Cement Manufacturing Process. *J. Clean. Prod.* **2016**, *136*, 119–132.
- (27) Morin, V.; Termkhajornkit, P.; Huet, B.; Pham, G. Impact of Quantity of Anhydrite, Water to Binder Ratio, Fineness on Kinetics and Phase Assemblage of Belite-Ye'elimitite-Ferrite Cement. *Cem. Concr. Res.* **2017**, *99*, 8–17.
- (28) Wang, F.; Long, G.; Bai, M.; Wang, J.; Shi, Y.; Zhou, X.; Zhou, J. L. A New Perspective on Belite-Ye'elimitite-Ferrite Cement Manufactured from Electrolytic Manganese Residue: Production, Properties, and Environmental Analysis. *Cem. Concr. Res.* **2023**, *163*, No. 107019.
- (29) Sabbah, A.; Zhutovsky, S. Effect of Sulfate Content and Synthesis Conditions on Phase Composition of Belite-Ye'elimitite-Ferrite (BYF) Clinker. *Cem. Concr. Res.* **2022**, *155*, No. 106745.
- (30) Elkneswaran, Y.; Noguchi, N.; Matumoto, K.; Morinaga, Y.; Chabayashi, T.; Kato, H.; Nawa, T. Characteristics of Ferrite-Rich Portland Cement: Comparison with Ordinary Portland Cement. *Front. Mater.* **2019**, *6*, 97.
- (31) Zhang, K.; Shen, P.; Yang, L.; Rao, M.; Nie, S.; Wang, F. Development of High-Ferrite Cement: Toward Green Cement Production. *J. Clean. Prod.* **2021**, *327*, No. 129487.
- (32) Yang, H. M.; Zhang, S. M.; Wang, L.; Chen, P.; Shao, D. K.; Tang, S. W.; Li, J. Z. High-Ferrite Portland Cement with Slag: Hydration, Microstructure, and Resistance to Sulfate Attack at Elevated Temperature. *Cem. Concr. Compos.* **2022**, *130*, No. 104560.
- (33) Sahu, S.; Meininger, R. C. Performance of CO₂-Reducing Cement Based on Calcium Silicates 15 Th International Congress on the Chemistry of Cement. In *International Congress on the Chemistry of Cement*; 2019.
- (34) Bremen, A. M.; Strunge, T.; Ostovari, H.; Spütz, H.; Mhamdi, A.; Renforth, P.; Van Der Spek, M.; Bardow, A.; Mitsos, A. Direct Olivine Carbonation: Optimal Process Design for a Low-Emission and Cost-Efficient Cement Production. *Ind. Eng. Chem. Res.* **2022**, *61* (35), 13177–13190.
- (35) Strunge, T.; Renforth, P.; der Spek, V. Towards a Business Case for CO₂ mineralisation in the Cement Industry. *Commun. Earth Environ.* **2022**, *3*, 59.
- (36) Kondraivendhan, B.; Bhattacharjee, B. Strength and w/c Ratio Relationship of Cement Based Materials through Pore Features. *Mater. Charact.* **2016**, *122*, 124–129.
- (37) Svanning, K.; Höskuldsson, A.; Justnes, H. Prediction of Potential Compressive Strength of Portland Clinker from Its Mineralogy. *Cem. Concr. Compos.* **2010**, *32* (4), 300–311.
- (38) Standards, B. *BS EN 197-1:2011*; 2011.
- (39) Dong, K.; Xie, F.; Wang, W.; Chang, Y.; Chen, C.; Gu, X. Calcination of Calcium Sulphoaluminate Cement Using Pyrite-Rich Cyanide Tailings. *Crystals (Basel)* **2020**, *10* (11), 971.
- (40) Vikström, A. *Separate Calcination in Cement Clinker Production: A Laboratory Scale Study on How an Electrified Separate Calcination Step Affects the Phase Composition of Cement Clinker*; Dissertation: Sweden, 2021.
- (41) Wan, B. *Energy Density of Methane - The Physics Factbook*. <https://hypertextbook.com/facts/2004/BillyWan.shtml> (accessed 2023-01-13).
- (42) Meng, R.; Zhao, Q.; Wu, M.; Long, Q.; Zhou, M. A Survey and Analysis on Electricity Consumption of Raw Material Mill System in China Cement Industry between 2014 and 2019. *Sustainability* **2021**, *13* (3), 1126.
- (43) Ahmed, A.; Esmaeil, K. K.; Irfan, M. A.; Al-Mufadi, F. A. Design Methodology of Organic Rankine Cycle for Waste Heat Recovery in Cement Plants. *Appl. Therm. Eng.* **2018**, *129*, 421–430.

- (44) Moreira, L. F.; Arrieta, F. R. P. Thermal and Economic Assessment of Organic Rankine Cycles for Waste Heat Recovery in Cement Plants. *Renew. Sustain. Energy Rev.* **2019**, *114*, No. 109315.
- (45) Our World in Data. *Carbon intensity of electricity*, 2022; Our World in Data. <https://ourworldindata.org/grapher/carbon-intensity-electricity> (accessed 2024–01–11).
- (46) Tiseo, I. *Carbon intensity of the power sector in China from 2000 to 2022*; Statista. <https://www.statista.com/statistics/1300419/power-generation-emission-intensity-china/#:~:text=The%20carbon%20intensity%20of%20electricity,two%20decades%2C%20it%20remains%20high>. (accessed 2023–11–24).
- (47) Voldsgård, M.; Gardarsdóttir, S. O.; De Lena, E.; Pérez-Calvo, J. F.; Jamali, A.; Berstad, D.; Fu, C.; Romano, M.; Roussanaly, S.; Anantharaman, R.; Hoppe, H.; Sutter, D.; Mazzotti, M.; Gazzani, M.; Cinti, G.; Jordal, K. Comparison of Technologies for CO₂ Capture from Cement Production—Part 1: Technical Evaluation. *Energies (Basel)* **2019**, *12* (3), 559.
- (48) Stadler, K. S.; Poland, J.; Galleste, E. Model Predictive Control of a Rotary Cement Kiln. *Control Eng. Pract.* **2011**, *19* (1), 1–9.
- (49) Skocek, J.; Zajac, M.; Ben Haha, M. Carbon Capture and Utilization by Mineralization of Cement Pastes Derived from Recycled Concrete. *Sci. Rep.* **2020**, *10* (1), 5614.



CAS BIOFINDER DISCOVERY PLATFORM™

STOP DIGGING THROUGH DATA — START MAKING DISCOVERIES

CAS BioFinder helps you find the right biological insights in seconds

Start your search



Potential of Reducing CO₂ Emissions in Cement Production through Altering Clinker Compositions

Franco Williams* and Aidong Yang



Cite This: *Ind. Eng. Chem. Res.* 2024, 63, 17158–17167



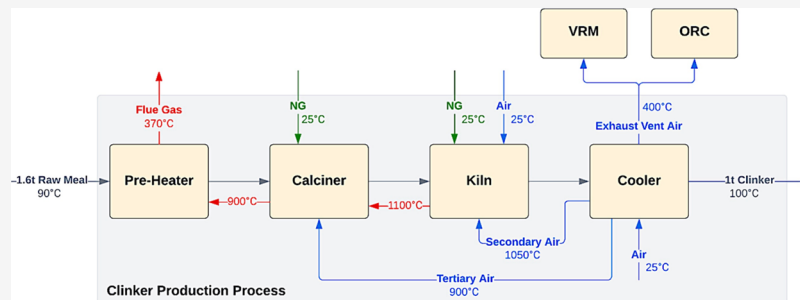
Read Online

ACCESS |

Metrics & More

Article Recommendations

Supporting Information



ABSTRACT: This study assessed seven cases of distinct raw material compositions with the aid of process simulation using Aspen Plus V12.1, focusing on reducing carbon dioxide (CO₂) emissions and energy demands from clinker production. Material and energy flows for the raw meal mixes were simulated in a natural gas-fueled plant. The results indicated up to 45.5% energy and 35.1% CO₂ reduction using alternative clinkers compared to ordinary Portland cement (OPC) clinker. Calcium silicate cement (CSC) clinker had the lowest energy consumption and CO₂ emissions, resulting from raw meal limestone reduction and a lower sintering temperature. Partially replacing OPC clinker with a supplementary cementitious material (SCM) from CO₂ mineralization reduced CO₂ emissions by ~45% compared to OPC. Location-dependent CO₂ emission analysis revealed that Brazil yielded the least emissions compared to the United States and China. These findings underscore the imperative for cement industries to adopt alternative clinkers, coupled with SCMs, as decarbonization measures.

INTRODUCTION

The global production of cement, the most used material in the world after water,¹ reached 4.4 billion tonnes in 2021 and reduced slightly to 4.1 billion tonnes in 2023.² Cement production was responsible for 2.9 billion tonnes of CO₂ emissions in 2021³ or about 8% of global anthropogenic carbon dioxide (CO₂) emissions.⁴ Toward the Net Zero targets by 2050 and aligning with the objectives established in the Paris Agreement, the World Business Council for Sustainable Development has urged the cement industry to achieve 20–25% CO₂ emission reductions by 2030.¹ These significant abatements are also widely expected by governmental bodies, financiers, and end users.⁵

Most of the CO₂ emissions of cement production arise from the process of producing clinker, the main component of ordinary Portland cement (OPC), which accounts for 95% of cement.⁶ Clinker production involves calcination, where limestone is decomposed into calcium oxide and CO₂,⁷ and the subsequent operation of the kiln, where clinker is formed.⁸ Both the calciner and the kiln require heating, which represents the main energy consumption in clinker production,⁹ along with electricity for grinding raw materials (known as raw meal),¹⁰ driving gas flows in the production process and other auxiliary uses.¹¹ In addition to the above-mentioned CO₂ production

from calcination, which accounts for ~60% of total emissions,¹² the combustion of fuels (predominantly coal or natural gas) in the calciner and kiln leads to about 28–35% CO₂ emissions from clinker production.^{9,13,14}

To tackle CO₂ emissions produced from cement production, carbon capture, utilization, and storage (CCUS) has been typically considered as a strategy to be applied to the flue gas of clinker production, which typically contains about 20% CO₂.¹⁵ CCUS has previously been reported to offer carbon capture efficiencies of 90%,¹⁶ 94%,¹⁷ and 99.7%¹⁸ through the use of MEA-based absorption, calcium looping, and advanced amine-based CO₂ capture, respectively. To aid CCUS, oxygen combustion (hereafter, oxy-combustion) offers more concentrated CO₂ to be produced from cement flue gases,⁷ leading to higher capture efficiencies up to 100%,¹⁷ and yields high-purity CO₂ streams, hence easing carbon capture.¹⁹ Although

Received: May 17, 2024

Revised: September 13, 2024

Accepted: September 13, 2024

Published: September 25, 2024



Table 1. Chemical Compositions of Raw Materials (wt %) in Six Different Simulated Clinker Cases^{a,b}

case ID	chemical composition of raw materials (wt %)					sintering temperature (°C)	compressive strength (MPa)	references
	CaCO ₃	SiO ₂	Al ₂ O ₃	Fe ₂ O ₃	CaSO ₄			
1. OPC	79.47	14.34	3.49	2.70	0.00	1500	32.5–55	37,38
2. HFC-a (4.34)	77.08	14.81	3.77	4.34	0.00	1375	73	31
3. HFC-b (3.72)	77.33	15.80	3.14	3.72	0.00	1350	60	32
4. HFC-c (3.93)	78.46	12.85	4.73	3.93	0.00	1350	45	30
5. BYFC	64.20	12.50	13.80	4.70	4.81	1350	45.9	28
6. CSC	61.86	35.61	1.93	0.59	0.00	1250	63	33
7. SCM + OPC	75% OPC + 25% SCM					Not specified; properties considered comparable with OPC		35

^aChemical compositions of raw materials, including CaCO₃, SiO₂, Al₂O₃, Fe₂O₃, and CaSO₄; with the addition of a case, where clinker is mixed with SCM; and including the combustion temperature of seven simulated cases (°C), ranging from 1250 to 1500 °C, with their respective mechanical strengths, where the strength of clinkers in case 7 was not identified as it was integrated with CO₂ mineralization but is assumed to be adequate as it shares similar raw material compositions as that of case 1, respectively. ^bIt is worth noting that the lower water-to-cement (w/c) ratio of CSC increases the compressive strength as less water relative to the amount of clinker is present.³⁶

substantial CO₂ emissions can be removed from the cement production process, the implementation of CCUS demands higher energy.¹⁸ Furthermore, while CCUS offers removal of CO₂ emissions from the cement production process, it does not prevent the generation of CO₂ but mitigates its release into the atmosphere.

Deep decarbonization in the cement sector necessitates the transition to cleaner production by reducing both the dependency on fossil fuels²⁰ and calcination-induced emissions.¹² Alternative fuels that have been considered for clinker production include hydrogen (H₂)^{9,21,22} and biomass.²³ Notably, a prior modeling study by Williams et al.⁹ achieved CO₂ reductions of ~28% in contrast with the conventional fossil fuel (natural gas based) process from the combustion with H₂ fuel. In industry, a report by Hanson Cement²⁴ successfully demonstrated the replacement of fossil fuels with a combination of H₂, biomass, and plasma-based energy supply at Hanson's Ribblesdale plant in the United Kingdom (UK), where it saved about 180,000 tonnes of CO₂ annually. Among alternative fuels, biomass demonstrated climate change mitigation of up to 31% in contrast with fossil fuels.¹² Modeling work by Association M. P. Ltd²⁵ demonstrated that alternative fuel replacement with 50% hydrogen and 50% biomass in the kiln and 83.3% biomass and 16.7% plasma in the calciner was used, leading to the removal of fuel-related CO₂ emissions. Despite these results, fuel-oriented measures alone can only achieve a limited extent of carbon abatement since they do not address emissions from calcination.⁹

The raw meal of Portland clinker consists of calcium carbonate (in the form of limestone, the main source of CO₂), argillaceous clays (silicon), aluminum, and iron, where the chemical compositions are CaCO₃, SiO₂, Al₂O₃, and Fe₂O₃.²⁶ The clinker product compositions include C₃S (alite), C₂S (belite), C₃A (calcium aluminate), and C₄AF (ferrite),⁷ in which C₃S (alite) is the most carbon-intensive component.¹ Targeting CO₂ reductions in calcination involves the use of different clinker types deviating from the conventional OPC clinker as follows:

1. Belite-ye'elinite ferrite (BYF) clinker, produced from a raw meal with a reduction in limestone²⁷ and an increase in aluminate, leads to a product containing ye'elinite (C₄A₃S) and elevated belite and ferrite in the absence of alite.²⁸ BYF also offers a reduction in the sintering temperature from the typical 1500 °C in the kiln for

producing OPC clinkers to the range of 1300–1350 °C.²⁹ BYF clinker displayed energy and CO₂ savings of 20% and 20–40% compared to the OPC clinker, respectively.²⁹

2. High-ferrite clinker (HFC), produced from a raw meal with increased Fe₂O₃ content, leads to a product containing increased ferrite (C₄AF) content. HFC decreases the combined proportion of C₂S and C₃S, offering a reduced sintering temperature by approximately 100 °C compared to traditional OPC.^{30,31} HFC demonstrated up to 20% energy and 18% CO₂ savings to be achieved relative to OPC.^{30–32}
3. Calcium silicate cement (CSC) clinker, which adopts a raw meal with increased silica to displace limestone, leads to a product containing low-lime calcium silicate phases and a significantly reduced sintering temperature at 1200°.³³ CO₂ and energy savings of 30% can be realized relative to OPC.³³

Along with holding potential for energy and CO₂ savings compared to OPC, these BYF, HFC, and CSC clinkers have been reported to offer sufficient mechanical properties needed for replacing OPC, as shown in refs 28, 30–32, and 33, respectively.

While the above-mentioned alternative clinkers are promising for the reduction of the inherent CO₂ emissions from calcination, to our knowledge, their production processes are yet to be systematically assessed and compared to quantify their potential on a consistent basis. By modeling these processes in the Aspen Plus V12.1 process simulator, this study aims to fill the gap and provide a comparative evaluation of these options in terms of energy consumption and CO₂ emissions. Additionally, recognizing the emerging proposal of supplementary cementitious materials (SCMs) derived from CO₂ mineralization that absorbs CO₂ emissions from cement production,^{34,35} a further option incorporating partial replacement of clinkers with SCMs is also evaluated in parallel with the alternative clinkers for comparison. The results from the study are poised to bring new insights into the carbon abatement potential of interventions from a materials perspective, complementing energy-oriented studies of cement production to promote deep decarbonization of this sector.

METHODS

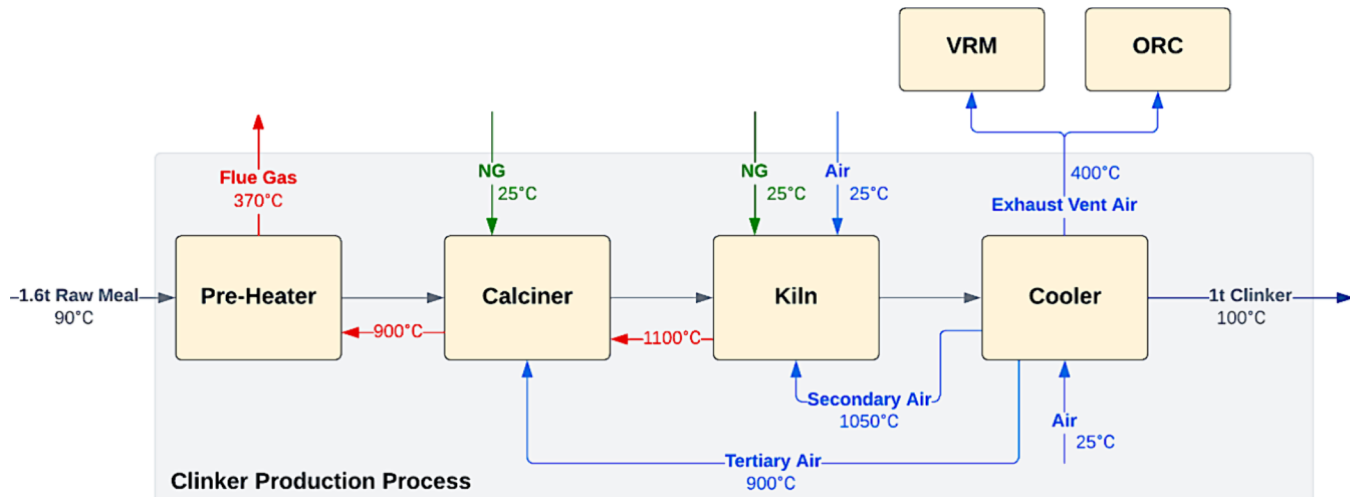
This study is centered on seven technical options for producing clinkers or equivalent products, which are introduced in the

Table 2. Chemical Reactions for the Formation of Clinker Components

cases	mineral component	chemical reaction
1–6	Belite	$2\text{CaO} + \text{SiO}_2 \rightarrow \text{C}_2\text{S}^{33}$
1–4	Alite	$\text{C}_2\text{S} + \text{CaO} \rightarrow \text{C}_3\text{S}^{33}$
1–4	Aluminate	$3\text{CaO} + \text{Al}_2\text{O}_3 \rightarrow \text{C}_3\text{A}^{33}$
1–5	Ferrite	$4\text{CaO} + \text{Al}_2\text{O}_3 + \text{Fe}_2\text{O}_3 \rightarrow \text{C}_4\text{AF}^{33}$
5	Calcium Sulfoaluminate	$3\text{Al}_2\text{O}_3 + 3\text{CaO} + \text{CaSO}_4 \rightarrow \text{Ca}_4\text{Al}_6\text{O}_{12}\text{SO}_4 (\text{C}_4\text{A}_3\text{S})^{39}$
6	Wollastonite	$\text{CaO} + \text{SiO}_2 \rightarrow \text{CaSiO}_3 (\text{CS})^{33}$
6	Rankinite	$3\text{CaO} + 2\text{SiO}_2 \rightarrow \text{Ca}_3\text{Si}_2\text{O}_7 (\text{C}_3\text{S}_2)^{33}$
6	Gehlenite/Melilite	$2\text{CaO} + \text{Al}_2\text{O}_3 + \text{SiO}_2 \rightarrow \text{Ca}_2\text{Al}_2\text{SiO}_7^{29}$

Table 3. Mineral Composition of Six Clinker Cases (wt %)^{29–33,37,38}

case ID	mineral composition of clinker cases (wt %)								
	C ₃ S	C ₂ S	C ₃ A	C ₄ AF	C ₄ A ₃ S	CS	C ₃ S ₂	melilite	amorphous
1. OPC	57.60	18.00	9.00	9.30	0	0	0	0	0
2. HFC-a (4.34)	42.10	28.40	2.80	18.10	0	0	0	0	0
3. HFC-b (3.72)	37.06	32.86	4.32	15.17	0	0	0	0	0
4. HFC-c (3.93)	59.10	8.60	8.50	17.20	0	0	0	0	0
5. BYFC	0	49.70	0	19.90	28.80	0	0	0	0
6. CSC	0	2.96	0	0	0	52.30	13.38	7.12	24.20

**Figure 1.** Schematic of the clinker production process. Air is represented in blue, natural gas in green, flue gas in red, and the material flows in gray. The raw meal mass flow rate and temperatures refer to the case of the OPC clinker production.

Cases for Evaluation section. The evaluation of these options is fundamentally based on the computer simulation of the clinker production processes, as presented in the **Process Simulation** section; the simulation results then provide the quantification of energy consumption and CO₂ emissions, following the approaches described in the **Quantification of Energy Demand and CO₂ Emissions of Clinker Production (Cases 1–6)** section and the **Quantification of Energy Demand and CO₂ Emissions for the Option Involving CO₂ Mineralization (Case 7)** section.

Cases for Evaluation. Seven cases were selected to scrutinize the effects of material composition on energy demand and CO₂ production, as shown in **Table 1**, where six cases contained distinct raw meal compositions for producing clinkers and one involved 25 wt % replacement of a clinker with an SCM produced through CO₂ mineralization. In all cases, natural gas was the assumed fuel for providing thermal energy.

For the reference case (case 1), the raw meal compositions were established following the parameters outlined in ref 11 to produce traditional OPC.

Cases two to four featured three variations of HFC based on the literature, with various Fe₂O₃ contents at 4.34 wt % (case 2),³¹ 3.72 wt % (case 3),³² and 3.93 wt % (case 4).³⁰ Also, according to these references, the sintering temperatures of these HFC cases are 100–150 °C lower than those of the OPC.

BYF clinker was adopted for case 5, with a lower lime (CaO) content and a greater alumina content in the raw meal. BYF required a lower sintering temperature similar to the HFC cases while containing a noticeably higher content of C₂S compared to the other clinkers.²⁹

Case 6 was introduced to represent the CSC clinker,³³ characterized by the lowest CaCO₃ content and the highest silica content in the raw meal among all clinker options. This was accompanied by the lowest sintering temperature of 1250 °C.

Case 7 integrated CO₂ mineralization (not explicitly modeled in this work) based on ref 35, with the utilization of CO₂ from cement flue gas to produce an SCM that contains 40% SiO₂, 50% MgCO₃, and 10% moisture, replacing 25% of OPC clinker.

In terms of the product properties, the literature-reported compressive strengths of the clinkers are listed in **Table 1**. There exist deviations between OPC and the alternative clinkers, although generally the latter have been considered being able to offer product properties comparable to OPC. The same comparability has been deemed valid for case 7,³⁵ although no specific measurements of mechanical strengths were reported.

The properties of each clinker are largely determined by its chemical composition.

Table 2 shows the chemical reactions leading to the key components of the clinkers. The composition of each clinker is shown in **Table 1**. Note that the composition of the raw meal for each of the cases (shown in **Table 1**) was determined according to its literature-reported clinker composition (shown in **Table 3**) by mass balance. Simulations in Aspen using these calculated raw meal inputs showed that the resultant clinker mineral compositions were consistent with the literature values.^{29–33}

Process Simulation. The mathematical modeling work of the clinker production process was based on adapting the Aspen Plus V12.1 simulation model established in an earlier study.⁹ The modeling itself was originally based on a plant producing 4200 tonnes of clinker daily in Alberta, Canada.¹¹ The process utilizes natural gas combustion in air, serving as a primary source of thermal energy, accompanied by electrical energy from the grid. A schematic representation of the production process is shown in **Figure 1**, with the Aspen Plus flowsheet provided in **Figure S1**. To produce OPC clinker, the process begins as the raw meal enters the preheater and is processed in the calciner, where limestone is decomposed at 900 °C to attain 95% calcination.⁴⁰ The calciner output then proceeds to the kiln, where decomposition, transition, and sintering reactions occur, with the sintering temperature reaching 1500 °C, before being cooled to 100 °C in the cooler and exiting the process. In the process, primary air and secondary air enter the kiln's combustor at 25 and 1050 °C, respectively, whereas tertiary air enters the calciner's combustor at 900 °C, following heat recovery.¹¹ The cooling vent air progresses through heat recovery phases, which supply a hot gas flow of 1762 kg/tonne clinker at 176.85 °C to satisfy the operation of a vertical roller mill.¹⁰ The remaining cooling exhaust coupled by the preheater exhaust then provides heat to operate the Organic Rankine Cycle (ORC) for further heat recovery.

The calciner and kiln combustors were modeled as stoichiometric reactors (RStoic), where a series of three RStoic reactors represented the three stages in the kiln. Heat losses were modeled for the combustors, including the calciner, kiln decomposition, kiln transition, and kiln sintering at 42.99 MJ/t clinker, 30.60 MJ/t clinker, 59.40 MJ/t clinker, and 90 MJ/t clinker, respectively.⁷

To simulate the production of an alternative clinker, the above Aspen Plus model was adapted by using a clinker-specific raw meal composition (**Table 1**), chemical reactions (**Table 2**), and their conversions as needed to attain the clinker composition (**Table 3**). Physical properties of new clinker components not present in the OPC clinker are summarized in **Table S1**. Clinker-specific sintering temperatures (**Table 1**) were also applied by adjusting the supply of natural gas and combustion air.

The physical property modeling of all the cases was also based on the previously established Aspen model for OPC clinker production.⁹ The information on new clinker components not available in the databases of Aspen is provided in **Table S1**.

Quantification of Energy Demand and CO₂ Emissions of Clinker Production (Cases 1–6).

Principal components responsible for the net energy consumption of the clinker production processes include the consumption of electrical (fans, raw meal preparation, and auxiliary) and thermal energy (natural gas), along with the recovery of thermal energy into electricity (ORC). The natural gas consumption values were extracted from Aspen simulations. The following assumptions were made in energetic analyses:

1. The scope of energy consumption modeling was set to “gate to gate”; processes that occur before or after the clinker production process were not included;
2. Natural gas was assumed to be 100% methane with a lower heating value of 50 MJ/kg;⁴¹
3. The auxiliary electricity consumption was assumed constant across all cases as 68 kWh/t clinker, according to ref 11;
4. Electricity required for raw meal preparation was presumed to be constant among the cases at 25.2 kWh/t clinker, as per ref 42.

The electrical energy demand for each fan (W_{fan}) was determined by scaling the reference fan power consumption, as per ref 11, where q_{ref} and W_{ref} are the volumetric gas flow and the power consumption of a reference fan, respectively, and q is the volumetric gas flow of the fan, as shown below:

$$W_{\text{fan}} = W_{\text{ref}} \times \left(\frac{q}{q_{\text{ref}}} \right)^3 \quad (1)$$

An ORC was incorporated into each clinker production process for waste heat recovery, which produces electricity to partially offset the process electricity demand. The ORC electricity output ($W_{\text{ORC}} = Q_{\text{in}} \times \eta_{\text{th}}$) was calculated using the recovered waste heat from the hot gas stream (Q_{in}), which was acquired from Aspen simulation results of each cooler. This represented the evaporator of the ORC, on the waste heat streams cooled to 130 °C, which was 20 °C higher (providing heat transfer driving force) compared to the working fluid of the ORC (at 110 °C), following the ORC design presented in ref 43. The ORC efficiency, η_{th} , was set to 0.225, according to the assumed organic working fluid.⁴⁴

On CO₂ emissions, both CO₂ directly emitted from the clinker production process, resulting from calcination and natural gas combustion (as quantified by Aspen simulations), and indirect emissions from the supply of grid electricity consumed in the clinker production process were considered. Other CO₂ emissions in the cement supply chain were not included. The carbon footprint of grid electricity is dependent on geographical locations. Three out of the top 10 cement producing countries with low, medium, and high carbon intensities (on a basis of kg of CO₂eq per MWh), namely, Brazil,⁴⁵ the United States,⁴⁵ and China,⁴⁶ were chosen to calculate location-sensitive emissions from electricity.

Quantification of Energy Demand and CO₂ Emissions for the Option Involving CO₂ Mineralization (Case 7). The CO₂ mineralization process was incorporated in case 7, involving the blending of 250 kg of SCM, derived from the mineralization of CO₂, with 750 kg of clinker, facilitating the production of 1 tonne of the final product, in accordance with ref 35. CO₂ was sourced by a monoethanolamide (MEA)-based process applied to the flue gas from clinker production with a capture efficiency of 90%.³⁵ The CO₂ mineralization process produced a stream of SCM consisting of 40% SiO₂, 50% MgCO₃, and 10% moisture (on a weight basis).³⁵

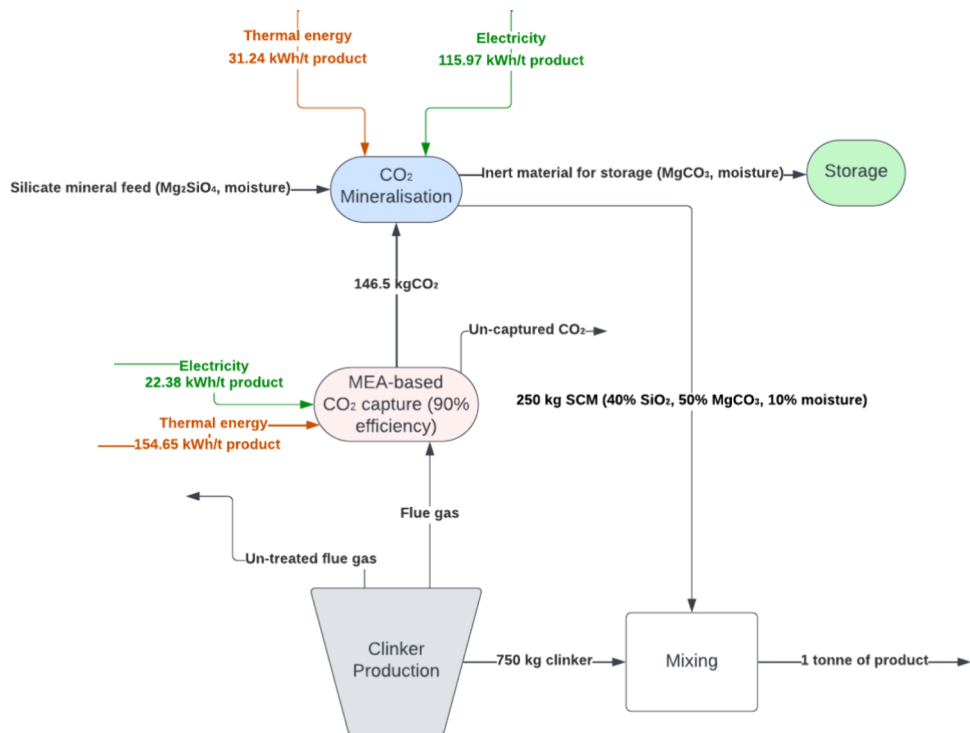


Figure 2. Process diagram for cases involving CO_2 mineralization. The electrical and thermal energy inputs were calculated from the paper;³⁰ the compositions of SCM were based on the literature.³⁵

Table 4. Key Players for the Electrical and Thermal Energy Demand of All Cases^a

	case 1 OPC	case 2 HFC-77.08	case 3 HFC-77.33	case 4 HFC-78.46	case 5 BYFC	case 6 CSC	case 7 SCM + OPC
Electrical Energy for clinker (kWh/t clinker)							
Fans (kWh/t)	165.66	86.65	77.76	91.63	62.28	37.20	124.25
Auxiliary (kWh/t)	68.00	68.00	68.00	68.00	68.00	68.00	51.00
ORC (kWh/t)	-73.79	-61.09	-59.33	-62.69	-48.15	-24.07	-55.34
Raw Meal Preparation (kWh/t)	25.20	25.20	25.20	25.20	25.20	25.20	18.90
MEA Capture (electrical)	N/A						22.38
Mineralization (electrical)							115.97
Total electrical energy (kWh/t clinker)	185.07	118.76	111.63	122.14	107.33	106.33	277.16
Thermal Energy for clinker (kWh/t clinker)							
Natural Gas (kWh/t)	1035.37	924.54	907.81	971.83	731.03	558.78	776.53
MEA Capture (thermal)	N/A						154.65
Mineralization (thermal)							31.24
Total thermal energy (kWh/t clinker)	1035.37	924.54	907.81	971.83	731.03	558.78	962.41
Net total energy (kWh/t clinker)	1220.44	1043.30	1019.45	1093.97	838.36	665.11	1239.57

^aAs CO_2 mineralization was only applicable to case 7, CO_2 mineralization energy (thermal and electrical) was not applicable to cases 1–6.

To determine the electrical and thermal energy requisites for the production of 750 kg of clinker, 75% of the corresponding values of the OPC (case 1) were taken, as illustrated in Figure 2.

For the production of 250 kg of SCM containing 40% or 100 kg of SiO_2 , the CO_2 demand was stoichiometrically determined to be 146.50 kg of CO_2 , according to the reaction equation of magnesium silicate carbonation (see eq 2). The thermal and electrical energy demands for MEA-based carbon capture were 3.8 MJ/kg CO_2 captured (thermal) and 0.55 MJ/kg CO_2 captured (electrical).⁴⁷ The electrical and thermal energy required for the CO_2 mineralization process leading to the production of 250 kg of SCM were 115.97 and 31.24 kWh, respectively.³⁵

The quantification of CO_2 emissions for case 7 included (see eq 1) (1) 75% CO_2 emissions from the production of 1 tonne of OPC clinker in case 1, as determined by the approach described in the Quantification of Energy Demand and CO_2 Emissions of Clinker Production (Cases 1–6) section; (2) deduction of 146.50 kg of CO_2 consumed by mineralization; (3) CO_2 emissions by the supply of thermal energy required for mineralization and MEA-based carbon capture at 241 kg CO_2/MWh ;³⁵ and (4) carbon footprint of the electricity consumed by mineralization and MEA-based carbon capture, based on the location-specific carbon intensities of grid electricity in the three chosen countries.

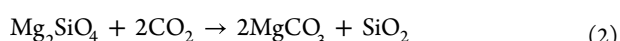


Table 5. CO₂ Emissions for Seven Simulated Cases in Three Different Geographical Locations of the United States (US), China, and Brazil

		OPC clinker production		SCM - MEA capture		SCM - CO ₂ mineralisation		net total CO ₂
		CO ₂ produced (kgCO ₂ /t clinker) - from Aspen	net electrical (kgCO ₂ /t clinker)	electrical (kgCO ₂ /t clinker)	thermal (kgCO ₂ /t clinker)	electrical (kgCO ₂ /t clinker)	thermal (kgCO ₂ /t clinker)	total (kgCO ₂ /t clinker)
Case 1 OPC	USA	741.50	67.92	N/A	N/A	N/A	N/A	809.42
	China	741.50	98.30	N/A	N/A	N/A	N/A	839.80
	Brazil	741.50	18.88	N/A	N/A	N/A	N/A	760.38
Case 2 HFC-a (4.34)	USA	695.80	43.58	N/A	N/A	N/A	N/A	739.38
	China	695.80	63.08	N/A	N/A	N/A	N/A	758.88
	Brazil	695.80	12.11	N/A	N/A	N/A	N/A	707.91
Case 3 HFC-b (3.72)	USA	694.43	40.97	N/A	N/A	N/A	N/A	735.40
	China	694.43	59.29	N/A	N/A	N/A	N/A	753.72
	Brazil	694.43	11.39	N/A	N/A	N/A	N/A	705.82
Case 4 HFC-c (3.93)	USA	718.62	44.83	N/A	N/A	N/A	N/A	763.45
	China	718.62	64.88	N/A	N/A	N/A	N/A	783.50
	Brazil	718.62	12.46	N/A	N/A	N/A	N/A	731.08
Case 5 BYF	USA	537.28	39.39	N/A	N/A	N/A	N/A	576.67
	China	537.28	57.01	N/A	N/A	N/A	N/A	594.29
	Brazil	537.28	10.95	N/A	N/A	N/A	N/A	548.23
Case 6 CSC	USA	481.34	39.02	N/A	N/A	N/A	N/A	520.36
	China	481.34	56.48	N/A	N/A	N/A	N/A	537.81
	Brazil	481.34	10.85	N/A	N/A	N/A	N/A	492.18
Case 7 SCM + OPC	USA	409.63	50.94	8.21	37.27	42.56	7.53	556.14
	China	409.63	73.73	11.89	37.27	61.60	7.53	601.63
	Brazil	409.63	14.16	2.28	37.27	11.83	7.53	482.69

RESULTS AND DISCUSSION

This section presents and discusses the results pertaining to energy consumption and carbon intensity, offering a comparative analysis of various cases. Specifically, we examine the thermal energy input from natural gas and the electrical energy requirement. The carbon intensity is assessed, determining the amount of CO₂ produced and the carbon footprint associated with electricity, which extends across three distinct locations, namely, the United States, China, and Brazil.

Energy Intensity. The energy consumption results are presented in Table 4. All alternative clinkers (cases 2–6) were predicted to gain energy savings compared to the OPC clinker (case 1), as projected in previous studies.^{29–33} In particular, case 6 (CSC clinker) is the most energy-efficient, with a total energy intensity of 665.1 kWh/tonne clinker, which represents a ~46% reduction in thermal and total energy, compared to case 1 (OPC). Its energy savings can be attributed to the significantly lower sintering temperature (1250 °C) and CaCO₃ input (989.7 kg/tonne clinker) corresponding to significantly lower contents of C₃S and C₂S. In comparison, case 1 (OPC) had a sintering temperature of 1500 °C and a CaCO₃ input of 1271.5 kg/tonne clinker, both demanding greater thermal energy input.

Case 5 (BYF) shared a similar CaCO₃ content with case 6 but with a higher sintering temperature (by 100 °C) and a substantial amount of C₂S in the clinker composition, making it the second most energy-efficient alternative clinker, saving thermal energy and total energy by 29.4 and 31.3%, respectively, compared to those of the case for the OPC.

Among the high-ferrite cases (cases 2–4), electricity and thermal energy consumption were comparable, with differences below 10%, resulting from minor variations in the raw meal and clinker compositions. Notably, among the high-ferrite options, case 3 (HFC-b), with the lowest alite content, exhibited the

lowest thermal and total energy consumption with 12.3 and 16.5% savings, respectively, compared to those of OPC.

The case involving SCM (case 7) was the most energy-intensive process, even more demanding than case 1, which supplied 75% of its product. This suggests that, on a basis of 1 kg of product (SCM or clinker), the energy required for mineralization and MEA-based carbon capture (1.30 kWh/kg SCM) was greater than that required for OPC clinker production (1.22 kWh/kg).

Finally, it is worth noting that thermal energy from natural gas emerged as the key contributor to the total energy demand, contributing 63–89% of the total energy demand across all the cases. Besides, it was observed that case 1 had the highest and case 6 had the lowest heat recovery value from ORC as the amount of recoverable waste heat was correlated with the natural gas input in the processes.

Carbon Intensity. As shown in Table 5, all non-OPC options (cases 2–7) were predicted to have a carbon intensity lower than that of the OPC clinker (case 1). Among the alternative clinkers (cases 2–6), the trend in carbon intensity agrees well with that in thermal energy consumption, where reduced natural gas consumption was coupled with a reduced CaCO₃ content in the raw meal, both contributing to the reduction of CO₂ emissions. Case 6 (CSC) was projected to achieve a 35.1% reduction in direct emissions (i.e., excluding carbon footprint of electricity) compared to case 1, followed by 27.5% and 3.1–6.4% reduction by case 5 (BYF) and cases 2–4 (HFC clinkers), respectively. These values of CO₂ savings were comparable to the literature, suggesting 30%, 20–40%, and up to 18% in contrast with OPC for CSC, BYF, and HFC clinkers, respectively^{29–33} (shown in Table 7). When the carbon footprint of electricity is included, the results differ between the three countries, although their difference was within 10% despite the significant gap in the carbon intensity of grid

electricity. This was a result of the relatively low share of electricity in total energy consumption. Comparing case 6 with case 1, the reductions of total carbon intensity for producing 1 tonne of clinker were 35.7, 36, and 35.3% for the US, China, and Brazil, respectively.

For the option involving CO₂ mineralization (case 7), the impact of replacing 250 kg of clinker with the SCM on total carbon intensity was dictated by the combined effect of three elements: (1) CO₂ removal through the mineralization process, (2) avoided CO₂ emissions from the replaced 250 kg of clinker, and (3) CO₂ emissions associated with the supply of electrical and thermal energy for CO₂ capture and mineralization. The second and third elements are differentially affected by the carbon intensity of the grid electricity in different locations. Compared to case 1 (OPC), case 7 clearly shows, for all three countries, that the benefit of CO₂ savings (elements 1 and 2) outweighs the CO₂ burden of additional energy consumption (element 3), leading to 31.3, 28.4, and 36.5% reduction in total carbon intensity for the US, China, and Brazil, respectively (shown in Table 5). These findings were comparable to the literature, where CO₂ savings of 33% were realized from the substitution of 25% SCM from CO₂ mineralization.³⁵ However, the comparison of case 7 with case 6 shows that while Brazil was predicted to (slightly) benefit from the SCM replacement from its rather “green” electricity grid, the higher energy consumption in the case involving the replacement resulted in a worse overall carbon intensity for the US and China compared to a low-carbon clinker (CSC).

Further Discussion. From the results presented above on alternative clinkers, lowering the sintering temperature and CaCO₃ content in the raw meal both played a role in reducing energy consumption and CO₂ emissions. A less understood aspect was the relative contributions of these two factors. To shed light on this, additional supporting simulation of OPC clinker production at 1400 °C (which is the lower end of the practical range⁴⁸) was conducted, as per Table 6. Furthermore,

Table 6. Reference of the OPC Case Compared to a Lower Sintering Temperature Scenario (1400 °C) and Hypothetical Additional Simulations with Changes to the Sintering Temperatures of 1350 °C (H1-OPC) and 1250 °C (H2-OPC)

reference OPC vs hypothetical supporting simulations	sintering temperature (°C)	energy consumption (kWh/t clinker)	CO ₂ produced (kgCO ₂ /t clinker)
OPC (reference)	1500	1220.4	741.5
OPC (low sintering T)	1400	1134.5	733.8
H1-OPC	1350	1063.8	730.1
H2-OPC	1250	1006.9	722.3

two hypothetical lower sintering temperatures for the OPC clinker, 1350 and 1250 °C, directly corresponding to those adopted for BYF and CSC clinkers, respectively, were simulated (see Tables 6, S2 and S3). These additional simulations showed reductions between 7.0 and 17.5% in total energy consumption and between 1.0 and 2.6% in average CO₂ emissions, all in contrast with case 1 (OPC). In comparison, and as shown earlier, the assessed alternative clinkers achieved up to 45.5% energy reductions and 35.1% CO₂ reductions. The contrast of these percentage savings suggests that adopting a low-limestone raw meal plays a more significant role in CO₂ and energy reductions in comparison to lowering the sintering temperature.

The alternative clinkers studied in this work have previously been considered to be able to achieve energy and CO₂ savings (shown in Table 7). Here, we can compare the previously stated

Table 7. Energy and CO₂ Savings from the Literature Compared to Traditional OPC Clinker, with Corresponding Literature References, and Energy and CO₂ Savings from the Results Compared to the Reference Case 1

alternative clinkers	energy savings (literature)	CO ₂ savings (literature)	energy savings (results)	CO ₂ savings (results)	literature references
HFC-a	17–20%	15–18%	14.5%	6.2%	31
HFC-b	N/A	N/A	16.5%	6.4%	32
HFC-c	5%	5%	10.4%	3.1%	30
BYF	20%	20–40%	31.3%	27.5%	29
CSC	30%	30%	45.5%	35.1%	33

CO₂ and energy performances with what was predicted in this study through consistent modeling. As shown in Table 7, both cases 5 (BYF) and 6 (CSC) demonstrate a notable agreement with the existing literature^{29,33} regarding CO₂ savings; however, the findings of this study indicate higher energy savings in comparison with the literature. This difference may be caused by the assessment’s consideration of various energy types and distinct comparison baselines. Whilst existing studies provide a comparison with coal-combusted OPC,^{29–33} this study uses natural gas-combusted OPC as a benchmark. In contrast, the HFC cases in the results only exhibited modest CO₂ savings of up to 6.4% from the calcination process in contrast with the literature, which projected CO₂ savings of up to 18%³¹ (shown in Table 7). This was predominantly a result of the minor reductions in the CaCO₃ content in the raw meal.

Examining the underlying chemical and physical mechanisms, the decomposition of CaCO₃ to CaO involves the decomposition reaction, $\text{CaCO}_3 \rightarrow \text{CaO} + \text{CO}_2$, releasing 0.44 kg of CO₂ per tonne of CaCO₃ converted. Additionally, the reaction requires an input of 179.4 kJ/kmol of heat at 900 °C.⁷ This emphasizes that both CO₂ and energy savings can be realized from the reduction of the CaCO₃ content in the raw material composition, a key target that has been aimed at by all the alternative clinkers. In the kiln processes, silica (SiO₂) reacts with CaO to form alite (C₃S) and belite (C₂S), which are the primary components of clinker, requiring 12.0 kJ/kmol and releasing 135.0 kJ/kmol of heat, respectively.⁷ Furthermore, the clinker raw materials, iron oxide (Fe₂O₃) and aluminum oxide (Al₂O₃), demand conversion temperatures of up to 1280 °C, releasing heat of 41.3 kJ/kmol and requiring 19.7 kJ/kmol, respectively, for the formation of C₄AF and C₃A.⁷ Energetically, the above suggests that C₂S and C₄AF would be preferred over C₃S and C₃A, respectively, which has been broadly reflected in the contrast of compositions between the OPC clinker and the alternative clinkers studied in this work.

With the use of SCMs, the main study presented above assumed 25% of replacement, although a lower-level replacement may be favored due to concerns such as product workability.⁴⁹ If 20% of clinker were to be replaced with SCMs, an additional option suggested by Strunge et al.,³⁵ our additional assessment showed that CO₂ reductions in the results observed in case 7 compared with case 1 would be 25.1, 22.8, and 29.2% for the United States, China, and Brazil, respectively. These reductions represent 6.2, 5.6, and 7.3% decreases in CO₂ savings compared to the scenario with 25% SCM replacement in

these respective countries. Despite these decreases, the CO₂ savings potential of this technical option remains significant.

As a final comment, although the electricity consumption is relatively minor compared to the thermal energy demand in clinker production that is dominated by thermal processes (i.e., the operation of the calciner and the kiln), the introduction of an SCM could potentially alter the picture, depending on the production method of the SCM. In the example included in this study, 22.4% of the total energy consumption of the CO₂ mineralization processes is electricity, higher than that of OPC production. A higher share of electricity in total energy consumption, among other impacts, will lead to greater differentiation in the total carbon emissions between countries with diverse carbon intensities in their electricity supply, potentially making some options more suitable for certain countries than others.

CONCLUSIONS

With the aid of process simulation, this work quantified how CO₂ emissions and energy consumption of the cement production process can be reduced by altering the composition of the clinker. The energy demand and CO₂ production in 7 evaluated cases were found to vary according to four key factors: limestone content in the raw meal, alite (C₃S) content in the clinker, sintering temperature, and substituting conventional clinker with SCMs from CO₂ mineralization.

1. The limestone (CaCO₃) content in the raw meal plays a key role, as the chemical reaction of calcination is a significant source of both thermal energy demand and direct CO₂ emissions. All the cases alternative to OPC clinker featured reduction of the use of CaCO₃, albeit to different extents, leading to reduced fuel consumption for calcination and lower combined CO₂ emissions from fuel combustion and CaCO₃ decomposition in the calcination step.
2. Reduction of the alite content of the clinker is advantageous in achieving lower CO₂ output from the cement production process, as particularly demonstrated by cases 5 (BYC) and 6 (CSC). This is in line with the literature, which determined that alite was the most carbon-intensive clinker mineral when compared to the rest.
3. The alternative clinkers were accompanied by a lower sintering temperature compared to OPC, which was a contributing factor to the lower energy demand and CO₂ emissions, although more significant contributions were shown to stem from the alteration of the raw meal and hence the clinker compositions.
4. The use of an SCM derived through mineralizing part of the CO₂ emissions from conventional clinker production (OPC) to partially substitute OPC clinkers demonstrated a significant reduction of CO₂. However, it did not lead to the lowering of energy demand due to the high energy (thermal and electrical) requirement of CO₂ mineralization.

Overall, case 6 (CSC) emerges as the winner in energy efficiency (45.5% energy reduction compared to case 1, OPC), with the lowest CaCO₃ content in the raw meal, zero alite in the clinker, the lowest sintering temperature, and the absence of the energy demand associated with SCM. In terms of direct CO₂ emissions from the production process (i.e., excluding the carbon footprint of electricity), CSC clinker achieved a 35.1%

reduction from the OPC clinker, which is the second best, next to case 7 (SCM + OPC), which achieved a 44.8% reduction. However, when the carbon footprint of electricity is included in the total CO₂ emissions, the SCM+OPC case retains its superiority over the CSC case only in Brazil from its low-carbon grid but only in China and the United States. This indicates the importance of decarbonizing electricity generation, particularly in production options, where the electrical energy demand is significant.

The encouraging results of this modeling study on alternative clinkers warrant further experimental testing of these products, as well as their production processes, so that their potential in decarbonizing the cement industry can be firmly established. Additionally, future work can explore cements used in concretes with equivalent performance, allowing for more detailed and in-depth comparisons.

ASSOCIATED CONTENT

Data Availability Statement

All energy and flow data are referenced within the main text with simulation data obtained using Aspen Plus software.

Supporting Information

The Supporting Information is available free of charge at <https://pubs.acs.org/doi/10.1021/acs.iecr.4c01885>.

Data involving the physical properties of clinker minerals, energy and CO₂ performance of hypothetical cases, and process flow diagram for Aspen Plus V12.1 modeling for the cement production process ([PDF](#))

AUTHOR INFORMATION

Corresponding Author

Franco Williams – Department of Engineering Science, University of Oxford, Oxford OX1 3PJ, U.K.;  orcid.org/0000-0001-8192-312X; Email: franco.williams@eng.ox.ac.uk

Author

Aidong Yang – Department of Engineering Science, University of Oxford, Oxford OX1 3PJ, U.K.;  orcid.org/0000-0001-5974-247X

Complete contact information is available at: <https://pubs.acs.org/10.1021/acs.iecr.4c01885>

Author Contributions

F.W.: Conceptualization, methodology, investigation, software, analysis, writing—original draft. A.Y.: Conceptualization, supervision, validation, writing—review and editing.

Notes

The authors declare no competing financial interest.

ACKNOWLEDGMENTS

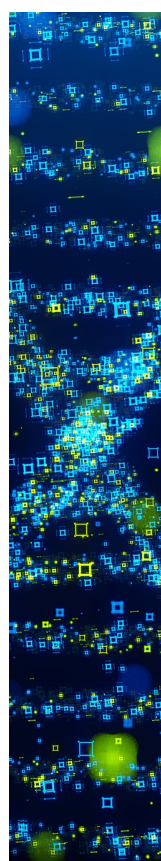
The authors are grateful to Till Strunge for providing supporting data on CO₂ mineralization for this paper.

REFERENCES

- (1) Scrivener, K. L.; John, V. M.; Gartner, E. M. Eco-Efficient Cements: Potential Economically Viable Solutions for a Low-CO₂ Cement-Based Materials Industry. *Cem. Concr. Res.* **2018**, *114*, 2–26.
- (2) Jaganmohan, M. Production volume of cement worldwide from 1995 to 2023; Statista. <https://www.statista.com/statistics/1087115/global-cement-production-volume/> (accessed 2024-07-01).

- (3) Supriya; Chaudhury, R.; Sharma, U.; Thapliyal, P. C.; Singh, L. P. Low-CO₂ Emission Strategies to Achieve Net Zero Target in Cement Sector. *J. Clean. Prod.* **2023**, *417*, No. 137466.
- (4) Cormos, C. C. Decarbonization Options for Cement Production Process: A Techno-Economic and Environmental Evaluation. *Fuel* **2022**, *320*, No. 123907.
- (5) Nie, S.; Zhou, J.; Yang, F.; Lan, M.; Li, J.; Zhang, Z.; Chen, Z.; Xu, M.; Li, H.; Sanjayan, J. G. Analysis of Theoretical Carbon Dioxide Emissions from Cement Production: Methodology and Application. *J. Clean. Prod.* **2022**, *334*, No. 130270.
- (6) British Geological Survey. *Cement Raw Materials British Geological Survey Mineral Profile*; United Kingdom, 2005.
- (7) Faria, D. G.; Carvalho, M. M. O.; Neto, M. R. V.; de Paula, E. C.; Cardoso, M.; Vakkilainen, E. K. Integrating Oxy-Fuel Combustion and Power-to-Gas in the Cement Industry: A Process Modeling and Simulation Study. *Int. J. Greenh. Gas Control* **2022**, *114*, No. 103602.
- (8) The European Cement Association *The Story of Cement Manufacture*; Cembureau. <https://cembureau.eu/media/wm0jmdw/cementmanufacturing.pdf> (accessed 2024-01-09).
- (9) Williams, F.; Yang, A.; Nhuchhen, D. R. Decarbonisation Pathways of the Cement Production Process via Hydrogen and Oxy-Combustion. *Energy Convers. Manag.* **2024**, *300*, No. 117931.
- (10) Ghalandari, V.; Esmaeilpour, M.; Payvar, N.; Toufiq Reza, M. A Case Study on Energy and Exergy Analyses for an Industrial-Scale Vertical Roller Mill Assisted Grinding in Cement Plant. *Adv. Powder Technol.* **2021**, *32* (2), 480–491.
- (11) Nhuchhen, D. R.; Sit, S. P.; Layzell, D. B. Decarbonization of Cement Production in a Hydrogen Economy. *Appl. Energy* **2022**, *317*, No. 119180.
- (12) Cavalett, O.; Watanabe, M. D. B.; Voldsgaard, M.; Roussanaly, S.; Cherubini, F. Paving the Way for Sustainable Decarbonization of the European Cement Industry. *Nat. Sustain.* **2024**, *7* (5), 568–580.
- (13) Antunes, M.; Santos, R. L.; Pereira, J.; Rocha, P.; Horta, R. B.; Colaço, R. Alternative Clinker Technologies for Reducing Carbon Emissions in Cement Industry: A Critical Review. *Materials (Basel)* **2022**, *15*, 209.
- (14) Klee, H. *The Cement Sustainability Initiative - Cement Industry Energy and CO₂ Performance*; 2009.
- (15) Baker, R. W.; Freeman, B.; Kniep, J.; Huang, Y. I.; Merkel, T. C. CO₂ Capture from Cement Plants and Steel Mills Using Membranes. *Ind. Eng. Chem. Res.* **2018**, *57* (47), 15963–15970.
- (16) Gardarsdóttir, S. O.; De Lena, E.; Romano, M.; Roussanaly, S.; Voldsgaard, M.; Pérez-Calvo, J. F.; Berstad, D.; Fu, C.; Anantharaman, R.; Sutter, D.; Gazzani, M.; Mazzotti, M.; Cinti, G. Comparison of Technologies for CO₂ Capture from Cement Production—Part 2: Cost Analysis. *Energies (Basel)* **2019**, *12* (3), 542.
- (17) Rolfe, A.; Huang, Y.; Haaf, M.; Pita, A.; Rezvani, S.; Dave, A.; Hewitt, N. J. Technical and Environmental Study of Calcium Carbonate Looping versus Oxy-Fuel Options for Low CO₂ Emission Cement Plants. *Int. J. Greenh. Gas Control* **2018**, *75*, 85–97.
- (18) Jiang, K.; Yu, H.; Sun, Z.; Lei, Z.; Li, K.; Wang, L. Zero-Emission Cement Plants with Advanced Amine-Based CO₂ Capture. *Environ. Sci. Technol.* **2024**, *58* (16), 6978–6987.
- (19) Guo, Y.; Luo, L.; Liu, T.; Hao, L.; Li, Y.; Liu, P.; Zhu, T. A Review of Low-Carbon Technologies and Projects for the Global Cement Industry. *J. Environ. Sci.* **2024**, *136*, 682–697.
- (20) Chatterjee, A.; Sui, T. Alternative Fuels—Effects on Clinker Process and Properties. *Cem. Concr. Res.* **2019**, *123*, No. 105777.
- (21) El-Emam, R. S.; Gabriel, K. S. Synergizing Hydrogen and Cement Industries for Canada's Climate Plan—Case Study. *Energy Sources A: Recovery Util. Environ. Eff.* **2021**, *43* (23), 3151–3165.
- (22) Juangsa, F. B.; Cezeliano, A. S.; Darmanto, P. S.; Aziz, M. Thermodynamic Analysis of Hydrogen Utilization as Alternative Fuel in Cement Production. *S. Afr. J. Chem. Eng.* **2022**, *42*, 23–31.
- (23) Kusuma, R. T.; Hiremath, R. B.; Rajesh, P.; Kumar, B.; Renukappa, S. Sustainable Transition towards Biomass-Based Cement Industry: A Review. *Renew. Sustain. Energy Rev.* **2022**, *163*, No. 112503.
- (24) Hanson. *Hydrogen trial | Hanson UK*. <https://www.hanson.co.uk/en/socialvalue/climate/hydrogen-trial> (accessed 2023-05-09).
- (25) Association, M. P.; Ltd, C. *Options for switching UK cement production sites to near zero CO₂ emission fuel: Technical and financial feasibility*. https://assets.publishing.service.gov.uk/government/uploads/system/uploads/attachment_data/file/866365/Phase_2_-_MPA_-_Cement_Production_Fuel_Switching.pdf (accessed 2023-07-11).
- (26) Mikulčić, H.; Klemes, J. J.; Vujanović, M.; Urbaniec, K.; Duić, N. Reducing Greenhouse Gases Emissions by Fostering the Deployment of Alternative Raw Materials and Energy Sources in the Cleaner Cement Manufacturing Process. *J. Clean. Prod.* **2016**, *136*, 119–132.
- (27) Morin, V.; Termkhajornkit, P.; Huet, B.; Pham, G. Impact of Quantity of Anhydrite, Water to Binder Ratio, Fineness on Kinetics and Phase Assemblage of Belite-Ye'elimitite-Ferrite Cement. *Cem. Concr. Res.* **2017**, *99*, 8–17.
- (28) Wang, F.; Long, G.; Bai, M.; Wang, J.; Shi, Y.; Zhou, X.; Zhou, J. L. A New Perspective on Belite-Ye'elimitite-Ferrite Cement Manufactured from Electrolytic Manganese Residue: Production, Properties, and Environmental Analysis. *Cem. Concr. Res.* **2023**, *163*, No. 107019.
- (29) Sabbah, A.; Zhutovsky, S. Effect of Sulfate Content and Synthesis Conditions on Phase Composition of Belite-Ye'elimitite-Ferrite (BYF) Clinker. *Cem. Concr. Res.* **2022**, *155*, No. 106745.
- (30) Elkneswaran, Y.; Noguchi, N.; Matumoto, K.; Morinaga, Y.; Chabayashi, T.; Kato, H.; Nawa, T. Characteristics of Ferrite-Rich Portland Cement: Comparison with Ordinary Portland Cement. *Front. Mater.* **2019**, *6*, 97.
- (31) Zhang, K.; Shen, P.; Yang, L.; Rao, M.; Nie, S.; Wang, F. Development of High-Ferrite Cement: Toward Green Cement Production. *J. Clean. Prod.* **2021**, *327*, No. 129487.
- (32) Yang, H. M.; Zhang, S. M.; Wang, L.; Chen, P.; Shao, D. K.; Tang, S. W.; Li, J. Z. High-Ferrite Portland Cement with Slag: Hydration, Microstructure, and Resistance to Sulfate Attack at Elevated Temperature. *Cem. Concr. Compos.* **2022**, *130*, No. 104560.
- (33) Sahu, S.; Meininger, R. C. Performance of CO₂-Reducing Cement Based on Calcium Silicates 15 Th International Congress on the Chemistry of Cement. In *International Congress on the Chemistry of Cement*; 2019.
- (34) Bremen, A. M.; Strunge, T.; Ostovari, H.; Spütz, H.; Mhamdi, A.; Renforth, P.; Van Der Spek, M.; Bardow, A.; Mitsos, A. Direct Olivine Carbonation: Optimal Process Design for a Low-Emission and Cost-Efficient Cement Production. *Ind. Eng. Chem. Res.* **2022**, *61* (35), 13177–13190.
- (35) Strunge, T.; Renforth, P.; der Spek, V. Towards a Business Case for CO₂ mineralisation in the Cement Industry. *Commun. Earth Environ.* **2022**, *3*, 59.
- (36) Kondraivendhan, B.; Bhattacharjee, B. Strength and w/c Ratio Relationship of Cement Based Materials through Pore Features. *Mater. Charact.* **2016**, *122*, 124–129.
- (37) Svanning, K.; Höskuldsson, A.; Justnes, H. Prediction of Potential Compressive Strength of Portland Clinker from Its Mineralogy. *Cem. Concr. Compos.* **2010**, *32* (4), 300–311.
- (38) Standards, B. *BS EN 197-1:2011*; 2011.
- (39) Dong, K.; Xie, F.; Wang, W.; Chang, Y.; Chen, C.; Gu, X. Calcination of Calcium Sulphoaluminate Cement Using Pyrite-Rich Cyanide Tailings. *Crystals (Basel)* **2020**, *10* (11), 971.
- (40) Vikström, A. *Separate Calcination in Cement Clinker Production: A Laboratory Scale Study on How an Electrified Separate Calcination Step Affects the Phase Composition of Cement Clinker*; Dissertation: Sweden, 2021.
- (41) Wan, B. *Energy Density of Methane - The Physics Factbook*. <https://hypertextbook.com/facts/2004/BillyWan.shtml> (accessed 2023-01-13).
- (42) Meng, R.; Zhao, Q.; Wu, M.; Long, Q.; Zhou, M. A Survey and Analysis on Electricity Consumption of Raw Material Mill System in China Cement Industry between 2014 and 2019. *Sustainability* **2021**, *13* (3), 1126.
- (43) Ahmed, A.; Esmaeil, K. K.; Irfan, M. A.; Al-Mufadi, F. A. Design Methodology of Organic Rankine Cycle for Waste Heat Recovery in Cement Plants. *Appl. Therm. Eng.* **2018**, *129*, 421–430.

- (44) Moreira, L. F.; Arrieta, F. R. P. Thermal and Economic Assessment of Organic Rankine Cycles for Waste Heat Recovery in Cement Plants. *Renew. Sustain. Energy Rev.* **2019**, *114*, No. 109315.
- (45) Our World in Data. *Carbon intensity of electricity*, 2022; Our World in Data. <https://ourworldindata.org/grapher/carbon-intensity-electricity> (accessed 2024–01–11).
- (46) Tiseo, I. *Carbon intensity of the power sector in China from 2000 to 2022*; Statista. <https://www.statista.com/statistics/1300419/power-generation-emission-intensity-china/#:~:text=The%20carbon%20intensity%20of%20electricity,two%20decades%2C%20it%20remains%20high>. (accessed 2023–11–24).
- (47) Voldsgård, M.; Gardarsdóttir, S. O.; De Lena, E.; Pérez-Calvo, J. F.; Jamali, A.; Berstad, D.; Fu, C.; Romano, M.; Roussanaly, S.; Anantharaman, R.; Hoppe, H.; Sutter, D.; Mazzotti, M.; Gazzani, M.; Cinti, G.; Jordal, K. Comparison of Technologies for CO₂ Capture from Cement Production—Part 1: Technical Evaluation. *Energies (Basel)* **2019**, *12* (3), 559.
- (48) Stadler, K. S.; Poland, J.; Galleste, E. Model Predictive Control of a Rotary Cement Kiln. *Control Eng. Pract.* **2011**, *19* (1), 1–9.
- (49) Skocek, J.; Zajac, M.; Ben Haha, M. Carbon Capture and Utilization by Mineralization of Cement Pastes Derived from Recycled Concrete. *Sci. Rep.* **2020**, *10* (1), 5614.



CAS BIOFINDER DISCOVERY PLATFORM™

STOP DIGGING THROUGH DATA — START MAKING DISCOVERIES

CAS BioFinder helps you find the right biological insights in seconds

Start your search

